FIU Sea Level Solutions Center
FLORIDA INTERNATIONAL UNIVERSITY

Sea Level Solutions Center (SLSC), Institute of Environment, Florida International University

Updating the Statewide Extreme Rainfall Projections

Final Report - June 1, 2021

Dr. Jayantha Obeysekera, P.E., Director (SLSC, Lead PI)
Dr. Mike Sukop, P.G., C.Hg., Professor (SLSC, Co-PI)
Dr. Tiffany Troxler, Director of Science (SLSC, Co-PI)
Dr. Anupama John, Post-doctoral Associate (SLSC)

FIU Sea Level Solutions Center
FLORIDA INTERNATIONAL UNIVERSITY

Final Report (June 1, 2021)

Updating the Statewide Extreme Rainfall Projections

Florida Department of Business and Professional Regulation
Florida Building Commission, Hurricane Research Advisory Committee

and

Sea Level Solutions Center (SLSC), Florida International University (FIU)

Project Team

Project Investigators:

1. Dr. Jayantha Obeysekera, P.E., Lead PI (Technical lead, guidance in all aspects)
   Director, Sea Level Solutions Center, FIU.
2. Dr. Mike Sukop, Co-PI (modeling)
   Professor, Department of Earth & Environment.
3. Dr. Tiffany Troxler, Co-PI (Florida Building Code)
   Director of Science, Sea Level Solutions Center, FIU.
4. Dr. Anupama John, Post-doctoral Associate, Sea Level Solutions Center, FIU

Acknowledgment: Dr. Obeysekera, PI, is a collaborator in a project on rainfall extremes, funded by the South Florida Water Management District (SFWMD) and awarded to US Geological Survey (USGS) with Michelle Irizarry, P.E. as its Principal Investigator, John Stamm, Ph.D. (USGS) and Carolina Maran, Ph.D, P.E. (SFWMD) serving as lead members of the project team. His participation in and input during weekly calls on that project has been beneficial to the current state-wide effort as it will ensure that, the results produced by SFWMD are consistent with the current products of this effort. We have made an extensive effort to use consistent analytical techniques and data and have received excellent collaboration from USGS. Also, SFWMD, in their project with USGS, included a task for FIU to facilitate an expert review panel. FIU SLSC appreciates receiving previously published data and computer codes from the USGS that was developed for the SFWMD. With permission from USGS, the codes may available from the GitHub sites:
mirizarry-ortiz/ddf_code: Provisional DDF code (github.com)
mirizarry-ortiz/etccdi_code: Python code to compute ETCCDI climate indices for DDF project (github.com)

Table of Contents

List of Tables

List of Figures

List of Abbreviations and Acronyms

AMS	Annual Maximum Series
ASCE	American Society of Civil Engineers
CD	Climate Division
CF	Change Factor
CMIP	Coupled Model Intercomparison Project
CORDEX	Coordinated Regional Downscaling Experiment
DDF	Depth-Duration-Frequency
EAP	External Advisory Panel
ETCCDI	Expert Team on Climate Change Detection and Indices
EVT	Extreme Value Theory
FAWN	Florida Automated Weather Network
FBC	Florida Building Code
FDEP	Florida Department of Environmental Protection
FDOT	Florida Department of Transportation
FIU	Florida International University
GCM	Global Circulation Model
GEV	Generalized Extreme Value
GHG	Greenhouse Gas
GPD	Generalized Pareto Distribution
IDF	Intensity-Duration-Frequency
IFAS	Institute of Food and Agricultural Sciences
IPC	International Plumbing Code
IPCC	Intergovernmental Panel of Climate Change
LOCA	Localized Constructed Analogues

MACA	Multivariate Adaptive Constructed Analogs
MCI	Model Climate performance Index
MVI	Model Variability Index
MQDM	Multiplicative Quantile Delta Mapping
NA-CORDEX	North America - Coordinated Regional Downscaling Experiment
NARCCAP	North American Regional Climate Change Assessment Program
NOAA	National Oceanic and Atmospheric Administration
NRMSE	Normalized Root-Mean-Squared-Error
PDF	Probability Distribution Function
PFDS	Precipitation Frequency Data Server
POT	Peaks Over Threshold
PRISM	Parameter-elevation Regressions on Independent Slopes Model
RCM	Regional Climate Model
RCP	Representative Concentration Pathway
RFA	Regional Frequency Analysis
RMSE	Root-Mean-Squared-Error
ROI	Region of Interest
SFWMD	South Florida Water Management District
SFWMM	South Florida Water Management Model
SLSC	Sea Level Solutions Center
SPC	Standard Plumbing Code
TIN	Triangulated Irregular Network
UF	University of Florida
USGS	United States Geological Survey

Executive Summary

The Florida Building Code (FBC) is one of the strongest in the nation for protection from extreme hazards. Communities are at risk of extreme flooding due to variations in rainfall extremes. In coastal regions, changes in rainfall patterns will have a compounding effect due to rising sea levels and rising groundwater levels. In 2019, the Florida Building Commission awarded a contract to the Sea Level Solutions Center (SLSC) in the Institute of Environment at Florida International University to assess potential updates to Miami-Dade County Flood and Rain Loads that may alter the flood risks, particularly in the current environment of changing conditions due to climate change. The focus of that study was on both sea level rise and changes in rainfall extremes but was limited to Miami-Dade County.

This new study, awarded by the Florida Building Commission through its Hurricane Research Advisory Committee, expands the Miami-Dade County study to update extreme rainfall projections state-wide. Information on Rain Loads in the current version of the Florida Building Code is quite dated (likely dating back to the 1970s) and needs to be updated and projected under future conditions. This update is necessary for two reasons: (a) extensive rainfall data have been collected throughout the State since the early 1970s; and (b) recent research on implications of climate change suggest a new paradigm is needed for planning and design, one that is based on the concept of nonstationarity, which means that the historical observations cannot be used to predict future rainfall.

This study leveraged a similar, ongoing study being conducted by the United States Geological Survey (USGS) and funded by the South Florida Water Management District (SFWMD). Extensive efforts were made to ensure the same datasets and similar technical approaches are used in both studies. However, the USGS/SFWMD study is limited only to the regions within the SFWMD boundary whereas the current study covers the entire state. The Principal Investigator of the current project is an active collaborator in the USGS/SFWMD study.

Because of the rapidly emerging research associated with predicting rainfall due to climate change and to ensure technical rigor, the study team assembled an Expert Advisory Panel (EAP) to seek input and review the technical strategy used in this study. The EAP membership included twelve members who are highly qualified and experienced professionals from SFWMD, St. Johns River WMD, Tampa Bay Water, academia (UF and UM), several state agencies (FDOT and FDEP), Broward County, RAND Corporation, and three federal agencies (USGS, NOAA, USACE). Following the collection of extensive datasets that were needed for the study and the development of the technical strategy, the study team held a meeting with the EAP to present the strategy and seek input and feedback.

Early in the project, several available rainfall datasets were assembled for use in selecting the best climate models. Datasets included both station rainfall data at numerous locations

within Florida as well as gridded rainfall data. As one of the most recent, commonly used rainfall Depth-Duration-Frequency (DDF) datasets, publicly available Atlas 14 station curves were selected as the reference data that would be projected into the future. The Atlas 14 DDF curves selected for the project cover 242 locations distributed within Florida and are available from the data server published by NOAA (http://hdsc.nws.noaa.gov/hdsc/pfds). The general strategy formulated for projecting future extreme rainfall consists of determining a multiplier, known as a Change Factor (CF), for determining DDF curves that are appropriate for a selected future period.This approach allows historical observations and the results of multiple future climate models to be objectively integrated to determine nonstationarity of future extreme rainfall. Where computed CFs deviate from 1, Atlas 14 DDF curves recommended for the current condition need to be adjusted before using them for stormwater drainage project planning and design The CFs have been regionalized for five Florida Climate Divisions that are based on those typically used by NOAA.

As the best available, gridded historical data, the daily PRISM dataset available for 1981 through 2005 was used. For predicting the future potential realization of rainfall, downscaled climate model data available from a variety of sources were used. Downscaling, a process for simulating regional rainfall from Global Climate Models, uses both statistical and dynamic approaches. The following downscaled datasets were acquired for the project:

1. Coordinated Regional Downscaling Experiment (CORDEX), dynamically downscaled
2. Localized Constructed Analogues (LOCA), statistically downscaled
3. Multivariate Adaptive Constructed Analogs (MACA), statistically downscaled

In the report, these are referenced as CORDEX, LOCA, and MACA datasets. Typically, each climate model data set is available for the period 1950 through 2099, covering both historical and future periods.

An important step in selecting the best models for computing future DDF curves was a process known as model culling, where the best models are found by comparing model output representing a historical period to the selected gridded observational dataset (PRISM) using a set of metrics representing extremes. The best models were selected based on their ability to represent both the climatology (means) and the interannual variability of the selected metrics when compared to the PRISM datasets. The best models for each Florida Climate Division were identified for further analysis.

A rigorous statistical modeling approach for computing DDF curves from the climate datasets (historical and future periods) was used. Historical and future DDF curves were produced using the Peaks Over Threshold (POT) approach involving the Generalized Pareto Distribution (GPD). The ratio of the DDF estimates corresponding to future and historical periods computed from climate model datasets yielded the CF for all Florida Atlas 14 stations.

Finally, the results were compiled according to the following categories:

1. Climate dataset (CORDEX, LOCA, and MACA)
2. Rainfall duration in days (1, 3, 7, and 10)
3. Two future periods of analysis (2030-2069 and 2060-2099, labeled as NEAR and FAR respectively relative to the "baseline" period, 1966-2005)
4. Florida Climate Divisions or Regions (1 through 5 shown in Figure 11)
5. Return Period (5, 10, 25, 50, 100, and 200 years)

The CFs generally ranged from 1 to 1.6, indicating that the multiplier for Atlas 14 DDF curves is greater than 1. This finding implies that future extreme rainfall is predicted to be larger than what is provided by the Atlas 14 DDF curves.

It is recommended that the Florida Building Commission adopt the Atlas-14 DDFs together with the CFs presented in this report. While the Code may adopt the 50^{th} percentile CF for the middle dataset in some circumstances, it is also recommended that design professionals and engineers be aware of the impact of variability among climate datasets used and of within-climate-dataset variability as expressed by the percentiles depending on the risk tolerance of projects.

Introduction and Purpose

Communities across Florida are frequently at risk of flooding due to extreme rainfall. Recent research suggests that there is a potential for this risk to increase in the future although local and regional information on exact predictions is not readily available. Extreme rainfall data used in the Florida Building Code is quite dated (probably dating back to the 1970s) and needs to be updated and projected under future conditions. In this project, the Florida International University (FIU) Sea Level Solutions Center (SLSC) (henceforth FIU SLSC) has extended the rainfall projections of the 2018 Miami-Dade pilot study titled "Potential Implications of Sea-Level Rise and Changing Rainfall in Florida Building Code for Communities in Florida using Miami-Dade County as a Case Study" (Obeysekera et al. 2019) to all communities across the State of Florida. This updated extreme rainfall information will be invaluable for all future infrastructure planning and design projects across all communities in Florida.

Literature Review

Engineers, municipal planners, and policy makers rely on design storms, often developed using historical data, as a tool to guide design, planning and policy decisions. Evidence suggests that current rainfall standards, based on historical observations (i.e., assuming stationarity) can misrepresent future conditions, particularly rainfall extremes (Milly et al. 2008; Sugahara et al. 2009; Srivastav et al., 2015) leaving communities and infrastructure vulnerable to climate-related hazards like flooding. Design storms need to be kept up-to-date with the current data and reflect the future projected scenarios of rainfall extremes to support informed decision-making and resiliency.

Design storms can be defined using Depth-Duration-Frequency (DDF) or Intensity-Duration Frequency (IDF) curves, which are an objective, probabilistic assessment of rainfall occurrence (Panthou et al., 2014). DDF/IDF curves provide the relationship between the depth/intensity and duration of rainfall for storms with various return periods. They are developed by fitting a theoretical probability distribution to rainfall data from a long time record of observations. For this reason, DDF/IDF curves summarize conditional probability. They do not represent actual storms but present integrated data from numerous different storms, and the depths of rainfall are averages over the selected duration (Bedient et al., 2013). DDF/IDF curves are developed by 1) fitting a probability distribution function (PDF) to rainfall data for different durations, 2) relating the maximum rainfall depth to the corresponding return period from the cumulative distribution function, and 3) determining the maximum rainfall depth from the known cumulative frequency and duration using a theoretical distribution function (Srivastav et al., 2015). For applications that require rainfall intensities over an area, Intensity-Duration-Area-Frequency (IDAF) curves were established. IDAF curves are a spatial extension of the IDF curves and are developed by combining IDF curves with Areal Reduction Factors (ARFs). Due to their heavy data requirements, applications of IDAFs are limited to regions where rainfall data with high spatial and temporal resolution exist (Borga et al., 2005; Gerold & Watkins, 2005; Nhat et al., 2007; Bara et al., 2009; Ben-Zvi, 2009; Overeem et al., 2009; Awadallah, 2011; Ariff et al., 2012; Panthou et al., 2014).

Theoretical distribution functions from Extreme Value Theory (EVT) are used in analyzing rainfall extremes and developing DDF/IDF curves. The Annual Maximum Series (AMS) modeling using Generalized Extreme Value (GEV) is a widely used EVT method (Jenkinson, 1955; Buishand, 1991; Durrans & Brown, 2001; Overeem et al., 2008; Overeem et al., 2009; Buishand & Hanel, 2010; Fontanazza et al., 2011). The GEV models the maxima of a series of independent and identically distributed observations using the method of moments, L-moments, or the maximum likelihood (ML). Based on the shape parameter from the fit, the distributions may be Gumbel, Frechet, or Weibull (Coles, 2001). A drawback of the GEV method is the tendency to ignore significant values that may be lower than the highest value in the block maxima. This can be overcome by using another widely applied method, the peaks-over-threshold (POT) approach using the Generalized Pareto Distribution (GPD) (Davison & Smith, 1990; Palychuk & Guo, 2008; Norlida et al., 2011). The POT uses a threshold value to define the significant extreme values resulting in a larger sample size and more robust estimates of fitting parameters. A stochastic model is fit to the exceedances above a threshold (Davison & Smith, 1990). When historical rainfall data are used in the methods described above, stationarity is assumed, which makes the developed DDF/IDF curves unreliable for future climate scenarios.

Nonstationary conditions can be derived from Global Circulations Models (GCMs), presently one of the best tools to study climate change. These are complex models that discretize the planet into large grid cells and employ either governing physical laws (fundamental equations of motion, thermodynamics, conservations of mass etc.) or observational phenomena to predict atmospheric variables for future climate scenarios. They incorporate aspects of the dynamics, chemistry, and biology of the atmosphere, biosphere, and oceans (Kotamarthi et al., 2016). Currently available GCMs are based on 1) land-ocean-atmosphere coupling, 2) greenhouse gas (GHG) emissions, and 3) different initial conditions representing the state of the climate system (Srivastav et al., 2015). GCMs are influenced by GHG emissions, land-use, energy production, global and regional economy, and population growth (Srivastav et al., 2015). Over the last two decades, the Coupled Model Intercomparison Project (CMIP) by the World Climate Research Programme (WCRP) has developed high quality GCMs like the CMIP3, CMIP5 and the recent CMIP6, which have been widely applied. However, GCMs cannot be directly applied to represent local-scale processes such as extreme rainfall due to their coarse spatial (~100km-250km).

Regional Climate Models (RCMs) incorporate GCM boundary conditions to produce higher resolution grids but the process of generating realizations for atmospheric forcings is computationally intensive (Srivastav et al., 2015). A popular alternative is applying downscaling techniques to convert GCM/RCM outputs into locally representative projections (Southam et al., 1999; Coulibaly and Dibike, 2004; Palmer et al., 2004; Simonovic & Peck, 2009). Downscaling methods may be either dynamical or statistical. Dynamical downscaling is a physically-based method that utilizes limited-area models in two ways: 1) using a limited area model driven by GCM inputs or 2) a variable-resolution global model that zooms in on the area of interest during calculations. Some examples of

past dynamically downscaled products include NARCAAP using CMIP3 and NA-CORDEX using CMIP5. Although dynamical downscaling can produce meaningful output that captures nonstationary relationships at high spatial and temporal resolutions, a major drawback of this method is that it requires a lot of computational resources; hence, the statistical downscaling approach of using a mathematical transfer function is more widely applied (Pierce et al., 2014). Statistical downscaling methods range from simple linear regressions to complex applications like inhomogeneous Markov chains and non-parametric kernel density estimators. These methods are more flexible than dynamical downscaling techniques. They have been found to match high-resolution observations better than the physically-based methods; however, a major limitation is their dependency on observational data. In addition, they are limited by a lack of understanding of the fine-scale physical processes. For these reasons, there has been interest in developing hybrid dynamical-statistical techniques (Walton et al., 2015); however, data products from hybrid techniques are not considered in this work.

Scope of Work

The scope of the project included the following tasks.

Task 1. External Advisory Panel (EAP)

FIU SLSC established a diverse External Advisory Panel (EAP) to seek guidance on rainfall datasets, analysis methods, desirable predicted rainfall durations, and design return periods for engineering projects. As shown in Table 1, EAP includes twelve members who are highly qualified and experienced professionals from SFWMD, St. Johns River WMD, Tampa Bay Water, academia (UF and UM), several state agencies (FDOT and FDEP), Broward County, RAND Corporation and three federal agencies (USGS, NOAA, USACE). Many in the EAP are also members of the panel established for the SFWMD rainfall project and through the interaction with those panel members, valuable input on data, analytical methods, model validation, and new approaches has been received.

Eleven members of the EAP participated in a meeting organized for receiving technical input that was held on May 3, 2021. The meeting was also attended by the Primary Investigator of the USGS project, Michelle Irizarry, P.E., who collaborated with the FIU team during the entire project. Details of the climate datasets, technical approach, and the nature of the final product were presented to EAP.

EAP provided valuable comments for the current project as well as suggestions for future research. The panel recognized the fact there is no single regional climate model for the State of Florida as a whole and concurred with the approach of using the best available climate model data. In particular, several members suggested the possible use of the high-resolution, CMIP6 class of models that are becoming available for use in the next report by the Intergovernmental Panel on Climate Change (IPCC). Because the CMIP6 data distribution is still ongoing, the associated new datasets are still being evaluated by climate modelers and we did not explore their use for this project. The use of CMIP6 may be

considered in future research on updating extreme rainfall. The State of Florida is also contemplating the establishment of what is known as a "FloodHub" at the University of South Florida and the panel members encouraged the collaboration of extreme rainfall research with that effort.

Concerning the dated information on extreme rainfall in the current Florida Building Code, the panel observed the fact that the Florida Department of Transportation (FDOT) has already updated its DDF curves to Atlas 14 data published by NOAA; this is being used as the recommended current baseline in the current project. There is a desire to standardize the methods and data across the State of Florida and provide regionally specific DDF curves.

Table 1. External Advisory Panel (EAP) established for the FBC Rainfall Update Project

Panel Member	Institution	Title
Ana Carolina Coelho Maran, Ph.D., P.E.	South Florida Water Management District	District Resiliency Officer
Brian J. Soden, Ph.D.	The University of Miami	Professor
Chou Fang, Ph.D.	St. Johns River Water Management District	Technical Program Manager
Christopher D. Frans, Ph.D, P.E.	United States Army Corps of Engineers	Civil Engineer
Jennifer Green, P.E.	Florida Department of Transportation	State Drainage Engineer
Jennifer Jurado, Ph.D.	Broward County	Chief Resiliency Officer
Johnna Infanti, Ph.D.	National Oceanic and Atmospheric Administration	Scientist
Michelle Miro, Ph.D.	RAND Corporation	Engineer
Stacey A. Archfield, Ph.D.	United States Geological Survey	Research Hydrologist
Tirusew Asefa, Ph.D., P.E.	Tampa Bay Water	Planning & Decision Support Manager
Wendy D. Graham, Ph.D.	University of Florida	Professor and Director, Water Institute
Whitney Gray	Florida Department of Environmental Protection	Administrator, Florida Resilient Coastlines Program

Task 2. Development of Future Conditions Extreme Rainfall Data

Task 2.1. Acquisition and Assessment of current datasets

Duration and Return Periods:

Chapter 14-86 FAC defines a Critical Duration as follows: *"Critical Duration" means the length of time of a specific storm frequency which creates the largest volume or highest*

rate of net stormwater runoff (post-improvement runoff less pre-improvement runoff) for typical durations up through and including the 10-day duration for closed basins, i.e. without a positive outlet, and up through the 3-day duration for basins with positive outlets. The critical duration for a given storm frequency is determined by calculating the peak rate and volume of stormwater runoff for various storm durations and then comparing the pre-improvement and post-improvement conditions for each of the storm durations. The duration resulting in the highest peak rate or largest net total stormwater volume is the "critical duration" storm (volume is not applicable for basins with positive outlets).

To meet the above requirement, the rainfall durations selected for updating extreme rainfall include 1 day, 3 days, 5 days, 7 days, and 10 days. These selected durations will be sufficient to meet the requirements of stormwater criteria typically used by state agencies such as FDOT and all the Water Management Districts.

Return periods selected for updating Depth-Duration curves include but are not limited to 5 years, 10 years, 25 years, 50 years, and 100 years.

The following historical rainfall data sets were acquired for this project:

Station Data:
1. AMS of precipitation from NOAA Atlas 14 for durations from 5 minutes to 60 days and the DDF data available from PF Data Server-PFDS/HDSC/OWP (noaa.gov)
2. University of Florida Institute of Food and Agricultural Sciences (IFAS), Florida Automated Weather Network (FAWN) (https://fawn.ifas.ufl.edu/)
3. Rainfall data at rainfall stations in the State of Florida from the Climatologist's Office at FSU (COAPS) (www.coaps.fsu.edu)

Gridded Data
4. PRISM data (PRISM Climate Group, Oregon State University, http://prism.oregonstate.edu)
5. South Florida Water Management District (SFWMD) daily gridded dataset

The historical data above are being used for evaluating the skills of the future climate model datasets with due consideration to differences in spatial resolution among the datasets.

NOAA Atlas 14 Data Set
NOAA Atlas 14 (NOAA 2013) contains estimates of precipitation DDF curves along with associated 90% confidence intervals for the United States and territories at weather stations and as a gridded product with 30 arc-second resolution (approx. 0.5 mi). Supplementary information available as part of this product includes the AMS data used in developing the DDF curves, analysis of the AMS seasonality and trends, and the temporal distribution of heavy precipitation. The results are published through the Precipitation Frequency Data Server (PFDS) at http://hdsc.nws.noaa.gov/hdsc/pfds. The AMS data are generally available up to the years 2011-2012, depending on the station. Volume 9 of NOAA Atlas 14 covers the Southeastern states including Florida.

AMS data have been downloaded from the PFDS for 242 weather stations in the State of Florida (Figure 1). Although data were available for over 450 stations, only 242 locations were selected based on the criteria that the record length should be sufficiently long to obtain reasonably accurate estimates of DDF using extreme value modeling. Periods of records at these stations can go back as far as 1840 and end in 2011-2012.

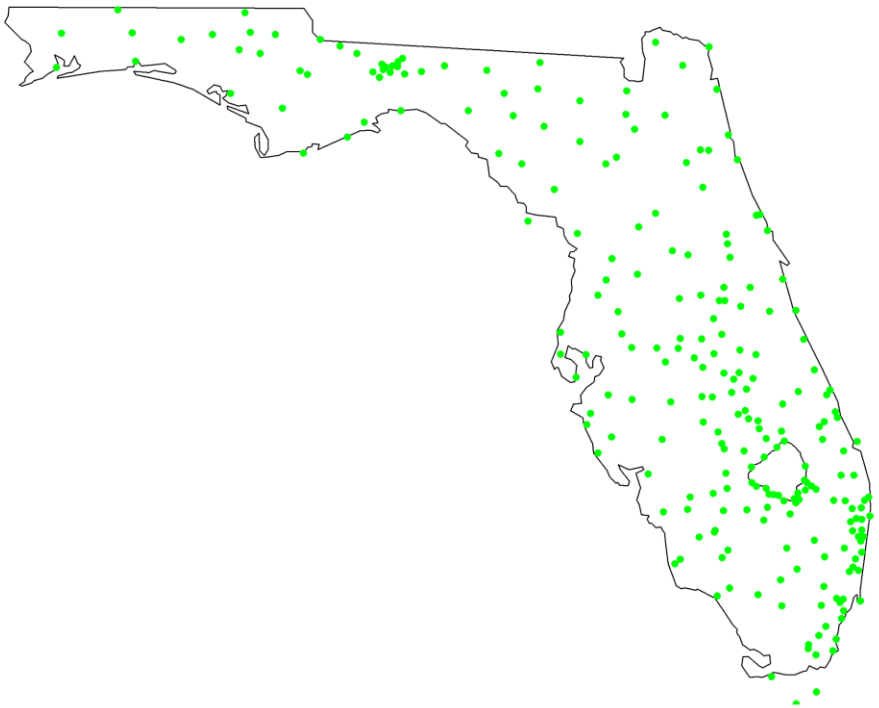

Figure 1. Locations of the 242 selected rainfall gage locations in Florida available from the NOAA Atlas 14 portal.

The NOAA Atlas 14 project portal provides the DDF data for all stations in Florida. These official Atlas 14 DDF curves for the Southeastern region have been developed by fitting a GEV distribution to the extremes (*unconstrained* AMS) for each duration of interest independently (Irizarry et al. 2017). Regional frequency analysis (RFA), which uses data from nearby stations that are expected to have similar frequency distributions, was used to obtain regional estimates of L-moment ratios. Regional L-moment ratios for the region of interest (ROI) were then used to estimate higher-order L-moments at the target station for that particular duration. The parameters of the GEV distribution were then estimated from the at-station average L-moments for each duration. As a final step, the GEV fits were smoothed across durations to improve the shape of the DDF curves. An example of a

typical DDF curve for a station in the state of Florida is shown in Figure 2. Many other examples of the DDF curves are shown in Appendix I.

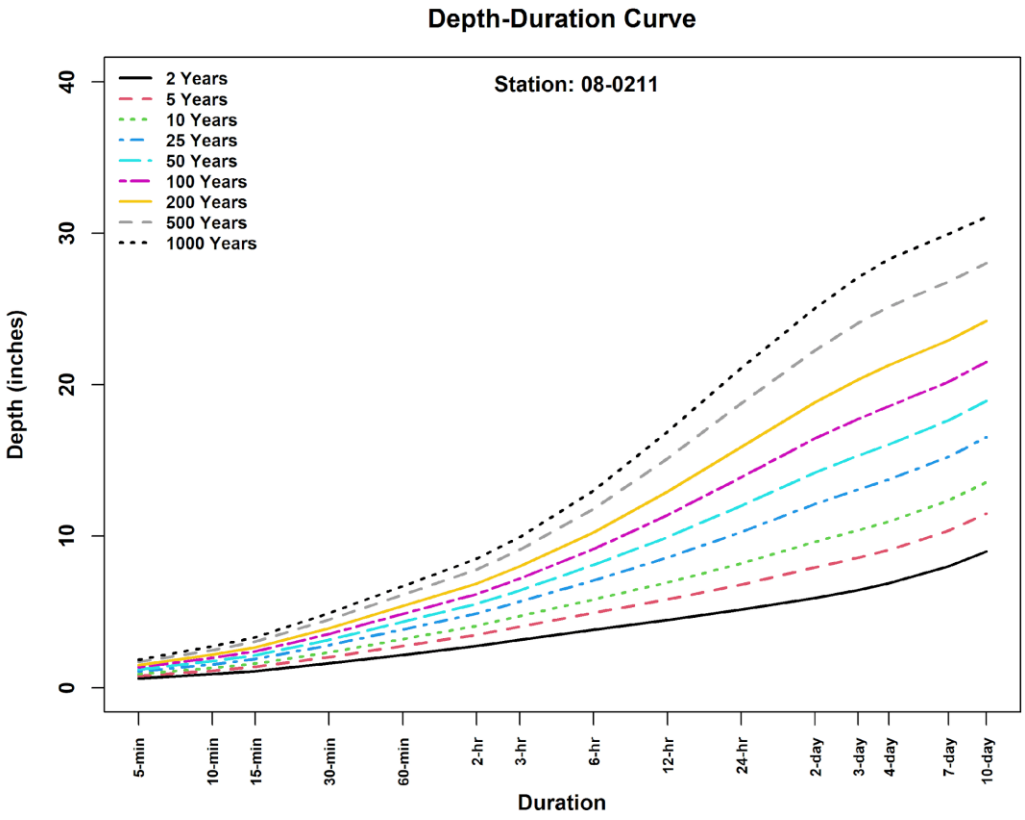

Figure 2. Official Atlas 14 DDF Curves at Station 08-0211, located near the Apalachicola Airport in northwest Florida. Legend entries indicate the return period corresponding to the DDF curves.

The DDF curves published by NOAA (2013) are generally accepted as the best available information on rainfall DDF data for Florida and many agencies are beginning to adopt these data for planning purposes. For this project, we assume that the DDF curves available for the 242 stations across the state of Florida represent the best available historical data on rainfall depth, duration, and frequency information. As explained below, our approach focused on adjusting these curves under future conditions incorporating climate change. As specified in the Scope of Work, two future periods (e.g. ~2050, and ~2080) have been considered.

University of Florida's IFAS FAWN rainfall data

The University of Florida's Institute of Food and Agricultural Sciences (IFAS) Florida Automated Weather Network (FAWN) provides near-real-time weather information directed towards agricultural users throughout the state of Florida (https://fawn.ifas.ufl.edu/) (Figure 3). Historical rainfall, precipitation, and other weather

data are available for download at timesteps ranging from 15 minutes to daily, at https://fawn.ifas.ufl.edu/data/fawnpub/. FAWN datasets corresponding to 15-minute intervals have been downloaded from the above site. These data are available from 1997 to 2020.

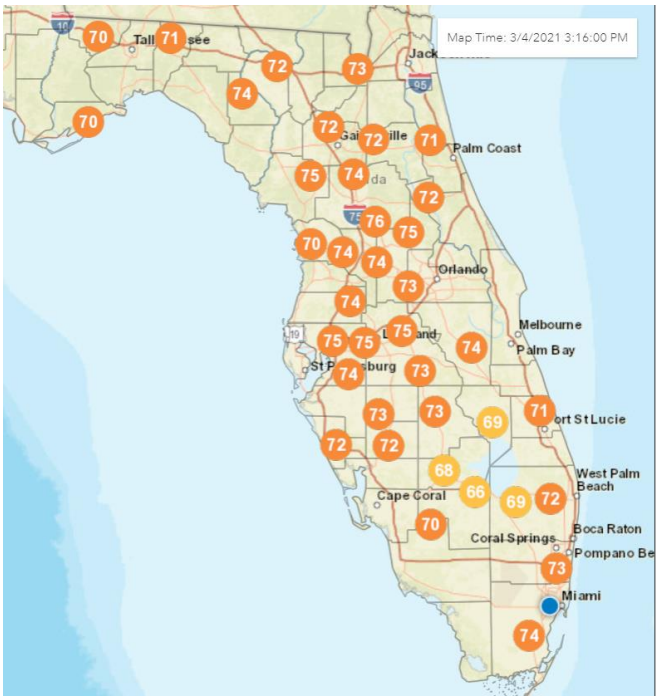

Figure 3. Locations of UF's FAWN data.

PRISM Data Set

PRISM stands for Parameter-elevation Regressions on Independent Slopes Model (Daly et al. 2008). PRISM is a set of monthly, yearly, and single-event gridded data products of mean temperature and precipitation, max/min temperatures, and dewpoints, primarily for the United States (PRISM High-Resolution Spatial Climate Data for the United States: Max/min temp, dewpoint, precipitation | NCAR - Climate Data Guide (ucar.edu). In-situ point measurements are ingested into the PRISM statistical mapping system and it uses a weighted regression scheme to account for complex climate regimes associated with orography, rain shadows, temperature inversions, slope aspect, coastal proximity, and other factors. Climatologies (normals) are available at 30-arcsec (800 meters) and monthly data are available at 2.5-arcmin (4 km) resolution.

For this project, we have acquired the daily gridded PRISM data for the period 10/1/1981 through 12/31/2005. These data are used for evaluating the skills of the climate models. Because it has a high spatial resolution (4 km), PRISM's gridded rainfall should be representative of the rainfall observed at the nearest Atlas 14 station (see map in Figure 4).

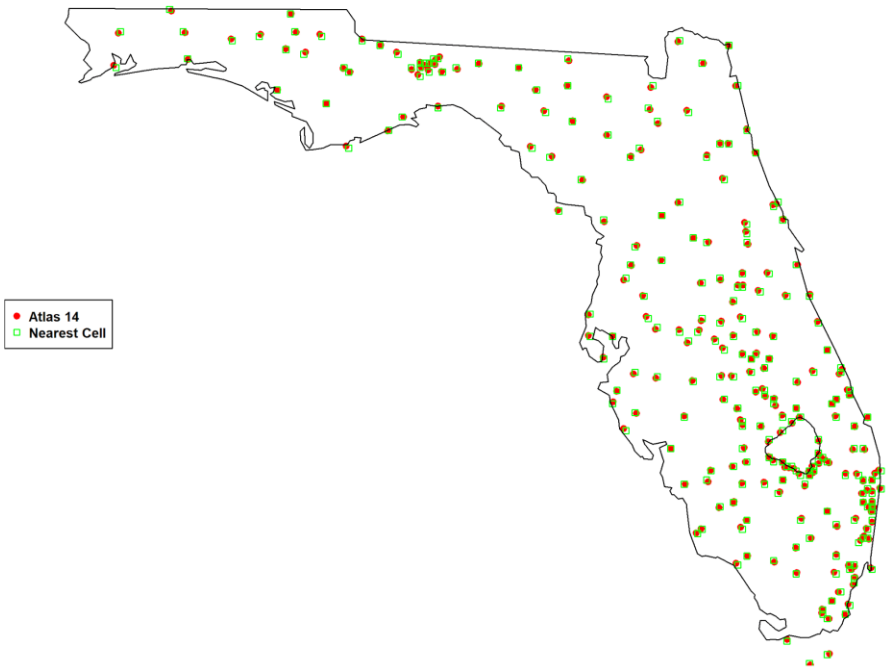

Figure 4. Atlas 14 rainfall stations and the nearest 4-km cell of the PRISM data set.

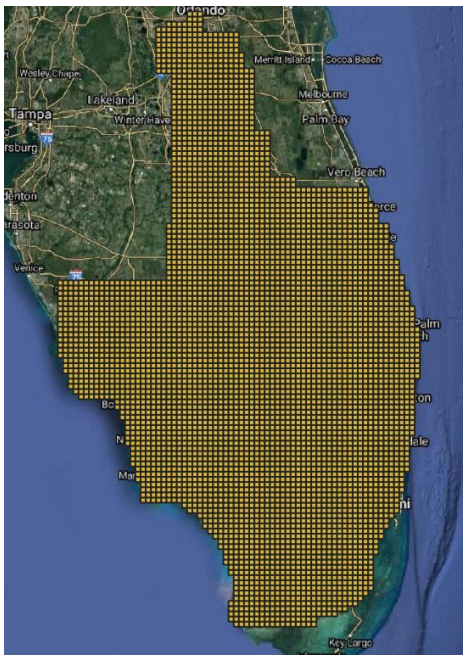

Figure 5. SFWMM 2 by 2 mile grid.

SFWMD Data Set

This daily, gridded data set is used as the primary input to SFWMD's premier regional hydrologic simulation model, the South Florida Water Management Model (SFWMM). The grid that covers the SFWMD's area in south Florida has a cell size of 2 miles by 2 miles and includes daily snapshots of rainfall over the region since 1914 (Figure 5). Records of hundreds of rainfall stations, with adequate quality control checks, have been used to estimate the gridded rainfall with a Triangulated Irregular Network (TIN) for interpolation. The model uses the period of record from 1965 to 2015. The density of rainfall stations during this period is high compared to earlier years and therefore the spatio-temporal pattern of rainfall for this period is considered to be accurate. This data set has been acquired for the project as one of the historical estimates of rainfall available for validation of

climate models. Although this data set covers only the southern half of the State of Florida, it is useful for the current research.

Task 2.2. Acquisition and assessment of Climate Model Data for Future Periods

GCMs can provide prediction information on changes in meteorology at coarse spatial and temporal scales. However, from an impact modeling perspective, their spatial resolution is too coarse to capture local variations, which have steep gradients in meteorological variables and circulation patterns (Abatzoglu & Brown, 2012). In complex terrains, even the finest GCM resolution of 100 by 100 km tends to aggregate multiple landscapes into one grid cell. Downscaling techniques are employed to produce RCMs covering smaller areas but providing projections at higher spatial resolutions required to capture localized extreme events. To date, the downscaling products can be categorized into two categories:

1. Statistical Downscaling
2. Dynamical Downscaling

As the name suggests, statistical downscaling employs statistical methods to project coarser GCM model output to a higher resolution (typically on the order of 10 km to 25 km) on the land surface. Several downscaled data sets have a national coverage developed using this technique. Dynamical downscaling is more physically based as it uses the higher-resolution RCMs, which use the GCMs for their boundary conditions. For this project we have acquired the following downscaled datasets:

1. Coordinated Regional Downscaling Experiment (CORDEX), dynamically downscaled
2. Localized Constructed Analogues (LOCA), statistically downscaled
3. Multivariate Adaptive Constructed Analogs (MACA), statistically downscaled

It is important to recognize that these data products do not provide absolute projections of future rainfall. They represent plausible realizations of future rainfall due to selected scenarios of climate change as characterized by alternative GHG emission scenarios of the atmosphere and the land-use trajectories. The Intergovernmental Panel on Climate Change (IPCC), in their latest assessment report, has defined four scenarios known as Representative Concentration Pathways (RCPs) and they are typically identified as RCP2.6, RCP4.5, RCP6.0, and RCP8.5. The number in the RCPs is the additional end-of-century radiative forcing (in watts per square meter, representing the GHG effect in the atmosphere) in the year 2100. The lowest concentration scenario is RCP2.6, recognized as the pathway necessary to keep the global temperature increase below 2°C (van Vuuren et al. 2011). RCP8.5 is the highest scenario, which assumes a continuing strong dependence on fossil fuels and is consistent with current trends and expectations through at least mid-century (Schwalm et al. 2020). The remaining scenarios RCP4.5 and RCP6.0 lie between these two extremes. In this project, we employ datasets corresponding to RCP8.5 and RCP4.5 representing the highest and one of the medium concentration pathways.

A summary of the data sets used for this project is presented in Table 2. The names of the GCMs used for different realizations of the climate models are shown in the last column of Table 2.

Table 2. Future rainfall data sets acquired for the project

Dataset	Climate Scenarios	Simulation Models	
Coordinated Regional Downscaling Experiment (CORDEX)	Historical	CanESM2.CanRCM4,	GFDL-ESM2M.WRF
	RCP85	CanESM2.CRCM5-UQAM	HadGEM2-ES.RegCM4
		CanESM2.RCA4	HadGEM2-ES.WRF
		EC-EARTH.HIRHAM5	MPI-ESM-LR.CRCM5-UQAM
		EC-EARTH.RCA4	MPI-ESM-LR.RegCM4
		GEMatm-Can.CRCM5-UQAM	MPI-ESM-LR.WRF
		GEMatm-MPI.CRCM5-UQAM	MPI-ESM-MR.CRCM5-UQAM
		GFDL-ESM2M.RegCM4	
	RCP45	CanESM2.CanRCM4	
		CanESM2.CRCM5-UQAM	
		CanESM2.RCA4	
		EC-EARTH.HIRHAM5	
		EC-EARTH.RCA4	
		MPI-ESM-LR.CRCM5-UQAM	
Localized Constructed Analogues (LOCA)	Historical	ACCESS1-0	GFDL-ESM2M
	RCP45	ACCESS1-3	GISS-E2-H
	RCP85	bcc-csm1-1-m	GISS-E2-R
		CanESM2	HadGEM2-AO
		CCSM4	HadGEM2-CC
		CESM1-BGC	HadGEM2-ES
		CESM1-CAM5	IPSL-CM5A-LR
		CMCC-CM	IPSL-CM5A-MR
		CMCC-CMS	MIROC5
		CNRM-CM5	MIROC-ESM
		CSIRO-Mk3-6-0	MIROC-ESM-CHEM
		EC-EARTH	MPI-ESM-LR
		FGOALS-g2	MPI-ESM-MR
		GFDL-CM3	MRI-CGCM3
		GFDL-ESM2G	NorESM1-M
Multivariate Adaptive Constructed Analogs (MACA)	Historical	bcc-csm1-1	HadGEM2-ES365
	RCP45	bcc-csm1-1-m	inmcm4
	RCP85	BNU-ESM	IPSL-CM5A-LR
		CanESM2	IPSL-CM5A-MR
		CCSM4	IPSL-CM5B-LR
		CNRM-CM5	MIROC5
		CSIRO-Mk3-6-0	MIROC-ESM
		GFDL-ESM2G	MIROC-ESM-CHEM
		GFDL-ESM2M	MRI-CGCM3
		HadGEM2-CC365	NorESM1-M

Coordinated Regional Climate Downscaling Experiment (CORDEX)

The Coordinated Regional Climate Downscaling Experiment (CORDEX) uses boundary conditions from the GCM simulations from the CMIP5 as boundary conditions to derive outputs from RCMs. Results for most of North America are available at North American CORDEX (NA-CORDEX) at spatial resolutions of 0.22º (25 km) or 0.44º (50 km) from 1950-2100 under different RCPs (Table 3).

Table 3. The spatial resolution of CORDEX dataset by climate models and RCPs

	RegCM4	WRF	CRCM5-OUR	CRCM5-UQAM	CanRCM4	RCA4	HIRHAM5	RCP
ERA-Int	50km	50km	0.22°	0.44°	0.44°	0.44°	0.44°	2.6, 4.5, 8.5
	25km	25km		0.22°	0.22°			
HadGEM2-ES	50km	50km						8.5
	25km	25km						
CanESM2				0.44°	0.44°	0.44°		4.5
					0.22°			
			0.22°	0.44°	0.44°	0.44°		8.5
				0.22°	0.22°			
GEMatm-Can				0.44°				8.5
				0.22°				
MPI-ESM-LR				0.44°				4.5
	50km	50km	0.22°	0.22°				8.5
	25km	25km		0.44°				
MPI-ESM-MR				0.44°				8.5
				0.22°				
GEMatm-MPI				0.44°				8.5
				0.22°				
EC-EARTH						0.44°		2.6
						0.44°	0.44°	4.5
						0.44°	0.44°	8.5
GFDL-ESM2M	50km	50km	0.22°					8.5
	25km	25km						

An example plot of a CORDEX model grid, the Atlas 14 station locations, and the nearest CORDEX cell of those stations are shown in Figure 6.

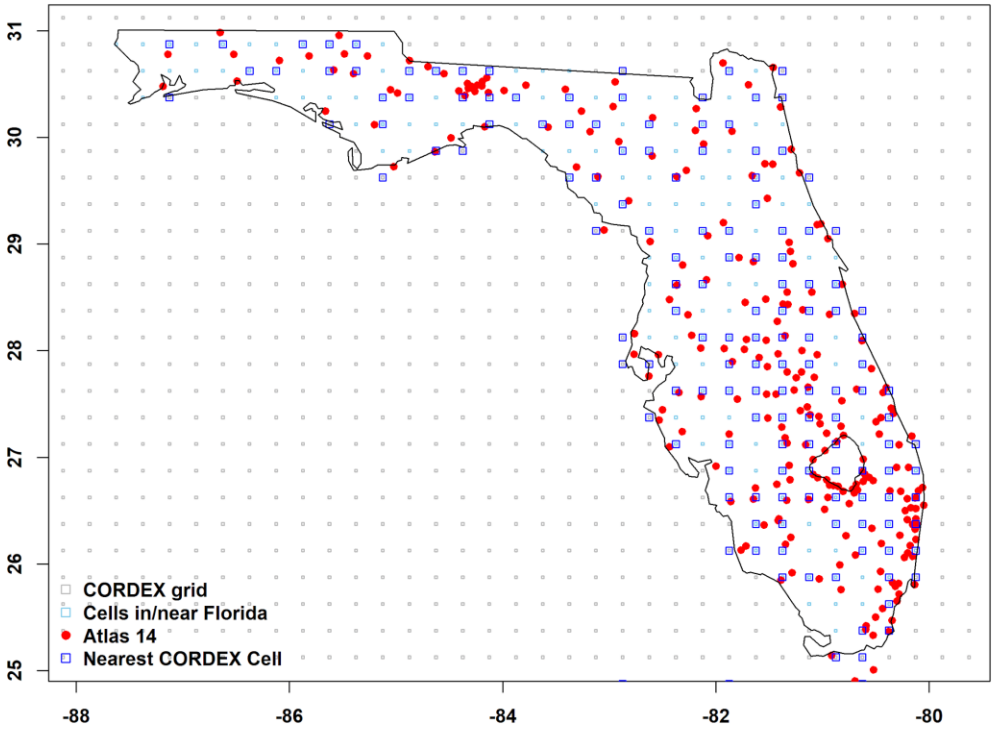

Figure 6. Example CORDEX grid in the region, its cells in and near Florida, Atlas 14 locations, and the nearest CORDEX cells.

Localized Constructed Analogues (LOCA)

The LOCA method was developed to address the issues that techniques like MACA encounter (next section) when using a weighted average of analog days. LOCA constructs the downscaled field using a single analog day (from a pool of 30 days) that best matches weather in the local region around the point being considered. The best matching observed day is scaled to match the amplitude of the modeled day being downscaled (additively for precipitation) and produce the final downscaled value (Pierce et al., 2014). In addition to the general limitations of statistical downscaling, LOCA is limited by the assumption that the relationship between local and area-averaged climate fields will not change in the future climate (Pierce et al., 2014).

The LOCA dataset covers North America from central Mexico through southern Canada at a 1/16th degree spatial resolution. The list of downloaded GCMs for scenarios for the LOCA model is presented in Table 2. An example of the LOCA grid, Atlas 14 stations, and the nearest LOCA cells are shown in Figure 7.

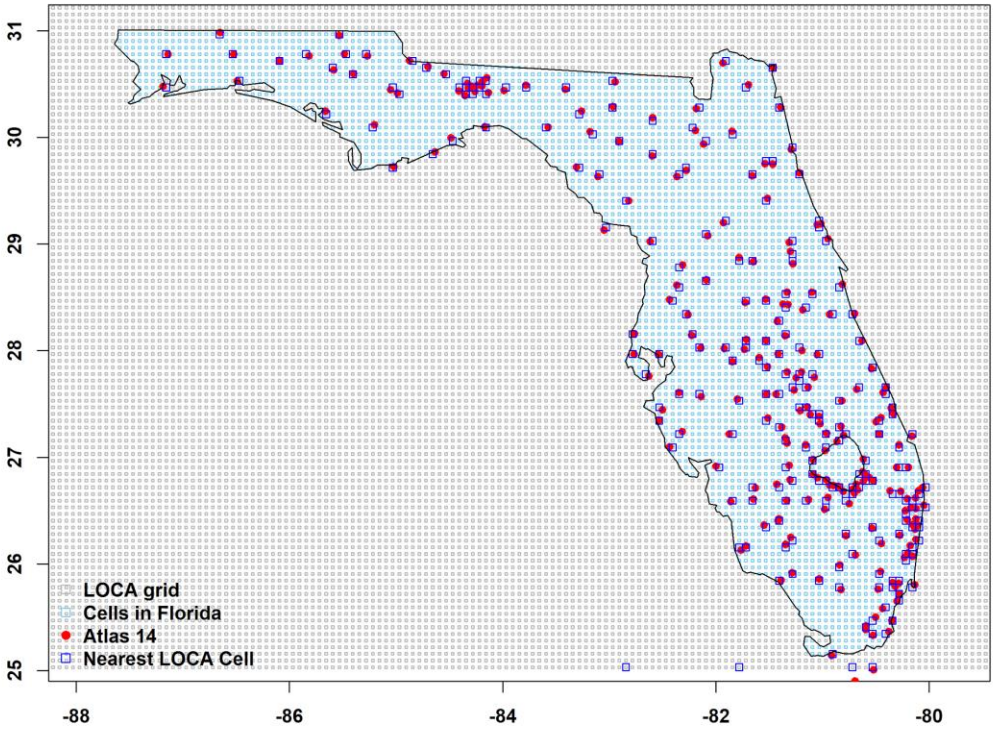

Figure 7. Example LOCA grid, the Atlas 14 stations, and the nearest LOCA cells.

Multivariate Adaptive Constructed Analogs (MACA)

The MACA method uses a multi-step process for developing fine-scale spatial patterns using historical observations. The technique uses 20 CMIP5 GCMs (see downloaded datasets in Table 2) providing daily meteorological variables for historical (1950-2011), RCP4.5, and RCP8.5 scenarios, which are bias-corrected using training data from two datasets: 1) Livneh et al. (2013) daily dataset from 1950-2011 with a 6 km ($1/16^{th}$ degree) spatial resolution; and 2) gridMet daily dataset from 1979-2012 with a 4 km ($1/24^{th}$ degree) spatial resolution. The MACA method identifies the 30 best matching analog days in the historical occurrence and combines these analog days, using a weighted average method, to reproduce the target pattern (Abatzoglu & Brown, 2012, Pierce et al., 2014). The datasets cover the contiguous United States. The downloaded datasets are presented in Table 2.

Unlike direct interpolation methods, the MACA technique is advantageous as it uses historical observations to produce meteorological data with a high spatial resolution (needed by impact studies) while preserving the time-scales and patterns simulated by GCMs. The obvious limitation is that any imperfections in the training data are carried over while bias correcting. Also, GCM signals may be preserved for the period of the bias-correction but not at longer time-scales (Abatzoglu & Brown, 2012). Since multiple analogs are averaged together to construct the downscaled field, there is a tendency to

dampen the extremes and increase the spatial coherence of downscaled fields, but there is also production of drizzle in areas where no precipitation exists in the original model (Pierce et al., 2014).

Figure 8 shows an example of the MACA grid, the Atlas 14 stations, and the nearest MACA grid cells.

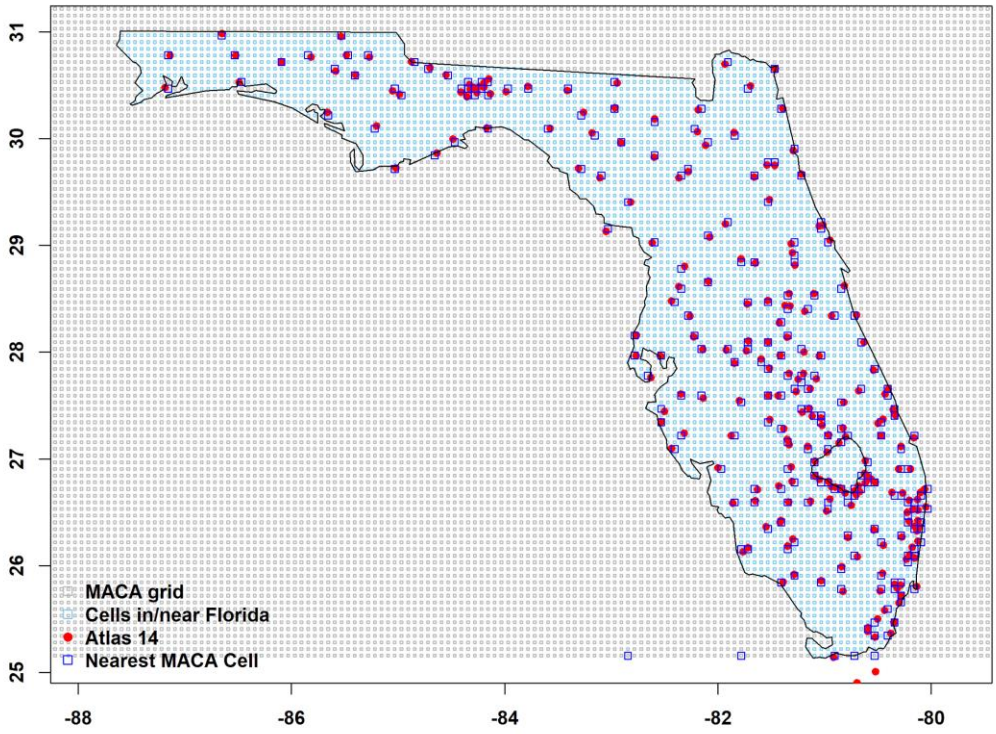

Figure 8. Example MACA grid, the Atlas 14 stations, and the nearest MACA cells.

Task 2.3 Extreme Rainfall Modeling

The recommended approach for determining future DDF curves is to adjust the Atlas 14 curves using what are known as Change Factors (CFs), which represent adjustments to the published curves provided by NOAA. The concept of CFs is illustrated using Figure 9.

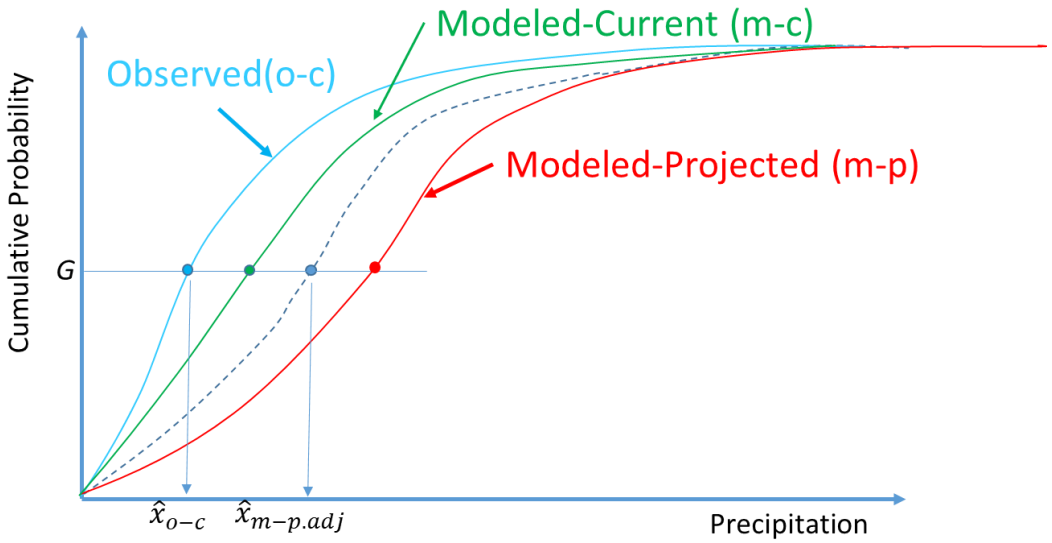

Figure 9. Illustration of the concept of the Change Factor. Dashed curve is the adjusted curve using, observed, modeled-current, and modeled-project probability distributions and the Change Factor defined in the text below.

As shown in Figure 9, a CF is associated with three cumulative probability distributions: (1) Observed (F_{o-c}); (2) Modeled-Current (F_{m-c}); and (3) Modeled-Projected (F_{m-p}). Modeled-Current and Observed probability distributions correspond to the same historical period. The Modeled-Projected distribution represent the future precipitation for a specific future period.

It is well known that the extreme rainfall predicted by climate models has a large negative bias. Typically, bias correction techniques are used to correct such biases. For this project, we will use what is known as the **Multiplicative Quantile Delta Mapping** (MQDM) method for adjusting the future. The expression for adjusting future rainfall quantiles is (Irizarry et al. 2016, 2017):

$$\hat{x}_{m-padj.} = F^{-1}_{m-padj.}(G) = F^{-1}_{m-p}(G) * \left\{ \frac{F^{-1}_{o-c}(G)}{F^{-1}_{m-c}(G)} \right\}$$

The variables used in MQDM are defined as follows: $\hat{x}_{m-padj.}$ is the adjusted quantile for the model (m) projections (p) for the future period, F_{o-c} is the Cumulative Distribution

Function, CDF, of the observations (*o*) in the current baseline period (*c*), F_{m-c} is the CDF of the model (*m*) in the current baseline period (*c*), and F_{m-p} is the CDF for the model (*m*) projections (*p*) for the future period. *G* is the annual non-exceedance probability (CDF value) and is equal to *1-P*, *P* is the annual exceedance probability (AEP) which is related to the return period *T* by *1/P = T* (i.e., *G=1-1/T*), F^{-1} is the quantile function.

Finally, the adjusted rainfall for the future is given by Eq (1) which allows the adjustment of the rainfall quantile corresponding to a given return period *T = 1/p* by combining estimates obtained from historical data (*o-c*), model output for the current period (*m-c*) and the model output for the future period.

$$\hat{x}_{m-padj} = F_{o-c}^{-1}(G)\left[\frac{F_{m-p}^{-1}(G)}{F_{m-c}^{-1}(G)}\right]$$

The quantity inside the large square brackets is the CF. For the present project, we will provide CFs corresponding to all frequencies (5- to 100-year return periods) and durations (1 day to 10 days) for adjusting the Atlas 14 frequency curves at each of the 242 locations. This work uses the R-software as specified in the SOW.

The overall approach for processing the historical data and the climate model outputs is shown in Figure 10

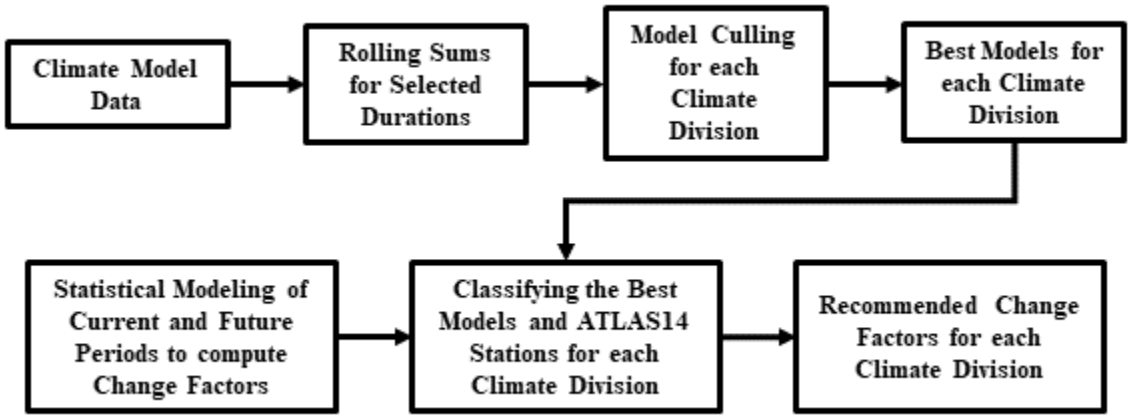

Figure 10. Approach for processing data and outputs.

First, the daily time series of the three climate model datasets (LOCA, MACA, and CORDEX) were aggregated to produce rolling sums for the selected durations (1, 3, 7, and 10 days). For each dataset, the number of rolling sums files correspond to the available models for each climate scenario denoted as RCPs and corresponding to the future

scenarios of GHG emissions. For this project, we include two RCPs, known as RCP4.5 and RCP8.5, representing a low and high emissions respectively. The underlying assumption is that future emissions influence the precipitation generation process in a region and thus change its regime. Second, we perform a selection process (also known as model culling) to find models which can reproduce the statistical characteristics of the historical observations. Only such models will be used for computing CFs. Third, the CF for each model was computed using a rigorous statistical modeling approach to produce the model-based, cumulative probability distribution as shown in Figure 9. Finally, the best models resulting from the model culling were combined with the CF for all models to determine the recommended values for the CFs. Because climatology across the State of Florida is not homogenous, the above analysis was performed for each of NOAA's Florida Climate Divisions (Figure 11).

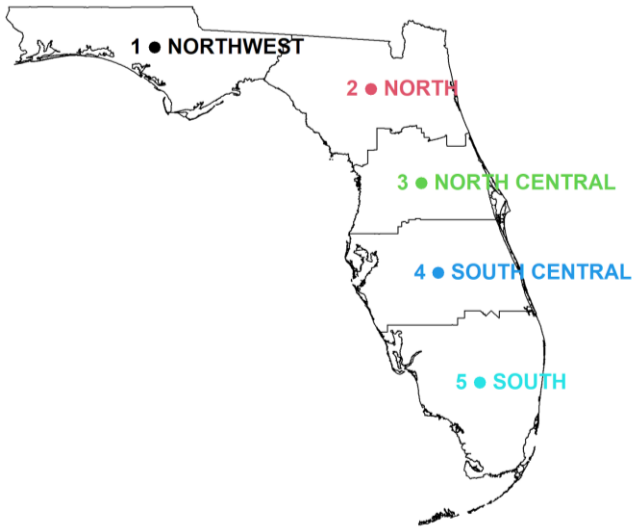

Figure 11. Selected Climate Divisions in the State of Florida

Task 2.3.1 Model Culling

Among the climate datasets (LOCA, MACA, and CORDEX), the number of models available for each RCP is not identical. Only a subset of these models may be capable of reproducing the characteristics of precipitation within a climate division (CD). The selection of "best' models for each CD through a process known as model culling was accomplished by comparing standard climate indices of models with those of standard observation sets. For this purpose, the daily PRISM dataset was used as the "reference dataset". As indicated above, PRISM grid covers the entire state with a high spatial resolution, at a daily time step (from 1981 to 2005), and therefore this dataset was deemed to be appropriate for culling climate models.

For comparing observations with models, we used the indices of climate extremes developed by the Expert Team on Climate Change Detection and Indices (ETCCDI)

(Sillmann et al. 2013; Srivastava et al. 2020). The initial set of indices selected for model evaluation is shown in Table 4.

Table 4. ETCCDI indices used for model culling

ID	Indicator Name	Definition	Units
PRCPTOT	Annual total wet days	Annual total, days > 1mm	inches
R10mm	Heavy precipitation days	# of days with > 10mm	days
R20mm	Heavy precipitation days	# of days with > 20mm	days
SDII	Daily intensity index	Ratio Annual precipitation / #wet days	inches/day
CDD	Consecutive dry days	#max. consecutive days < 1 mm	days
CWD	Consecutive wet days	#max. consecutive days > 1 mm	days
RX1day	Max 1-day precipitation amount	Annual maxima of 1-day precipitation	inches
R95p	Very wet days	Annual precip from days > 95%	inches
R99p	Extreme wet days	Annual precip from days > 99%	inches
RX3day	Max 3-day precipitation amount	Annual maxima of 3-day precipitation	inches
RX5day	Max 5-day precipitation amount	Annual maxima of 5-day precipitation	inches
RX7day	Max 7-day precipitation amount	Annual maxima of 7-day precipitation	inches
RX10day	Max 10-day precipitation amount	Annual maxima of 10-day precipitation	inches

Although the model evaluation considered all of the metrics shown in Table 4, only the indices that reflect extreme rainfall (highlighted in bold) were used for final model selection. First, for each performance index, I in Table 4, the root-mean-squared-error (RMSE) statistic was computed using

$$RMSE_{m,I} = \left[\frac{1}{N}\sum_{n=1}^{n=N}\left(\underline{I_{m,n}} - \underline{I_{o,n}}\right)^2\right]^{1/2}$$

where, $\underline{I_{m,n}}$ is the average of the index for model m, and grid cell n (1:N), $\underline{I_{o,n}}$ is the average of the index for the reference dataset, o (i.e. PRISM) and grid cell n, and N is the total number of grid cells in the model domain. Low RMSE values indicate better models in representing the climatological average of the reference dataset. Second, each RMSE is normalized by the median of all the models using

$$NRMSE_{m,I} = \frac{RMSE_{m,I} - RMSE_{median,I}}{RMSE_{median,I}}$$

where $NRMSE_{m,I}$ is the normalized RMSE for model *m* and index *I*, and $RMSE_{median,I}$ is median across all models. Finally, a Model Climate performance Index (MCI) is computed as the average of all NRMSE values across all indices.

To assess the performance of models concerning interannual variability, we used the Inter-annual Variability Skills Score (IVSS) as

$$IVSS_{m,I} = \left[\frac{1}{N}\sum_{n=1}^{n=N}\left(\frac{\sigma_{m,n,I}}{\sigma_{o,n,I}} - \frac{\sigma_{o,n,I}}{\sigma_{m,n,I}}\right)^2\right]$$

where $\sigma_{m,n,I}$ is the iterquartile range for model *m* (*o* for reference data), cell *n*, and index *I*. As in the case of MCI, the IVSS score is normalized using

$$NIVSS_{m,I} = \frac{IVSS_{m,I} - IVSS_{median,I}}{IVSS_{median,I}}$$

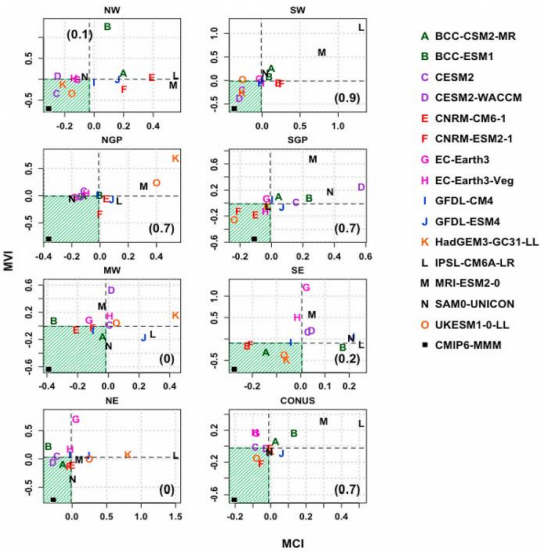

Figure 12. Climate performance Index (MCI) versus Model Variability Index (MVI) (Srivastava et al. 2020).

where $IVSS_{median,I}$ is the median across all models for index *I* as before. The Model Variability Index, MVI is given by the average of all NIVASS values across all indices.

The overall performance of all models of a particular dataset is evaluated by plotting MVI vs. MCI. An example of such a plot for different regions across the United States is shown in Figure 12 (Srivastava et al. 2020). In this scatter plot, models that have MVI and MCI values below zero (i.e., in the lower left quadrant) are better than all others in the other quadrants.

For the present project, MCI vs. MVI plots were produced for each dataset (LOCA, MACA, and CORDEX) and each CD (Regions 1 through 5). The scatter plots were produced for both (a) all indices in Table 4; and (b) only the indices representing extremes (shown in bold in the first column of Table 4)

Figure 13 shows an example MVI vs MCI plot for Climate Division I (Region 1) for the MACA data set. The annotation of each point shows an abbreviated version of the model name. Figure 14 shows the same plot but only considering the climate indices RX1day through RX7day. Combined results for all datasets and all regions are shown in Figure 15 (shows only the lower left quadrant of the

MVI vs. MCI scatter plot). From these results, the best models for each region were tabulated. They were used for computing CFs.

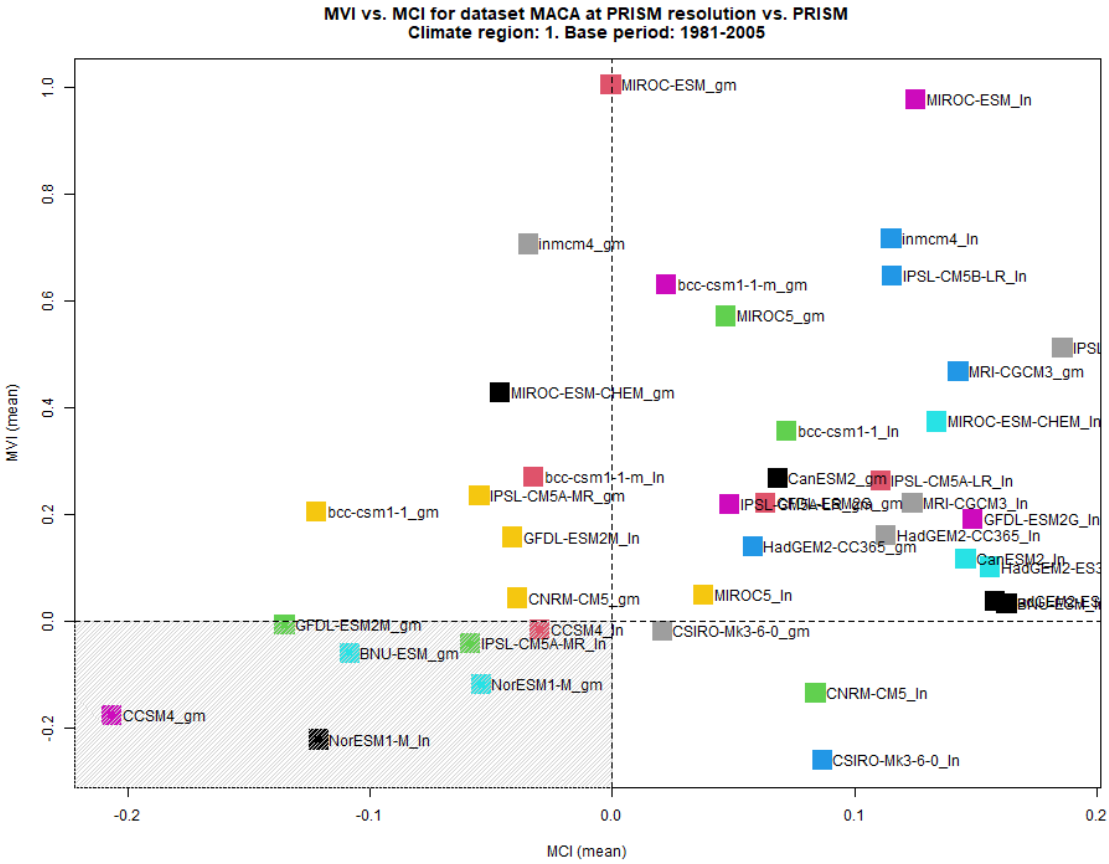

Figure 13. Scatter diagram of MVI versus MCI for the MACA dataset, for all indices in Climate Division identified as Region-1.

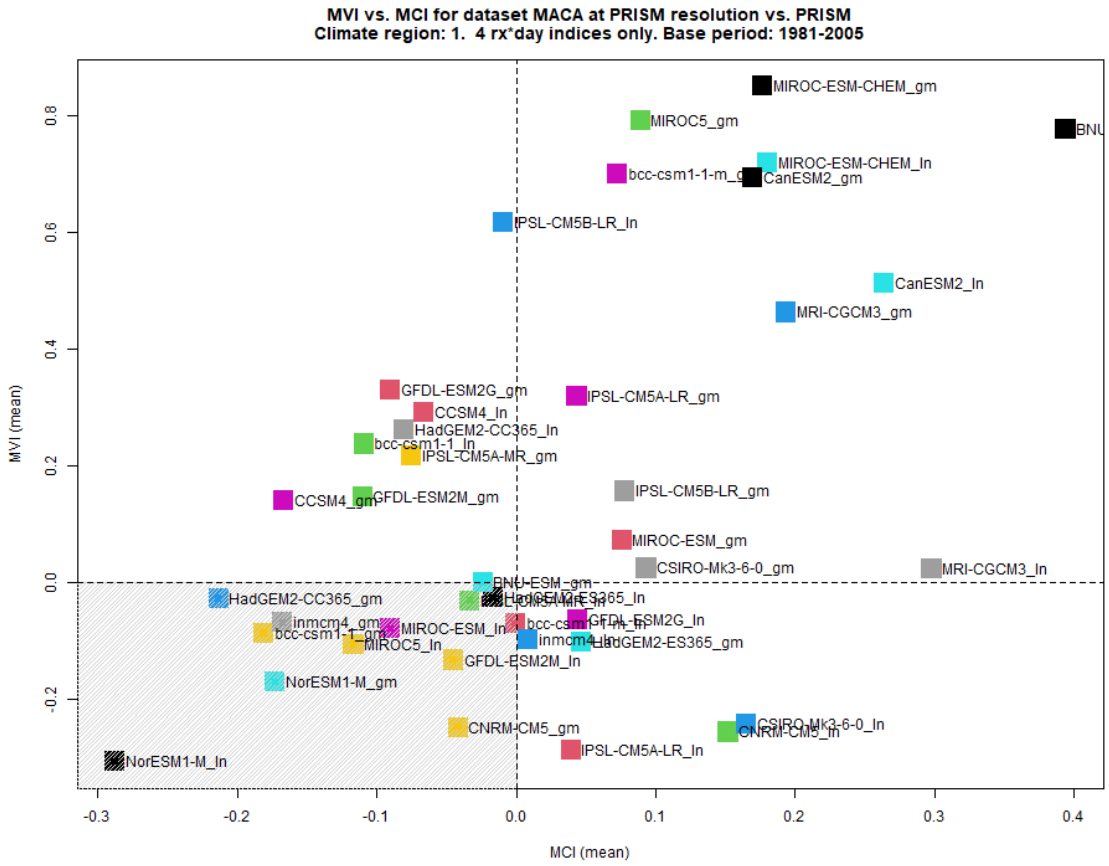

Figure 14. Scatter diagram of MVI versus MCI for the MACA dataset, for four extreme indices (bold in column in 1 of Table 4) in Climate Division identified as Region-1.

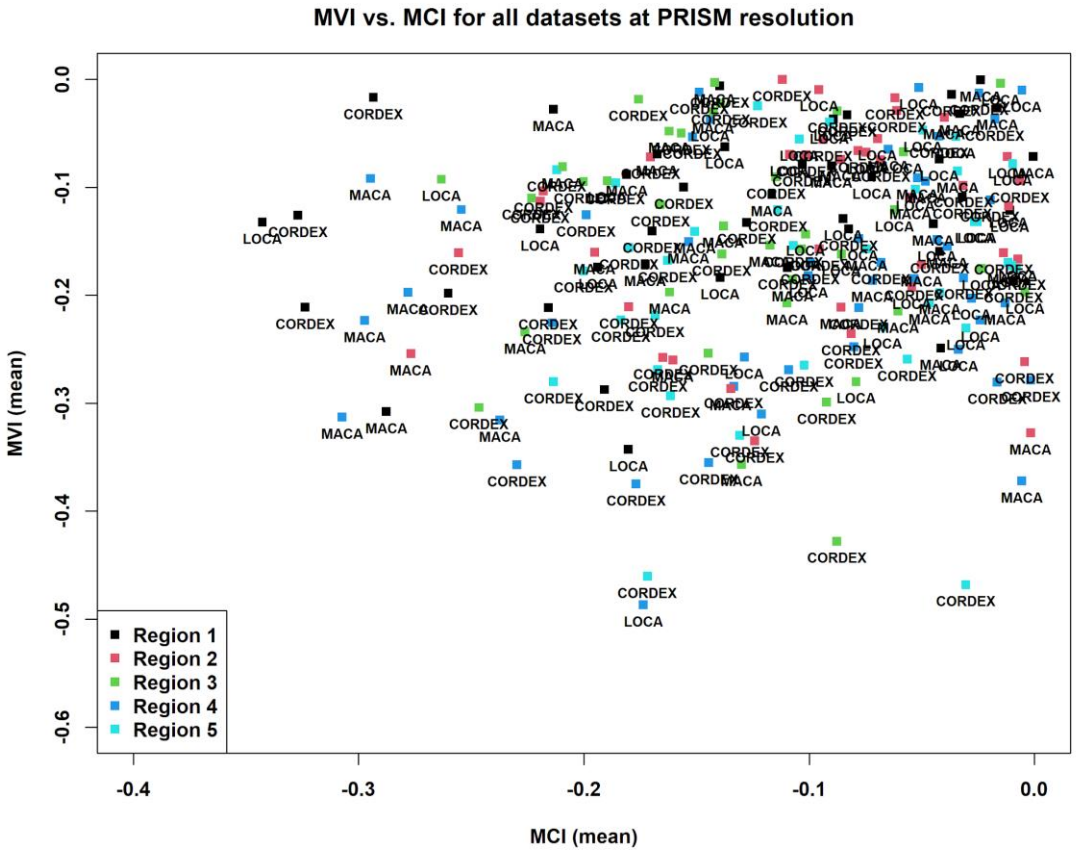

Figure 15. Scatter diagram of MVI versus MCI for all datasets and all regions for the climate extreme indices. This figure shows only the lower left quadrant of the MVI-MCI plot. These results were used to select "best models" for each region.

Task 2.3.2 Statistical Modeling of Extreme Rainfall

As outlined in the SOW, extreme value modeling uses two approaches for modeling:

1. Generalized Extreme Value (GEV) Distribution Fit for Annual Maxima Series (AMS)
2. Generalized Pareto Distribution (GPD) Fit for the Peaks Over Threshold (POT) Series

The conceptual frameworks for AMS (also known as Block Maxima) and POT are illustrated in Figure 16. For AMS, a maximum value is determined for each block (in the present case, one year), whereas for POT, all peaks above a particular threshold are considered. Both methods will be described below. The POT methods were ultimately used in this project.

The general approach for the project is to fit the probability distributions for two periods:

1. 1966 up to 2005 (considered the base or historical period for computing CFs)
2. Future forty-year periods 2030-2069 and 2060 to 2099

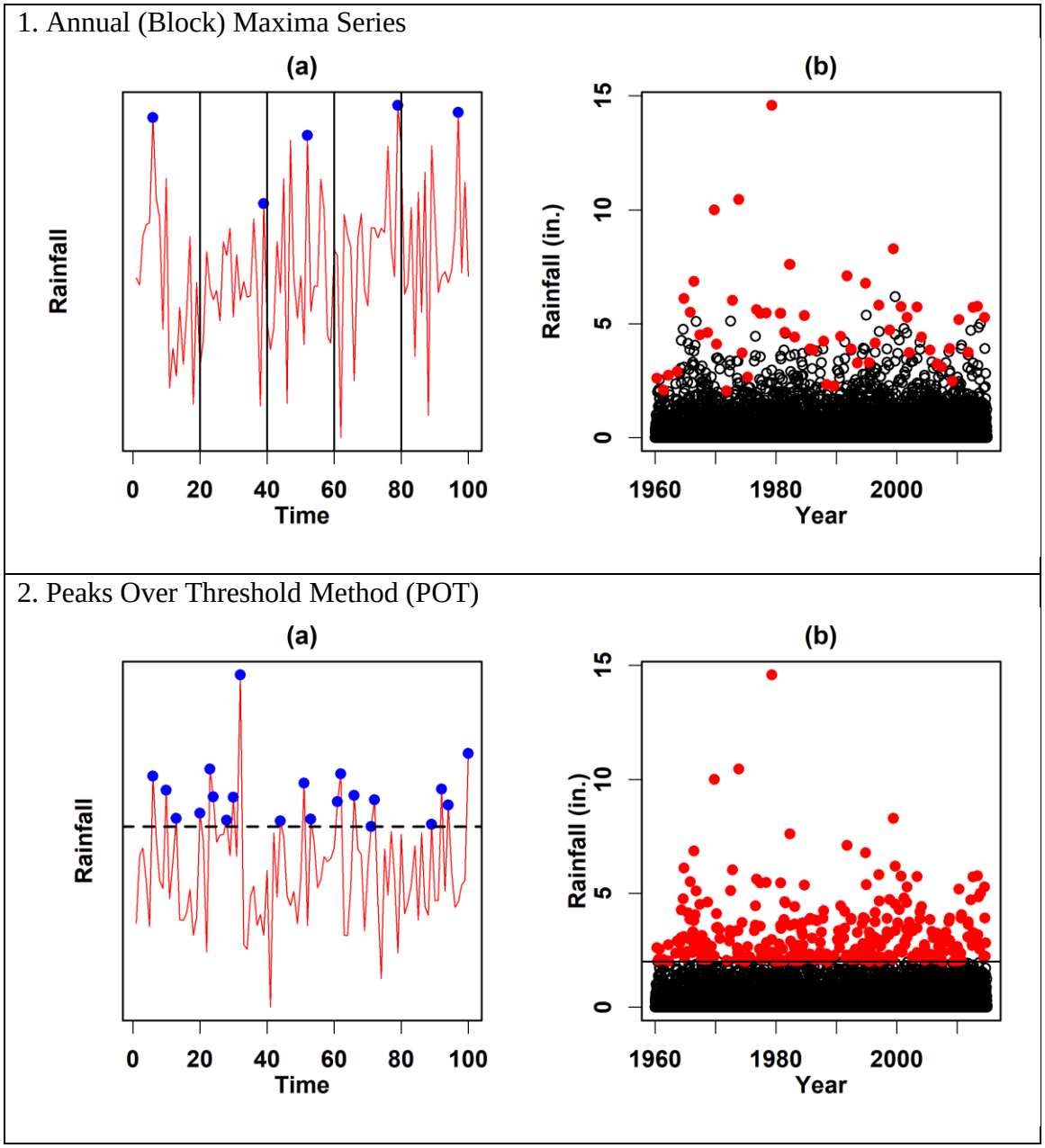

Figure 16. Illustration of Annual Maxima and Peaks Over Threshold.

We describe the technical details of both AMS and POT approaches.

AMS Modeling using Generalized Extreme Value (GEV) Distribution

The GEV distribution provides a model for the distribution of block maxima (Coles, 2001). It may be expressed as,

$$G(z) = exp\left\{-\left[1+\xi\left(\frac{z-\mu}{\sigma}\right)\right]^{-1/\xi}\right\}$$

defined on the set

$$\left\{z: 1+\xi\left(\frac{z-\mu}{\sigma}\right) > 0\right\},$$

where

$$-\infty < \mu < \infty,$$
$$\sigma > 0,$$
$$-\infty < \xi < \infty,$$

and ξ is the shape parameter, μ is the location parameter and σ is the scale parameter. Depending on the values of the shape parameter ξ, the three different families of GEVs are defined as Gumbel ($\xi = 0$), Fréchet ($\xi > 0$), and Weibull ($\xi < 0$).

Estimates of the extreme quantiles of the AMS are obtained by inverting the above equation and it is given by:

$$z_p = \mu - \frac{\sigma}{\xi}\left[1 - {y_p}^{-\xi}\right],$$

where

$$y_p = -log\,(1-p)\,,$$

$G(z_p) = 1-p$, and z_p is the return level for the return period $1/p$. The return level plot, which is a plot of z_p vs y_p, is linear when for Gumbel, convex with the asymptotic limit for Weibull, and concave with no finite bound for Fréchet (Coles, 2001).

Since the GEV models are implemented by blocking the data, the method is limited by the choice of the block size. Block selection can be a trade-off between bias and variance. Large blocks result in fewer block maxima while small blocks, which depending on the data recording may not be an available choice, can result in bias in estimation and extrapolation (Coles, 2001). The next section presents another method to overcome some of these limitations.

Peaks-Over-Threshold (POT) using Generalized Pareto Distribution (GPD)

The POT approach was first developed by hydrologists in the 1970s. This method fits a stochastic model to the exceedances over a threshold (u) and an independent exponential random variable to the model the amount of exceedance (Davison & Smith, 1990). The main advantage of employing the POT method is the increased sample size which results in more robust estimations of the shape parameter. Threshold models have previously been applied for rainfall depth and duration analysis (Palychuk & Guo, 2008). The POT approach used in this project is based on the family of distributions called GPDs. The GPD,

which implies the classical Pareto Distribution (Picklands, 1975; Davison & Smith, 1990; Madsen et al., 1997), models the amount of exceedance and the distribution function is given by (Coles, 2001):

$$H(y) = 1 - \left(1 + \frac{\xi y}{\tilde{\sigma}}\right)^{-1/\xi},$$

defined on the set

$$\{y: y > 0 \; and \; \left(1 + \frac{\xi y}{\tilde{\sigma}}\right) > 0\}$$

where

$$\tilde{\sigma} = \sigma + \xi(u - \mu).$$

Like the GEV, the shape parameter ξ is dominant in determining the behavior of the GPD, but unlike the GEV, the block size does not affect the value of the GPD parameters (Coles, 2001).
Early versions model the times of exceedances over the threshold using a non-homogenous Poisson process. In this project, we use the Poisson process of exceedance times with the GPD. It is given by,

$$F_Z^t(z) = exp\left[-\Lambda(t)\left(1 + \frac{\xi(z-u)}{\tilde{\sigma}}\right)^{-1/\xi}\right]$$

where *t* is the period of interest, $\Lambda(t)$ is the number of events over time *t*, and $\tilde{\sigma}$ and ξ are parameters.

Similar to the GEV, the shape parameter ξ is dominant in determining the qualitative behavior of the GPD. The distribution is unbounded when $\xi = 0$, has no upper limit when $\xi > 0$, and is bounded by an upper limit of $u - \tilde{\sigma}/\xi$ when $\xi < 0$.

The *N*-year return level (or quantile) is given by (Coles, 2001):

$$z_N = u + \frac{\tilde{\sigma}}{\xi}\left[\left(Nn_y\zeta_u\right)^{-\xi} - 1\right],$$

where n_y is the number of periods in a year (for daily this is 365.25), and ζ_u is the probability of an individual observations exceeding the threshold. This probability is typically estimated as the ratio of the number of exceedances and the length of the entire time series.

A constrained estimation procedure that fits all durations at once to overcome issues with crossing curves typically experienced when fitting one duration at a time (Irizarry et al. 2017; Xu & Tung, 2009) has been used. In this approach, the scale and shape parameters are assumed to be a linear function of the duration, *d*:

$$\tilde{\sigma}(d) = \alpha_0 + \alpha_1 d$$
$$\xi(d) = \beta_0 + \beta_1 d,$$

where $\alpha_0, \alpha_1, \beta_0, and\ \beta_1$ are the parameters of this formulation. In this approach, rainfall data corresponding to all durations are pooled and the above four parameters are estimated using the Maximum Likelihood Estimation (MLE) method. In the MLE method, checks are made during every iteration to ensure that the crossing of DDF curves is minimal. We found this Constrained MLE approach characterized by the simultaneous fitting of all durations together to minimize the crossing of distributions. For the fitting of the GPD using the Constrained MLE method, scripts were written using R-language software and made available to FIU SLSC.

The fitted GPD for current and future periods were used to compute the DDF curves and CFs.

Task 2.4. Change Factors (CFs)

Using the process illustrated in Figure 10, the CFs were computed for grid cells nearest to Atlas 14 stations for all climate datasets. The results were compiled according to the following categories:

1. Climate dataset (CORDEX, LOCA, and MACA)
2. Rainfall duration in days (1, 3, 7, and 10)
3. Two future periods of analysis (2030-2069 and 2060-2099, labeled as NEAR and FAR respectively relative to the "baseline" period, 1966-2005)
4. Florida Climate Divisions or Regions (1 through 5 shown in Figure 11)
5. Return Period (5,10, 25, 50, 100, and 200 years)

As described in the preceding sections, ensembles of "best models" according to the performance of climate model output relative the reference dataset (i.e., PRISM) were selected for each CD. These were selected from the MCI vs. MVI plots. The final outcome of this process was a set of best models for each CD. The CFs computed by fitting the Generalized Pareto Probability distribution for each of the two future periods were then parsed to identify only those that correspond to the best models. For each CD we identified all the Atlas 14 stations that are located inside its spatial domain.

In view of the large number of climate model outputs corresponding to the three datasets, it is not surprising that there is a significant variability of CFs within and across CDs. In order to simplify the final guidance for adjusting Atlas DDFs, we decided to regionalize the values of CFs for each CD. This approach simplifies the application of the CF to compute future DDFs for each of the Atlas 14 stations. The tabulation of CFs by CD allows the user to select a particular value of CF corresponding to a desired return period and future period (NEAR or FAR) and that can be used to adjust the Atlas 14 DDF curve for any location in that region or CD.

For a specific CD, the number of CF values used in regionalization will vary according to the number of Atlas 14 stations in that region. They will also vary in magnitude, and in some cases result in seemingly unrealistic, large CFs values. Considering this variability, each sample of CFs within a CD was analyzed statistically to compute percentiles corresponding to 17th, 50th (median) and 83%. This step was applied to determine the range of CF values that represent a majority, which in this case would be about two-thirds of the sample values (66%). These percentiles were recorded for each combination of the categories mentioned at the beginning of this section.

The behavior of CFs across the climate datasets was first inspected to understand the relative variability among them. Specifically, Figure 17 illustrates the relative magnitude of the median CF for each climate dataset when all values are combined for each duration (1, 3, 7, and 10). There is a clear pattern of CF variability across the climate datasets. The CFs corresponding to LOCA datasets is the lowest in general, while MACA datasets show some of the highest values. The CF values for CORDEX are generally in between LOCA and MACA, but that is not always the case. In addition, these plots show that the median values of CF are above 1 and they are in the range of 1 to about 1.5. The multipliers for the Atlas 14 DDF values are greater than 1, implying that the projected future rainfall extremes will be larger than those corresponding to the historical period as represented by the Atlas 14 DDF curves. This has significant implications for the planning and design of the stormwater drainage systems associated with civil infrastructure.

Variation of median CFs across all CDs for each return period and each downscaled dataset was investigated separately for each duration and each future period (Figure 18 through Figure 25). We first assess the variability of CFs for the 1-day duration for both NEAR (2030-2069) and FAR (2060-2069) future periods (Figure 18 and Figure 19). For the NEAR term, the median CFs are generally in the range of 1 to 1.5 for all CDs except for CDs 3 and 5 where CFs are lower with a range of 1 to 1.4. As observed previously, the MACA CF values are the highest, and the LOCA CFs are the lowest in general. The median CFs increase with increasing return periods, a pattern consistent for all CDs. However, this rate of increase appears to be the lowest for the LOCA dataset. From these results, it can be concluded that the CFs for high return periods are higher, implying that the percent increase from the Atlas 14 DDF values is larger.

The CFs for the FAR period generally mimic the patterns for the NEAR period described above except that the high end of the median CF values is about 1.6 as opposed to 1.5 for the NEAR term. Generally, CF vales for years in the FAR period are higher. It is noted that the foregoing discussion of CFs is relative to the median values and the CF range can be larger when the focus is on 17th and 83rd percentiles. In addition, the behavior of CFs as a function of return period for each climate dataset is similar for all other durations, namely 3 days, 7 days, and 10 days (see Figure 20 through Figure 25).

The actual data for CFs corresponding to each CD are provided in Appendix I of this report.

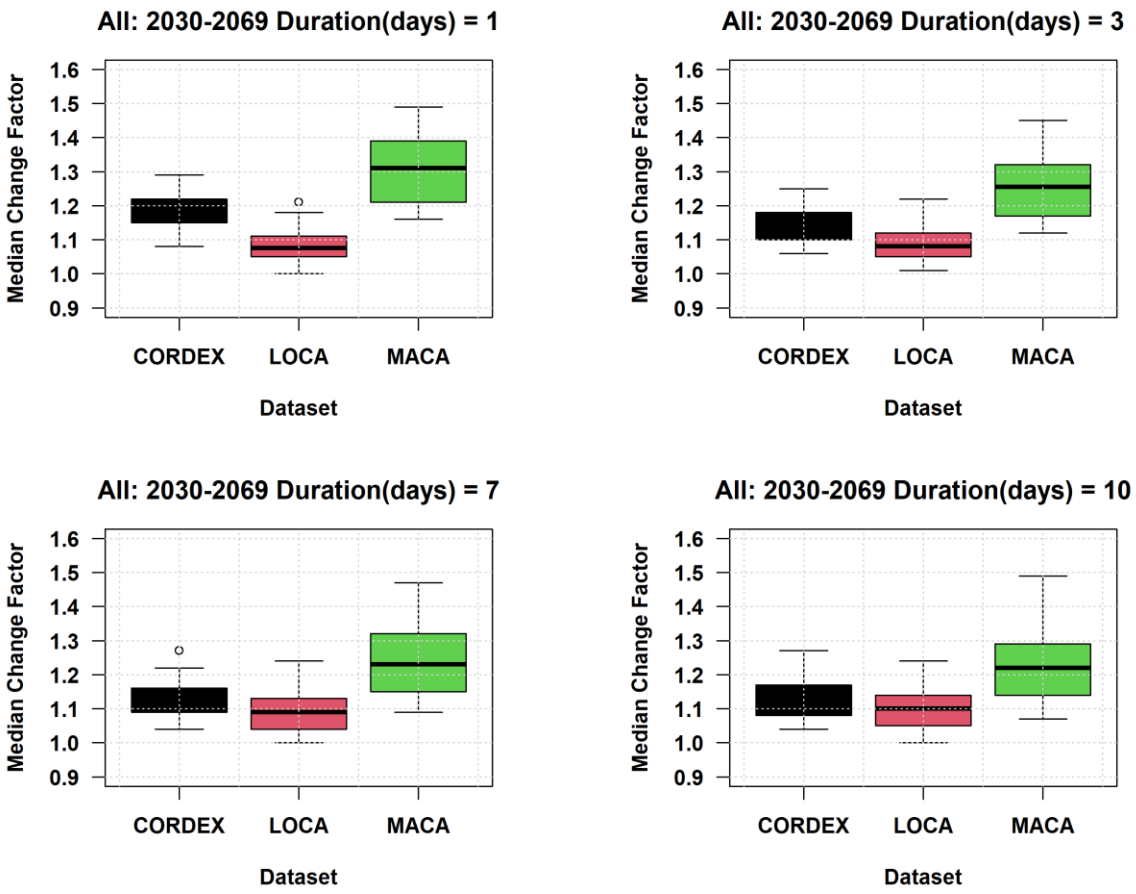

Figure 17. Box plots of Change Factors values for each climate dataset, all Florida Climate Divisions, and durations 1, 3, 7, and 10 days. The data used in this plot are for 2030 to 2069 relative to 1966 to 2005.

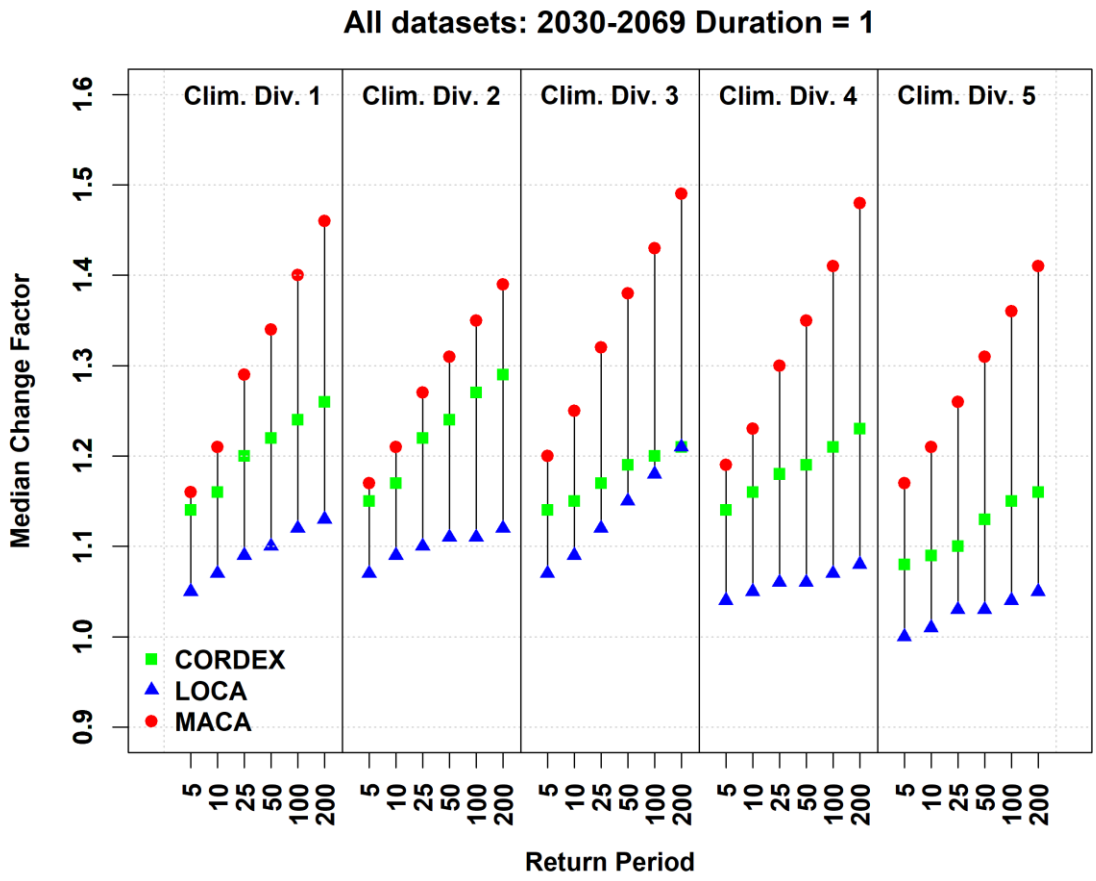

Figure 18. Ranges of median change factors as a function of return period in years for each climate dataset (CORDEX, LOCA, and MACA) and each Climate Division. The data shown are for NEAR period (2030-2069) and 1-day duration.

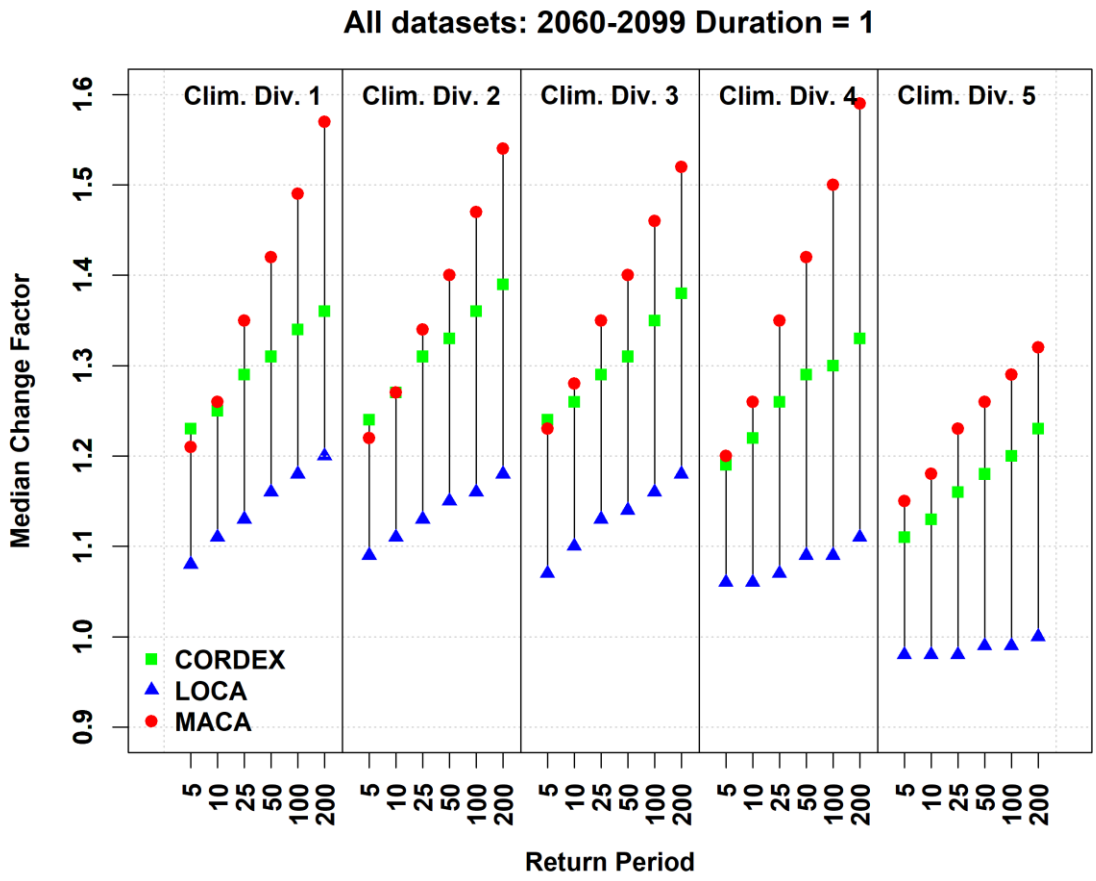

Figure 19. Ranges of median change factors as a function of return period in years for each climate dataset (CORDEX, LOCA, and MACA) and each Climate Division. The data shown are for the FAR period (2069-2099) and 1-day duration

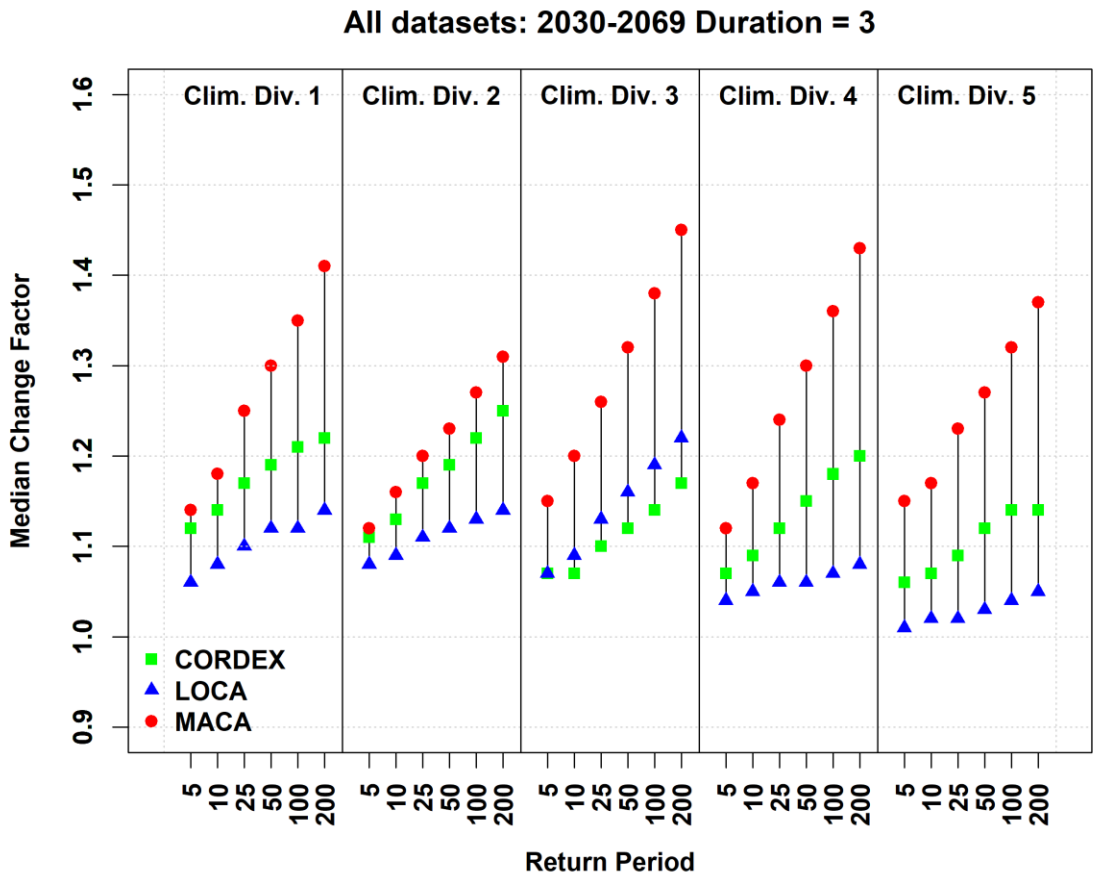

Figure 20. Ranges of median change factors as a function of return period in years for each climate dataset (CORDEX, LOCA, and MACA) and each Climate Division. The data shown are for NEAR period (2030-2069) and 3-day duration.

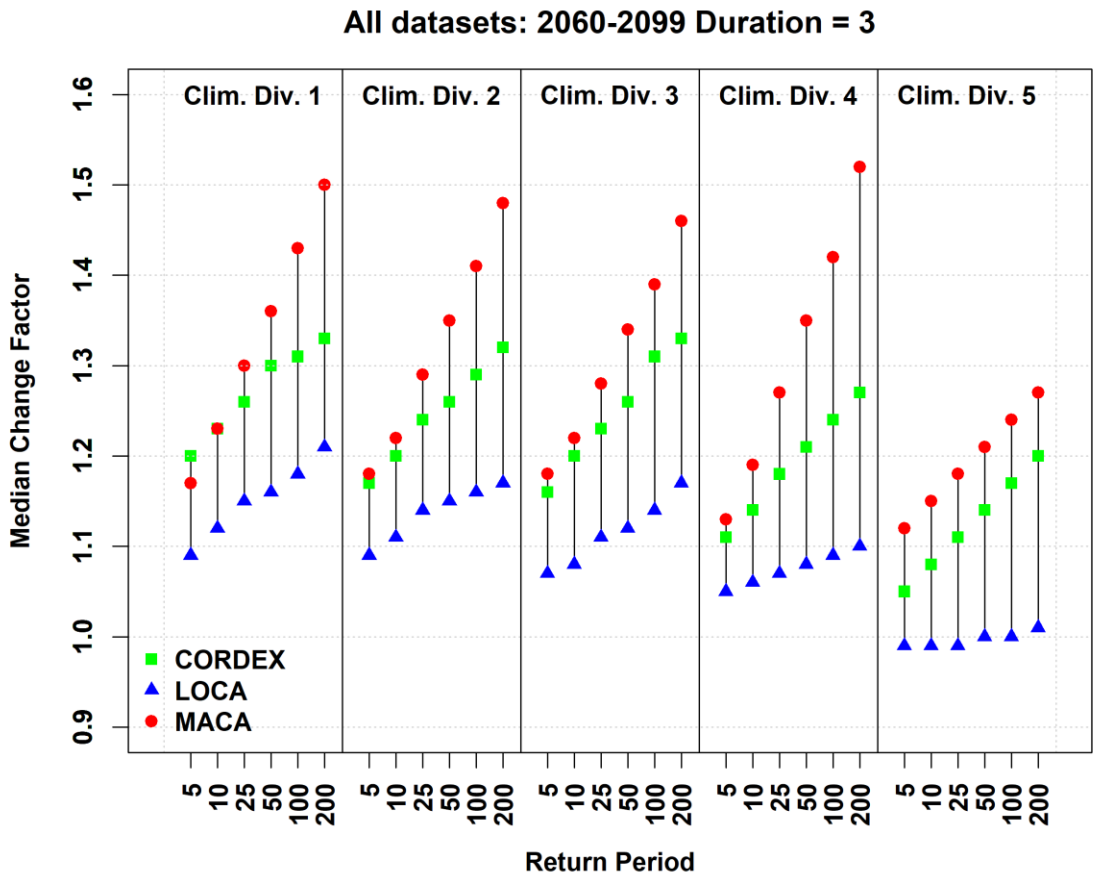

Figure 21. Ranges of median change factors as a function of return period in years for each climate dataset (CORDEX, LOCA, and MACA) and each Climate Division. The data shown are for the FAR period (2060-2099) and 3-day duration

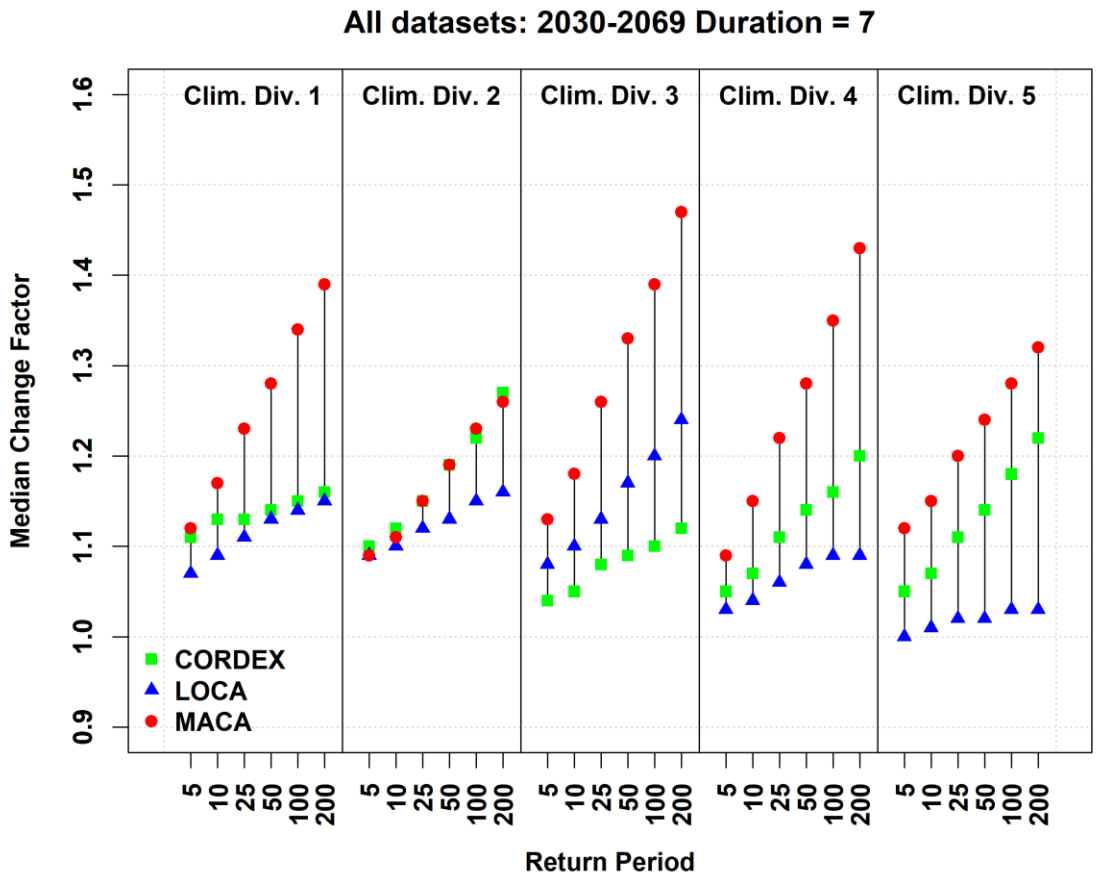

Figure 22. Ranges of median change factors as a function of return period in years for each climate dataset (CORDEX, LOCA, and MACA) and each Climate Division. The data shown are for the NEAR period (2030-2069) and 7-day duration

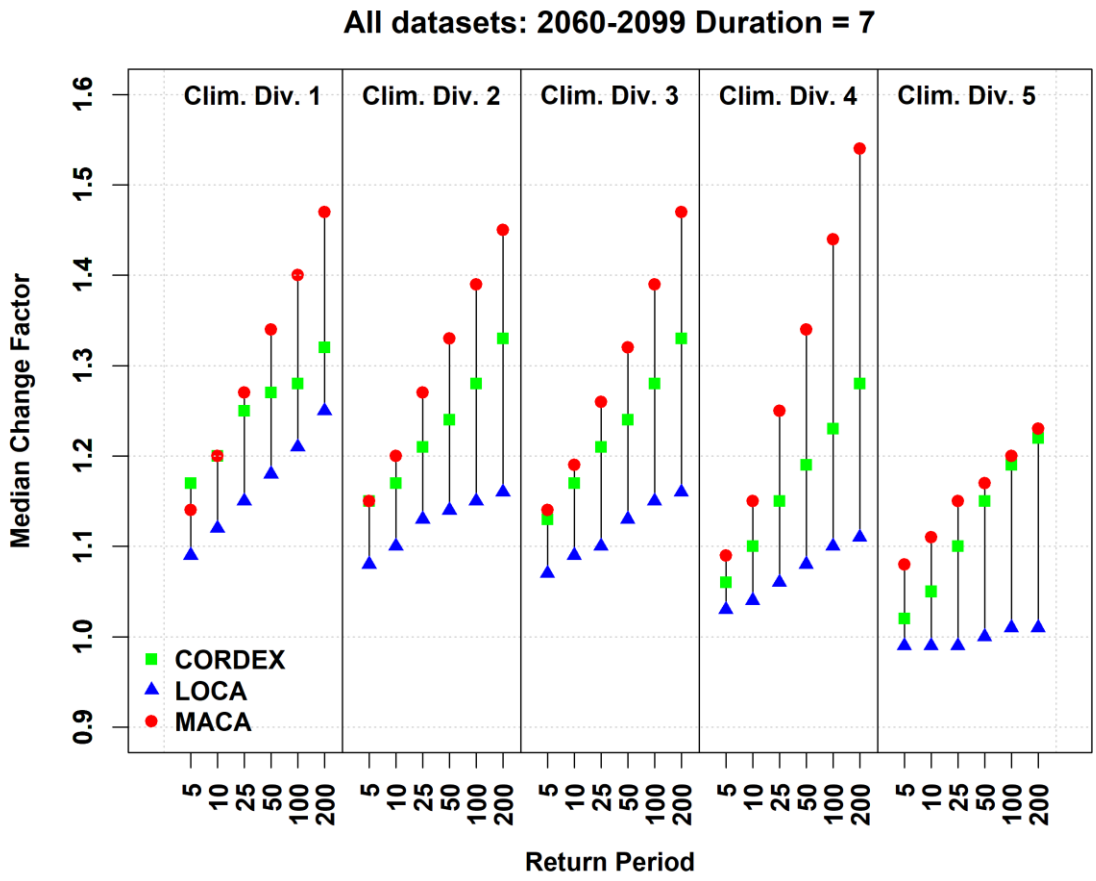

Figure 23. Ranges of median change factors as a function of return period in years for each climate dataset (CORDEX, LOCA, and MACA) and each Climate Division. The data shown are for the FAR period (2060-2099) and 7-day duration

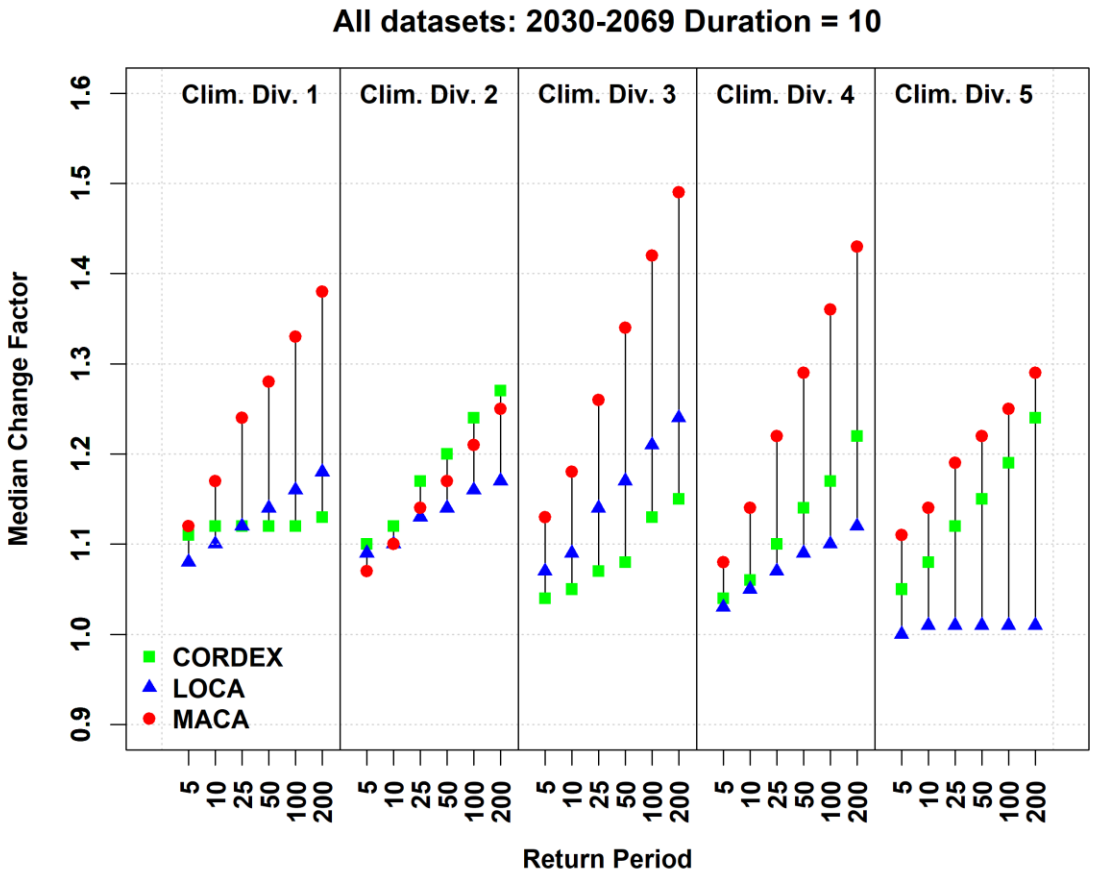

Figure 24. Ranges of median change factors as a function of return period in years for each climate dataset (CORDEX, LOCA, and MACA) and each Climate Division. The data shown are for the NEAR period (2030-2069) and 10-day duration

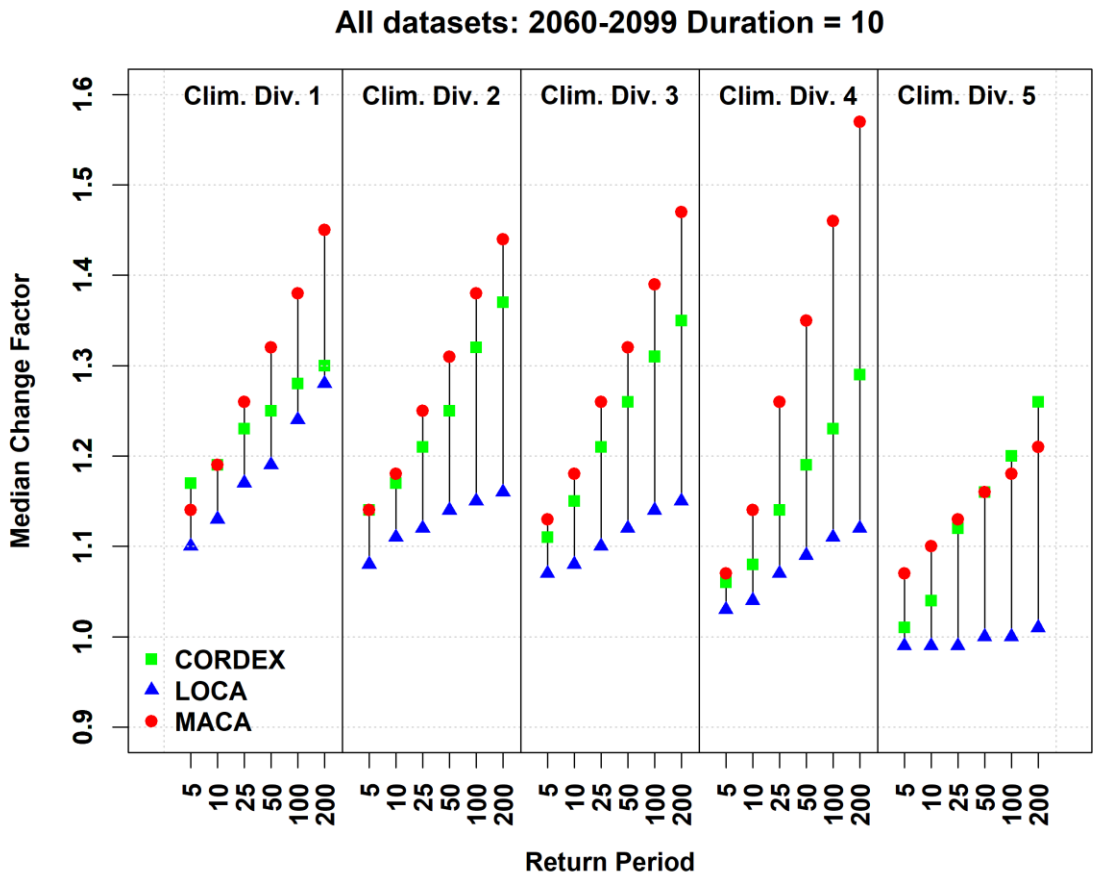

Figure 25. Ranges of median change factors as a function of return period in years for each climate dataset (CORDEX, LOCA, and MACA) and each Climate Division. The data shown are for the FAR period (2060-2099) and 10-day duration

Task 2.5. Adjustment of Atlas 14 DDF values using Change Factors (CFs)

In this section, general guidance is provided on how to use the CFs listed in Appendix I for a given Atlas 14 station to project its DDF values for future conditions. Because, the median values of the CFs have been regionalized according to the CD, application of the CFs for a specific Atlas 14 station requires the identification of its corresponding CD. Tables of Atlas 14 stations sorted by CD are provided in Appendix II. For a given duration (1, 3, 7, or 10 days), tables in Appendix I can be used to determine the CF for each Return Period. Because there are three climate datasets to choose from (i.e., CORDEX, LOCA, and MACA), there will be three sets of CF for that CD. One obvious challenge is to select an appropriate set of CFs from these three sets of CFs. Because of the particular model selection approach that was used, one cannot discard any of the sets and all must be considered in the application. From the results, we do know that the median CFs range in general from 1 to about 1.6, and among them LOCA has the lowest value in most cases while MACA is associated with the highest CF.

We recommend that the user consider CF values corresponding to all three climate datasets and select an appropriate value based on the particular setting of the project under consideration. That setting may be characterized by design life, objectives of the stormwater project, size of the infrastructure, and the design return period. Using a higher CF value will lead to a larger anticipated magnitude of extreme rainfall when adjusting the Atlas 14 DDF curves and this may lead to a larger design but a lower risk of failure. Choosing a lower CF will have the opposite effect of a smaller design and a larger risk of failure. If the user prefers a more conservative design (hence a larger CF), the uncertainty range as represented by the 17th to 83rd percentiles must also be considered.

Task 2.6. Evaluation of the Florida Building Code (FBC)-related requirements

The FIU SLSC team has expanded the previous FBC-funded Miami-Dade County project to update extreme rainfall projections state-wide and has evaluated the potential implications of changing rainfall on the Florida Building Code for all communities across the State of Florida. The changes to the rain loads and their implications for Rain Loads as applied to Figure 1611.1 and Figure 1106.1 of the FBC, Plumbing were evaluated. Information on Rain Loads in the current version of the Florida Building Code is quite dated and needs to be updated and projected under future conditions. This update is necessary for two reasons: (a) extensive rainfall data have been collected throughout the State since the early 1970s; and (b) recent research on implications of climate change suggest that a new paradigm based on the concept of nonstationarity is needed for planning and design, which means that historical observations cannot be used to predict future rainfall.

Objective 2.6.1:
Evaluate the current Florida Building Code requirements to recommend what additional steps will be necessary to incorporate the results of the study into relevant sections of the Codes. Specifically, the changes to the rain loads and their implications for Rain Loads as applied to Figure 1611.1 and Figure 1106.1 of the FBC, Plumbing shall be recommended.

The context for evaluation: Rain loads contribute to the design specifications of a structure through weight of water and drainage of water from the structure's roof. Rain loads applied to building and plumbing are interconnected, as the size of the drainage system determines how fast water can drain from a roof, reducing the potential for structural failures. But also, structural considerations for rain loads extend to the combination of loads that must be computed by adding rain load to other loads of the structure.

FBC – Plumbing
Chapter 11, Storm Drainage
Figure 1106.1

Current code: Roofs shall be designed for the maximum possible depth of water that will pond. The published roof drain flow rate, based on the head of water above the roof drain,

shall be used to size the storm drainage system in accordance with Section 1106. The maximum possible depth of water includes the height of the water required above the inlet of the secondary roof drainage to achieve the required flow rate of the secondary drainage to accommodate the design rainfall rate, and assuming all primary roof drainage is blocked (FBC 2017). Fundamentally, the code implies use of a flow rate for sizing the storm drainage piping that is based on the maximum anticipated ponding at the roof drain (Section 1105.2, FBC 2017).

The size of the vertical conductors and leaders, building *storm drains*, building storm sewers and any horizontal branches of such drains or sewers shall be based on the 100-year hourly rainfall rate indicated in Figure 1106.1 or on other rainfall rates determined from *approved* local weather data (FBC 2017).

The 100-yr, hourly rainfall (i) and the roof area serviced by a single drainage system is used to determine flow rate for a single drainage system by Q = 0.0104Ai (ASCE 7-05). Static head (d_s) is the depth of water on the undeflected roof up the inlet of the secondary drainage system when the primary drainage is blocked, provided Q and Table 1106.2. Hydraulic head (d_h) is the additional depth of water on the undeflected roof above the inlet of the secondary drainage system at its design flow, and can be determined from the minimum required flow for the secondary drain, referencing ASCE/SEI 7-16 (in Patterson and Mehta (2018)). Computing the total depth of water on the roof when the primary system is blocked ($d_s + d_h$) * 5.2 gives the design rain load in psf.

Results of data analyses: The updated 100-year, 1- to 10-day duration rainfall rates determined for the five climate divisions (Figure 11) across the State of Florida were both higher and more spatially-variable than indicated in Figure 1106.1/1611.1, and depended on the climate dataset used. For instance, median CFs for 100-yr, 1-day duration rainfall varied from ~ 5% in CD 5 using the LOCA dataset to ~40% in CD 3 using the MACA dataset for the 2030-2069 time horizon (Figure 18). Assuming CFs can be similarly applied to hourly events as to 1-day duration events, this time horizon is well within the design life of buildings and construction regulated by the FBC. See also Appendices I and II.

Additional literature research: In a paper presented to the 33rd RCI International Convention and Trade Show in 2018, Patterson and Mehta noted some limitations of using 100-year, hourly rainfall. One, that 100-year, hourly rainfall is often not a constant rainfall rate over the 60-minute period. Two, the secondary or overflow drainage system is intended as a safety provision against failures (e.g., roof collapse, pipe-fitting separation, pulled hanger from pre-stressed concrete floor/ceiling, flood of upper-balcony decks, fitting component failure, flooding in upper building floors due to pipe failure, Ballanco 2012) in the case that the primary drainage system is compromised. Patterson and Mehta (2018) noted that past codes had used higher rainfall rates for the secondary drainage system. In 1991, the National Standard Plumbing Code (SPC) of the Plumbing- Heating-Cooling Contractors National Association required overflow drainage to be designed to 100-year, 15-minute rainfall rate. The first International Plumbing Code (IPC) published in 1995 divided in half the drainage capacity of the secondary system, effectively doubling the

design rainfall rate for overflow drainage. Among Ballanco's (2012) recommendations for code changes were new sizing requirements to be based on two rainfall rates: 100-year, hourly rainfall and 10-year, 5-minute rainfall rates, and applying the rate that accommodates the greatest amount of expected ponding (p.73). The SPC continues to use 100-year, 15-minute rainfall rate for the secondary drainage system. In fact, ASCE 7-16 apparently also recommends using 100-year, 15-minute rainfall rates to accommodate those heavy, short duration storms.

FBC - Building
Chapter 16, Structural Design
Figure 1611.1

Current Code: Similarly, design rain loads (R) are determined for each portion of a roof to sustain the load of rainwater that will accumulate on it if the primary drainage system for that portion is blocked (static head = d_s) plus the uniform load caused by water that rises above the inlet of the secondary drainage system (hydraulic head = d_h) at its design flow ($R = 5.2 (d_s + d_h)$). The design rainfall is based on the 100-year hourly rainfall rate indicated in Figure 1611.1 or on other rainfall rates determined from *approved* local weather data (FBC 2017).

Results of data analyses: As described above, the updated 100-year, 1- to 10-day duration rainfall rate determined for the five climate divisions (Figure 11) across the State of Florida were both higher and more spatially-variable than indicated in Figure 1106.1/1611.1, and depended on the climate dataset used. For instance, median CFs for 100-year, 1-day duration rainfall varied from ~ 5% in CD 5 using the LOCA dataset to ~40% in CD 3 using the MACA dataset for the 2030-2069 time horizon (Figure 18). Assuming CFs can be similarly applied to hourly events as to 1-day duration events, this time horizon is well within the design life of buildings and construction regulated by the FBC. See also Appendices I and II.

Key Recommendations: Three recommendations are proposed related to Rain Loads for Storm Drainage in the Plumbing volume and Structural Design in the Building volume of the FBC.

1. Currently, the FBC allows Figure 1106.1/1611.1 to be used to determine 100-year, hourly rainfall to determine flows and rain loads for structural and plumbing design. Updated data and guidance in relevant international and national codes suggest that the 100-year, hourly rainfall maps for the State be based on updated data. Further, 100-year, 15-minute rainfall rate data should also be reviewed, and updated as needed, to facilitate consideration of new code language that the higher of the 100-year, hourly rainfall rate or 100-year, 15-minute rainfall rate be applied for the secondary drainage system.

2. Large roof areas may result in the exceedance of the flow capacities provided in Tables 1106.2 and 1106.3. It is recommended to recompute the flow capacities provided in Tables 1106.2 and 1106.3 with large roof areas using the new rain load data.
3. Similar to the Southeast Florida Regional Climate Change Compact (2019) guidance on use of projected sea level rise based on expected design life or criticality of buildings, consideration of projected, future rainfall evaluated on division-by-division basis and applying the CF for a 100-year rainfall event is recommended to ensure expected building performance. At a minimum, the current 100-yr rainfall should be updated using the CFs provided in Appendix I prior to evaluating rain loads.

References

Abatzoglou J. T. " Development of gridded surface meteorological data for ecological applications and modeling " International Journal of Climatology. (2011), https://dx.doi.org/10.1002/joc.3413

Abatzoglou J.T. & Brown T.J. (2012). International Journal of Climatology. "A comparison of statistical downscaling methods suited for wildfire applications, https://dx.doi.org/10.1002/joc.2312

Ariff, N., Jemain, A., Ibrahim, K., and Wan Zin, W. (2012). IDF relationships using bivariate copula for storm events in Peninsular Malaysia, J. Hydrol., 470–471, 158–171.

Awadallah, A. (2011). Developing Intensity-Duration-Frequency Curves in Scarce Data Region: An Approach using Regional Analysis and Satellite Data, Engineering, 03, 215–226.

Ballanco, J. (2012). Storm drainage system research project: Flow rate through roof drains. American Society of Plumbing Engineers Research Foundation, Inc. 121p. http://www.floridabuilding.org/fbc/commission/FBC_0816/TAC_Chair/ASPERFStormDrainageReportForDistribution.pdf

Bara, M., Kohnová, S., Gaál, L., Szolgay, J., and Hlavcoá, K. (2009). Estimation of IDF curves of extreme rainfall by simple scaling in Slovakia, Contributions to Geophysics and Geodesy, 39, 187–206.

Bedient, P. B., Huber, W. C., Vieux, B. E., & Mallidu, M. (2013). Hydrology and floodplain analysis. Harlow: Pearson Education.

Ben-Zvi, A. (2009). Rainfall intensity-duration-frequency relationships derived from large partial duration series, J. Hydrol., 367, 104–114.

Borga, M., Vezzani, C., and Fontana, G. D. (2005). Regional rainfall depth-duration-frequency equations for an Alpine region, Natural Hazards, 36, 221–235.

Buishand T. A. (1991). Extreme rainfall estimation by combining data from several sites. Hydrol Sci J 36(4):345-365.

Buishand T. A., Hanel M. (2010). On the value of hourly precipitation extremes in regional climate model simulations. Journal of Hydrology 393:265-273.

Coles, S. (2001). An Introduction to Statistical Modeling of Extreme Values. Springer-Verlag, 219 p. https://dx.doi.org/10.1007/978-1-4471-3675-0

Coulibaly, P. and Dibike, Y. B. (2004). Downscaling of Global Climate Model Outputs for Flood Frequency Analysis in the Saguenay River System. Final Project Report prepared for the Canadian Climate Change Action Fund, Environment Canada, Hamilton, Ontario, Canada.

Daly, C., Halbleib, M., Smith, J. I., Gibson, W. P., Doggett, M. K., Taylor, G. H., et al. (2008). Physiographically sensitive mapping of climatological temperature and precipitation across the conterminous United States. *International Journal of Climatology*, *28*(15), 2031–2064. https://doi.org/10.1002/joc.1688

Davison, A.C., and Smith, R.L. (1990). Models for exceedances over high thresholds: Journal of the Royal Statistical Society. Series B v. 52, no. 3. p. 393-442. https://doi.org/10.1111/j.2517-6161.1990.tb01796.x

Durrans S. R., Brown P. A. (2001). Estimation and internet-based dissemination of extreme rainfall information. Transp Res Rec 1743:41–48.

Fontanazza C. M., Freni G., Loggia G. L., Notaro V. (2011). Uncertainty evaluation of design
rainfall for urban flood risk analysis. Water Sci Technol 63(11):2641-2650.

Gerold, L. and Watkins, D. (2005). Short Duration Rainfall Frequency Analysis in Michigan Using Scale-Invariance Assumptions, J. Hydrol. Eng., 10, 450–457.

Irizarry M., Obeysekera J., Dessalegne T. (2016). Determination of Future Intensity-Duration-Frequency Curves for Level of Service Planning Projects. Task 2 - Deliverable 2.1 to SFWMD - Conduct an extreme rainfall analysis in climate model outputs to determine temporal changes in IDF curves.

Irizarry, M. M., Dessalegne, T., & Obeysekera, J. (2017). Assessment of Methods for Future Depth-Duration-Frequency Curve Development under Climate Change for the State of Florida, World Environmental and Water Resources Congress. 2017. 188–202. https://doi.org/10.1061/9780784480601.018

Jenkinson, A.F. (1955). The frequency distribution of the annual maximum (or minimum) values of meteorological elements. Q J R Meteorol Soc 81:158−171.

Kotamarthi, R., L. Mearns, K. Hayhoe, C.L. Castro, and D. Wuebble. (2016). Use of Climate Information for Decision-Making and Impacts Research: State of Our Understanding. Prepared for the Department of Defense, Strategic Environmental Research and Development Program. 55pp.

Livneh B, E.A. Rosenberg, C. Lin, V. Mishra, K. Andreadis, E.P. Maurer, and D.P. Lettenmaier. " A Long-Term Hydrologically Based Dataset of Land Surface Fluxes and States for the Conterminous United States: Update and Extensions. J. Climate, 26, 9384–9392.(2013). https://doi.org/10.1175/JCLI-D-12-00508.1

Livneh, B., T. J. Bohn, D. W. Pierce, F. Munoz-Arriola, B. Nijssen, R. Vose, D. R. Cayan, and L. Brekke, 2015: A spatially comprehensive, hydrometeorological data set for Mexico, the U.S., and Southern Canada 1950-2013. Scientific Data, v. 2, article 150042 (2015). https://dx.doi.org/10.1038/sdata.2015.42.

Madsen, H., Pearson, C.P., Rosbjerg, D. (1997). Comparison of annual maxima series and partial duration series methods for modeling extreme hydrologic events. 1. At-site modeling: Water Resources Research, v. 33, no. 4, p. 747-757. https://doi.org/10.1029/96WR03848

Milly P. C. D., J. Betancourt, M. Falkenmark, Robert M Hirsch, Zbigniew W Kundzewicz, Dennis P Lettenmaier, Ronald J Stouffer (2008) Stationarity Is Dead: Whither Water Management? Science. 319 (5863), 573-574. [DOI:10.1126/science.1151915]

Nhat, L., Tachikawa, Y., Sayama, T., and Takara, K. (2007). A simple scaling characteristics of rainfall in time and space to derive intensity duration frequency relationships, Annu. J. Hydraul. Eng., 51, 73–78.

NOAA (National Oceanic and Atmospheric Administration). (2013). *Precipitation-Frequency Atlas of the United States, Southeastern States. NOAA Atlas 14 Volume 9 Version 2.0*, S. Perica, D. Martin, S. Pavlovic, I. Roy, M. St. Laurent, C. Trypaluk, D. Unruh, M. Yekta, G. Bonnin, NOAA, National Weather Service, Silver Spring, MD.

Norlida M. D., Abustan I., Abdullah R., Yahaya A. S., Sazali O., Mohd Nor M. D., Lariyah M.S.: Intensity-Duration-Frequency Estimation using Generalized Pareto Distribution for Urban Area in a Tropical Region. In: Proceedings of 12th International Conference on Urban Drainage, Porto Alegre/Brazil, 11-16 September 2011.

Obeysekera, J, M. Sukop, T. Troxler, M. Irizarry, M. Rogers. (2019). Potential Implications of Sea-Level Rise and Changing Rainfall for Communities in Florida using Miami-Dade County as a Case Study, report submitted to the Florida Department of Business and Professional Regulation by the FIU Sea Level Solutions Center. fbc_fiu_finalreport_22aug2019.pdf

Overeem A., Buishand T. A., Holleman I. (2008). Rainfall depth-duration-frequency curves
and their uncertainties. J Hydrol 348:124-134.

Overeem, A., Buishand, T. A., and Holleman, I. (2009). Extreme rainfall analysis and estimation of depth-duration-frequency curves using weather radar, Water Resour. Res., 45, W10424, doi:10.1029/2009WR007869.

Palmer, R. N., Clancy, E., VanRheenen, N. T., and Wiley, M. W. (2004). The Impacts of Climate Change on The Tualatin River Basin Water Supply: An Investigation into Projected Hydrologic and Management Impacts. Department of Civil and Environmental Engineering, University of Washington, Seattle, Washingtom.

Palychuk, B., and Guo, P., (2008) Threshold analysis of rainstorm depth and duration statistics at Toronto, Canada. Journal of Hydrology. v. 348. no 3–4. p. 535-545, ISSN 0022-1694. https://doi.org/10.1016/j.jhydrol.2007.10.023

Panthou, G., Vischel, T., Lebel, T., Quantin, G., and Molinié, G. (2014). Characterising the space–time structure of rainfall in the Sahel with a view to estimating IDAF curves, Hydrol. Earth Syst. Sci., 18, 5093–5107, https://doi.org/10.5194/hess-18-5093-2014

Patterson, S., and M. Mehta. (2018). Roof drainage design, roof collapses and the codes. Proceedings of the 33rd RCI International Convention and Trade Show, March 22-27, 2018, P.121-131.

Pickands, J. (1975). Statistical inference using extreme order statistics: Annals of Statistics, v. 3. p. 1190131. https://dx.doi.org/10.1214/aos/1176343003

Pierce D. W., Cayan D. R., Thrasher B. L. (2014). Statistical downscaling using Localized Constructed Analogs (LOCA). Journal of Hydrometeorology 15:2558–2585. https://doi.org/10.1175/JHM-D-14-0082.1

Serinaldi, F., and Kilsby, C.G. (2014) Rainfall extremes. Toward reconciliation after the battle of distributions: Water Resources Research. v. 50. p. 336-352. https://doi.org/10.1002/2013WR014211

Schwalm, C. R., Glendon, S., & Duffy, P. B. (2020). RCP8.5 tracks cumulative CO2 emissions. Proceedings of the National Academy of Sciences, 117(33), 19656–19657. https://doi.org/10.1073/pnas.2007117117

Sillmann, J., V. V. Kharin, X. Zhang, F. W. Zwiers, and D. Bronaugh (2013), Climate extremes indices in the CMIP5 multimodel ensemble: Part 1. Model evaluation in the present climate, J. Geophys. Res. Atmos., 118, 1716–1733, doi:10.1002/jgrd.50203.

Simonovic, Slobodan P. and Peck, Angela, "Updated Rainfall Intensity Duration Frequency Curves for the City of London under the Changing Climate" (2009). Water Resources Research Report. 29.

Southam, C. F., Mills, B. N., Moulton, R. J., and Brown, D. W. (1999). “The potential impact of climate change in Ontario's Grand River Basin: Water supply and demand issues.” Canadian Water Resources Journal, 24(4), 307-330.

Southeast Florida Regional Climate Change Compact. (2019). Unified Sea Level Rise Projection Southeast Florida. South Florida Regional Climate Change Compact's Sea Level Rise Ad Hoc Work Group. 35p.

Sugahara Shigetoshi, Rocha RP, Silveira R (2009) Non-stationary frequency analysis of extreme daily rainfall in Sao Paulo , Brazil, 29, 1339–1349. doi:10.1002/joc.

Srivastav R. and Slobodan P. Simonovic (2015). Computerized Tool for the Development of Intensity-Duration-Frequency Curves under a Changing Climate. Water Resources Research Report no. 089, Facility for Intelligent Decision Support, Department of Civil and Environmental Engineering, London, Ontario, Canada, 52 pages. ISBN: (print) 978-0-7714-3087-9; (online) 978-0-7714-3088-6.

Srivastava, A., R. Grotjahn, and P. A. Ullrich, 2020: Evaluation of historical cmip6 model simulations of extreme precipitation over contiguous us regions. Wea. Climate Extremes, 29, 100268, https://doi.org/ 10.1016/j.wace.2020.100268.

Taylor, K.E., R.J. Stouffer, G.A. Meehl: An Overview of CMIP5 and the experiment design. MS-D-11-00094.1. (2012).

Xu, YP., Tung, YK. Constrained scaling approach for design rainfall estimation. *Stoch Environ Res Risk Assess* **23,** 697–705 (2009). https://doi.org/10.1007/s00477-008-0250-6

van Vuuren, D. P., Edmonds, J., Kainuma, M., Riahi, K., Thomson, A., Hibbard, K., Hurtt, G. C., Kram, T., Krey, V., Lamarque, J-. F., Masui, T., Meinshausen, M., Nakicenovic, N., Smith, S. J., & Rose, S. K. (2011). The representative concentration pathways: an overview. *Climatic Change* 109, 5-31. https://doi.org/10.1007/s10584-011-0148-z

Walton, D.B., F. Sun, A. Hall, and S. Capps, 2015, "A Hybrid Dynamical-Statistical Downscaling Technique, Part I: Development and Validation of the Technique," Journal of Climate 28(12):4597–4617

Data Citations

MACAv2-LIVNEH
Climate forcings in the MACAv2-LIVNEH were drawn from a statistical downscaling of global climate model (GCM) data from the Coupled Model Intercomparison Project 5 (CMIP5, Taylor et al. 2010) utilizing a modification of the Multivariate Adaptive Constructed Analogs (MACA, Abatzoglou and Brown, 2012) method with the Livneh (Livneh et.al.,2013) observational dataset as training data.

MACAv2-METDATA

Climate forcings in the MACAv2-METDATA were drawn from a statistical downscaling of global climate model (GCM) data from the Coupled Model Intercomparison Project 5 (CMIP5, Taylor et al. 2010) utilizing a modification of the Multivariate Adaptive Constructed Analogs (MACA, Abatzoglou and Brown, 2012) method with the METDATA (Abatzoglou, 2011) observational dataset as training data.

APPENDIX I. Tables of Change Factors for all Climate Divisions

Table I-1. Change Factor Values for Climate Division 1.

Dataset	Period	CD	RP	1D17	1D50	1D83	3D17	3D50	3D83	7D17	7D50	7D83	10D17	10D50	10D83
CORDEX	NEAR	1	5	1.05	1.14	1.26	1.05	1.12	1.22	1.04	1.11	1.22	1.04	1.11	1.22
LOCA	NEAR	1	5	0.94	1.05	1.16	0.98	1.06	1.16	0.99	1.07	1.18	1	1.08	1.2
MACA	NEAR	1	5	1.06	1.16	1.31	1.05	1.14	1.25	1.03	1.12	1.24	1.02	1.12	1.25
CORDEX	NEAR	1	10	1.04	1.16	1.3	1.05	1.14	1.26	1.04	1.13	1.25	1.02	1.12	1.25
LOCA	NEAR	1	10	0.94	1.07	1.2	0.97	1.08	1.19	0.98	1.09	1.21	0.98	1.1	1.24
MACA	NEAR	1	10	1.07	1.21	1.41	1.06	1.18	1.34	1.03	1.17	1.34	1.01	1.17	1.36
CORDEX	NEAR	1	25	1.03	1.2	1.38	1.05	1.17	1.33	1.01	1.13	1.31	0.99	1.12	1.32
LOCA	NEAR	1	25	0.92	1.09	1.26	0.95	1.1	1.25	0.95	1.11	1.28	0.95	1.12	1.32
MACA	NEAR	1	25	1.08	1.29	1.58	1.07	1.25	1.51	1.02	1.23	1.52	1	1.24	1.55
CORDEX	NEAR	1	50	1.02	1.22	1.45	1.04	1.19	1.38	0.99	1.14	1.37	0.93	1.12	1.37
LOCA	NEAR	1	50	0.89	1.1	1.33	0.93	1.12	1.31	0.93	1.13	1.35	0.93	1.14	1.41
MACA	NEAR	1	50	1.08	1.34	1.73	1.07	1.3	1.66	1.01	1.28	1.68	0.97	1.28	1.72
CORDEX	NEAR	1	100	1.01	1.24	1.56	1.03	1.21	1.47	0.97	1.15	1.44	0.91	1.12	1.43
LOCA	NEAR	1	100	0.86	1.12	1.41	0.9	1.12	1.37	0.9	1.14	1.44	0.9	1.16	1.51
MACA	NEAR	1	100	1.08	1.4	1.92	1.07	1.35	1.85	1	1.34	1.89	0.95	1.33	1.93
CORDEX	NEAR	1	200	0.99	1.26	1.69	1.02	1.22	1.59	0.94	1.16	1.5	0.87	1.13	1.48
LOCA	NEAR	1	200	0.84	1.13	1.5	0.87	1.14	1.47	0.87	1.15	1.55	0.86	1.18	1.63
MACA	NEAR	1	200	1.08	1.46	2.14	1.07	1.41	2.08	0.98	1.39	2.12	0.92	1.38	2.2
CORDEX	FAR	1	5	1.09	1.23	1.36	1.09	1.2	1.31	1.09	1.17	1.29	1.08	1.17	1.29
LOCA	FAR	1	5	0.97	1.08	1.23	0.99	1.09	1.21	1	1.09	1.2	1	1.1	1.21
MACA	FAR	1	5	1.07	1.21	1.36	1.07	1.17	1.3	1.05	1.14	1.28	1.03	1.14	1.28
CORDEX	FAR	1	10	1.08	1.25	1.42	1.1	1.23	1.35	1.09	1.2	1.33	1.08	1.19	1.34
LOCA	FAR	1	10	0.96	1.11	1.29	0.98	1.12	1.24	1	1.12	1.26	1	1.13	1.28
MACA	FAR	1	10	1.09	1.26	1.48	1.08	1.23	1.41	1.05	1.2	1.38	1.02	1.19	1.4

Dataset	Period	CD	RP	1D17	1D50	1D83	3D17	3D50	3D83	7D17	7D50	7D83	10D17	10D50	10D83
CORDEX	FAR	1	25	1.08	1.29	1.5	1.09	1.26	1.44	1.07	1.25	1.43	1.06	1.23	1.42
LOCA	FAR	1	25	0.94	1.13	1.38	0.97	1.15	1.34	1	1.15	1.37	1	1.17	1.39
MACA	FAR	1	25	1.09	1.35	1.68	1.07	1.3	1.58	1.03	1.27	1.57	1	1.26	1.6
CORDEX	FAR	1	50	1.08	1.31	1.6	1.09	1.3	1.51	1.07	1.27	1.49	1.04	1.25	1.51
LOCA	FAR	1	50	0.93	1.16	1.47	0.96	1.16	1.43	0.99	1.18	1.46	0.98	1.19	1.51
MACA	FAR	1	50	1.09	1.42	1.88	1.07	1.36	1.76	1.02	1.34	1.75	0.98	1.32	1.8
CORDEX	FAR	1	100	1.05	1.34	1.72	1.08	1.31	1.61	1.04	1.28	1.54	1.02	1.28	1.6
LOCA	FAR	1	100	0.9	1.18	1.57	0.94	1.18	1.55	0.97	1.21	1.58	0.95	1.24	1.65
MACA	FAR	1	100	1.09	1.49	2.12	1.07	1.43	1.98	1	1.4	1.97	0.96	1.38	2.02
CORDEX	FAR	1	200	1.03	1.36	1.85	1.08	1.33	1.73	1.02	1.32	1.64	1	1.3	1.72
LOCA	FAR	1	200	0.89	1.2	1.69	0.93	1.21	1.69	0.94	1.25	1.74	0.92	1.28	1.8
MACA	FAR	1	200	1.09	1.57	2.4	1.06	1.5	2.23	0.99	1.47	2.22	0.93	1.45	2.28

NEAR=Period 2030 – 2069; FAR = Period 2060-2099; CD = Climate Division; RP = Return Period; 1D17 is 1 Day 17th percentile. All others column headers use this format

Table I-2. Change Factor Values for Climate Division 2.

Dataset	Period	CD	RP	1D17	1D50	1D83	3D17	3D50	3D83	7D17	7D50	7D83	10D17	10D50	10D83
CORDEX	NEAR	2	5	1.05	1.15	1.28	1.03	1.11	1.22	1.02	1.1	1.2	1.02	1.1	1.2
LOCA	NEAR	2	5	0.98	1.07	1.19	1	1.08	1.17	1.01	1.09	1.19	1	1.09	1.2
MACA	NEAR	2	5	1.06	1.17	1.29	1.03	1.12	1.21	1	1.09	1.19	0.98	1.07	1.19
CORDEX	NEAR	2	10	1.04	1.17	1.33	1.03	1.13	1.26	1.01	1.12	1.25	1.01	1.12	1.27
LOCA	NEAR	2	10	0.96	1.09	1.22	1	1.09	1.21	1	1.1	1.22	0.99	1.1	1.23
MACA	NEAR	2	10	1.06	1.21	1.38	1.04	1.16	1.29	1	1.11	1.26	0.97	1.1	1.26
CORDEX	NEAR	2	25	1.03	1.22	1.42	1.02	1.17	1.35	1	1.15	1.36	0.99	1.17	1.38
LOCA	NEAR	2	25	0.94	1.1	1.3	0.97	1.11	1.27	0.98	1.12	1.29	0.97	1.13	1.31
MACA	NEAR	2	25	1.06	1.27	1.53	1.03	1.2	1.42	0.99	1.15	1.37	0.96	1.14	1.38
CORDEX	NEAR	2	50	1.02	1.24	1.51	1.01	1.19	1.44	0.99	1.19	1.47	0.97	1.2	1.51
LOCA	NEAR	2	50	0.91	1.11	1.36	0.94	1.12	1.33	0.96	1.13	1.37	0.94	1.14	1.4
MACA	NEAR	2	50	1.06	1.31	1.65	1.01	1.23	1.53	0.98	1.19	1.47	0.95	1.17	1.52
CORDEX	NEAR	2	100	1	1.27	1.61	0.99	1.22	1.54	0.97	1.22	1.59	0.94	1.24	1.63
LOCA	NEAR	2	100	0.88	1.11	1.43	0.92	1.13	1.41	0.92	1.15	1.45	0.92	1.16	1.5
MACA	NEAR	2	100	1.04	1.35	1.79	1	1.27	1.67	0.96	1.23	1.62	0.93	1.21	1.67
CORDEX	NEAR	2	200	0.98	1.29	1.72	0.98	1.25	1.64	0.95	1.27	1.69	0.92	1.27	1.79
LOCA	NEAR	2	200	0.85	1.12	1.52	0.89	1.14	1.48	0.89	1.16	1.56	0.88	1.17	1.61
MACA	NEAR	2	200	1.02	1.39	1.95	0.99	1.31	1.82	0.94	1.26	1.78	0.92	1.25	1.87
CORDEX	FAR	2	5	1.12	1.24	1.41	1.07	1.17	1.32	1.04	1.15	1.28	1.03	1.14	1.26
LOCA	FAR	2	5	0.99	1.09	1.23	1.01	1.09	1.19	1	1.08	1.18	1	1.08	1.18
MACA	FAR	2	5	1.1	1.22	1.32	1.07	1.18	1.26	1.03	1.15	1.24	1.03	1.14	1.24
CORDEX	FAR	2	10	1.11	1.27	1.47	1.08	1.2	1.39	1.06	1.17	1.36	1.04	1.17	1.34
LOCA	FAR	2	10	0.99	1.11	1.26	1.01	1.11	1.22	1.01	1.1	1.22	1.01	1.11	1.22
MACA	FAR	2	10	1.12	1.27	1.43	1.09	1.22	1.34	1.06	1.2	1.32	1.05	1.18	1.32
CORDEX	FAR	2	25	1.1	1.31	1.58	1.08	1.24	1.49	1.06	1.21	1.48	1.05	1.21	1.49
LOCA	FAR	2	25	0.98	1.13	1.33	1	1.14	1.27	1	1.13	1.28	0.98	1.12	1.29
MACA	FAR	2	25	1.13	1.34	1.59	1.1	1.29	1.48	1.08	1.27	1.47	1.07	1.25	1.5

Dataset	Period	CD	RP	1D17	1D50	1D83	3D17	3D50	3D83	7D17	7D50	7D83	10D17	10D50	10D83
CORDEX	FAR	2	50	1.08	1.33	1.71	1.07	1.26	1.6	1.06	1.24	1.6	1.03	1.25	1.61
LOCA	FAR	2	50	0.96	1.15	1.38	0.99	1.15	1.32	0.97	1.14	1.34	0.96	1.14	1.36
MACA	FAR	2	50	1.14	1.4	1.75	1.12	1.35	1.6	1.09	1.33	1.61	1.07	1.31	1.66
CORDEX	FAR	2	100	1.06	1.36	1.86	1.05	1.29	1.72	1.04	1.28	1.74	1.01	1.32	1.77
LOCA	FAR	2	100	0.93	1.16	1.45	0.96	1.16	1.4	0.95	1.15	1.43	0.93	1.15	1.45
MACA	FAR	2	100	1.14	1.47	1.92	1.13	1.41	1.75	1.1	1.39	1.77	1.07	1.38	1.86
CORDEX	FAR	2	200	1.05	1.39	2.04	1.04	1.32	1.88	1.02	1.33	1.9	0.99	1.37	1.93
LOCA	FAR	2	200	0.91	1.18	1.54	0.92	1.17	1.49	0.92	1.16	1.52	0.89	1.16	1.56
MACA	FAR	2	200	1.15	1.54	2.12	1.13	1.48	1.93	1.1	1.45	1.98	1.07	1.44	2.11

NEAR=Period 2030 – 2069; FAR = Period 2060-2099; CD = Climate Division; RP = Return Period; 1D17 is 1 Day 17th percentile. All others column headers use this format

Table I-3. Change Factor Values for Climate Division 3

Dataset	Period	CD	RP	1D17	1D50	1D83	3D17	3D50	3D83	7D17	7D50	7D83	10D17	10D50	10D83
CORDEX	NEAR	3	5	1.01	1.14	1.26	1	1.07	1.17	0.97	1.04	1.15	0.96	1.04	1.15
LOCA	NEAR	3	5	0.98	1.07	1.18	1	1.07	1.16	0.99	1.08	1.17	0.98	1.07	1.16
MACA	NEAR	3	5	1.1	1.2	1.32	1.08	1.15	1.25	1.05	1.13	1.23	1.03	1.13	1.24
CORDEX	NEAR	3	10	1.01	1.15	1.33	1	1.07	1.24	0.97	1.05	1.2	0.97	1.05	1.2
LOCA	NEAR	3	10	0.98	1.09	1.23	1	1.09	1.21	0.99	1.1	1.21	0.98	1.09	1.22
MACA	NEAR	3	10	1.1	1.25	1.43	1.08	1.2	1.33	1.06	1.18	1.33	1.05	1.18	1.35
CORDEX	NEAR	3	25	0.99	1.17	1.41	0.97	1.1	1.32	0.95	1.08	1.29	0.94	1.07	1.27
LOCA	NEAR	3	25	0.97	1.12	1.3	0.99	1.13	1.27	0.98	1.13	1.29	0.97	1.14	1.31
MACA	NEAR	3	25	1.1	1.32	1.6	1.09	1.26	1.48	1.06	1.26	1.51	1.05	1.26	1.55
CORDEX	NEAR	3	50	0.96	1.19	1.45	0.93	1.12	1.39	0.92	1.09	1.38	0.93	1.08	1.37
LOCA	NEAR	3	50	0.95	1.15	1.37	0.97	1.16	1.34	0.97	1.17	1.36	0.95	1.17	1.39
MACA	NEAR	3	50	1.09	1.38	1.75	1.08	1.32	1.63	1.05	1.33	1.67	1.04	1.34	1.74
CORDEX	NEAR	3	100	0.95	1.2	1.56	0.9	1.14	1.47	0.9	1.1	1.5	0.9	1.13	1.49
LOCA	NEAR	3	100	0.94	1.18	1.46	0.96	1.19	1.41	0.95	1.2	1.46	0.93	1.21	1.49
MACA	NEAR	3	100	1.09	1.43	1.91	1.07	1.38	1.81	1.05	1.39	1.87	1.04	1.42	1.96
CORDEX	NEAR	3	200	0.92	1.21	1.66	0.88	1.17	1.56	0.91	1.12	1.65	0.89	1.15	1.61
LOCA	NEAR	3	200	0.91	1.21	1.56	0.94	1.22	1.5	0.92	1.24	1.56	0.89	1.24	1.59
MACA	NEAR	3	200	1.08	1.49	2.1	1.06	1.45	2.01	1.03	1.47	2.11	1.03	1.49	2.21
CORDEX	FAR	3	5	1.11	1.24	1.4	1.07	1.16	1.29	1.04	1.13	1.25	1.02	1.11	1.24
LOCA	FAR	3	5	0.97	1.07	1.19	0.99	1.07	1.16	0.98	1.07	1.16	0.96	1.07	1.15
MACA	FAR	3	5	1.13	1.23	1.35	1.1	1.18	1.25	1.05	1.14	1.23	1.04	1.13	1.22
CORDEX	FAR	3	10	1.09	1.26	1.48	1.06	1.2	1.35	1.04	1.17	1.31	1.04	1.15	1.3
LOCA	FAR	3	10	0.96	1.1	1.25	1	1.08	1.2	0.97	1.09	1.2	0.97	1.08	1.22
MACA	FAR	3	10	1.15	1.28	1.44	1.12	1.22	1.34	1.08	1.19	1.32	1.07	1.18	1.31
CORDEX	FAR	3	25	1.07	1.29	1.58	1.04	1.23	1.47	1.02	1.21	1.41	1.01	1.21	1.45
LOCA	FAR	3	25	0.94	1.13	1.35	0.99	1.11	1.29	0.97	1.1	1.29	0.96	1.1	1.31

Dataset	Period	CD	RP	1D17	1D50	1D83	3D17	3D50	3D83	7D17	7D50	7D83	10D17	10D50	10D83
MACA	FAR	3	25	1.17	1.35	1.6	1.14	1.28	1.48	1.1	1.26	1.47	1.09	1.26	1.47
CORDEX	FAR	3	50	1.04	1.31	1.67	1.02	1.26	1.58	1.02	1.24	1.55	1.01	1.26	1.58
LOCA	FAR	3	50	0.93	1.14	1.43	0.98	1.12	1.37	0.96	1.13	1.38	0.94	1.12	1.39
MACA	FAR	3	50	1.18	1.4	1.74	1.16	1.34	1.61	1.11	1.32	1.61	1.1	1.32	1.64
CORDEX	FAR	3	100	1.01	1.35	1.75	1.01	1.31	1.67	1	1.28	1.75	1.01	1.31	1.77
LOCA	FAR	3	100	0.92	1.16	1.52	0.96	1.14	1.48	0.94	1.15	1.46	0.92	1.14	1.48
MACA	FAR	3	100	1.19	1.46	1.9	1.16	1.39	1.77	1.11	1.39	1.79	1.09	1.39	1.83
CORDEX	FAR	3	200	0.96	1.38	1.89	0.98	1.33	1.79	0.99	1.33	1.89	0.98	1.35	2
LOCA	FAR	3	200	0.9	1.18	1.64	0.94	1.17	1.58	0.92	1.16	1.57	0.9	1.15	1.58
MACA	FAR	3	200	1.19	1.52	2.11	1.16	1.46	1.96	1.12	1.47	2.01	1.09	1.47	2.06

NEAR=Period 2030 – 2069; FAR = Period 2060-2099; CD = Climate Division; RP = Return Period; 1D17 is 1 Day 17th percentile. All others column headers use this format

Table I-4. Change Factor Values for Climate Division 4

Dataset	Period	CD	RP	1D17	1D50	1D83	3D17	3D50	3D83	7D17	7D50	7D83	10D17	10D50	10D83
CORDEX	NEAR	4	5	1.01	1.14	1.26	0.99	1.07	1.19	0.96	1.05	1.15	0.95	1.04	1.14
LOCA	NEAR	4	5	0.95	1.04	1.15	0.96	1.04	1.13	0.95	1.03	1.13	0.95	1.03	1.13
MACA	NEAR	4	5	1.06	1.19	1.34	1.03	1.12	1.22	0.99	1.09	1.2	0.98	1.08	1.2
CORDEX	NEAR	4	10	1.01	1.16	1.32	0.99	1.09	1.23	0.95	1.07	1.2	0.94	1.06	1.19
LOCA	NEAR	4	10	0.93	1.05	1.19	0.94	1.05	1.17	0.94	1.04	1.17	0.94	1.05	1.17
MACA	NEAR	4	10	1.07	1.23	1.46	1.04	1.17	1.32	1.02	1.15	1.3	1.01	1.14	1.3
CORDEX	NEAR	4	25	1	1.18	1.43	0.96	1.12	1.32	0.94	1.11	1.3	0.94	1.1	1.31
LOCA	NEAR	4	25	0.9	1.06	1.24	0.92	1.06	1.23	0.91	1.06	1.24	0.91	1.07	1.26
MACA	NEAR	4	25	1.07	1.3	1.68	1.04	1.24	1.51	1.03	1.22	1.5	1.02	1.22	1.51
CORDEX	NEAR	4	50	0.99	1.19	1.53	0.95	1.15	1.41	0.94	1.14	1.41	0.92	1.14	1.42
LOCA	NEAR	4	50	0.87	1.06	1.3	0.9	1.06	1.28	0.89	1.08	1.31	0.88	1.09	1.34
MACA	NEAR	4	50	1.07	1.35	1.88	1.04	1.3	1.7	1.04	1.28	1.7	1.03	1.29	1.72
CORDEX	NEAR	4	100	0.98	1.21	1.63	0.94	1.18	1.51	0.92	1.16	1.53	0.91	1.17	1.54
LOCA	NEAR	4	100	0.84	1.07	1.36	0.87	1.07	1.34	0.87	1.09	1.39	0.86	1.1	1.42
MACA	NEAR	4	100	1.06	1.41	2.12	1.04	1.36	1.93	1.04	1.35	1.96	1.03	1.36	2
CORDEX	NEAR	4	200	0.95	1.23	1.76	0.91	1.2	1.64	0.89	1.2	1.67	0.88	1.22	1.69
LOCA	NEAR	4	200	0.81	1.08	1.44	0.85	1.08	1.41	0.84	1.09	1.47	0.84	1.12	1.52
MACA	NEAR	4	200	1.05	1.48	2.38	1.04	1.43	2.19	1.03	1.43	2.27	1.02	1.43	2.34
CORDEX	FAR	4	5	1.05	1.19	1.36	1.01	1.11	1.24	0.97	1.06	1.19	0.95	1.06	1.18
LOCA	FAR	4	5	0.94	1.06	1.17	0.95	1.05	1.14	0.94	1.03	1.13	0.93	1.03	1.12
MACA	FAR	4	5	1.08	1.2	1.34	1.02	1.13	1.23	0.97	1.09	1.22	0.96	1.07	1.21
CORDEX	FAR	4	10	1.04	1.22	1.41	1.01	1.14	1.3	0.96	1.1	1.26	0.95	1.08	1.24
LOCA	FAR	4	10	0.93	1.06	1.21	0.95	1.06	1.17	0.94	1.04	1.16	0.93	1.04	1.16
MACA	FAR	4	10	1.11	1.26	1.45	1.05	1.19	1.33	1.02	1.15	1.31	1.01	1.14	1.32
CORDEX	FAR	4	25	1.01	1.26	1.54	0.99	1.18	1.4	0.95	1.15	1.38	0.93	1.14	1.39
LOCA	FAR	4	25	0.91	1.07	1.26	0.93	1.07	1.22	0.93	1.06	1.22	0.9	1.07	1.23
MACA	FAR	4	25	1.14	1.35	1.64	1.09	1.27	1.51	1.07	1.25	1.52	1.05	1.26	1.55

Dataset	Period	CD	RP	1D17	1D50	1D83	3D17	3D50	3D83	7D17	7D50	7D83	10D17	10D50	10D83
CORDEX	FAR	4	50	1.01	1.29	1.64	0.97	1.21	1.49	0.93	1.19	1.52	0.91	1.19	1.52
LOCA	FAR	4	50	0.88	1.09	1.32	0.91	1.08	1.27	0.9	1.08	1.29	0.88	1.09	1.31
MACA	FAR	4	50	1.16	1.42	1.81	1.12	1.35	1.67	1.1	1.34	1.71	1.08	1.35	1.79
CORDEX	FAR	4	100	0.99	1.3	1.76	0.95	1.24	1.65	0.91	1.23	1.67	0.89	1.23	1.71
LOCA	FAR	4	100	0.86	1.09	1.38	0.89	1.09	1.33	0.88	1.1	1.35	0.86	1.11	1.39
MACA	FAR	4	100	1.17	1.5	2.01	1.13	1.42	1.88	1.12	1.44	1.97	1.11	1.46	2.1
CORDEX	FAR	4	200	0.96	1.33	1.87	0.92	1.27	1.79	0.88	1.28	1.85	0.86	1.29	1.88
LOCA	FAR	4	200	0.83	1.11	1.46	0.86	1.1	1.4	0.86	1.11	1.43	0.83	1.12	1.48
MACA	FAR	4	200	1.18	1.59	2.27	1.14	1.52	2.14	1.14	1.54	2.27	1.13	1.57	2.45

NEAR=Period 2030 – 2069; FAR = 2060-2099; CD = Climate Division; RP = Return Period; 1D17 is 1 Day 17th percentile. All others column headers use this format

Table I-5. Change Factor Values for Climate Division 5

Dataset	Period	CD	RP	1D17	1D50	1D83	3D17	3D50	3D83	7D17	7D50	7D83	10D17	10D50	10D83
CORDEX	NEAR	5	5	0.97	1.08	1.21	0.97	1.06	1.15	0.96	1.05	1.15	0.96	1.05	1.17
LOCA	NEAR	5	5	0.91	1	1.11	0.93	1.01	1.09	0.92	1	1.1	0.91	1	1.1
MACA	NEAR	5	5	1.05	1.17	1.34	1.04	1.15	1.27	1.01	1.12	1.24	1.01	1.11	1.23
CORDEX	NEAR	5	10	0.95	1.09	1.25	0.96	1.07	1.19	0.97	1.07	1.21	0.96	1.08	1.23
LOCA	NEAR	5	10	0.9	1.01	1.14	0.92	1.02	1.12	0.91	1.01	1.13	0.89	1.01	1.13
MACA	NEAR	5	10	1.06	1.21	1.43	1.05	1.17	1.34	1.03	1.15	1.31	1.01	1.14	1.3
CORDEX	NEAR	5	25	0.93	1.1	1.33	0.95	1.09	1.27	0.96	1.11	1.31	0.95	1.12	1.33
LOCA	NEAR	5	25	0.88	1.03	1.2	0.9	1.02	1.18	0.88	1.02	1.18	0.85	1.01	1.21
MACA	NEAR	5	25	1.07	1.26	1.56	1.06	1.23	1.46	1.03	1.2	1.42	1.01	1.19	1.42
CORDEX	NEAR	5	50	0.91	1.13	1.38	0.93	1.12	1.32	0.95	1.14	1.37	0.94	1.15	1.43
LOCA	NEAR	5	50	0.86	1.03	1.26	0.88	1.03	1.23	0.85	1.02	1.23	0.81	1.01	1.28
MACA	NEAR	5	50	1.06	1.31	1.69	1.06	1.27	1.56	1.02	1.24	1.54	0.99	1.22	1.54
CORDEX	NEAR	5	100	0.88	1.15	1.43	0.93	1.14	1.4	0.94	1.18	1.47	0.92	1.19	1.52
LOCA	NEAR	5	100	0.84	1.04	1.34	0.85	1.04	1.29	0.81	1.03	1.3	0.77	1.01	1.37
MACA	NEAR	5	100	1.06	1.36	1.82	1.05	1.32	1.69	1	1.28	1.66	0.97	1.25	1.67
CORDEX	NEAR	5	200	0.87	1.16	1.53	0.91	1.14	1.51	0.93	1.22	1.58	0.92	1.24	1.65
LOCA	NEAR	5	200	0.81	1.05	1.43	0.82	1.05	1.36	0.78	1.03	1.38	0.73	1.01	1.47
MACA	NEAR	5	200	1.06	1.41	2	1.04	1.37	1.84	0.98	1.32	1.8	0.95	1.29	1.83
CORDEX	FAR	5	5	0.99	1.11	1.25	0.95	1.05	1.17	0.9	1.02	1.13	0.89	1.01	1.12
LOCA	FAR	5	5	0.87	0.98	1.09	0.88	0.99	1.08	0.88	0.99	1.09	0.87	0.99	1.09
MACA	FAR	5	5	1.01	1.15	1.32	1.01	1.12	1.25	0.98	1.08	1.22	0.97	1.07	1.22
CORDEX	FAR	5	10	0.99	1.13	1.29	0.95	1.08	1.21	0.92	1.05	1.2	0.9	1.04	1.19
LOCA	FAR	5	10	0.86	0.98	1.12	0.88	0.99	1.11	0.88	0.99	1.12	0.87	0.99	1.13
MACA	FAR	5	10	1.03	1.18	1.38	1.03	1.15	1.3	1	1.11	1.27	0.99	1.1	1.26
CORDEX	FAR	5	25	1	1.16	1.38	0.95	1.11	1.29	0.93	1.1	1.3	0.9	1.12	1.32
LOCA	FAR	5	25	0.84	0.98	1.17	0.87	0.99	1.15	0.86	0.99	1.17	0.84	0.99	1.2
MACA	FAR	5	25	1.04	1.23	1.5	1.05	1.18	1.39	1	1.15	1.37	0.98	1.13	1.37

Dataset	Period	CD	RP	1D17	1D50	1D83	3D17	3D50	3D83	7D17	7D50	7D83	10D17	10D50	10D83
CORDEX	FAR	5	50	0.99	1.18	1.43	0.96	1.14	1.37	0.91	1.15	1.39	0.88	1.16	1.43
LOCA	FAR	5	50	0.81	0.99	1.22	0.85	1	1.19	0.83	1	1.23	0.8	1	1.27
MACA	FAR	5	50	1.05	1.26	1.6	1.06	1.21	1.49	1	1.17	1.46	0.96	1.16	1.47
CORDEX	FAR	5	100	0.97	1.2	1.53	0.94	1.17	1.45	0.88	1.19	1.52	0.86	1.2	1.56
LOCA	FAR	5	100	0.79	0.99	1.28	0.82	1	1.25	0.8	1.01	1.3	0.76	1	1.36
MACA	FAR	5	100	1.05	1.29	1.72	1.05	1.24	1.61	0.99	1.2	1.58	0.93	1.18	1.58
CORDEX	FAR	5	200	0.94	1.23	1.66	0.93	1.2	1.59	0.87	1.22	1.66	0.85	1.26	1.7
LOCA	FAR	5	200	0.75	1	1.35	0.79	1.01	1.32	0.76	1.01	1.39	0.72	1.01	1.45
MACA	FAR	5	200	1.05	1.32	1.85	1.04	1.27	1.75	0.96	1.23	1.73	0.9	1.21	1.72

NEAR=Period 2030 – 2069; FAR = Period 2060-2099; CD = Climate Division; RP = Return Period; 1D17 is 1 Day 17th percentile. All others column headers use this format

APPENDIX II. Tables of Atlas 14 Stations

Table II-1. Atlas 14 stations in Climate Division 1

ID	Station Name	Longitude	Latitude	Climate Division
08-0211	APALACHICOLA AP	-85.0206	29.7258	1
08-0765	BLACKMAN	-86.65	30.9833	1
08-0804	BLOUNTSTOWN 2 SE	-85.05	30.45	1
08-1020	BRISTOL	-84.9861	30.4181	1
08-1356	CARRABELLE 1 NNW	-84.6333	29.8667	1
08-1388	CARYVILLE	-85.8167	30.7667	1
08-1544	CHIPLEY	-85.4847	30.7836	1
08-1775	COMPASS LAKE	-85.4	30.6	1
08-1986	CRESTVIEW BOB SIKES AP	-86.5225	30.7797	1
08-2220	DE FUNIAK SPRINGS 1 E	-86.0939	30.7244	1
08-3538	GRACEVILLE 1 SW	-85.5331	30.9575	1
08-5372	MARIANNA SCH FOR BOYS	-85.2667	30.7667	1
08-5793	MILTON EXP STN	-87.1414	30.7794	1
08-5879	MONTICELLO 5 SE	-83.7833	30.4922	1
08-5880	MONTICELLO 10 SW	-83.9858	30.4406	1
08-5990	MT PLEASANT 2 W	-84.7	30.6667	1
08-6240	NICEVILLE	-86.4928	30.5316	1
08-6828	PANACEA 1 S	-84.485	29.9989	1
08-6842	PANAMA CITY 5 N	-85.6606	30.2492	1
08-6997	PENSACOLA RGNL AP	-87.1869	30.4781	1
08-7429	QUINCY 3 SSW	-84.55	30.6	1
08-7867	ST MARKS 5 SSE	-84.1667	30.1	1
08-8758	TALLAHASSEE WSO AP	-84.3533	30.3931	1
08-9417	WAUSAU	-85.5833	30.6333	1
08-9566	WEWAHITCHKA	-85.2042	30.1192	1
08-9795	WOODRUFF DAM	-84.8742	30.7219	1
91-0602	HERRON STEEL SITE, SILVER	-84.4111	30.4383	1
91-0605	CHRISTIAN HERITAGE CHURCH	-84.3308	30.5053	1
91-0606	LAKE JACKSON FACILITY	-84.2992	30.4833	1
91-0610	TUCK PROPERTY, N. CENTERV	-84.15	30.5592	1
91-0613	CITY WELL @ LIMOGES DR.	-84.1956	30.4844	1
91-0616	LEON COUNTY LANDFILL, US	-84.1347	30.4203	1
91-0618	LAKE KANTURK OUTFALL @ CE	-84.1917	30.5272	1
91-0623	SAN LUIS CITY PARK	-84.3211	30.4586	1
91-0626	CHOWKEEBIN NENE NEAR MAGN	-84.2608	30.4331	1
91-0628	WEMBLEY WAY, EASTGATE NEI	-84.2392	30.4931	1

Table II-2. Atlas 14 stations in Climate Division 2

ID	Station Name	Longitude	Latitude	Climate Division
08-0975	BRANFORD	-82.9108	29.9625	2
08-1432	CEDAR KEY 1 WSW	-83.05	29.1333	2
08-1978	CRESCENT CITY	-81.5158	29.4292	2
08-2008	CROSS CITY 1 E	-83.1053	29.6333	2
08-2391	DOWLING PARK 1 W	-83.2594	30.2497	2
08-2915	FEDERAL POINT	-81.5389	29.755	2
08-2944	FERNANDINA BEACH	-81.4636	30.6589	2
08-3321	GAINESVILLE 3 WSW	-82.3667	29.6333	2
08-3326	GAINESVILLE RGNL AP	-82.2756	29.6919	2
08-3470	GLEN ST MARY 1 W	-82.1856	30.2717	2
08-3874	HASTINGS 4NE	-81.4669	29.7517	2
08-3956	HIGH SPRINGS	-82.5972	29.8286	2
08-3978	HILLIARD	-81.9333	30.7	2
08-4273	INGLIS 3 E	-82.6158	29.0253	2
08-4358	JACKSONVILLE INTL AP	-81.6936	30.495	2
08-4366	JACKSONVILLE BEACH	-81.3928	30.2875	2
08-4394	JASPER	-82.9447	30.5228	2
08-4731	LAKE CITY 2 E	-82.5942	30.1853	2
08-5099	LIVE OAK	-82.965	30.2889	2
08-5275	MADISON	-83.4119	30.4517	2
08-5391	MARINELAND	-81.215	29.67	2
08-5539	MAYO	-83.1819	30.0564	2
08-6753	PALATKA	-81.6606	29.6439	2
08-7025	PERRY	-83.5742	30.0986	2
08-7440	RAIFORD STATE PRISON	-82.1928	30.0678	2
08-7826	ST AUGUSTINE LH	-81.2917	29.8875	2
08-8529	STARKE	-82.1164	29.9381	2
08-8565	STEINHATCHEE 6 ENE	-83.3061	29.7236	2
08-9120	USHER TWR	-82.8186	29.4083	2
92-0038	BLACK CK MIDDLEBURG	-81.8488	30.0602	2

Table II--3. Atlas 14 stations in Climate Division 3

ID	Station Name	Longitude	Latitude	Climate Division
08-1046	BROOKSVILLE CHIN HILL	-82.3658	28.6164	3
08-1048	BROOKSVILLE 7 SSW	-82.4353	28.4811	3
08-1163	BUSHNELL 2 E	-82.0894	28.6664	3
08-1565	BITHLO	-81.1	28.55	3
08-1641	CLERMONT 9 S	-81.7233	28.4553	3
08-2150	DAYTONA BEACH	-81.0139	29.1894	3
08-2158	DAYTONA BEACH INTL AP	-81.0483	29.1828	3
08-2229	DELAND 1 SSE	-81.3106	29.0181	3
08-3840	HART LAKE	-81.1833	28.3833	3
08-4289	INVERNESS 3 SE	-82.3125	28.8031	3
08-4332	ISLEWORTH	-81.5333	28.4833	3
08-5076	LISBON	-81.7844	28.8728	3
08-5237	LYNNE	-81.9306	29.2003	3
08-5643	MERRITT ISLAND	-80.7	28.35	3
08-6210	NEW SMYRNA BEACH	-80.95	29.05	3
08-6414	OCALA	-82.0778	29.0803	3
08-6584	ORANGE CITY	-81.3	28.9333	3
08-6628	ORLANDO INTL AP	-81.325	28.4339	3
08-6638	ORLANDO WSO AP	-81.3333	28.55	3
08-7851	SAINT LEO	-82.26	28.3378	3
08-7982	SANFORD	-81.2778	28.8147	3
08-8942	TITUSVILLE	-80.8158	28.6242	3
90-0808	TAFT R	-81.3714	28.4361	3
92-0052	LK JOANNA	-81.646	28.8345	3

Table II-4. Atlas 14 stations in Climate Division 4

ID	Station Name	Longitude	Latitude	Climate Division
08-0228	ARCADIA	-81.8739	27.2181	4
08-0236	ARCHBOLD BIO STN	-81.3508	27.1819	4
08-0369	AVON PARK 2 W	-81.5253	27.5944	4
08-0390	BABSON PARK 1 ENE	-81.5167	27.85	4
08-0478	BARTOW	-81.8433	27.8986	4
08-0488	BASINGER	-81.0333	27.3833	4
08-0945	BRADENTON 5 ESE	-82.5014	27.4467	4
08-1632	CLEARWATER	-82.7667	27.9667	4
08-2288	DESOTO CITY 8 SW	-81.5136	27.3697	4
08-3137	FT DRUM 3 NW	-80.8167	27.5303	4
08-3153	FT GREEN 12 WSW	-82.1378	27.5706	4
08-3207	FT PIERCE	-80.3539	27.4622	4
08-3986	HILLSBOROUGH RIVER SP	-82.2269	28.1428	4
08-4242	INDIAN LAKE ESTATES	-81.3333	27.8	4
08-4625	KISSIMMEE 2	-81.4239	28.2764	4
08-4707	LAKE ALFRED EXP STN	-81.7144	28.1042	4
08-4797	LAKELAND	-81.9219	28.0206	4
08-4845	LAKE PLACID 2 SW	-81.3833	27.2833	4
08-5612	MELBOURNE WFO	-80.6308	28.0958	4
08-5973	MTN LAKE	-81.5928	27.9347	4
08-6065	MYAKKA RIVER SP	-82.3161	27.2417	4
08-6880	PARRISH	-82.3478	27.6089	4
08-7205	PLANT CITY	-82.1422	28.0236	4
08-7886	ST PETERSBURG	-82.6272	27.7631	4
08-8021	SARASOTA	-82.5333	27.35	4
08-8788	TAMPA WSCMO AP	-82.5403	27.9614	4
08-8824	TARPON SPGS SEWAGE PL	-82.7644	28.1586	4
08-9176	VENICE	-82.4364	27.1006	4
08-9184	VENUS	-81.3303	27.135	4
08-9219	VERO BEACH 4SE	-80.4031	27.6528	4
08-9401	WAUCHULA	-81.7994	27.5478	4
08-9707	WINTER HAVEN	-81.7331	28.0153	4
90-0023	AVONPK R	-81.2647	27.6317	4
90-0040	BLUEG R	-80.465	27.2197	4
90-0142	LOTELA R	-81.4353	27.5914	4
90-0221	MRF155	-81.0772	27.7528	4
90-0225	MRF159	-81.1439	27.4725	4
90-0238	MRF18	-81.3519	28.1403	4

ID	Station Name	Longitude	Latitude	Climate Division
90-0243	MRF187	-81.2064	27.4386	4
90-0248	MRF191	-81.2453	27.7458	4
90-0254	MRF205	-81.5286	28.0994	4
90-0274	MRF23	-81.1936	28.0017	4
90-0312	MRF27	-81.1981	27.8031	4
90-0354	MRF32	-81.1342	27.66	4
90-0404	MRF38	-81.1147	27.4014	4
90-0411	MRF39	-80.4506	27.3733	4
90-0423	MRF40	-80.4967	27.3325	4
90-0485	MRF5029	-80.4314	27.6081	4
90-0489	MRF5034	-80.8269	27.2903	4
90-0507	MRF5053	-80.3369	27.4103	4
90-0686	S133-R	-80.8008	27.2061	4
90-0765	S65DW R	-81.0219	27.3142	4
90-0766	S65E R	-80.9625	27.2253	4
90-0803	SNIVLY R	-81.4175	27.9717	4
92-0007	S-157	-80.5397	27.8304	4
92-0008	S-164	-80.9333	28.3406	4
92-0022	S-252D	-80.6789	27.6389	4
96-0020	KENANSVILLE	-81.05	27.963	4

Table II-5. Atlas 14 stations in Climate Division 5

ID	Station Name	Longitude	Latitude	Climate Division
08-0611	BELLE GLADE	-80.6711	26.6928	5
08-0735	BIG CORKSCREW	-81.5478	26.365	5
08-0845	BOCA RATON	-80.1108	26.3675	5
08-1276	CANAL POINT USDA	-80.6256	26.8639	5
08-1858	CORAL SPRINGS	-80.275	26.2678	5
08-2298	DEVILS GARDEN	-81.1292	26.6033	5
08-2418	DRY TORTUGAS	-82.8736	24.6281	5
08-2850	EVERGLADES	-81.3897	25.8489	5
08-3020	FLAMINGO RS	-80.9144	25.1422	5
08-3163	FT LAUDERDALE	-80.2011	26.1019	5
08-3165	FT LAUDERDALE INTL AP	-80.1536	26.0719	5
08-3186	FT MYERS PAGE FLD AP	-81.8614	26.585	5
08-3909	HIALEAH	-80.2858	25.8175	5
08-4091	HOMESTEAD EXP STN	-80.5	25.5	5
08-4198	HYPOLUXO	-80.05	26.55	5
08-4210	IMMOKALEE	-81.41	26.4217	5
08-4570	KEY WEST INTL AIRPORT	-81.7522	24.555	5
08-4662	LA BELLE	-81.4264	26.7458	5
08-5035	LIGNUMVITAE KEY	-80.696	24.9027	5
08-5182	LOXAHATCHEE	-80.2667	26.6833	5
08-5658	MIAMI BEACH	-80.1336	25.8064	5
08-5663	MIAMI INTL AP	-80.3164	25.7906	5
08-5668	MIAMI WSO CITY	-80.2833	25.7167	5
08-5678	MIAMI 12 SSW	-80.3	25.65	5
08-5895	MOORE HAVEN LOCK 1	-81.0872	26.84	5
08-6078	NAPLES	-81.7158	26.1686	5
08-6318	NORTH NEW RVR CANAL 1	-80.75	26.5667	5
08-6323	NORTH NEW RVR CANAL 2	-80.5372	26.3336	5
08-6406	OASIS RS	-81.0319	25.8581	5
08-6485	OKEECHOBEE	-80.8653	27.1508	5
08-6657	ORTONA LOCK 2	-81.3044	26.7897	5
08-6988	PENNSUCO 5 WNW	-80.4539	25.9297	5
08-7020	PERRINE 4W	-80.4361	25.5819	5
08-7293	PORT MAYACA S L CANAL	-80.6167	26.9833	5
08-7397	PUNTA GORDA 4 ESE	-81.9983	26.9164	5
08-7760	ROYAL PALM RANGER STA	-80.5936	25.3867	5
08-7859	ST LUCIE NEW LOCK 1	-80.2833	27.1167	5
08-8620	STUART	-80.1639	27.2	5

ID	Station Name	Longitude	Latitude	Climate Division
08-8780	TAMIAMI TRL 40 MI BEND	-80.8242	25.7608	5
08-8841	TAVERNIER	-80.5211	25.0069	5
08-9010	TRAIL GLADE RANGES	-80.4775	25.7647	5
08-9525	WEST PALM BCH INTL AP	-80.0994	26.6847	5
60-0352	MILES CITY	-81.2967	26.2483	5
60-0353	OCHOPEE	-81.2833	25.9167	5
90-0001	3A-36 R	-80.4492	26.1915	5
90-0003	3ANW R	-80.7795	26.2665	5
90-0004	3AS R	-80.6915	26.0821	5
90-0007	3ASW R	-80.8362	25.9898	5
90-0020	ALICO R	-80.9819	26.5128	5
90-0055	COLGOV R	-81.7625	26.1297	5
90-0106	G56-R	-80.1308	26.3278	5
90-0107	G57-R	-80.1242	26.2311	5
90-0143	LXWS R	-80.2222	26.4989	5
90-0153	MIALCK R	-80.8061	26.6819	5
90-0162	MRF102	-80.1539	26.3689	5
90-0176	MRF114	-80.2317	26.0603	5
90-0179	MRF117	-80.3442	25.8269	5
90-0185	MRF122	-80.3464	25.47	5
90-0186	MRF123	-80.3764	25.3669	5
90-0190	MRF125C	-80.9344	26.7386	5
90-0204	MRF133	-80.6836	26.7489	5
90-0207	MRF137	-80.5636	26.8131	5
90-0208	MRF138	-80.5253	26.7839	5
90-0240	MRF183	-80.7161	26.7003	5
90-0249	MRF198	-80.9617	26.7897	5
90-0255	MRF206	-81.6497	26.6069	5
90-0262	MRF212	-80.1222	26.4239	5
90-0263	MRF213	-80.2039	26.4167	5
90-0265	MRF220	-80.3675	26.6844	5
90-0294	MRF250	-81.6297	26.7125	5
90-0335	MRF300	-80.8533	26.7281	5
90-0336	MRF301	-80.0622	26.715	5
90-0464	MRF50	-80.9778	27.0653	5
90-0469	MRF5005	-81.4164	26.4072	5
90-0470	MRF5006	-81.3353	26.5956	5
90-0474	MRF5010	-81.3464	26.1844	5
90-0480	MRF5022	-81.3139	26.9244	5
90-0513	MRF54	-80.3039	26.9044	5

ID	Station Name	Longitude	Latitude	Climate Division
90-0516	MRF57	-80.6022	26.8419	5
90-0519	MRF60	-81.0467	26.8083	5
90-0577	MRF63	-80.8953	26.735	5
90-0579	MRF65	-80.6175	26.7744	5
90-0609	MRF73C	-80.7011	26.665	5
90-0614	MRF78	-80.1264	26.6189	5
90-0617	MRF80	-80.9483	26.6244	5
90-0618	MRF81	-80.205	26.6122	5
90-0621	MRF84	-80.1239	26.5208	5
90-0622	MRF85	-80.1703	26.5283	5
90-0684	S131 R	-81.09	26.9792	5
90-0705	S18C-R	-80.525	25.3306	5
90-0728	S332-R	-80.5897	25.4217	5
90-0774	S70 R	-81.1572	27.1186	5
90-0801	SIRG R	-80.1917	26.9072	5
95-1274	S36-R	-80.1784	26.1734	5

APPENDIX III. Change Factor Maps for NEAR period (2030-2069)

Presented herein are maps of the change factors across Florida for the NEAR period (2030-2069) generated using IDW interpolation with an exponent of 1. The maps were created for durations: 24-hr, 3-day, 7-day and 10-day, and return periods: 5-yr, 10-yr, 25-yr, 50-yr, 100-yr and 200-yr.

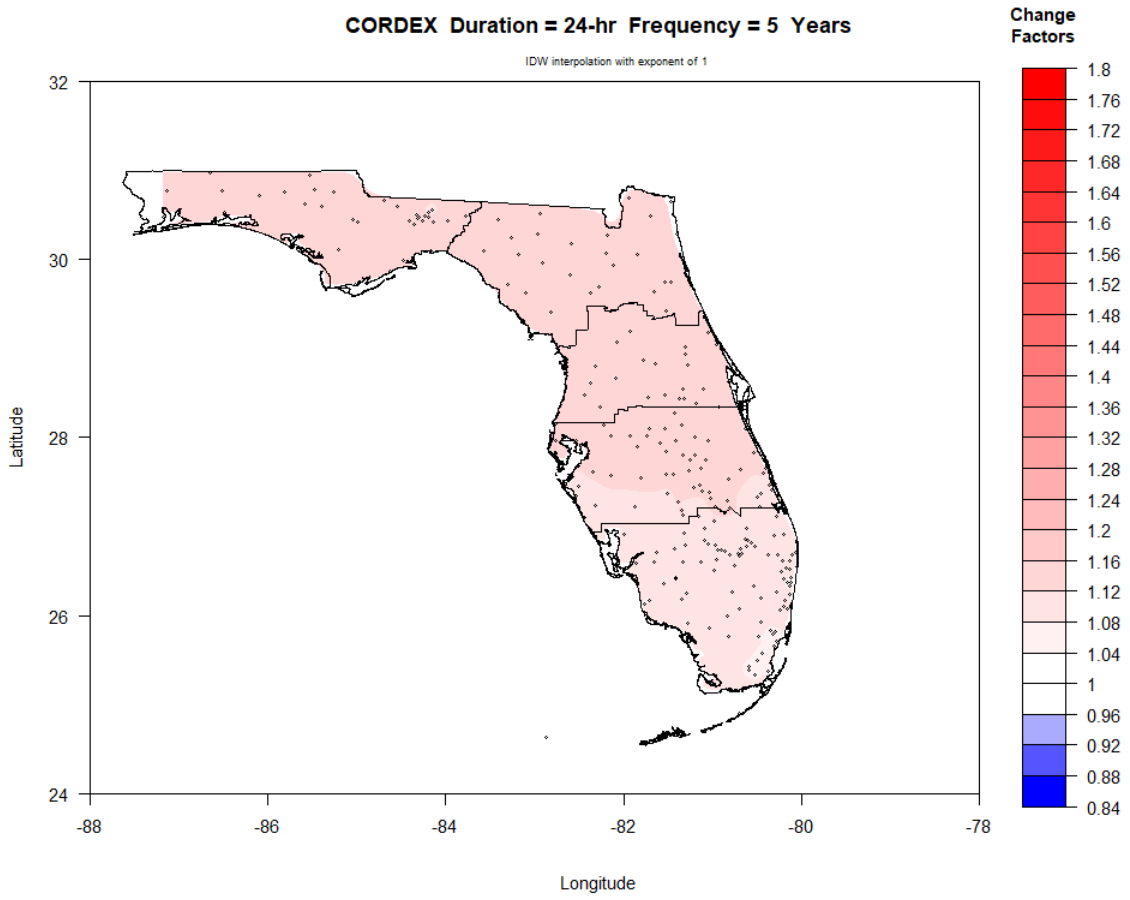

Figure III-1. Map of NEAR period (2030-2069) change factors across Florida for 24-hr duration and 5-year return period.

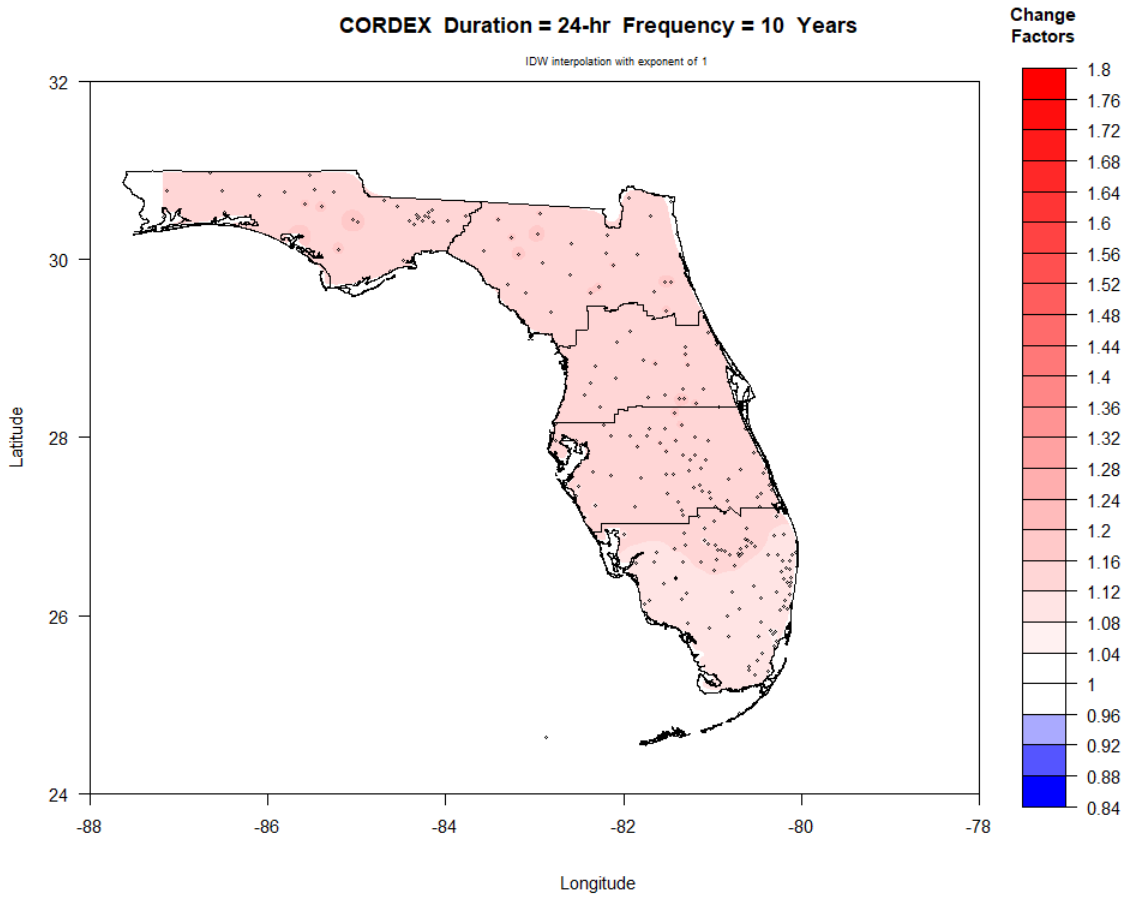

Figure III-2. Map of NEAR period (2030-2069) change factors across Florida for 24-hr duration and 10-year return period.

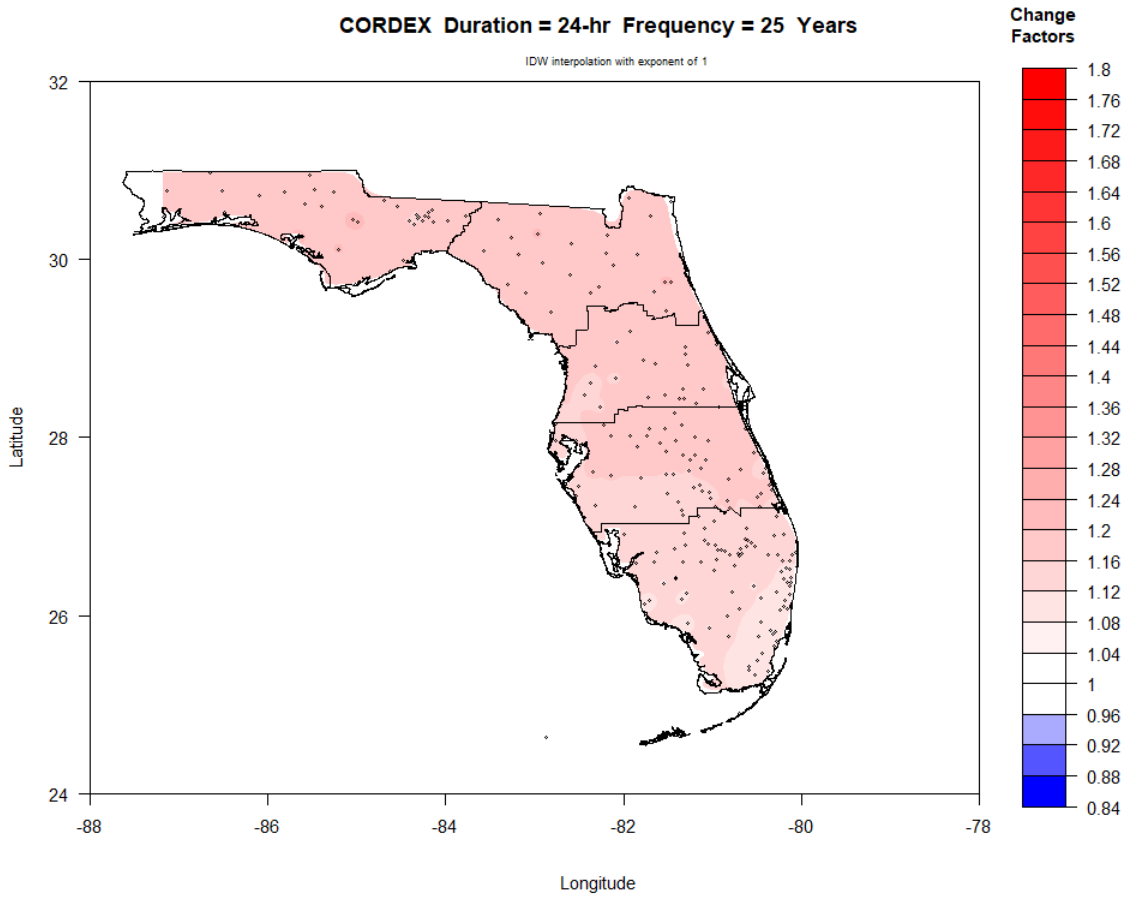

Figure III-3. Map of NEAR period (2030-2069) change factors across Florida for 24-hr duration and 25-year return period.

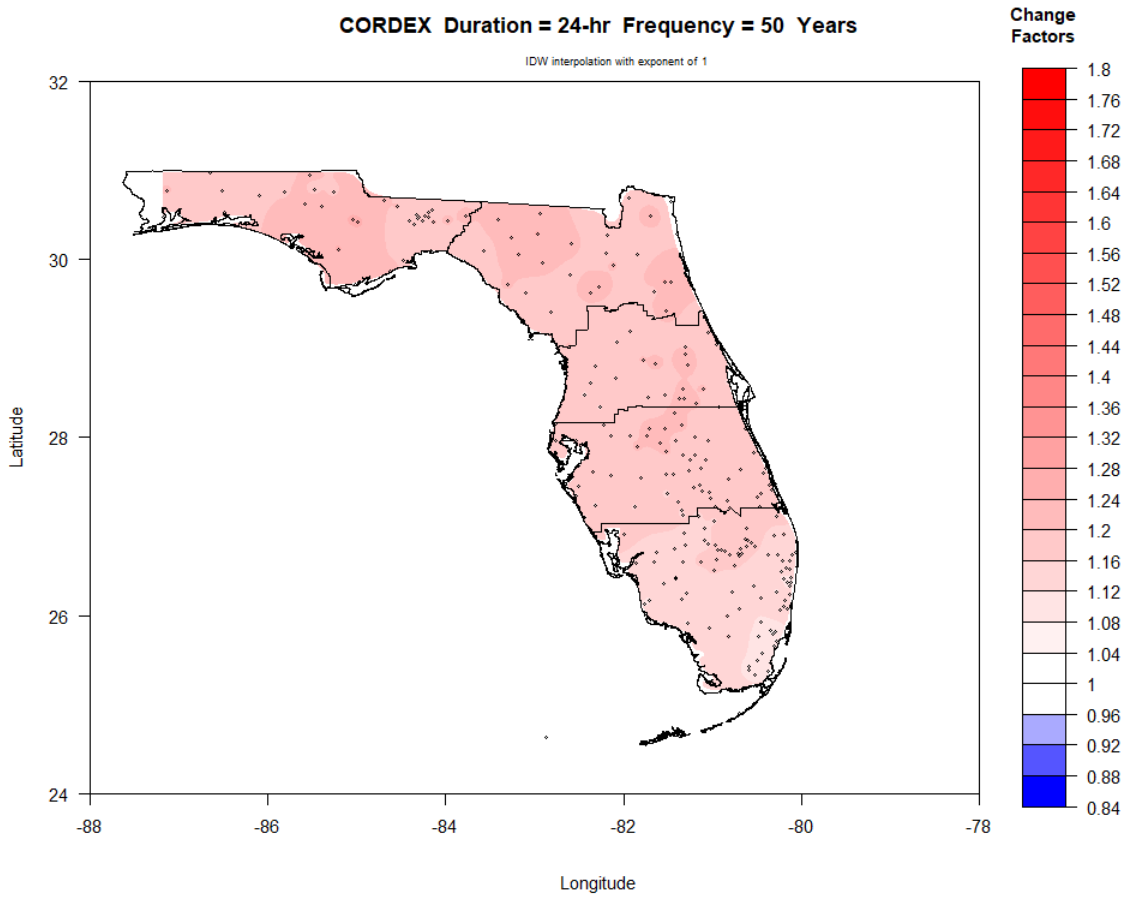

Figure III-4. Map of NEAR period (2030-2069) change factors across Florida for 24-hr duration and 50-year return period.

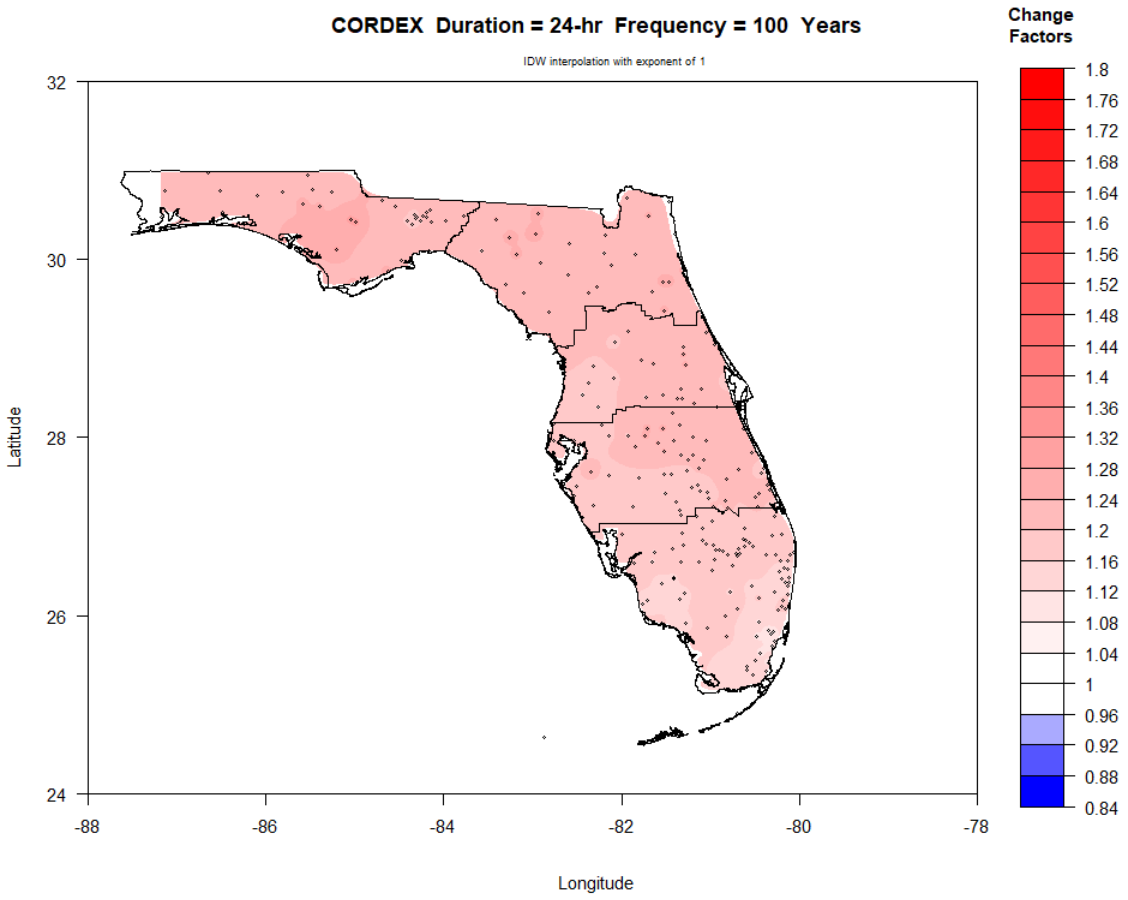

Figure III-5. Map of NEAR period (2030-2069) change factors across Florida for 24-hr duration and 100-year return period.

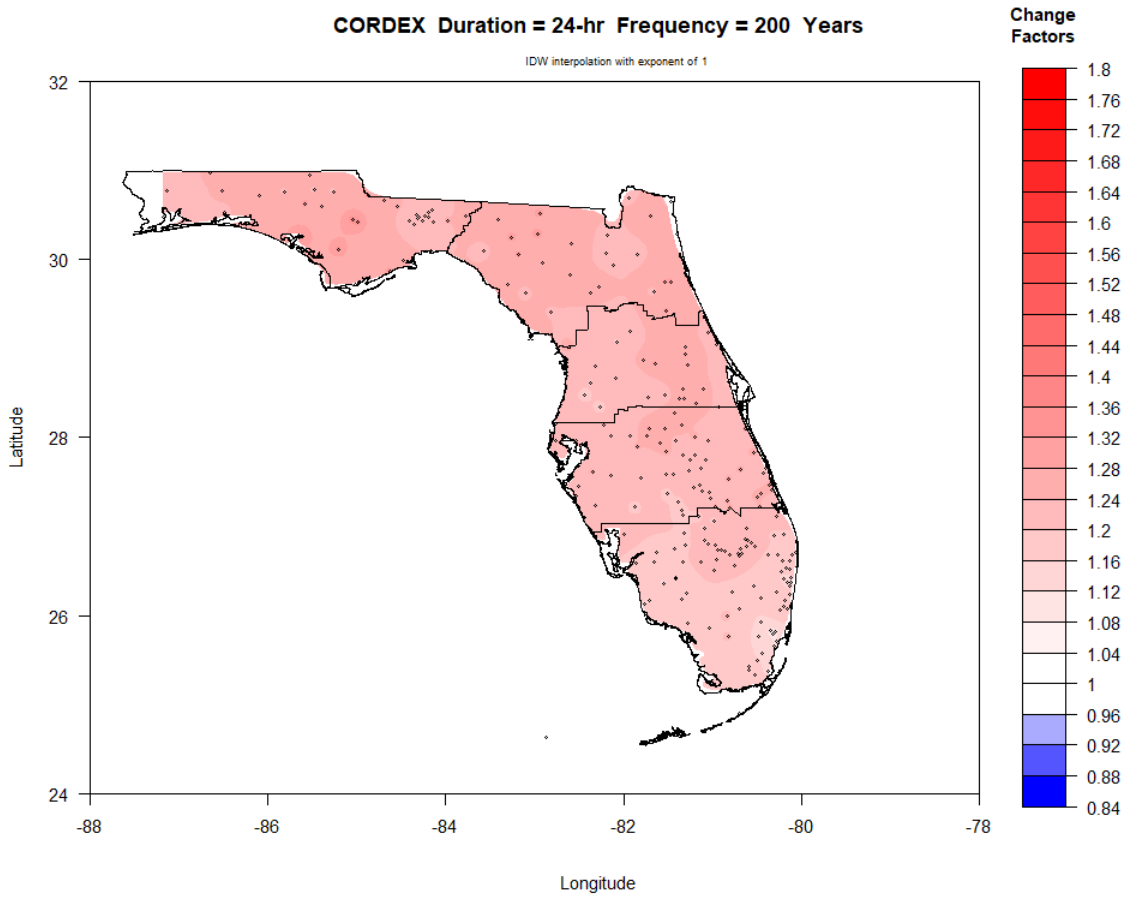

Figure III-6. Map of NEAR period (2030-2069) change factors across Florida for 24-hr duration and 200-year return period.

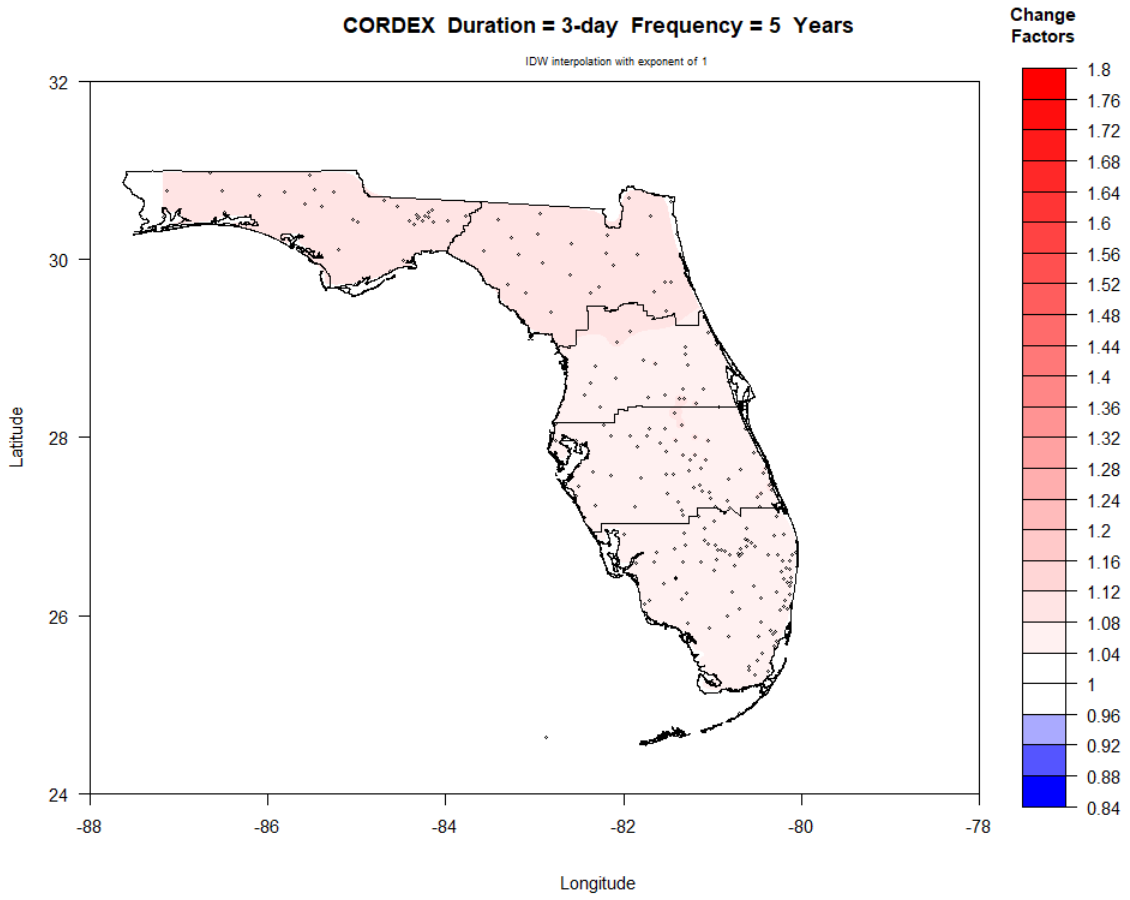

Figure III-7. Map of NEAR period (2030-2069) change factors across Florida for 3-day duration and 5-year return period.

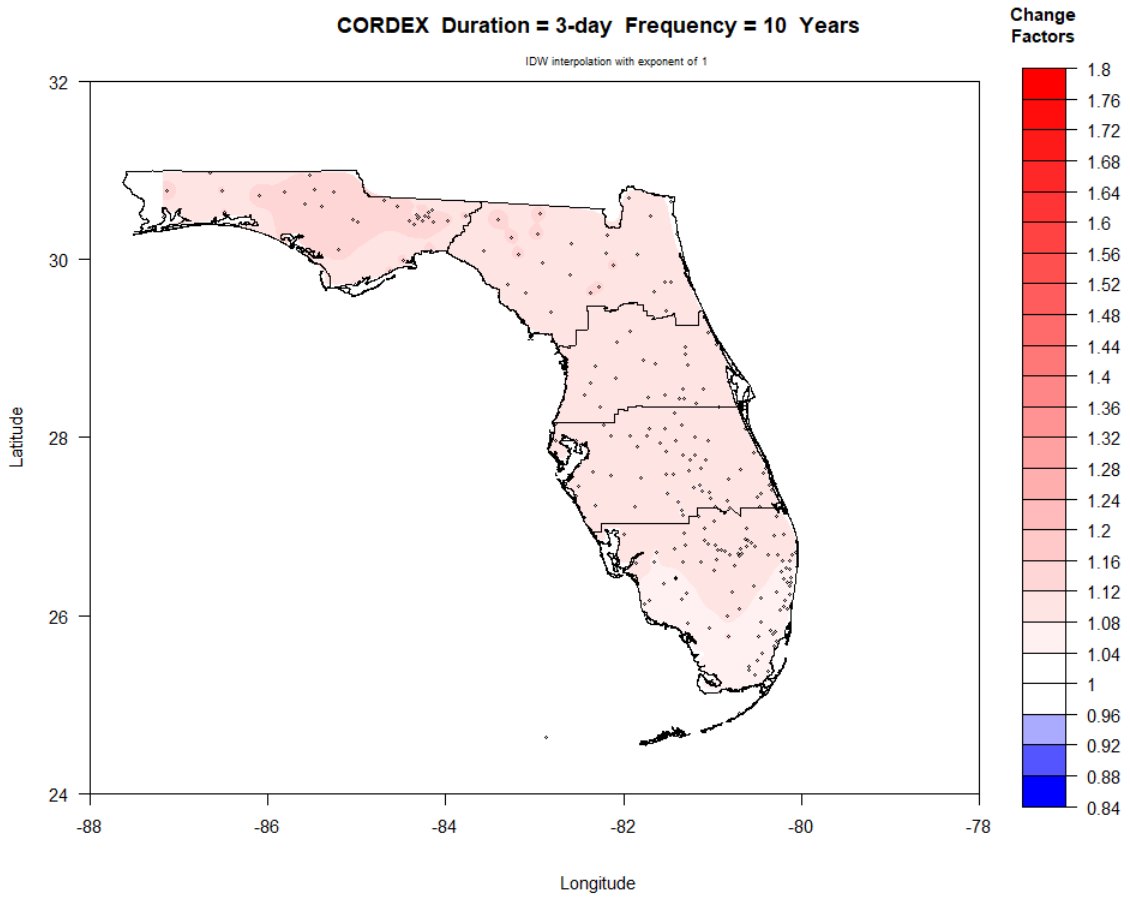

Figure III-8. Map of NEAR period (2030-2069) change factors across Florida for 3-day duration and 10-year return period.

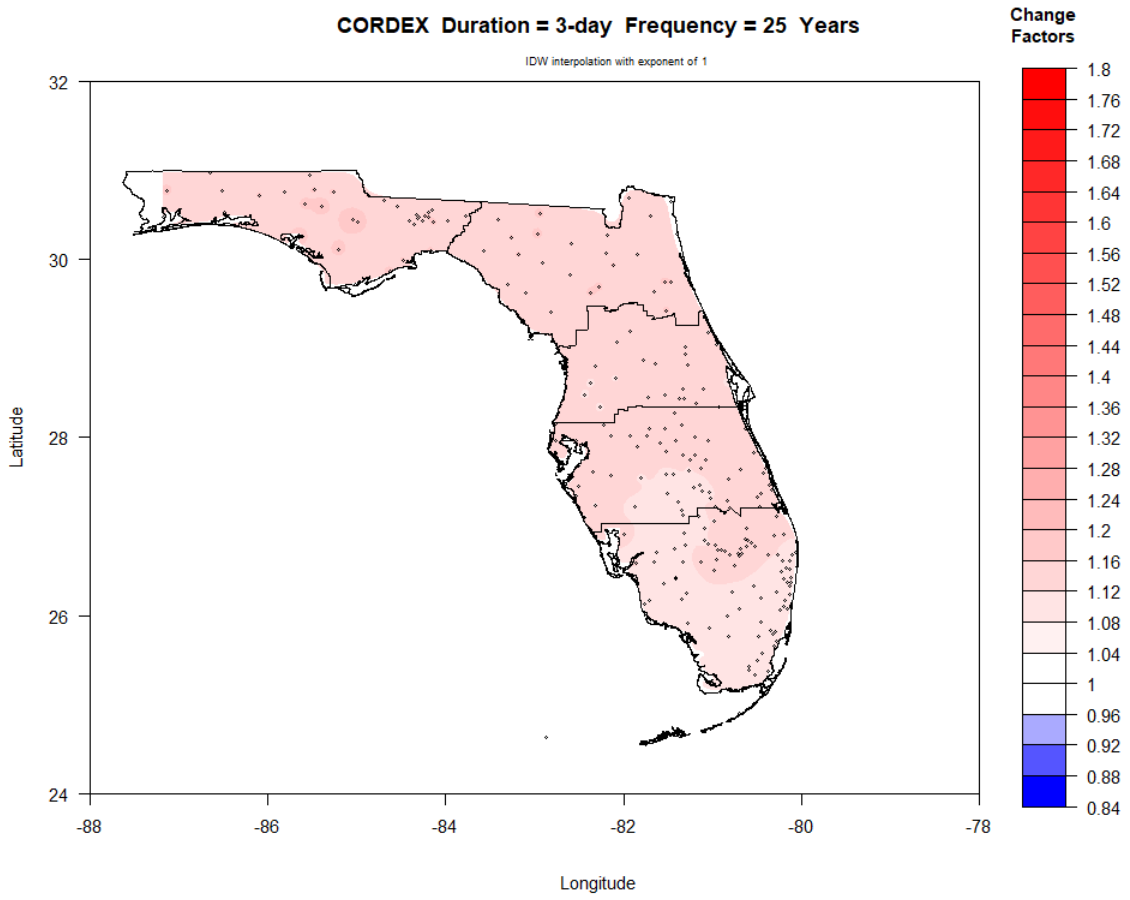

Figure III-9. Map of NEAR period (2030-2069) change factors across Florida for 3-day duration and 25-year return period.

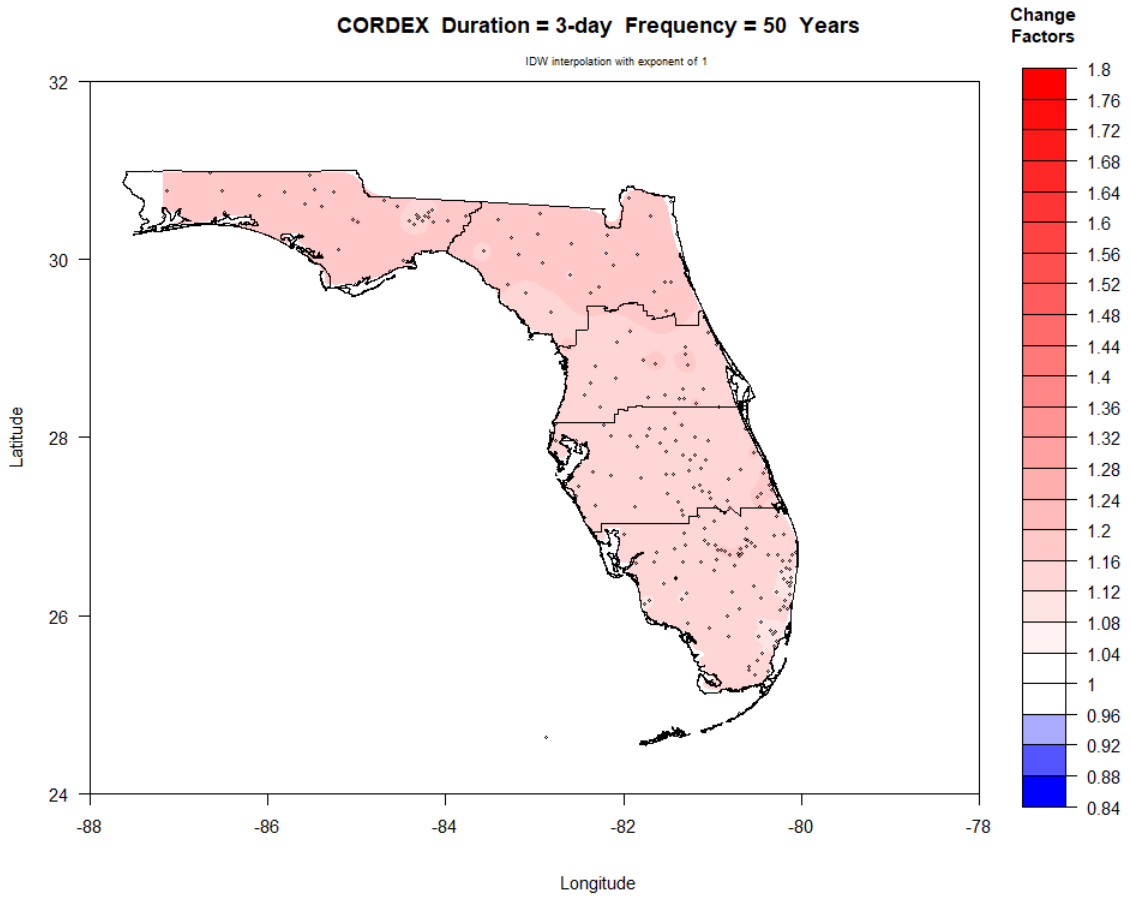

Figure III-10. Map of NEAR period (2030-2069) change factors across Florida for 3-day duration and 50-year return period.

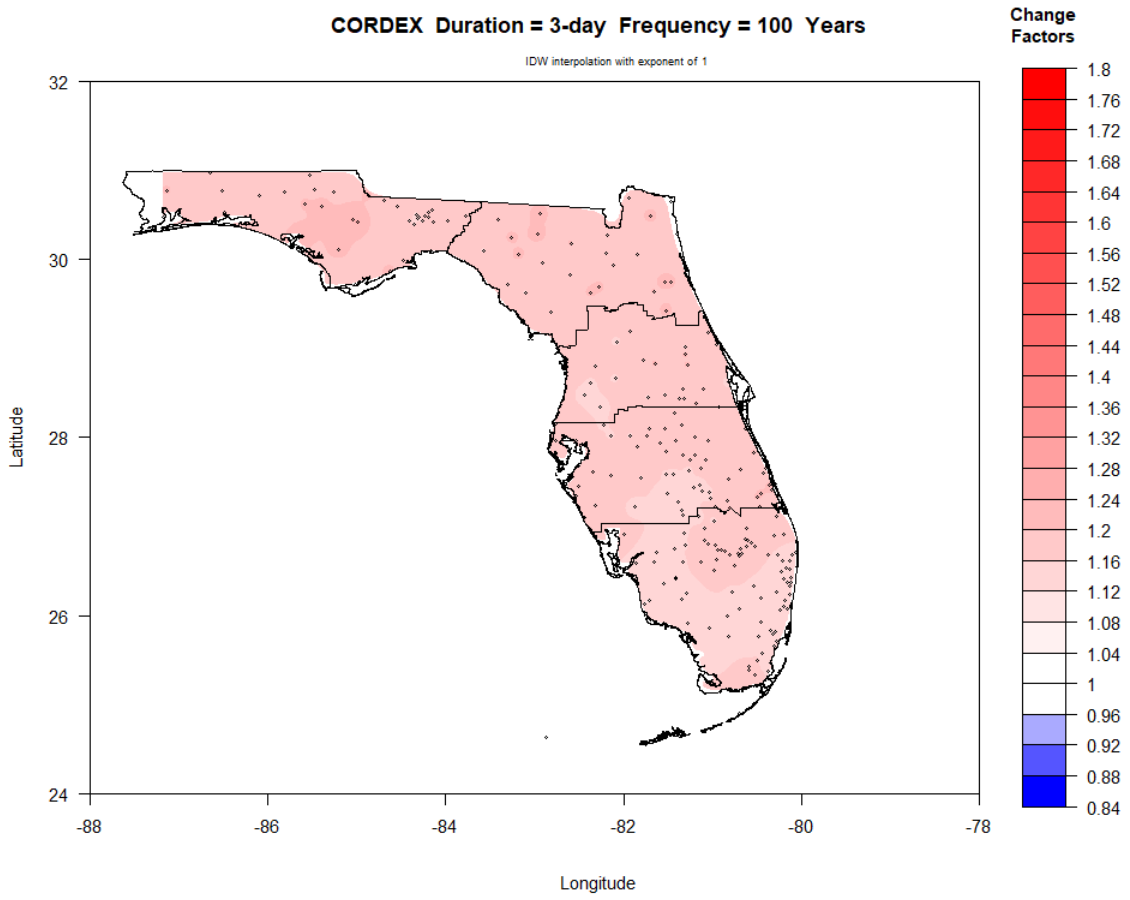

Figure III-11. Map of NEAR period (2030-2069) change factors across Florida for 3-day duration and 100-year return period.

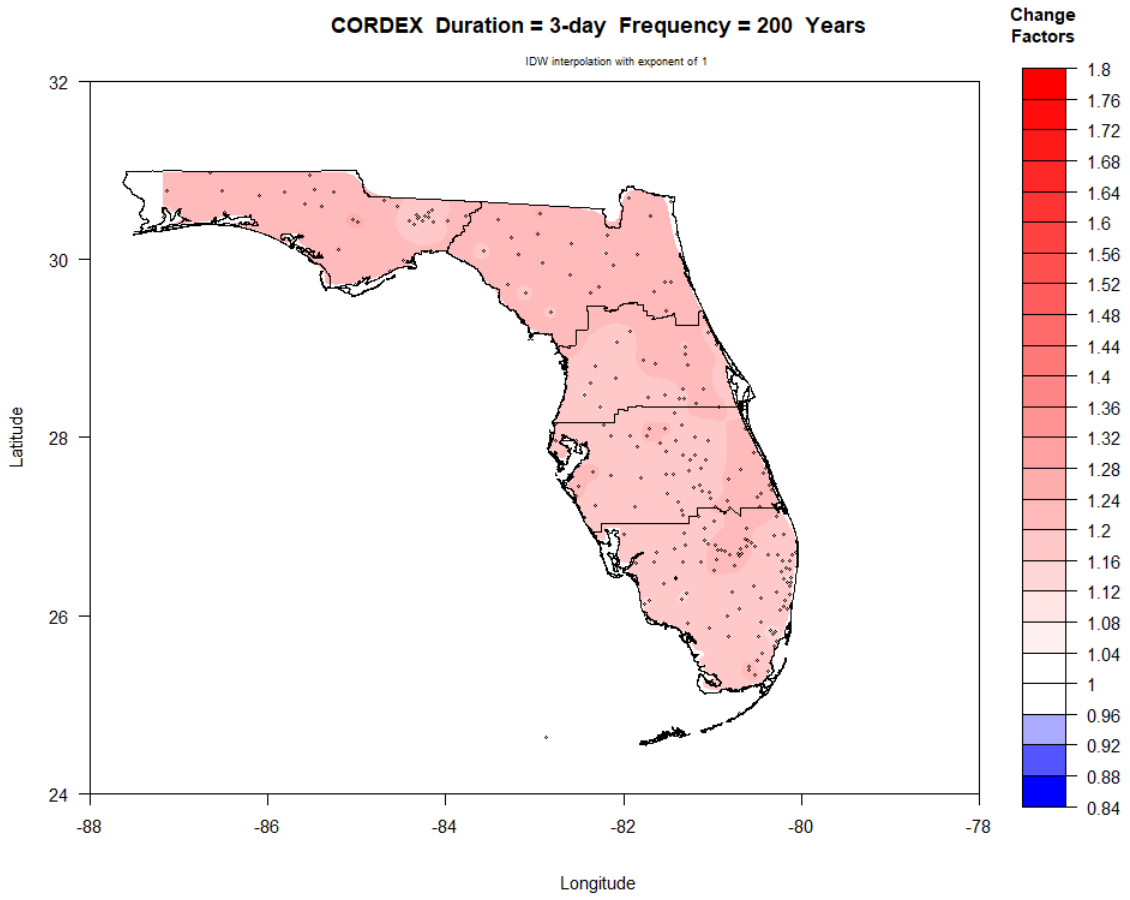

Figure III-12. Map of NEAR period (2030-2069) change factors across Florida for 3-day duration and 200-year return period.

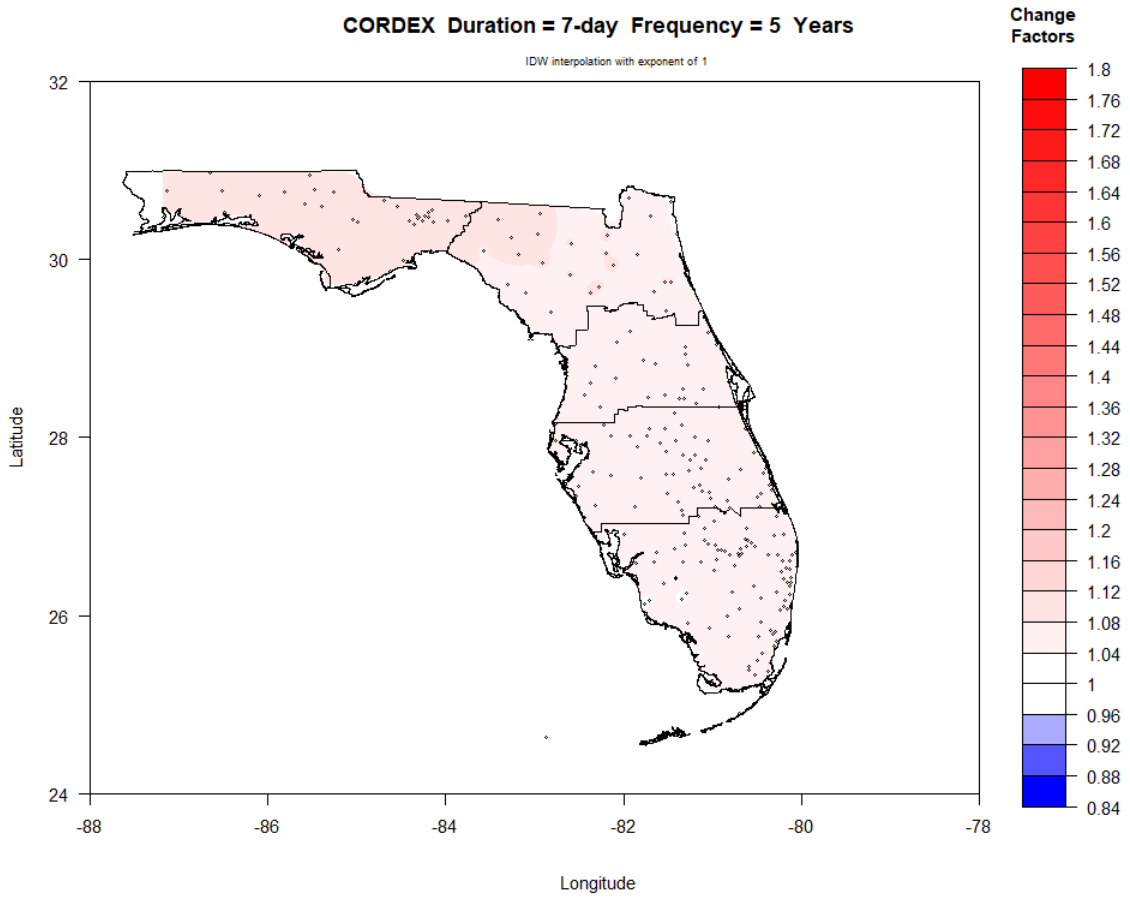

Figure III-13. Map of NEAR period (2030-2069) change factors across Florida for 7-day duration and 5-year return period.

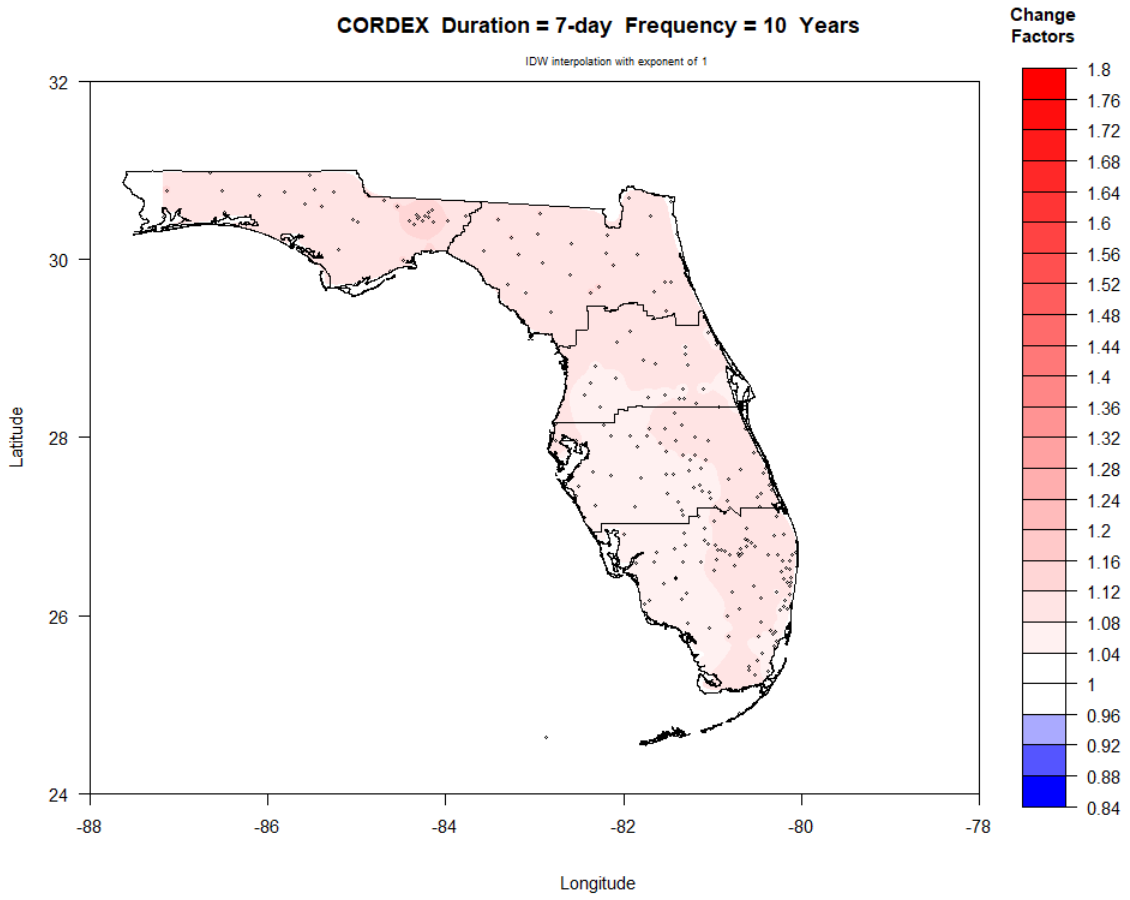

Figure III-14. Map of NEAR period (2030-2069) change factors across Florida for 7-day duration and 10-year return period.

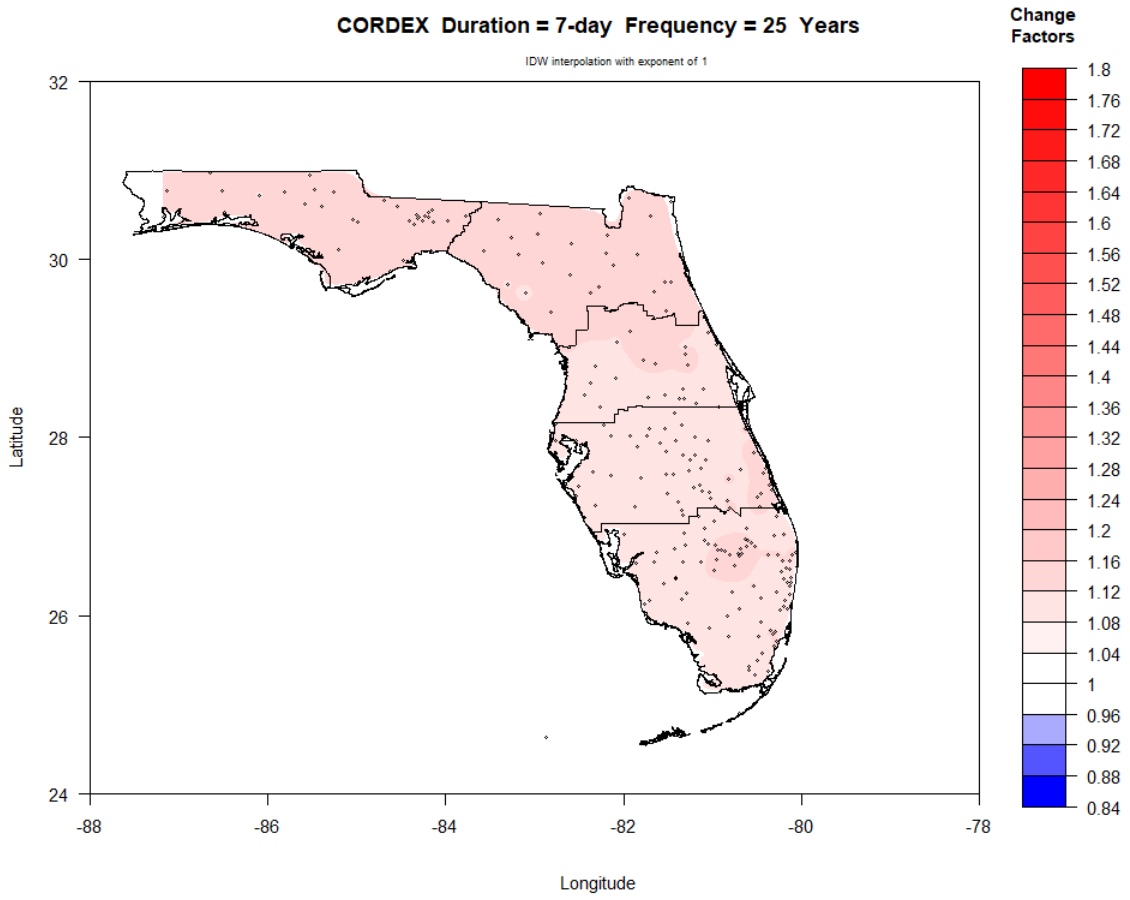

Figure III-15. Map of NEAR period (2030-2069) change factors across Florida for 7-day duration and 25-year return period.

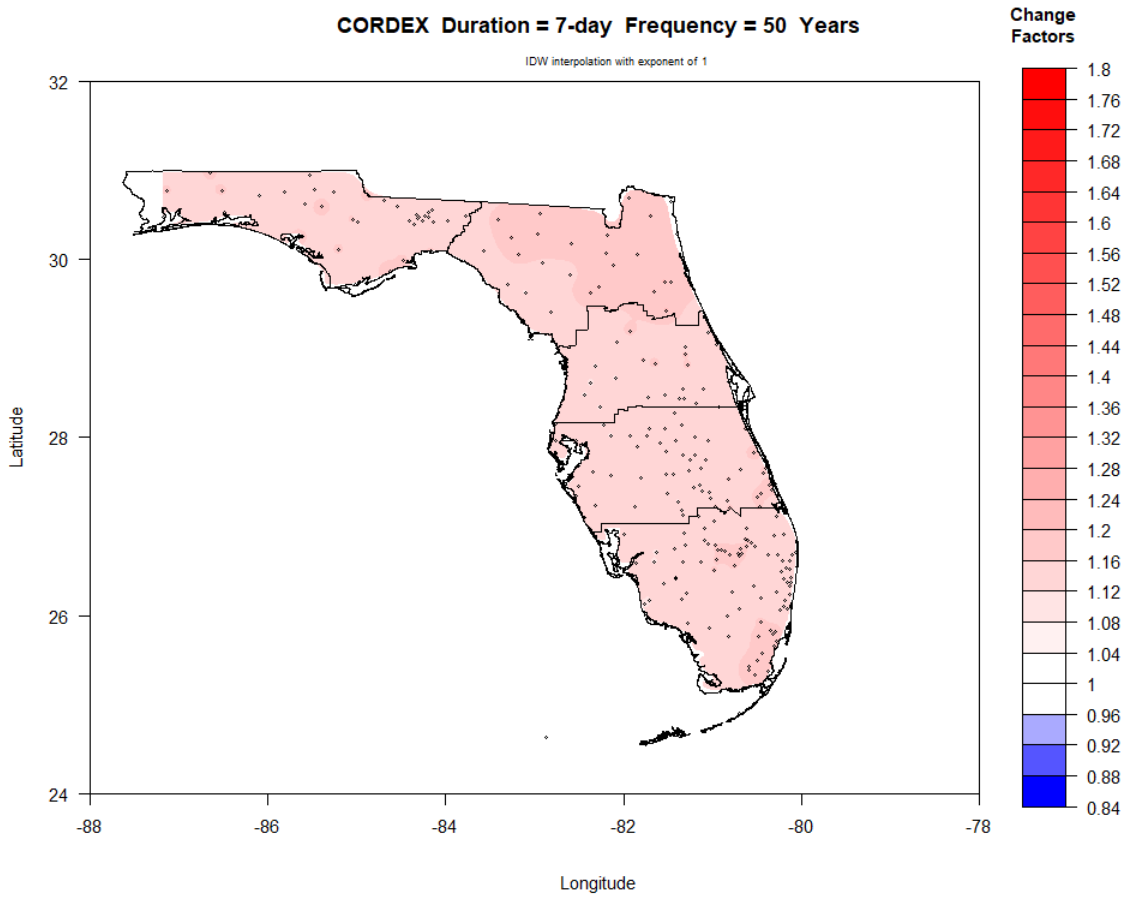

Figure III-16. Map of NEAR period (2030-2069) change factors across Florida for 7-day duration and 50-year return period.

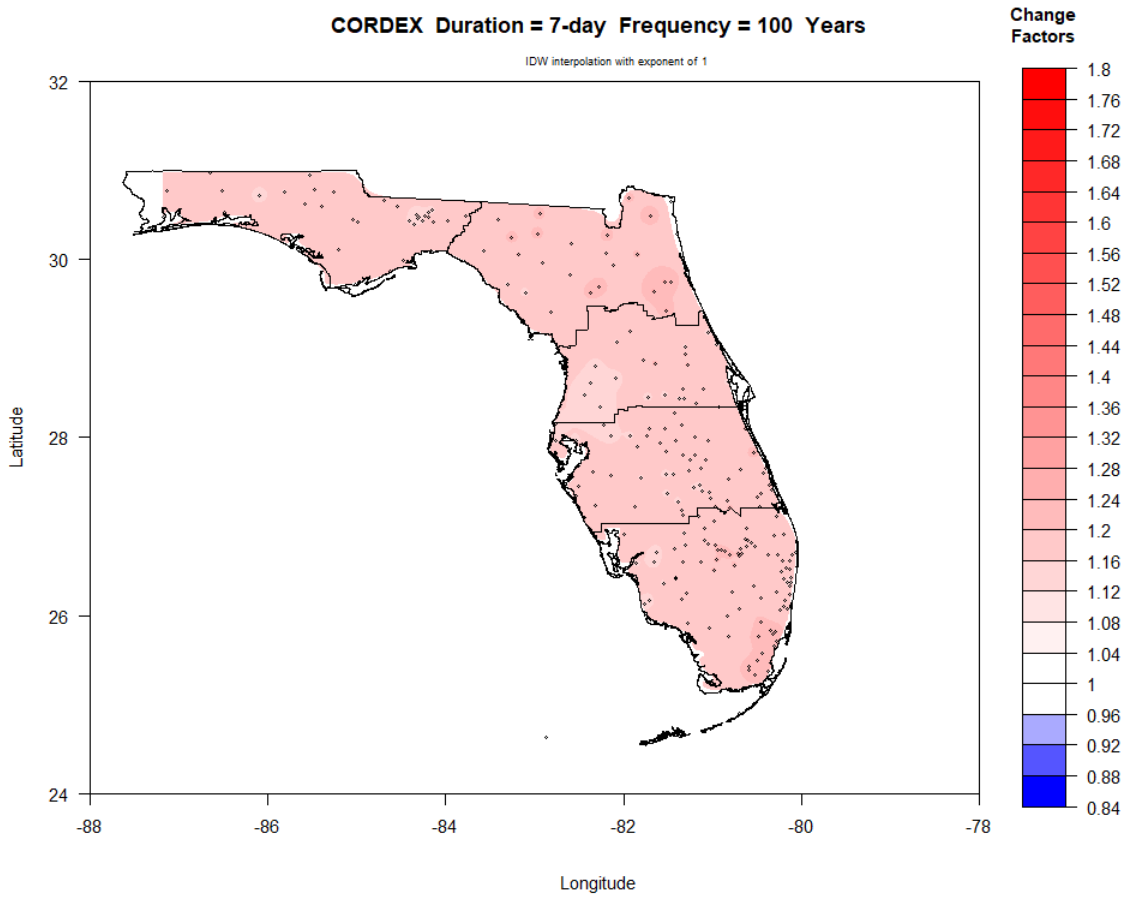

Figure III-17. Map of NEAR period (2030-2069) change factors across Florida for 7-day duration and 100-year return period.

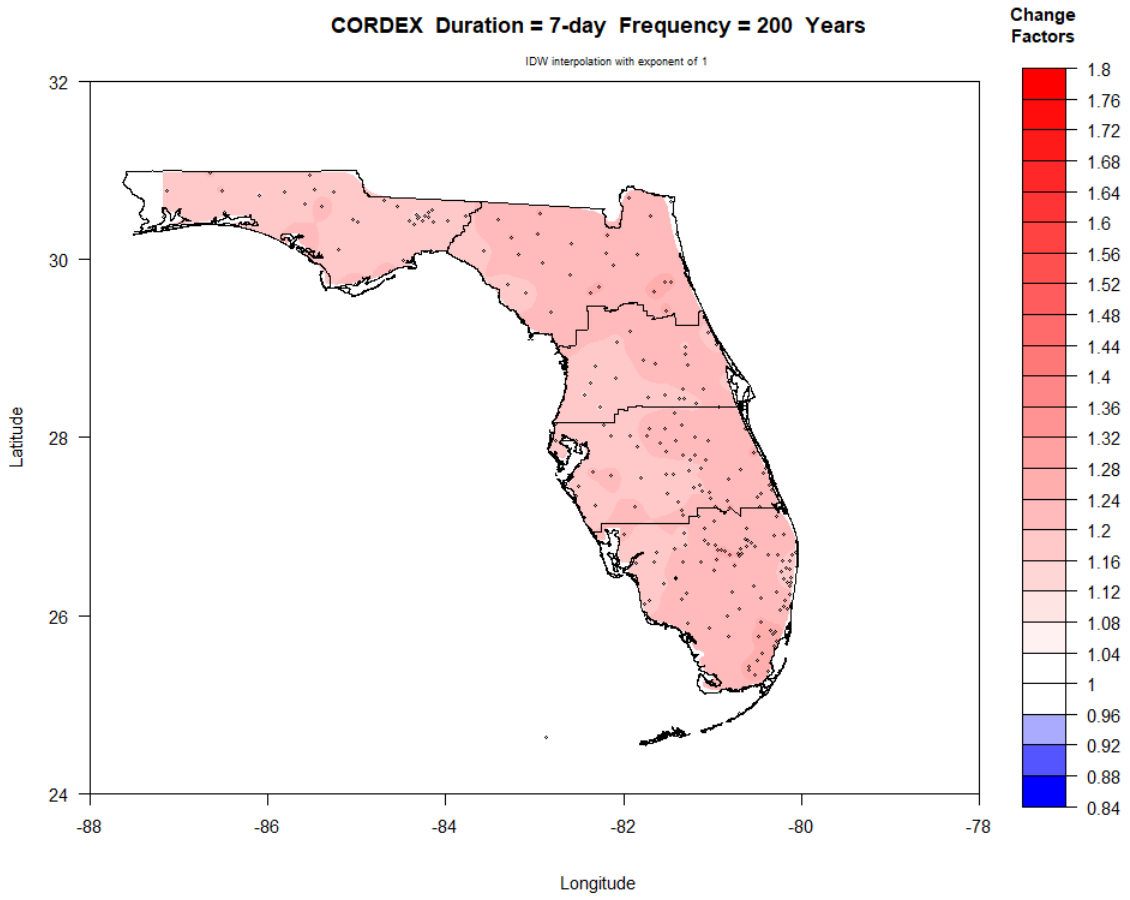

Figure III-18. Map of NEAR period (2030-2069) change factors across Florida for 7-day duration and 200-year return period.

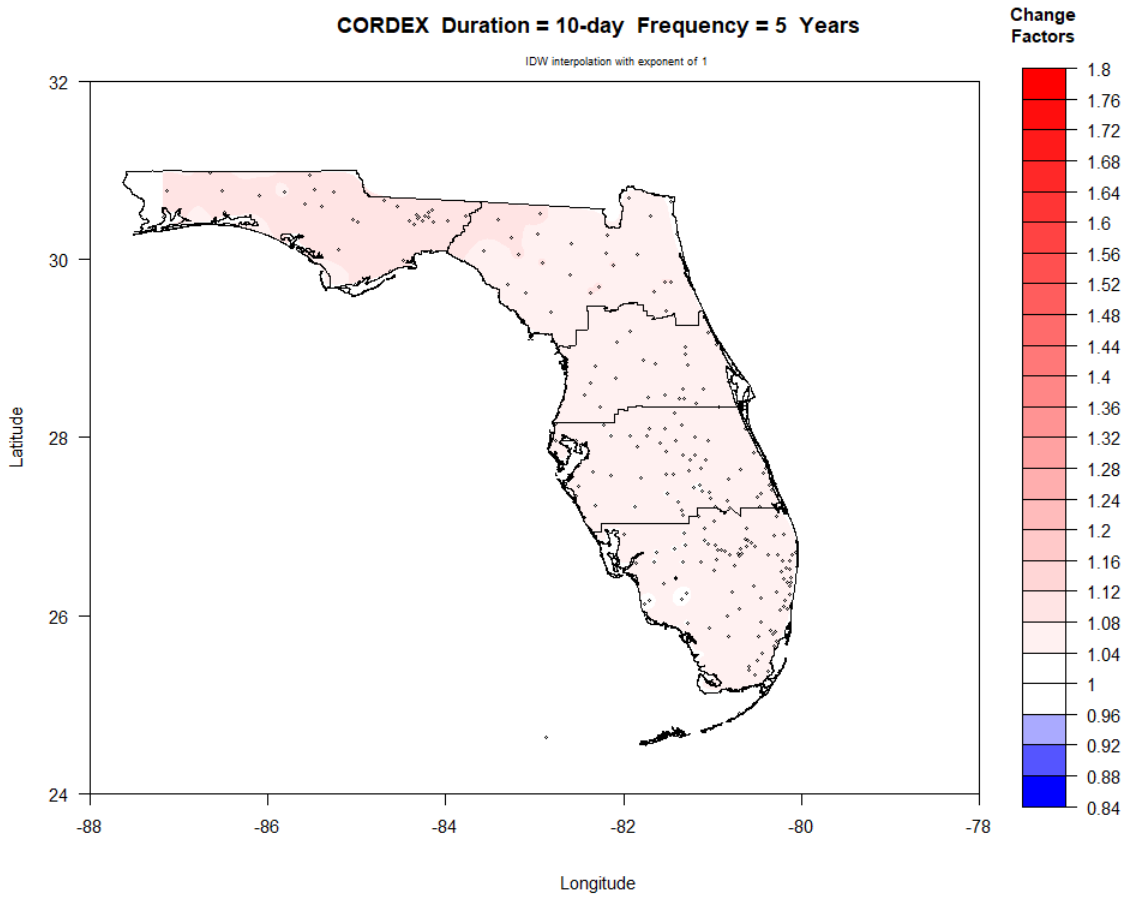

Figure III-19. Map of NEAR period (2030-2069) change factors across Florida for 10-day duration and 5-year return period.

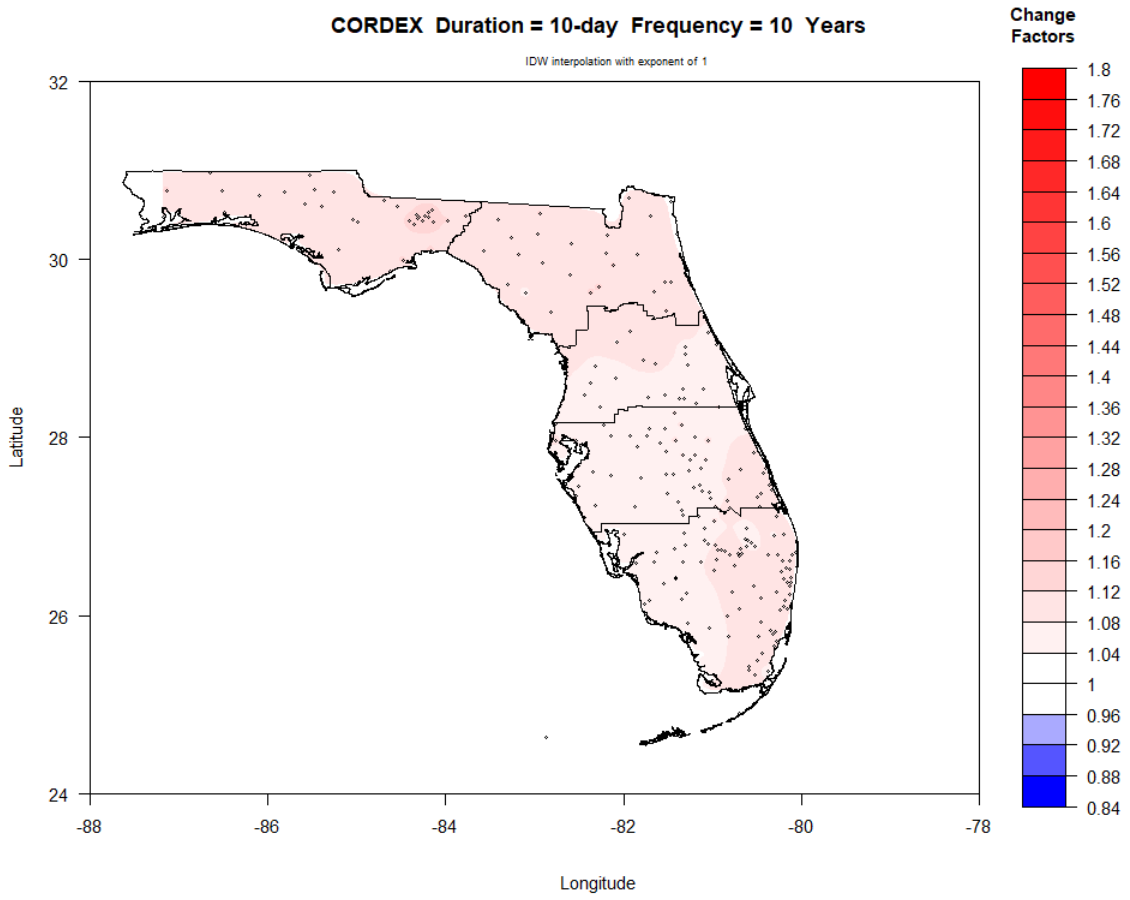

Figure III-20. Map of NEAR period (2030-2069) change factors across Florida for 10-day duration and 10-year return period.

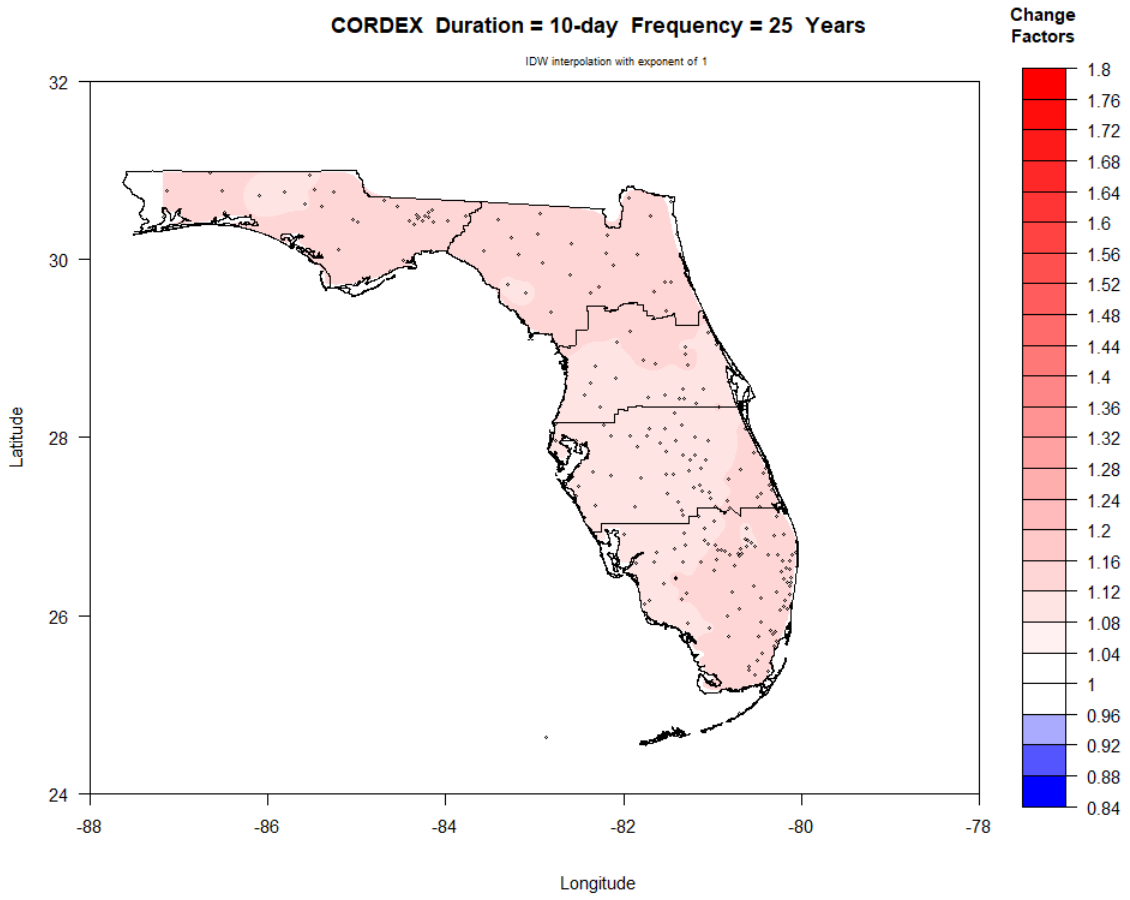

Figure III-21. Map of NEAR period (2030-2069) change factors across Florida for 10-day duration and 25-year return period.

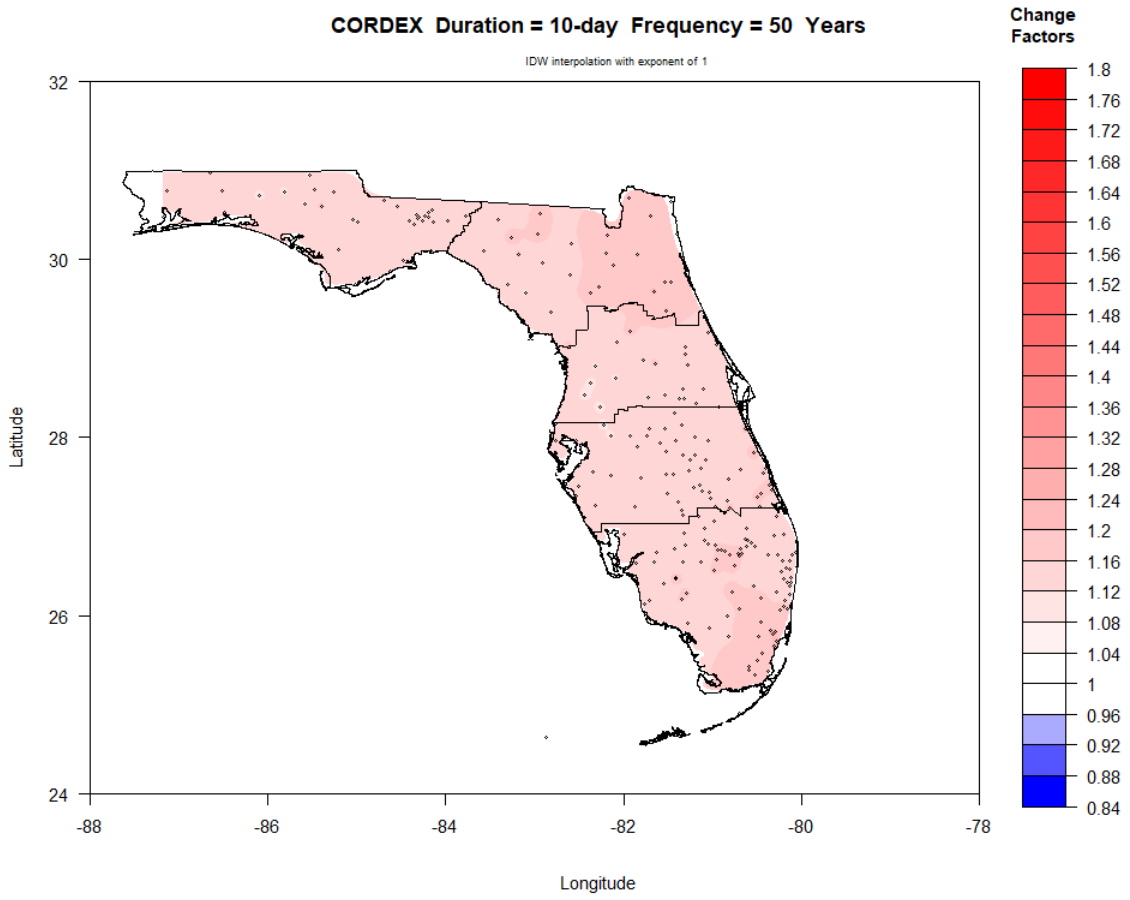

Figure III-22. Map of NEAR period (2030-2069) change factors across Florida for 10-day duration and 50-year return period.

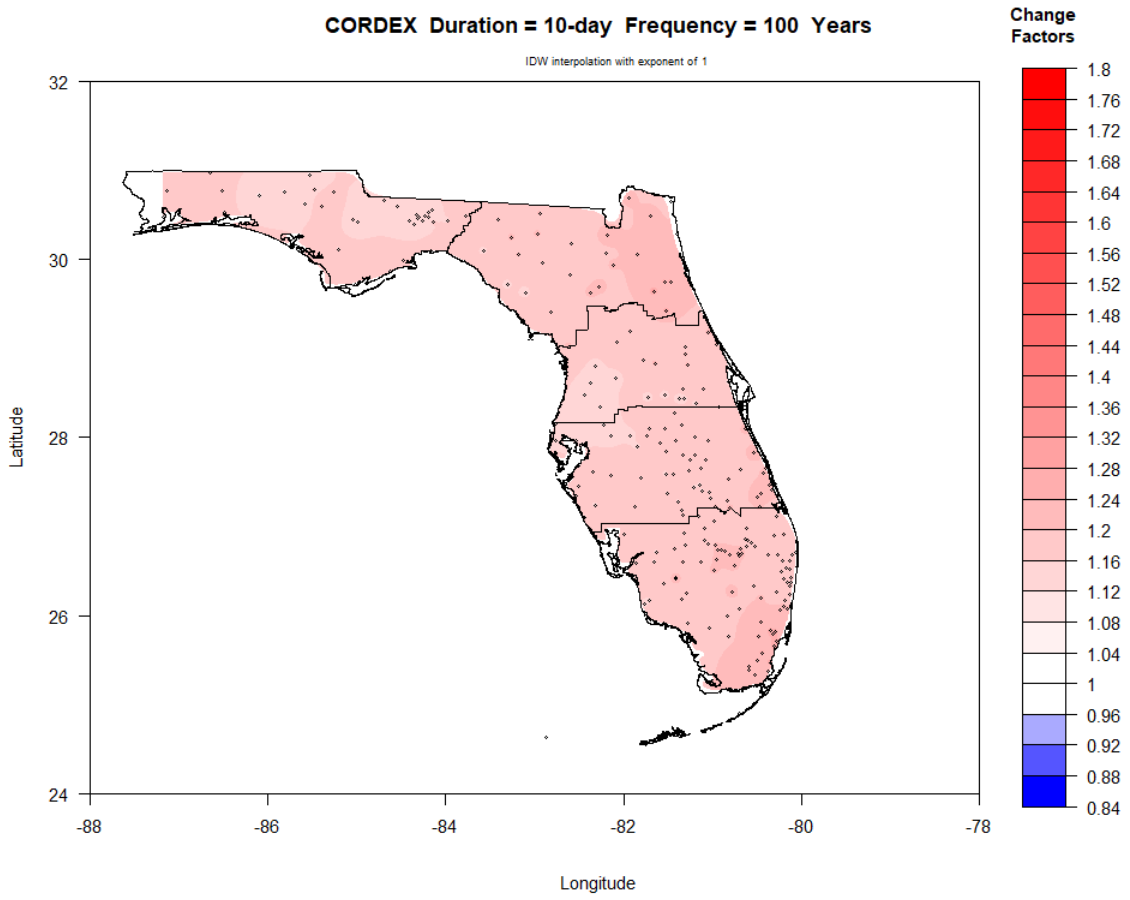

Figure III-23. Map of NEAR period (2030-2069) change factors across Florida for 10-day duration and 100-year return period.

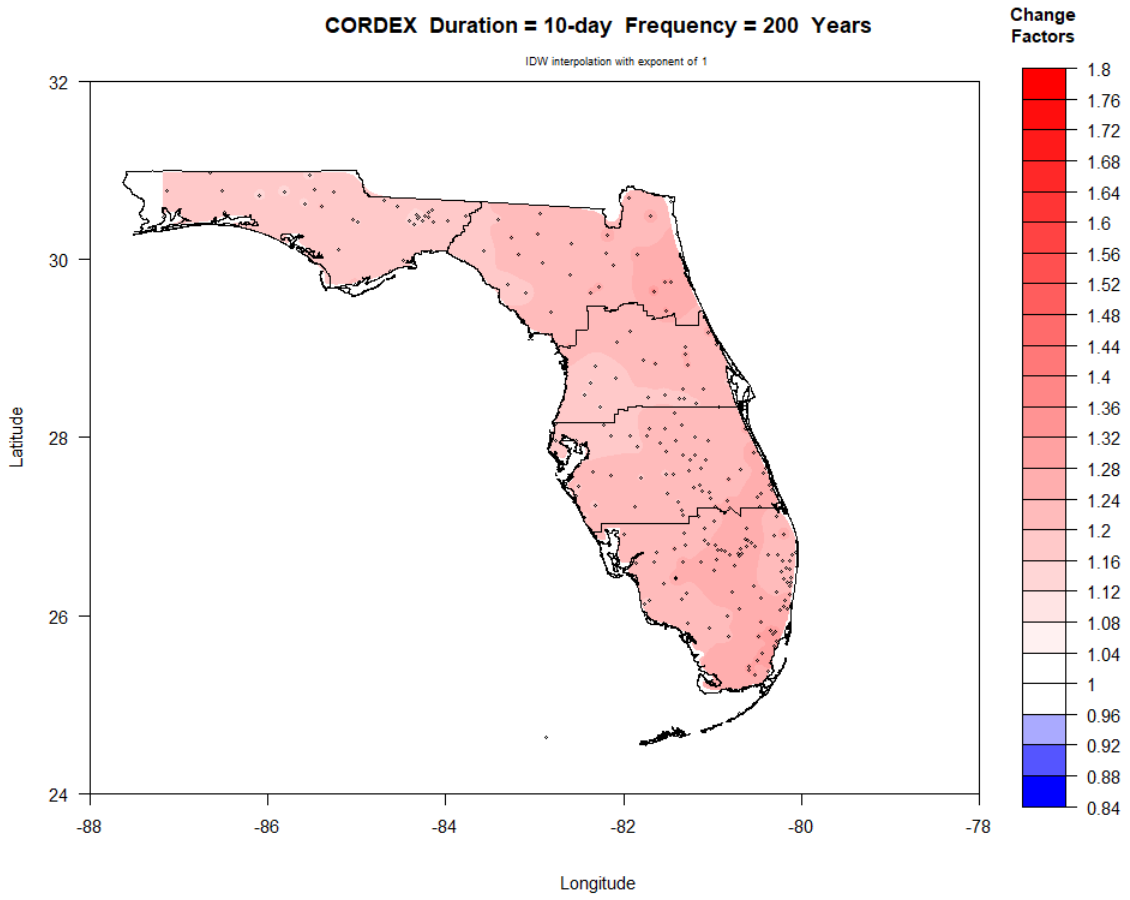

Figure III-24. Map of NEAR period (2030-2069) change factors across Florida for 10-day duration and 200-year return period.

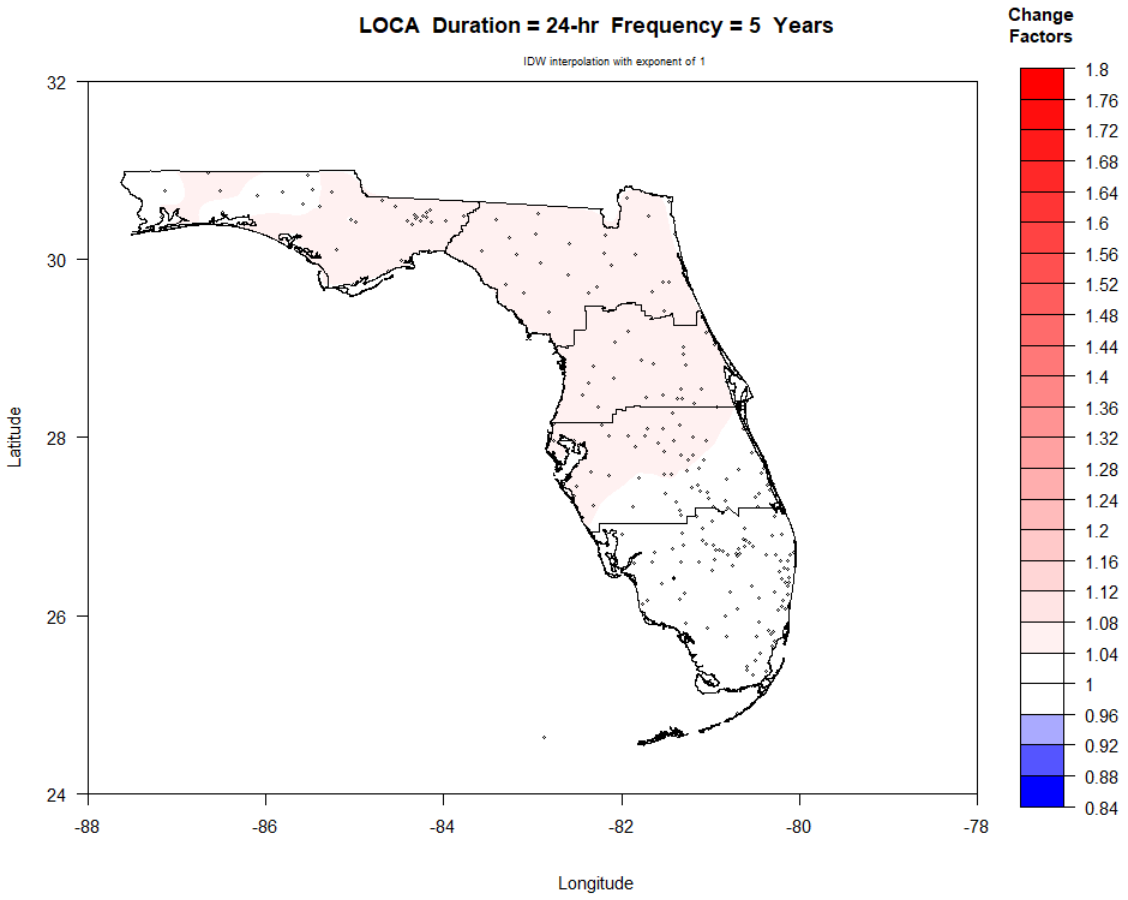

Figure III-25. Map of NEAR period (2030-2069) change factors across Florida for 24-hr duration and 5-year return period.

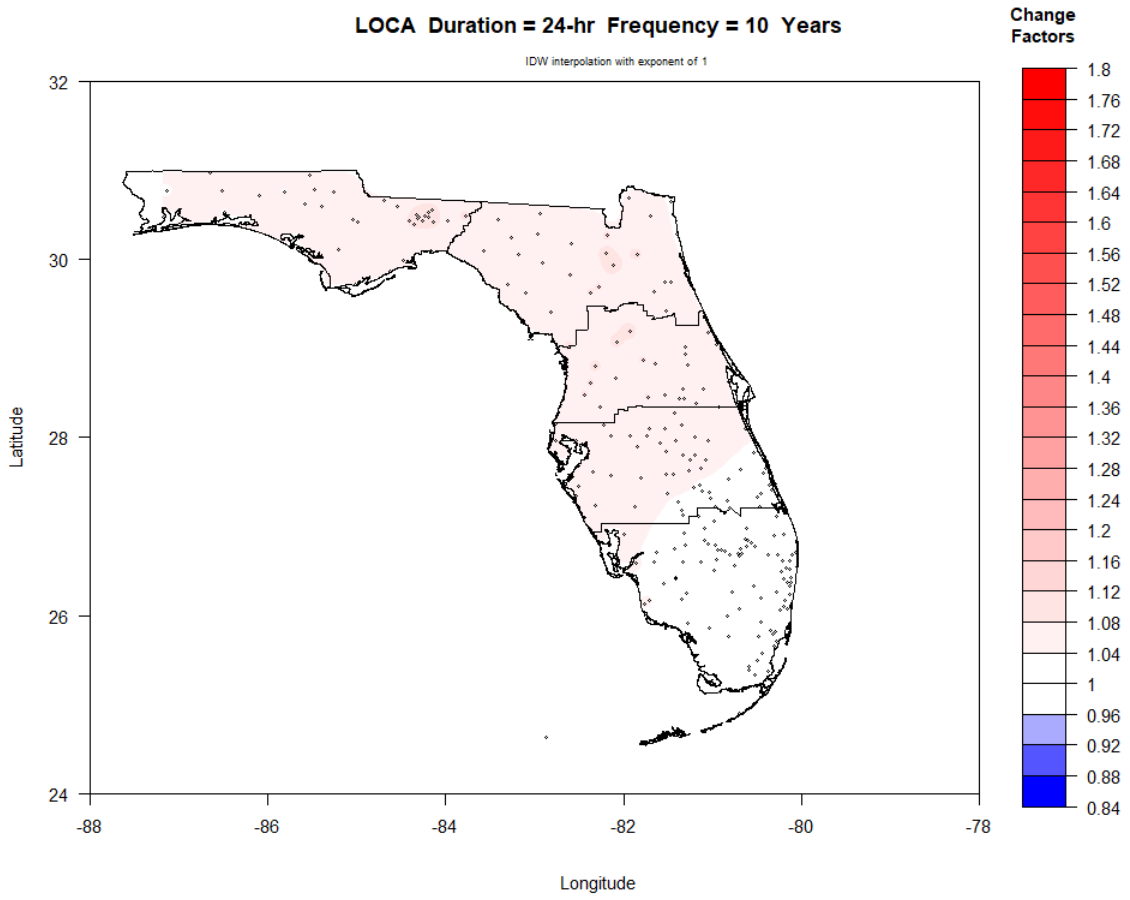

Figure III-26. Map of NEAR period (2030-2069) change factors across Florida for 24-hr duration and 10-year return period.

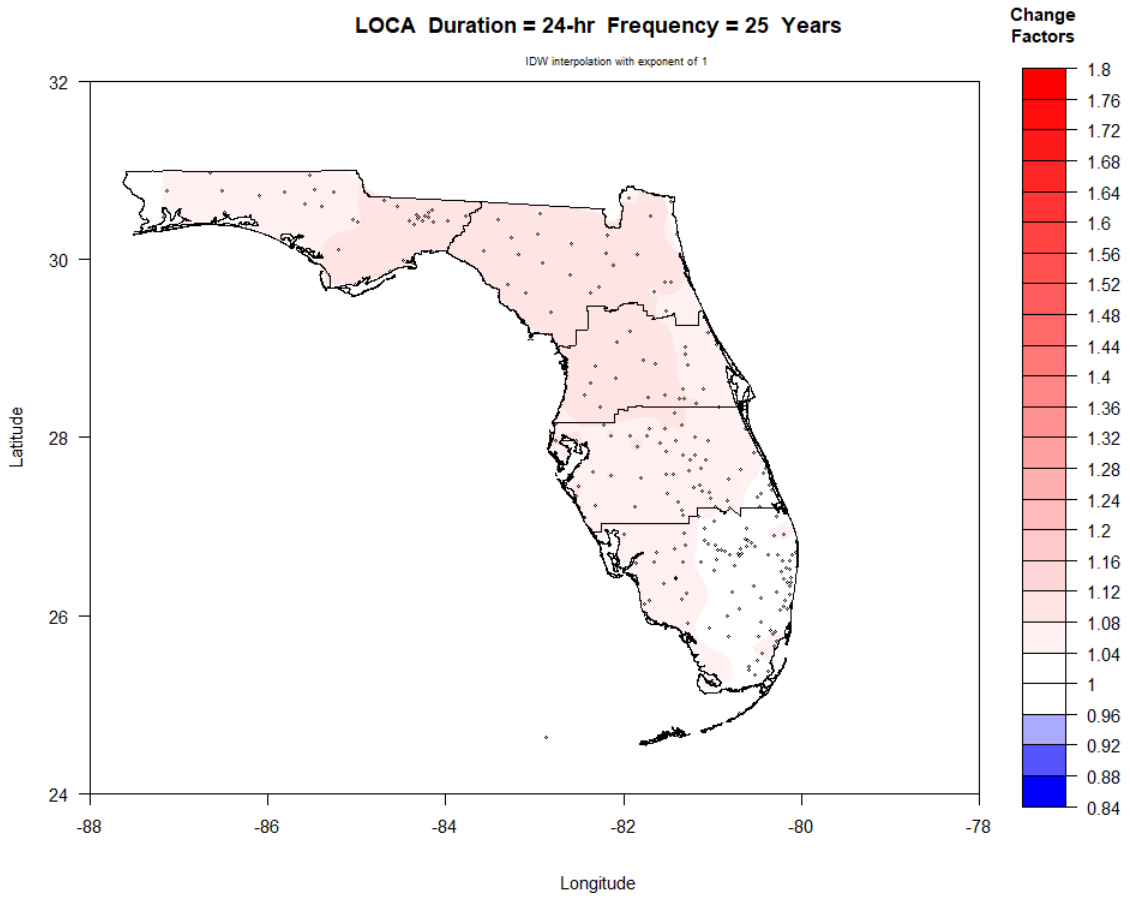

Figure III-27. Map of NEAR period (2030-2069) change factors across Florida for 24-hr duration and 25-year return period.

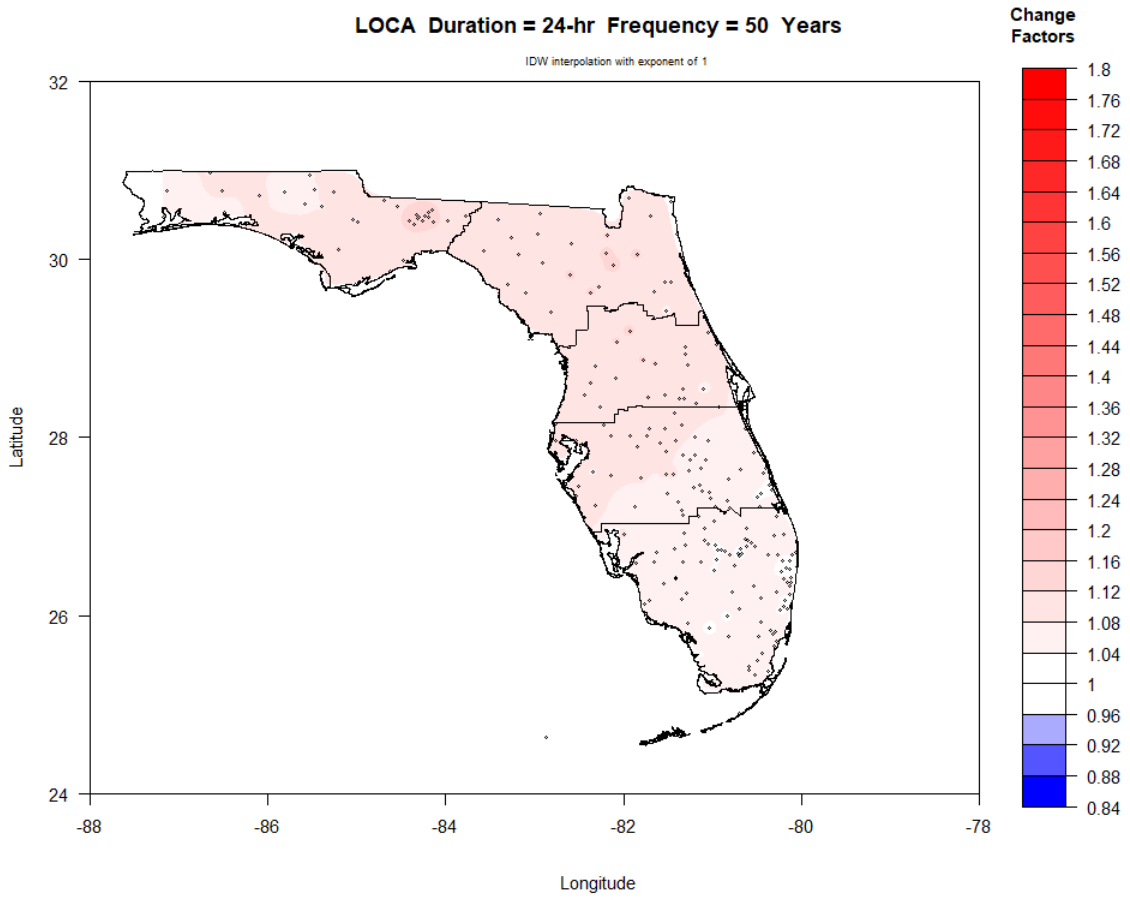

Figure III-28. Map of NEAR period (2030-2069) change factors across Florida for 24-hr duration and 50-year return period.

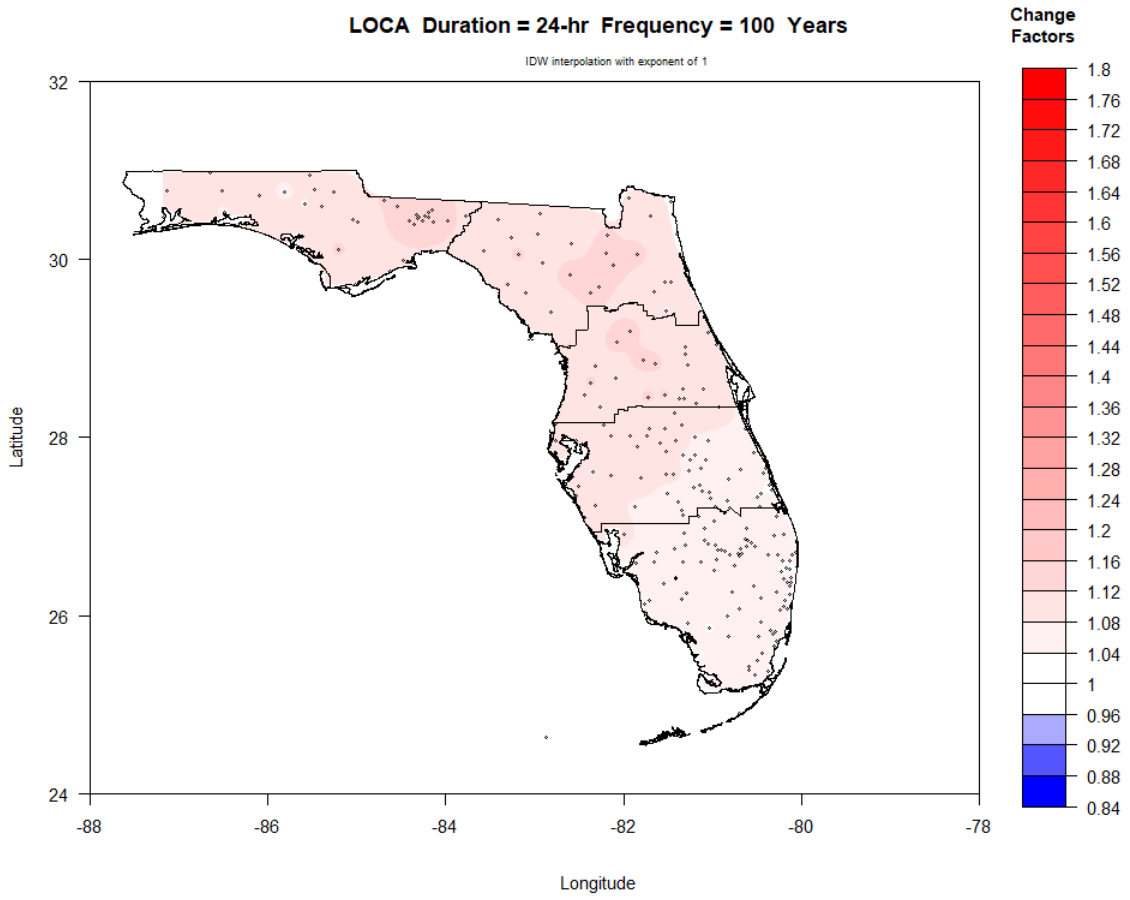

Figure III-29. Map of NEAR period (2030-2069) change factors across Florida for 24-hr duration and 100-year return period.

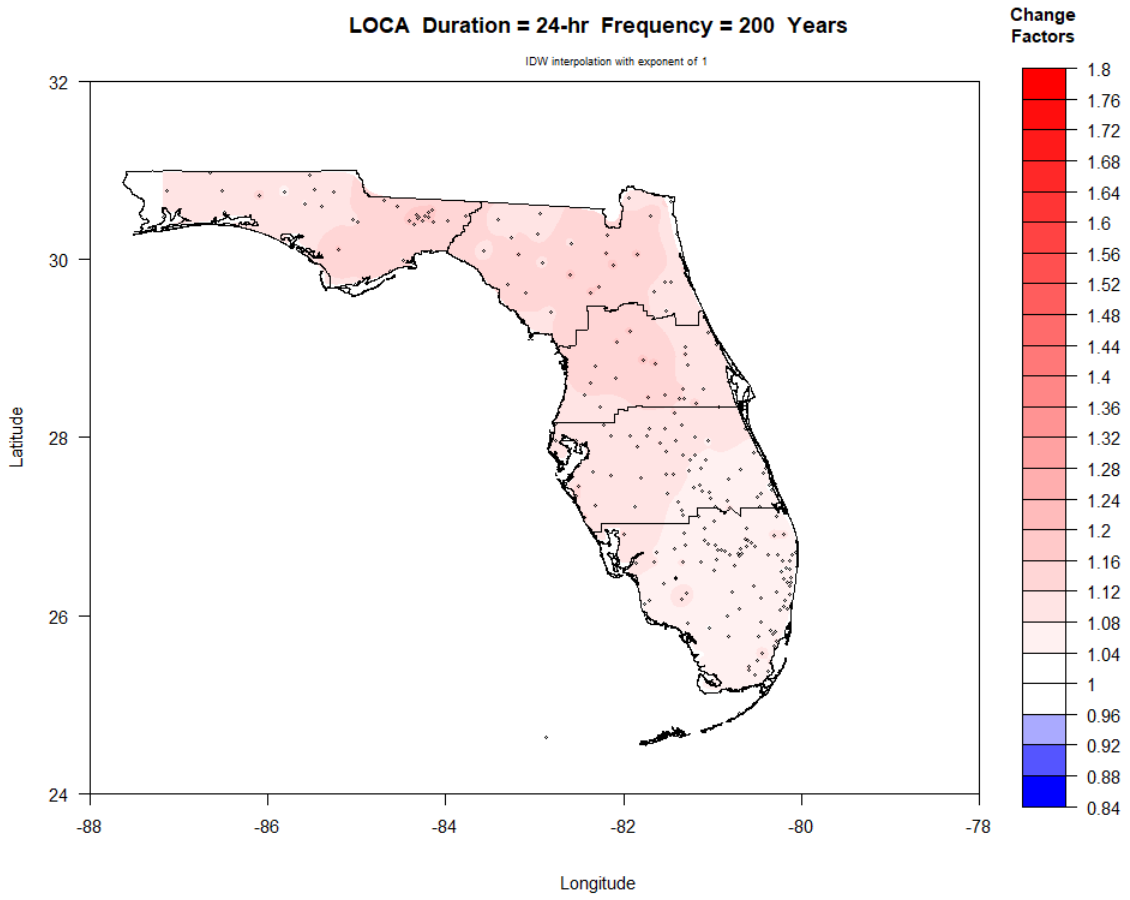

Figure III-30. Map of NEAR period (2030-2069) change factors across Florida for 24-hr duration and 200-year return period.

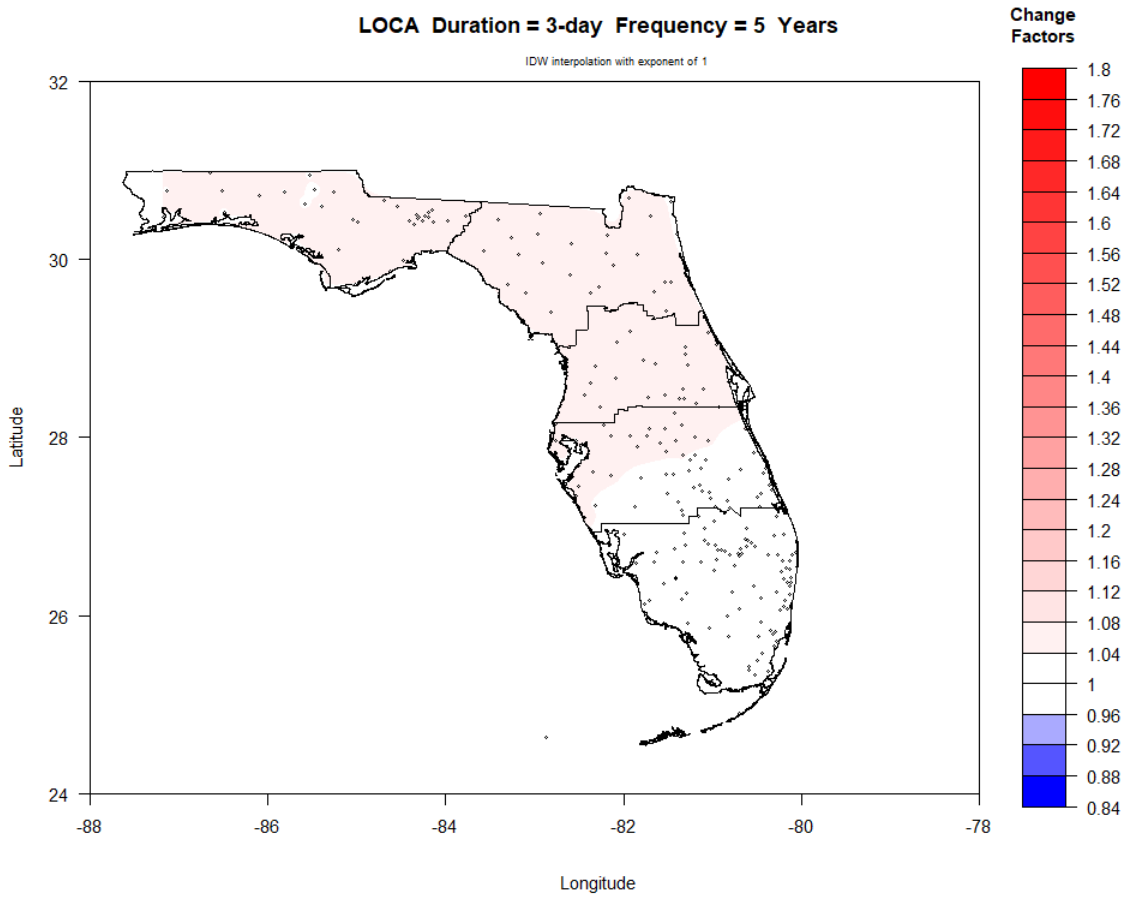

Figure III-31. Map of NEAR period (2030-2069) change factors across Florida for 3-day duration and 5-year return period.

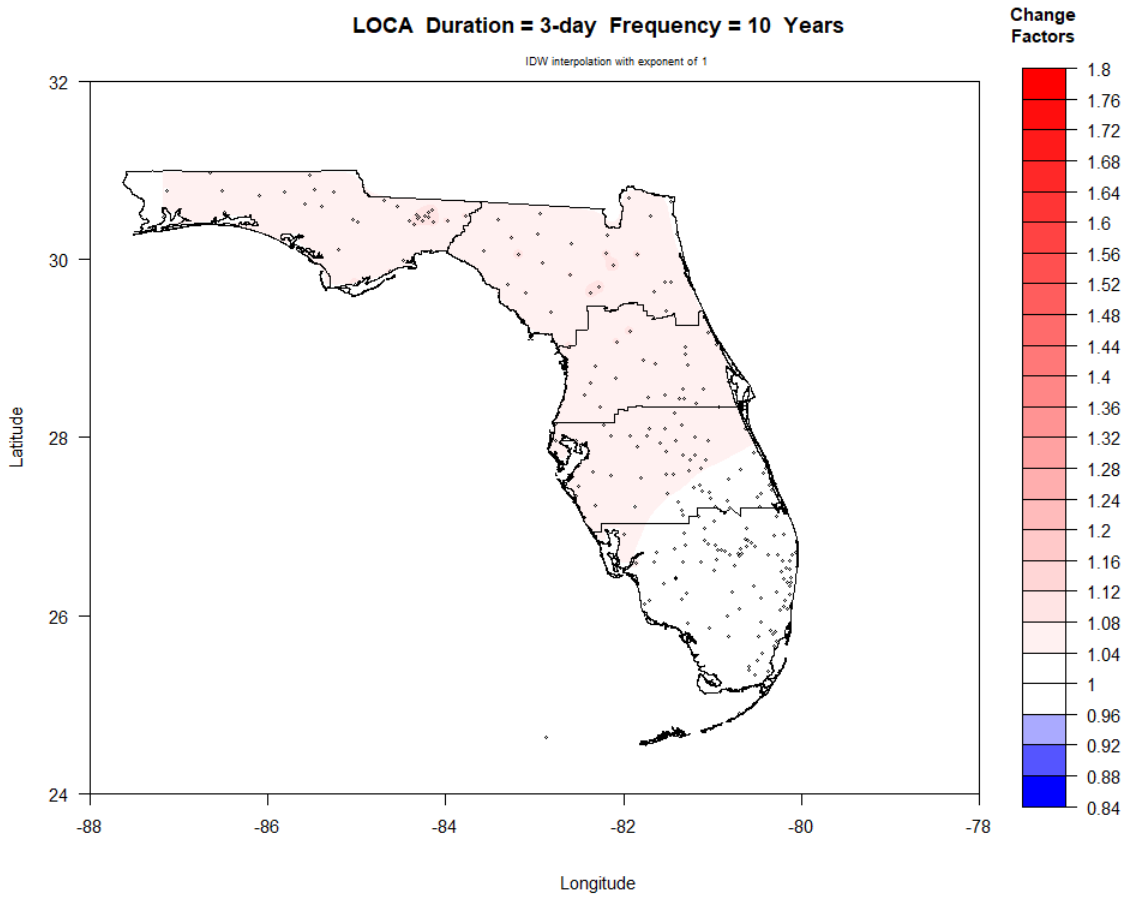

Figure III-32. Map of NEAR period (2030-2069) change factors across Florida for 3-day duration and 10-year return period.

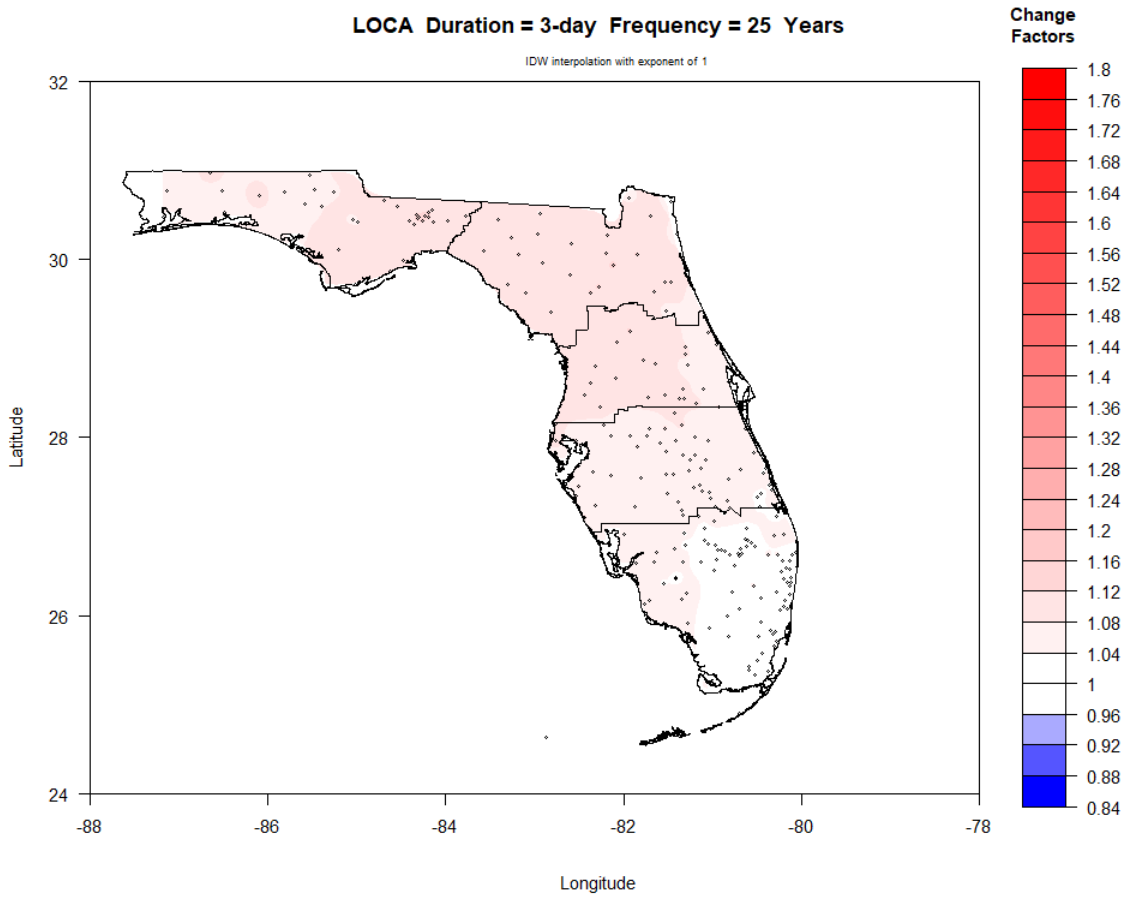

Figure III-33. Map of NEAR period (2030-2069) change factors across Florida for 3-day duration and 25-year return period.

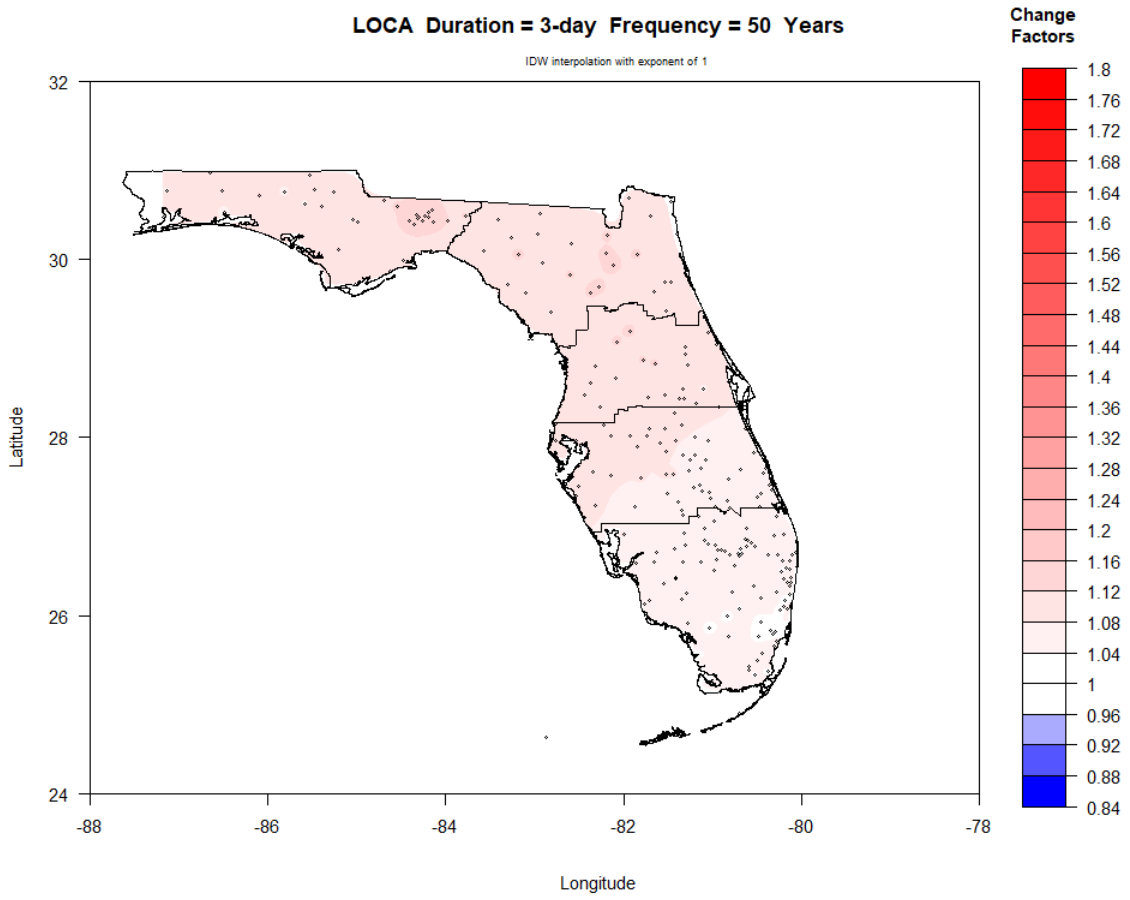

Figure III-34. Map of NEAR period (2030-2069) change factors across Florida for 3-day duration and 50-year return period.

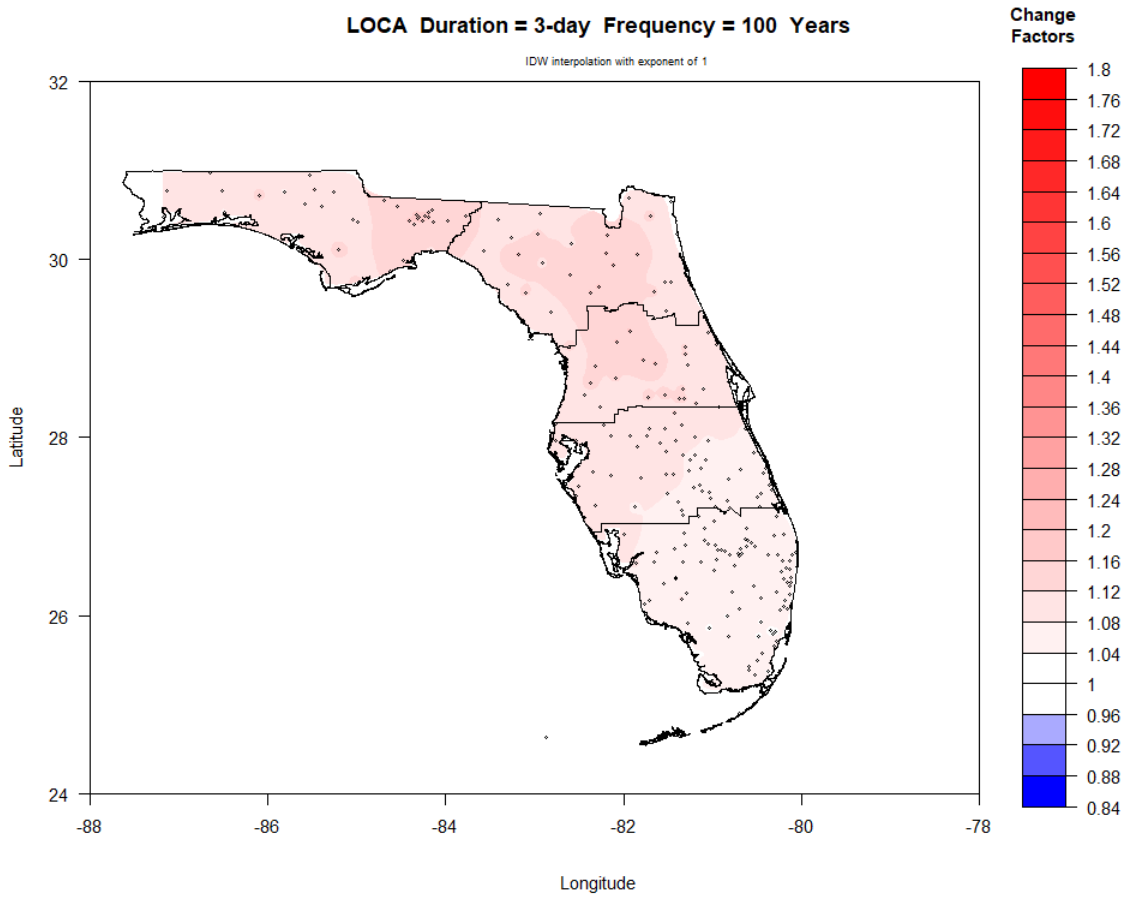

Figure III-35. Map of NEAR period (2030-2069) change factors across Florida for 3-day duration and 100-year return period.

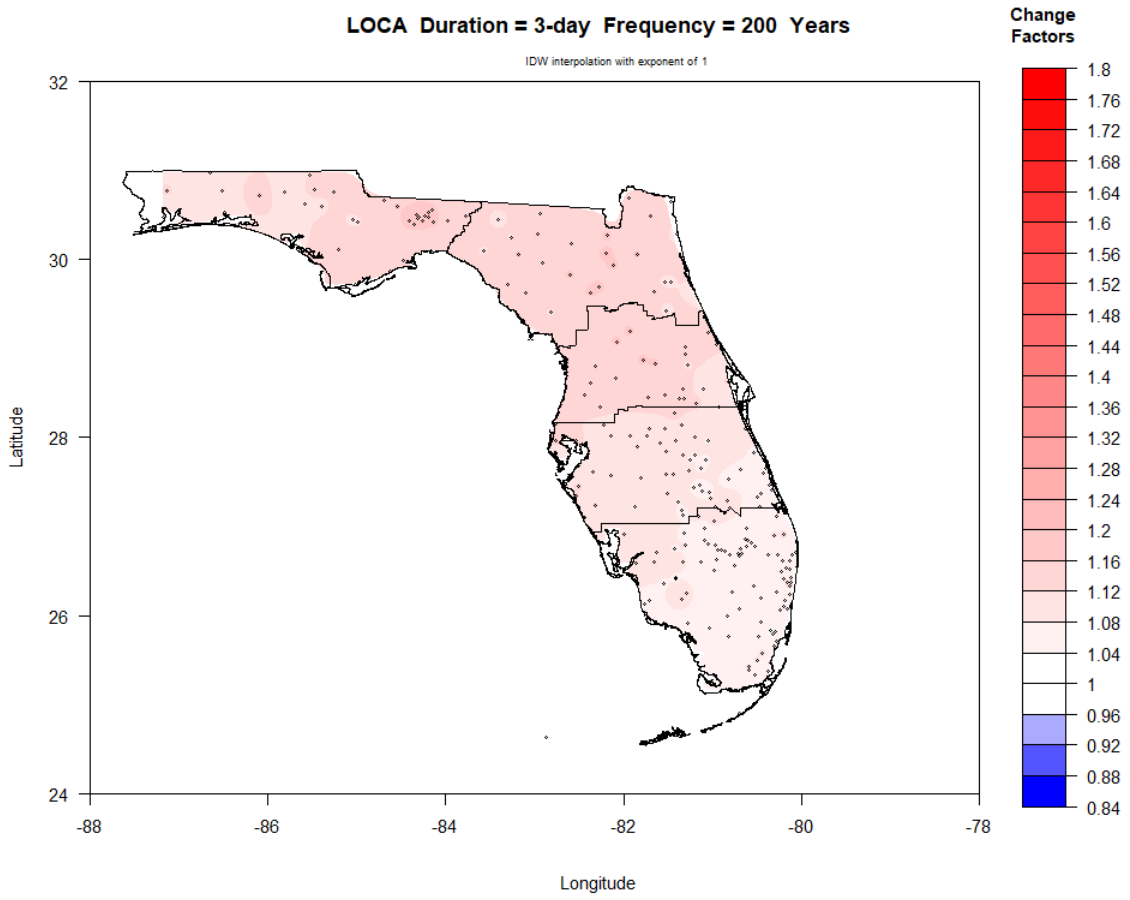

Figure III-36. Map of NEAR period (2030-2069) change factors across Florida for 3-day duration and 200-year return period.

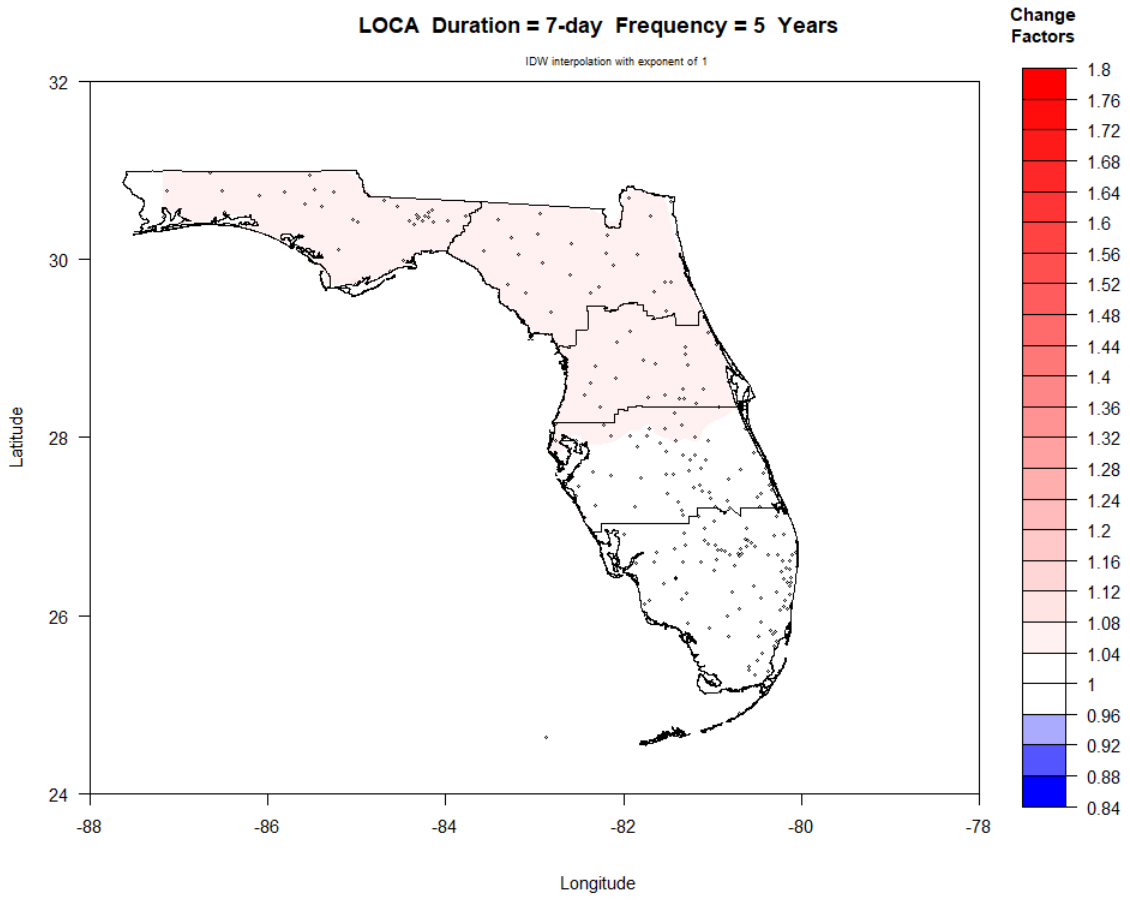

Figure III-37. Map of NEAR period (2030-2069) change factors across Florida for 7-day duration and 5-year return period.

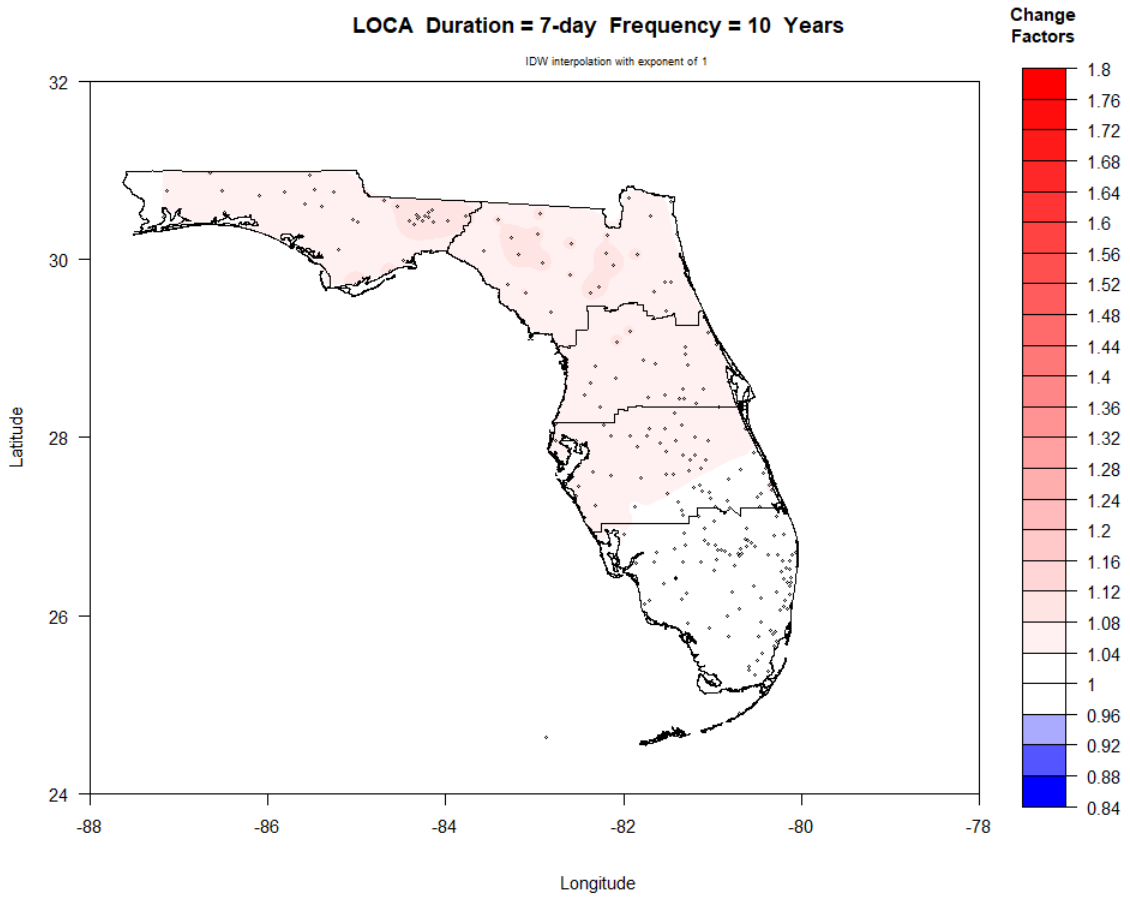

Figure III-38. Map of NEAR period (2030-2069) change factors across Florida for 7-day duration and 10-year return period.

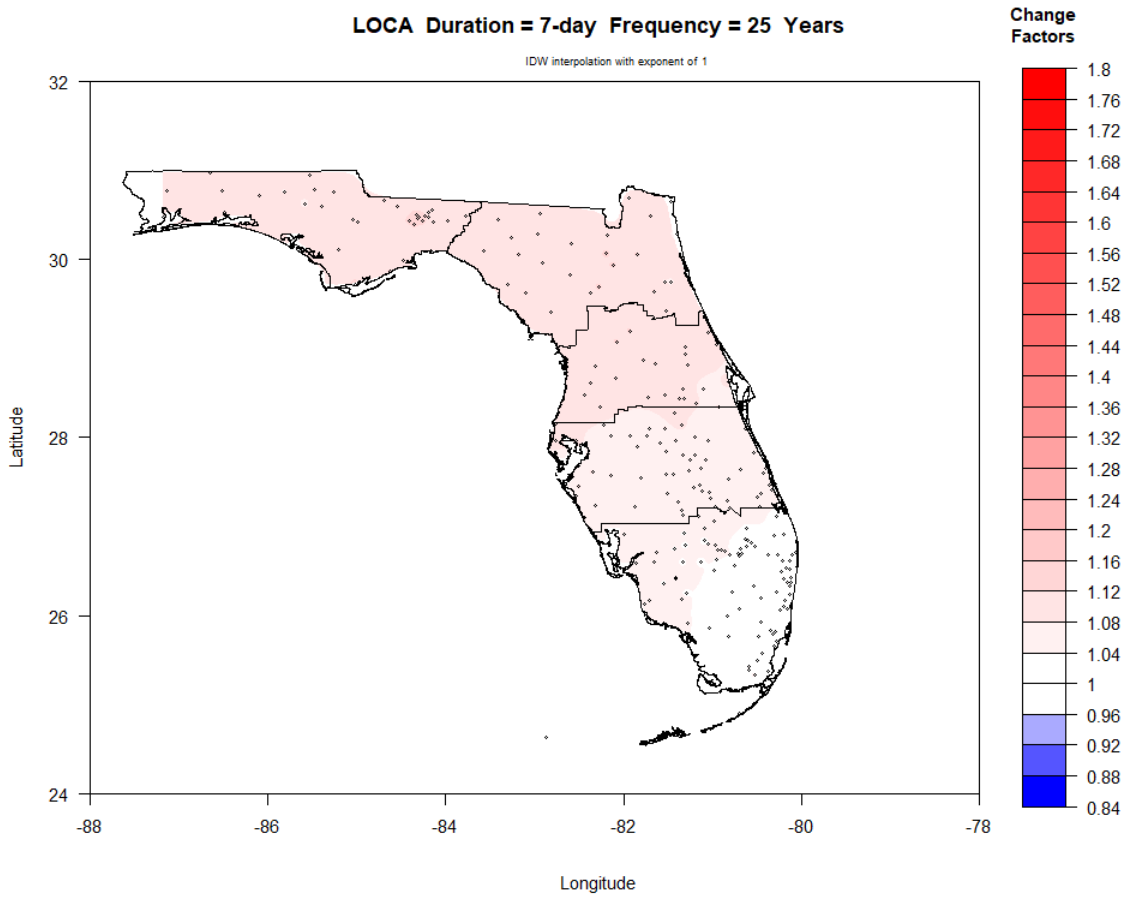

Figure III-39. Map of NEAR period (2030-2069) change factors across Florida for 7-day duration and 25-year return period.

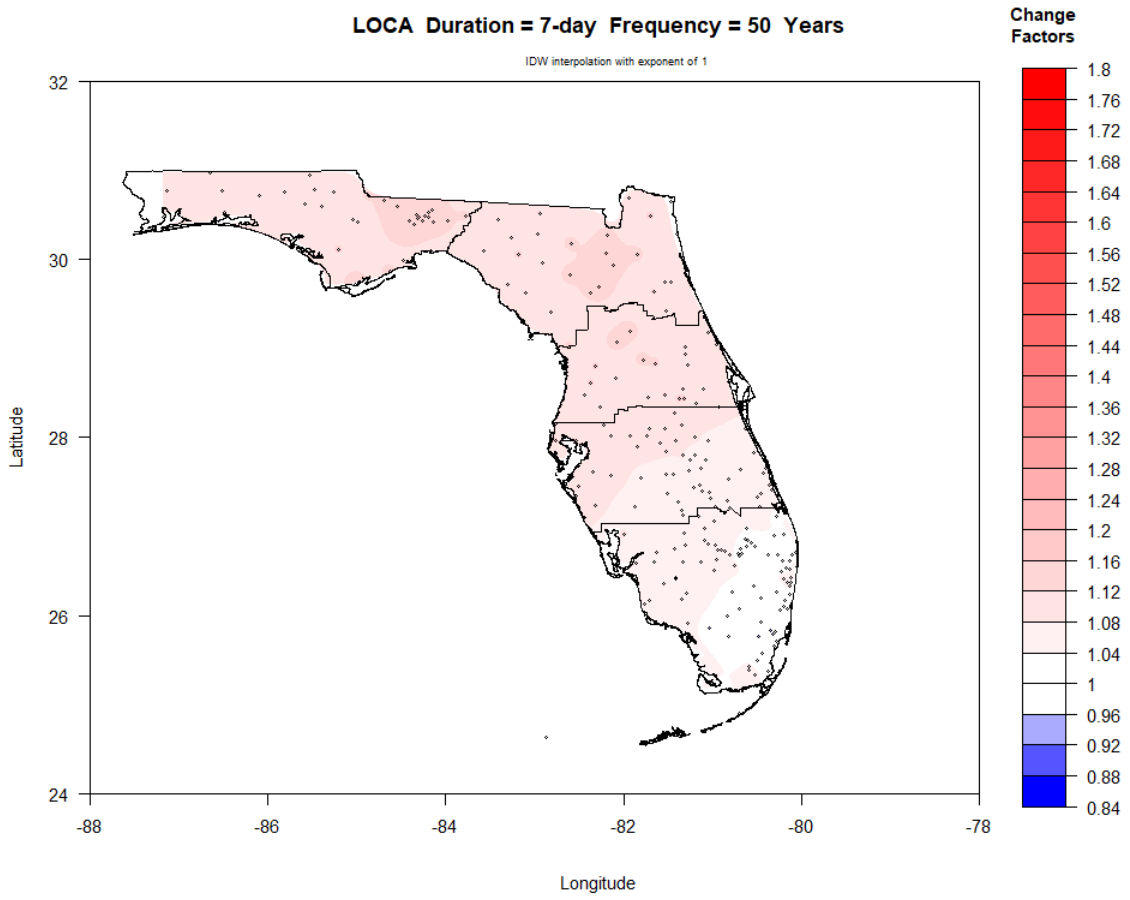

Figure III-40. Map of NEAR period (2030-2069) change factors across Florida for 7-day duration and 50-year return period.

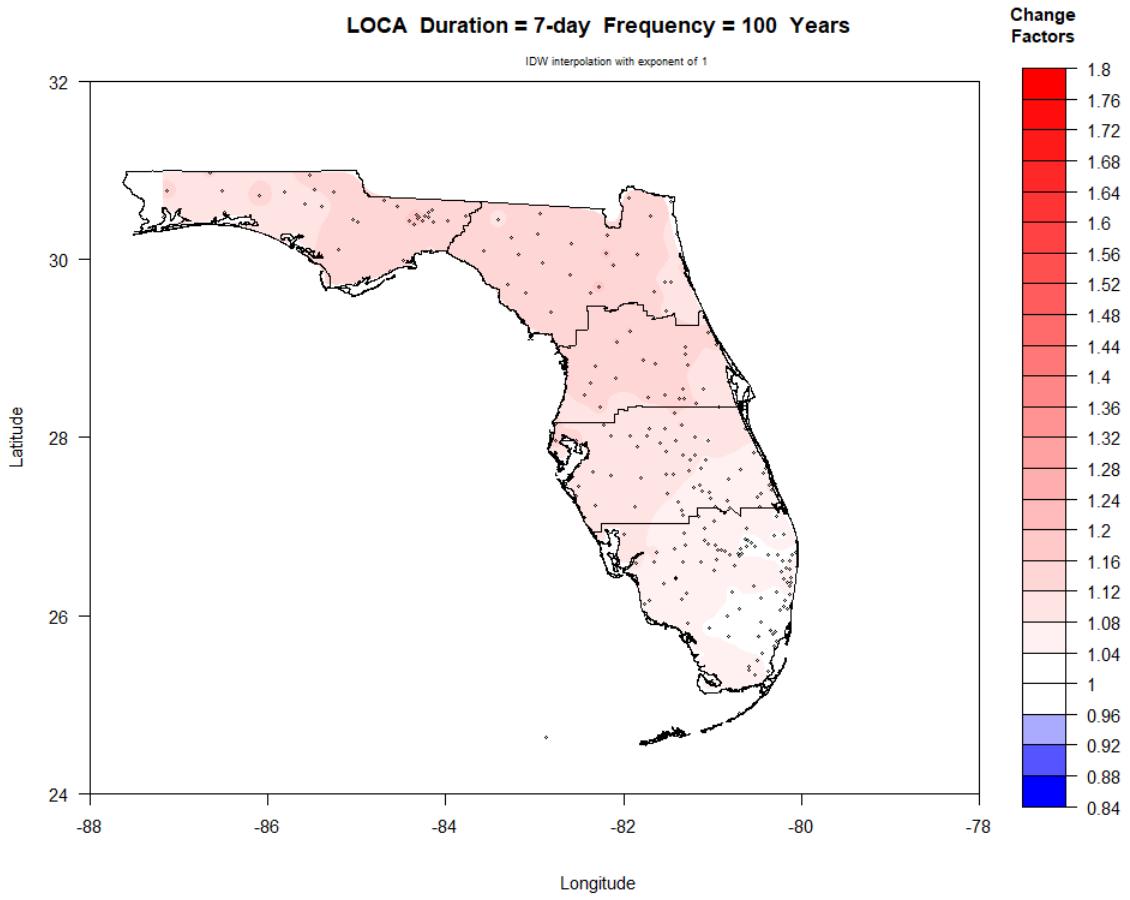

Figure III-41. Map of NEAR period (2030-2069) change factors across Florida for 7-day duration and 100-year return period.

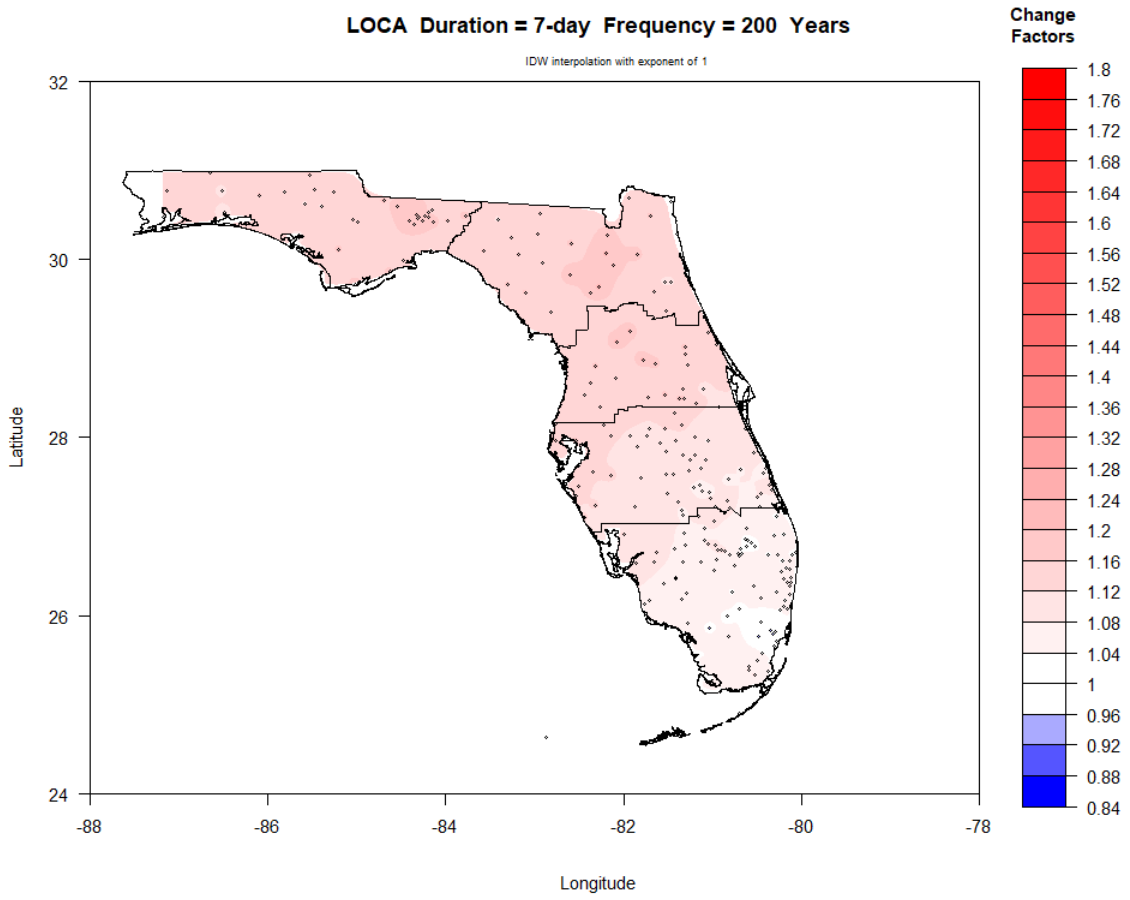

Figure III-42. Map of NEAR period (2030-2069) change factors across Florida for 7-day duration and 200-year return period.

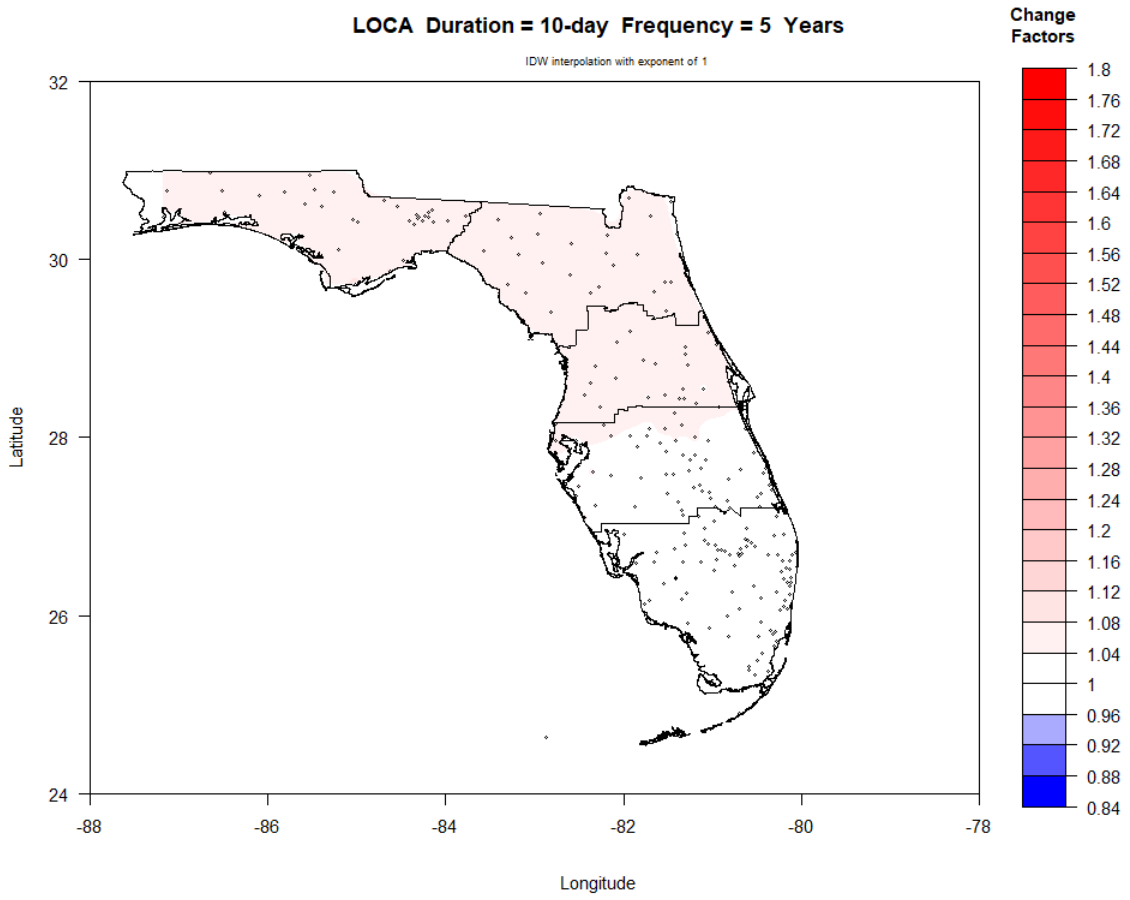

Figure III-43. Map of NEAR period (2030-2069) change factors across Florida for 10-day duration and 5-year return period.

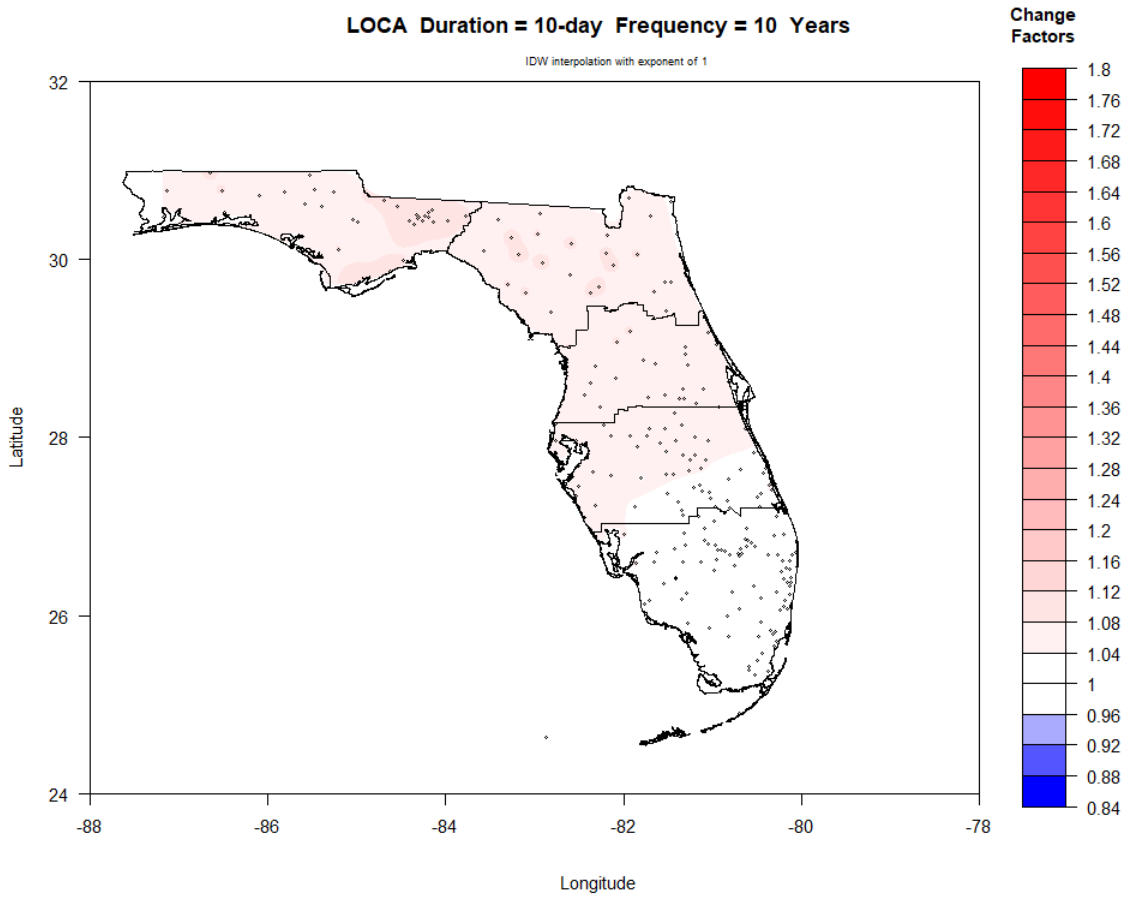

Figure III-44. Map of NEAR period (2030-2069) change factors across Florida for 10-day duration and 10-year return period.

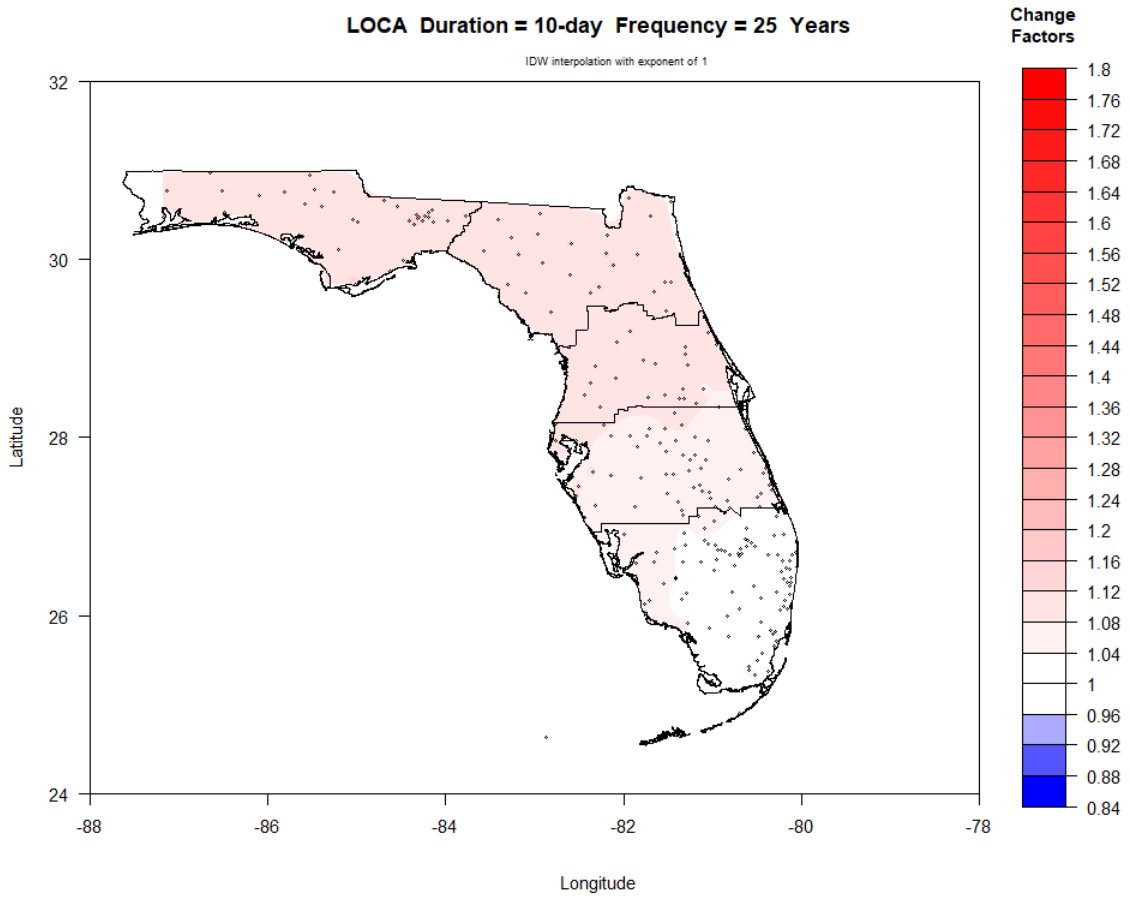

Figure III-45. Map of NEAR period (2030-2069) change factors across Florida for 10-day duration and 25-year return period.

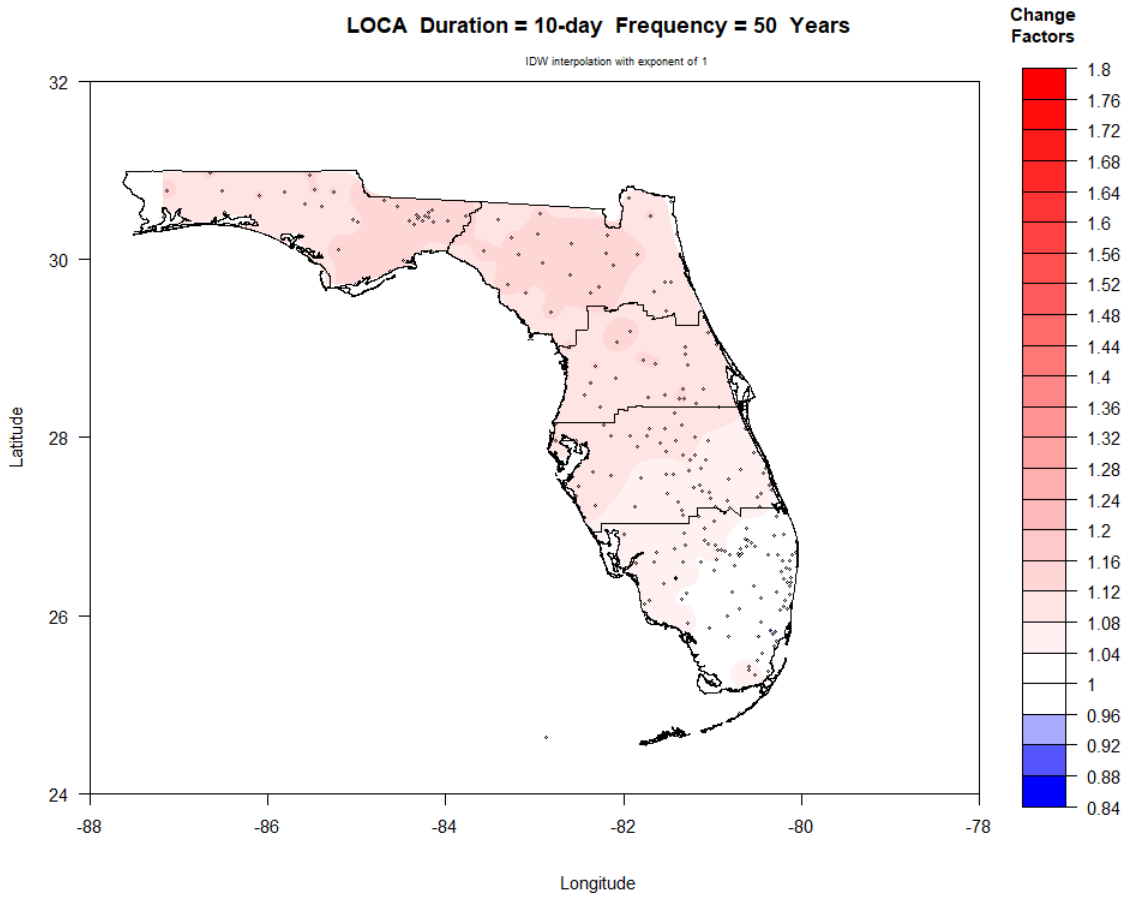

Figure III-46. Map of NEAR period (2030-2069) change factors across Florida for 10-day duration and 50-year return period.

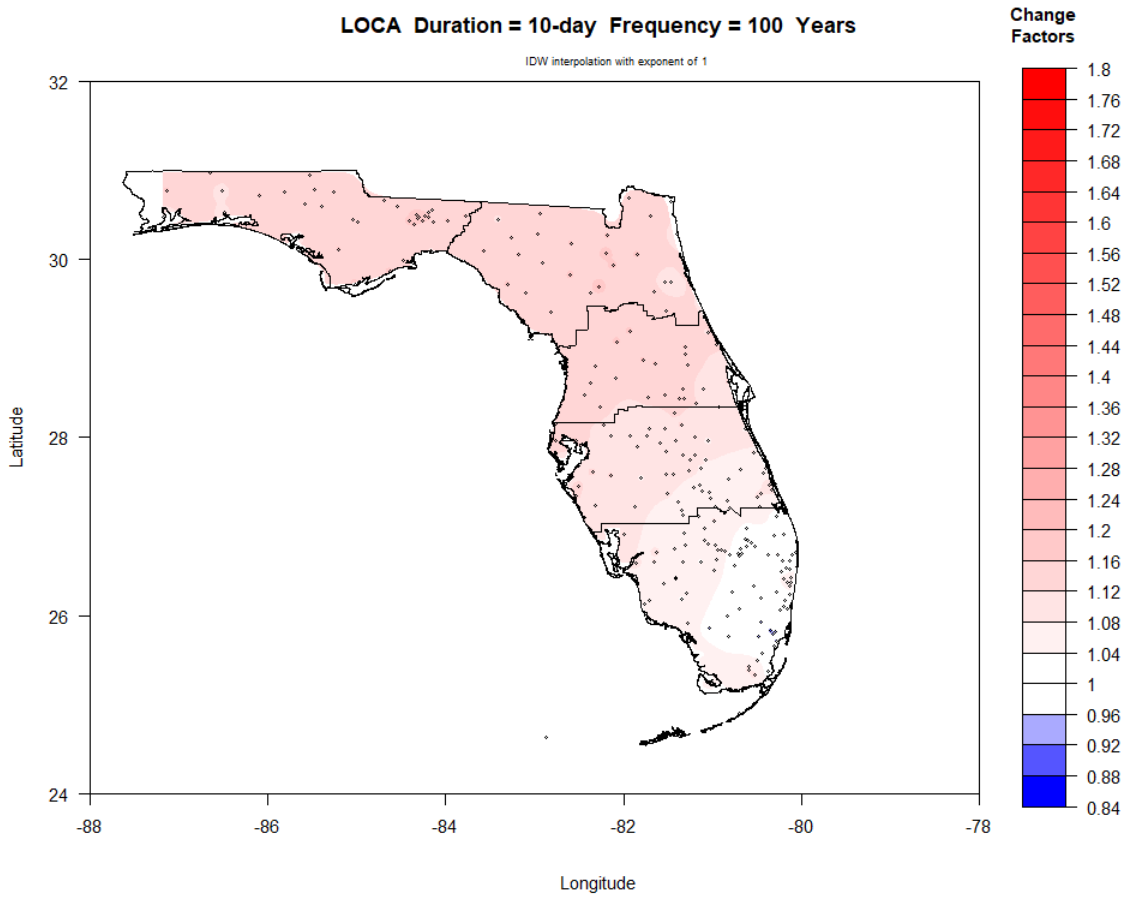

Figure III-47. Map of NEAR period (2030-2069) change factors across Florida for 10-day duration and 100-year return period.

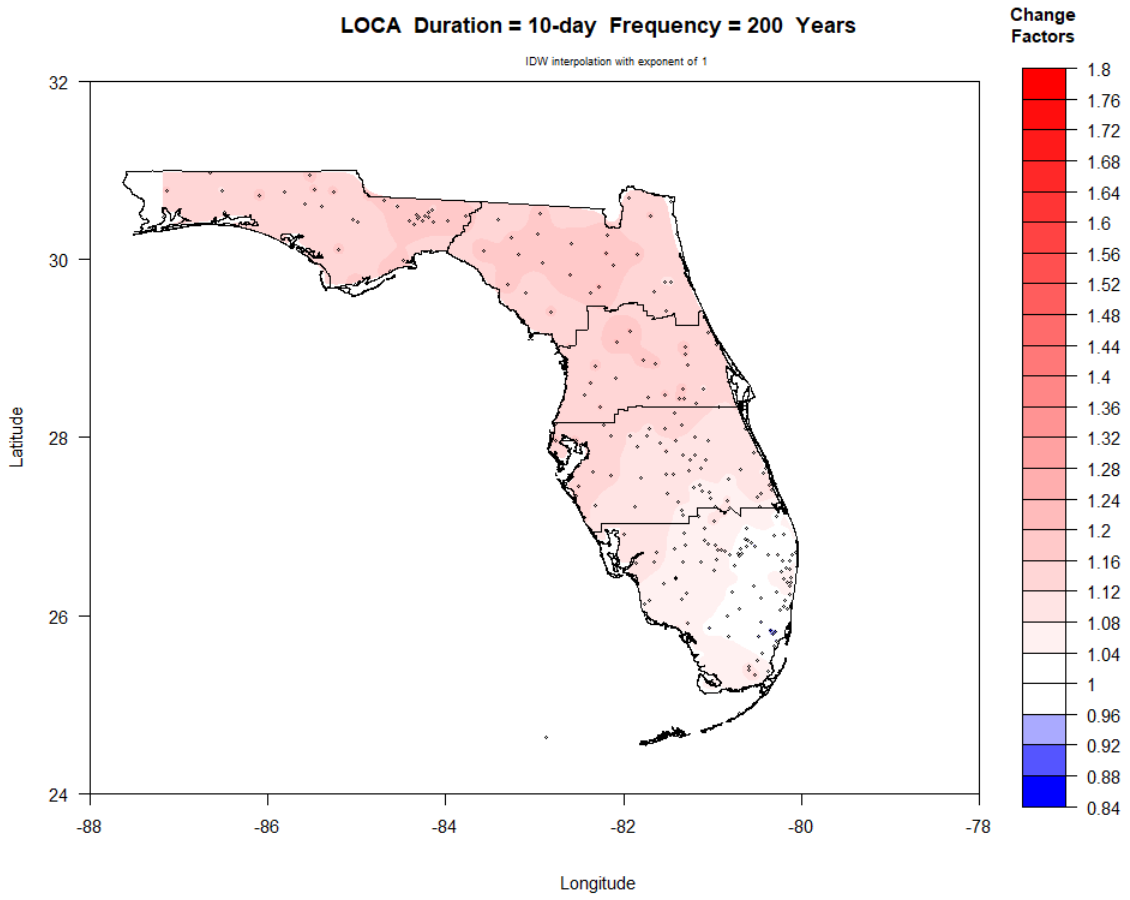

Figure III-48. Map of NEAR period (2030-2069) change factors across Florida for 10-day duration and 200-year return period.

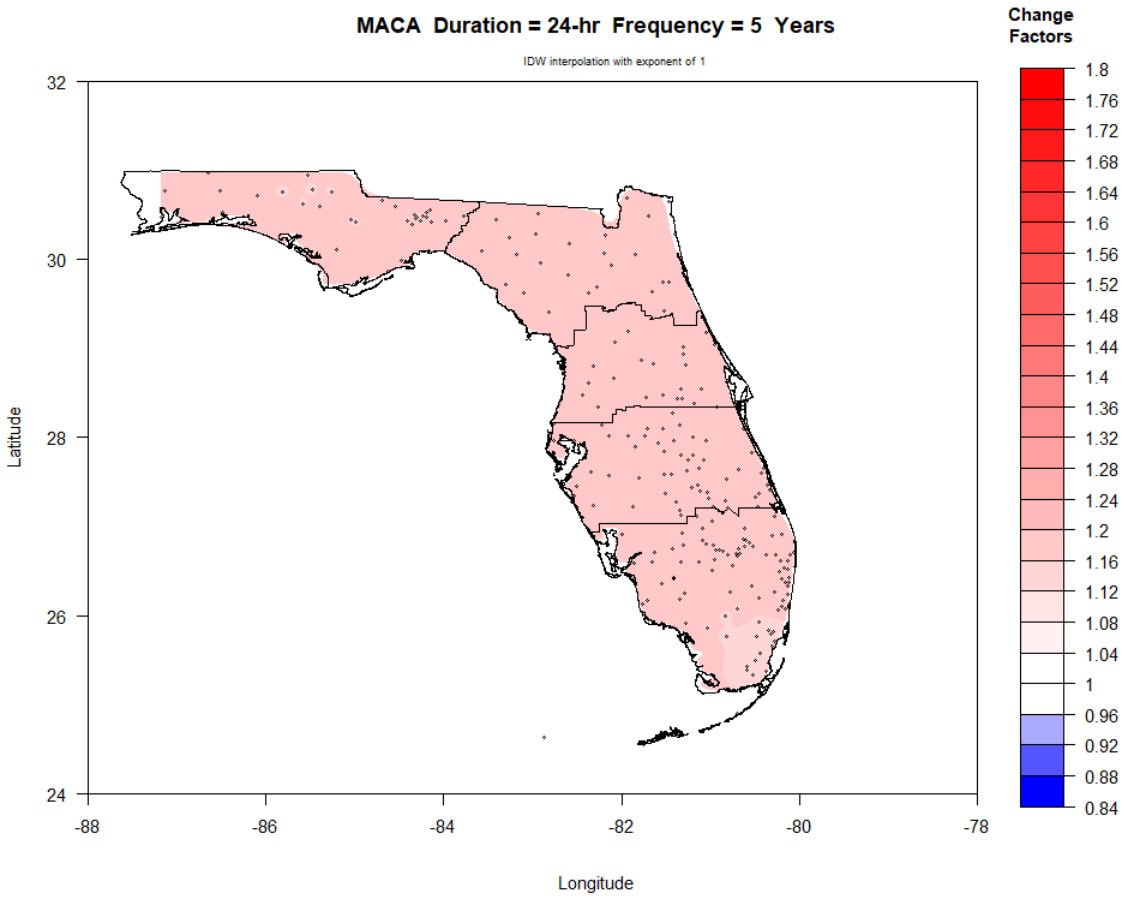

Figure III-49. Map of NEAR period (2030-2069) change factors across Florida for 24-hr duration and 5-year return period.

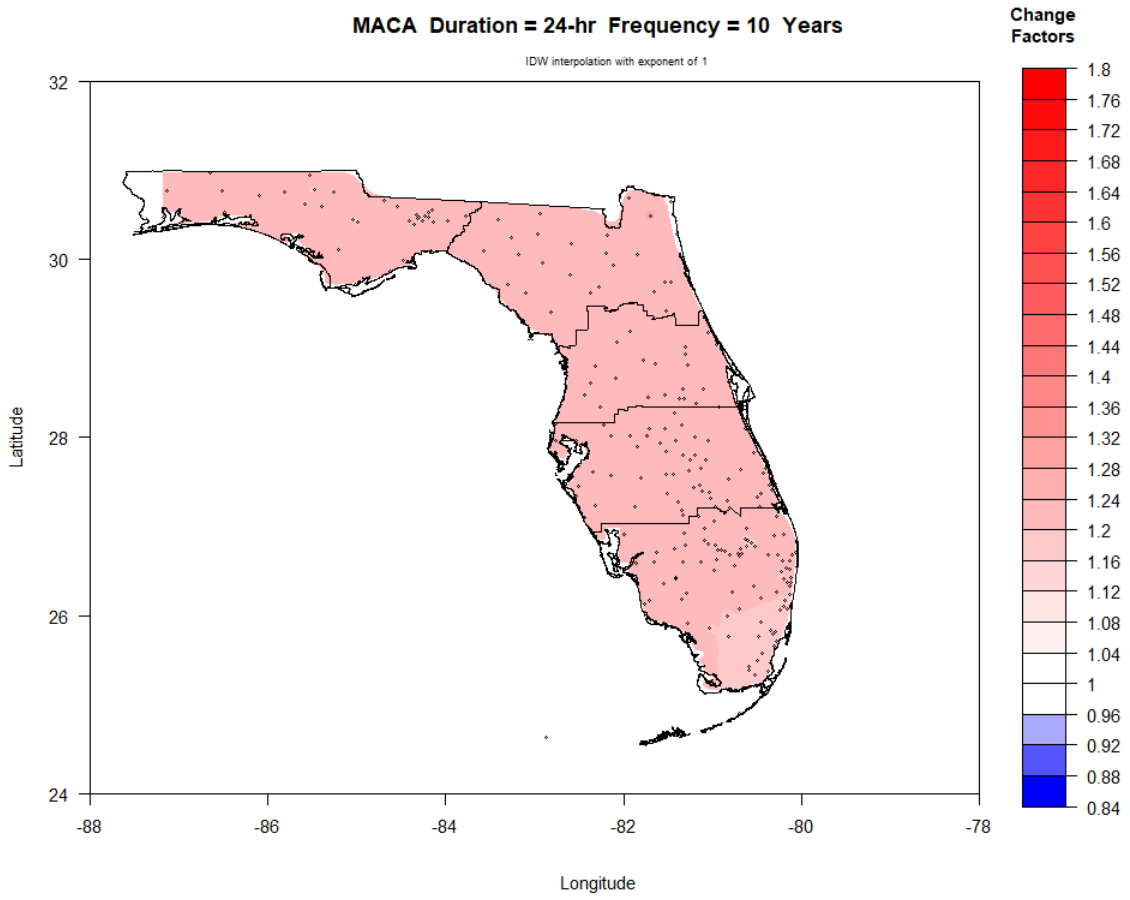

Figure III-50. Map of NEAR period (2030-2069) change factors across Florida for 24-hr duration and 10-year return period.

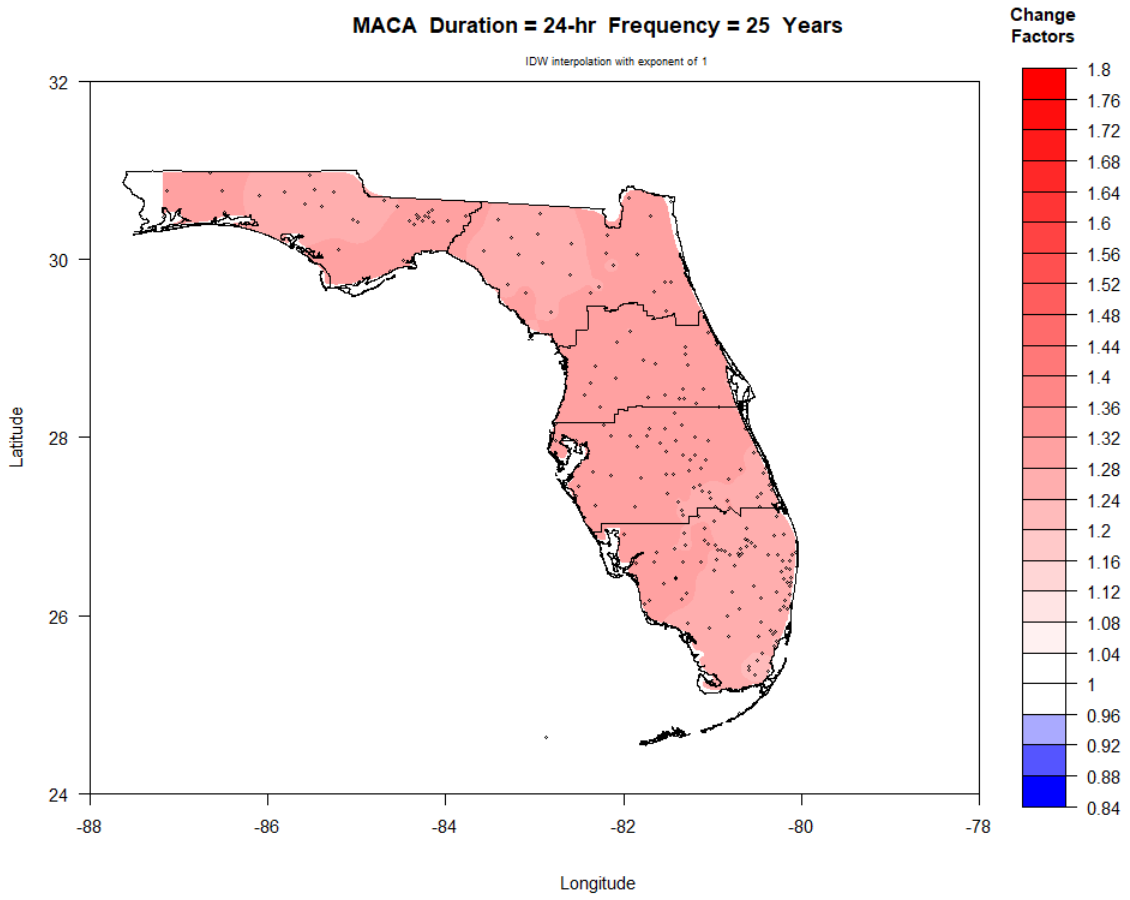

Figure III-51. Map of NEAR period (2030-2069) change factors across Florida for 24-hr duration and 25-year return period.

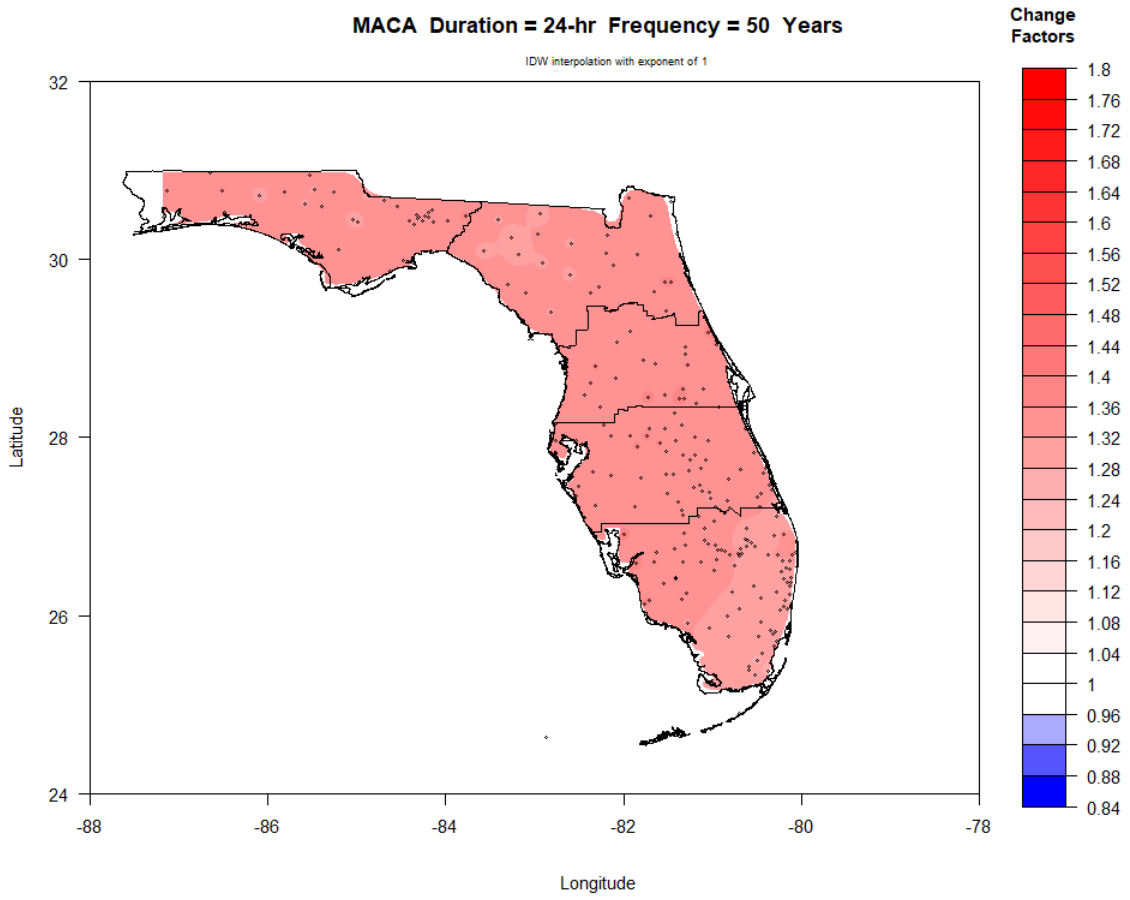

Figure III-52. Map of NEAR period (2030-2069) change factors across Florida for 24-hr duration and 50-year return period.

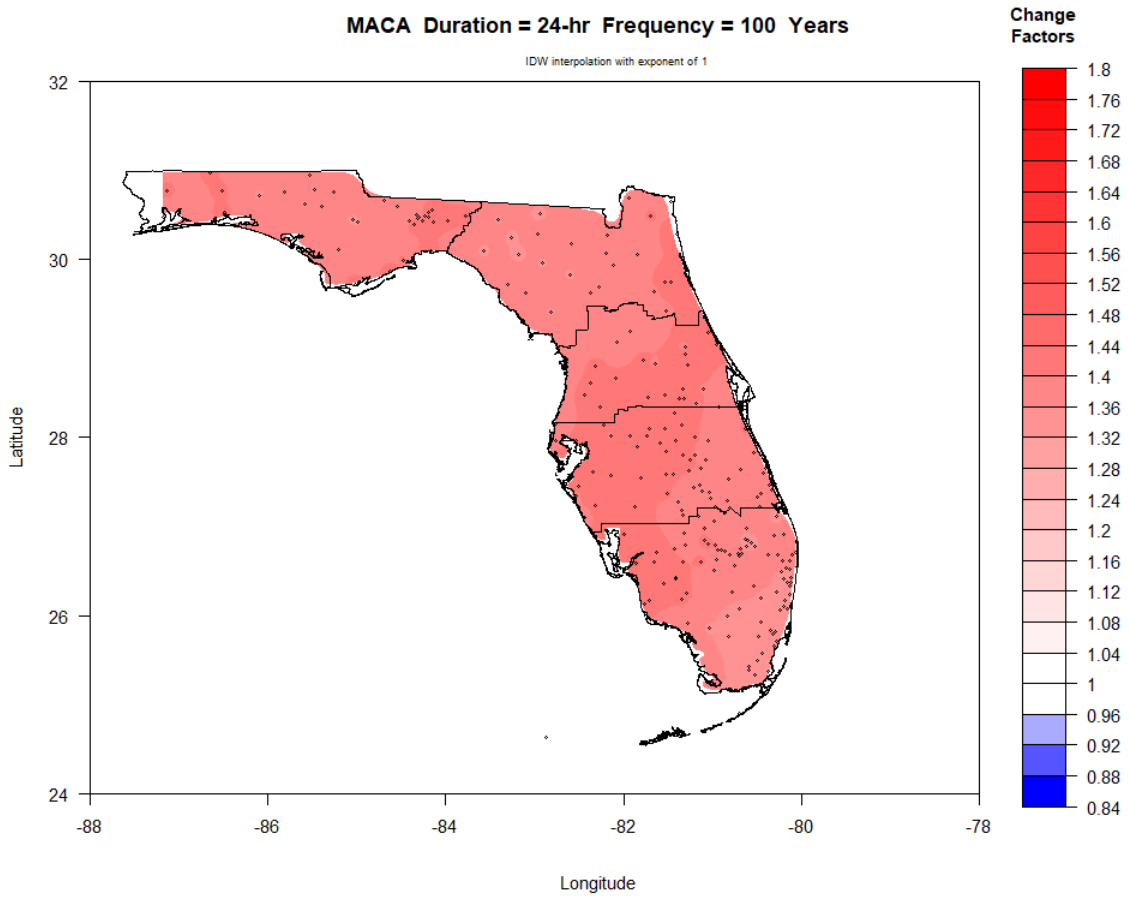

Figure III-53. Map of NEAR period (2030-2069) change factors across Florida for 24-hr duration and 100-year return period.

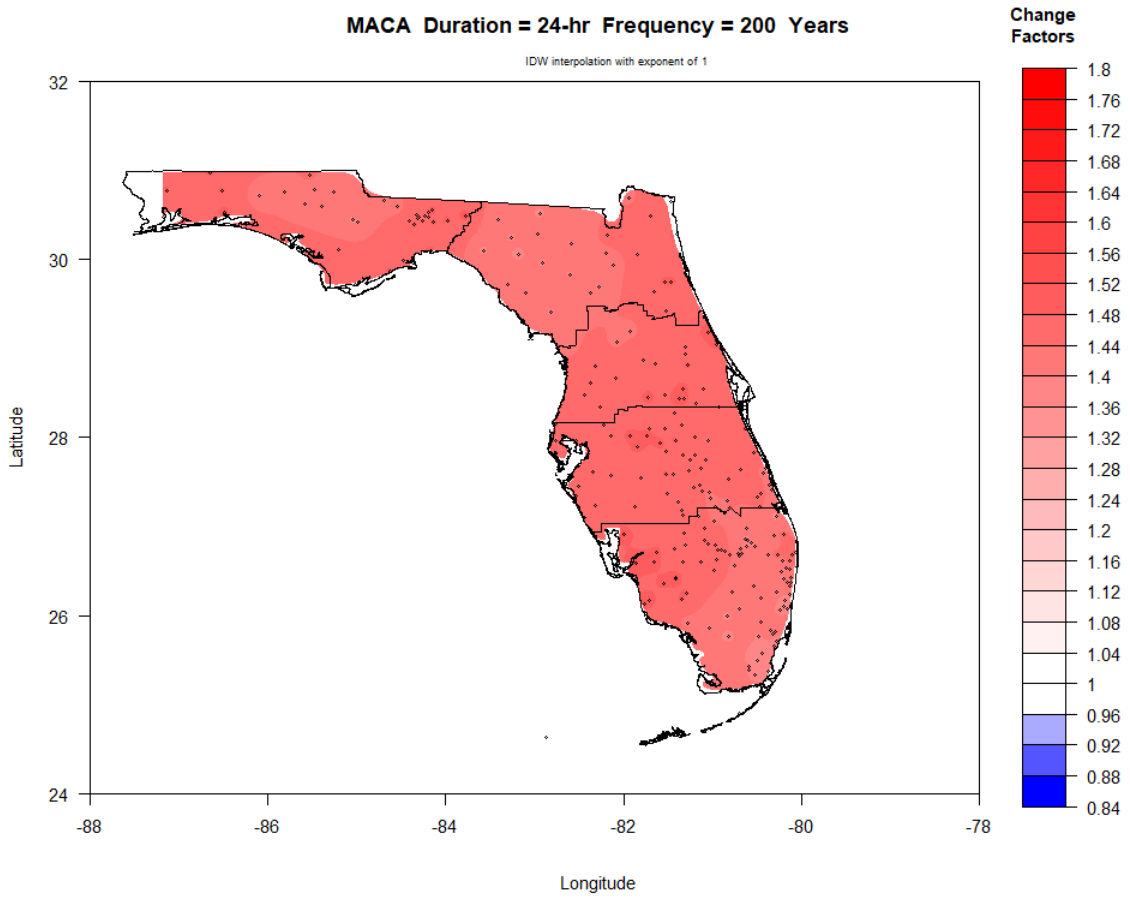

Figure III-54. Map of NEAR period (2030-2069) change factors across Florida for 24-hr duration and 200-year return period.

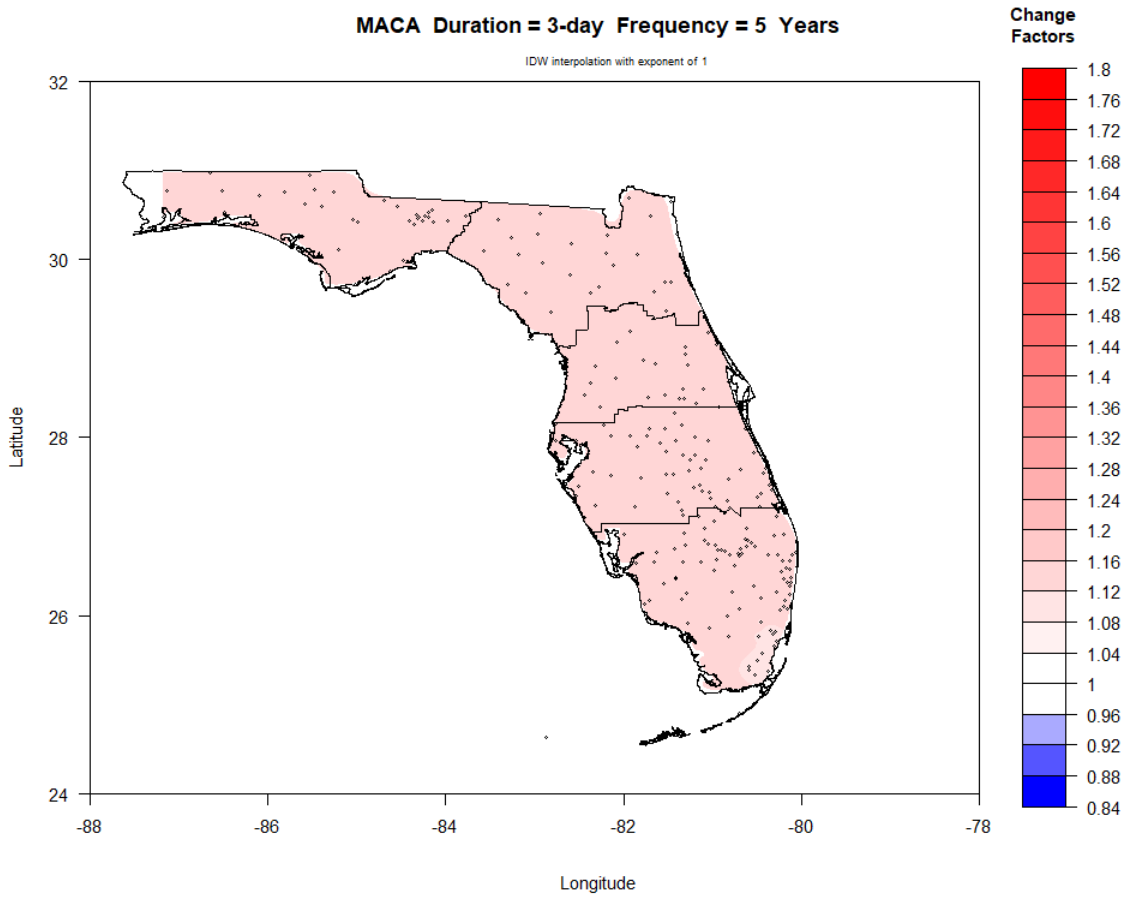

Figure III-55. Map of NEAR period (2030-2069) change factors across Florida for 3-day duration and 5-year return period.

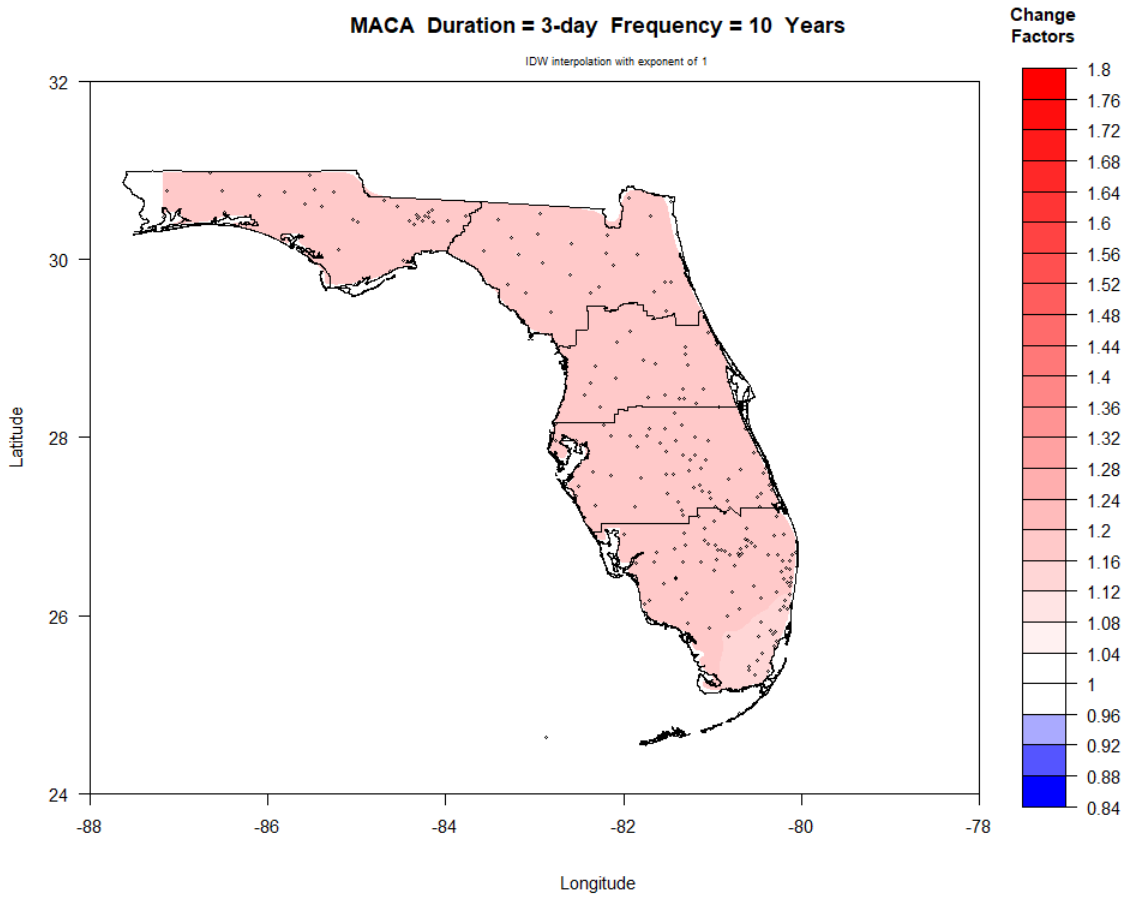

Figure III-56. Map of NEAR period (2030-2069) change factors across Florida for 3-day duration and 10-year return period.

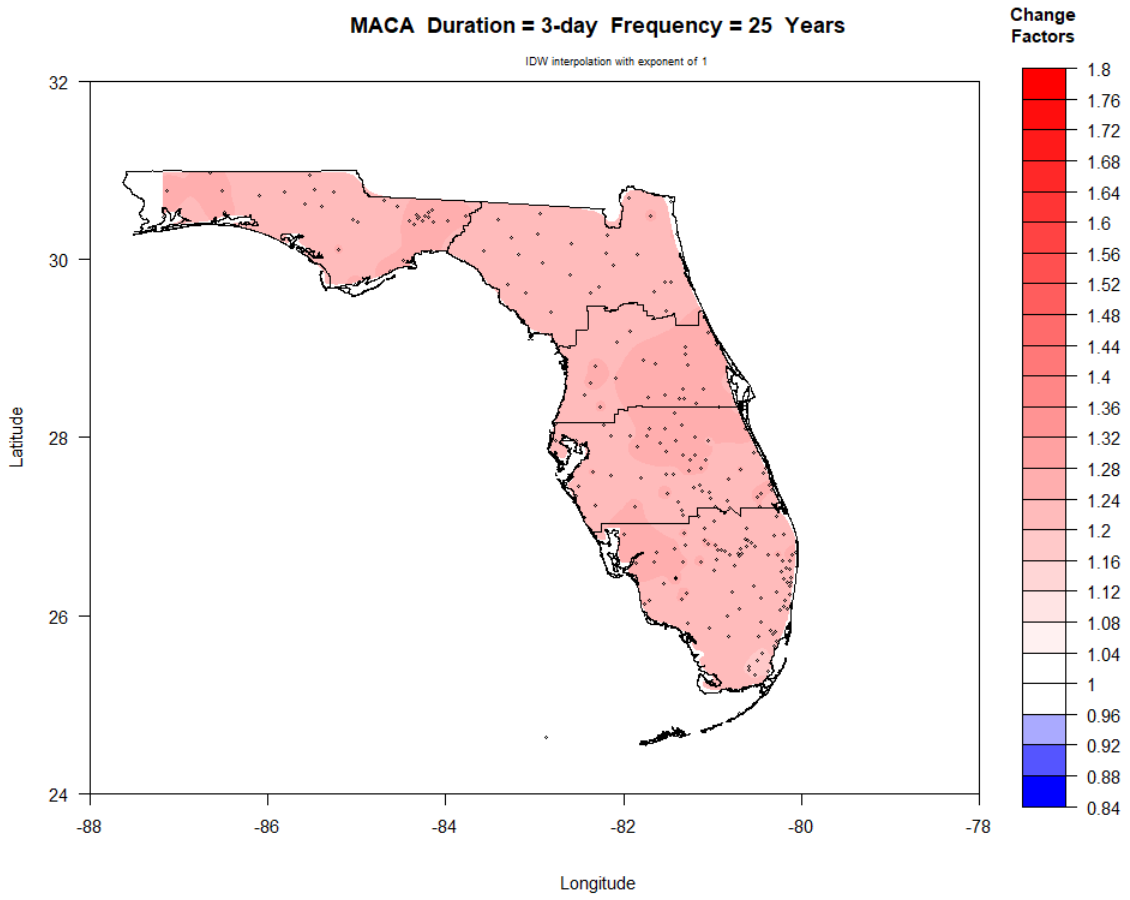

Figure III-57. Map of NEAR period (2030-2069) change factors across Florida for 3-day duration and 25-year return period.

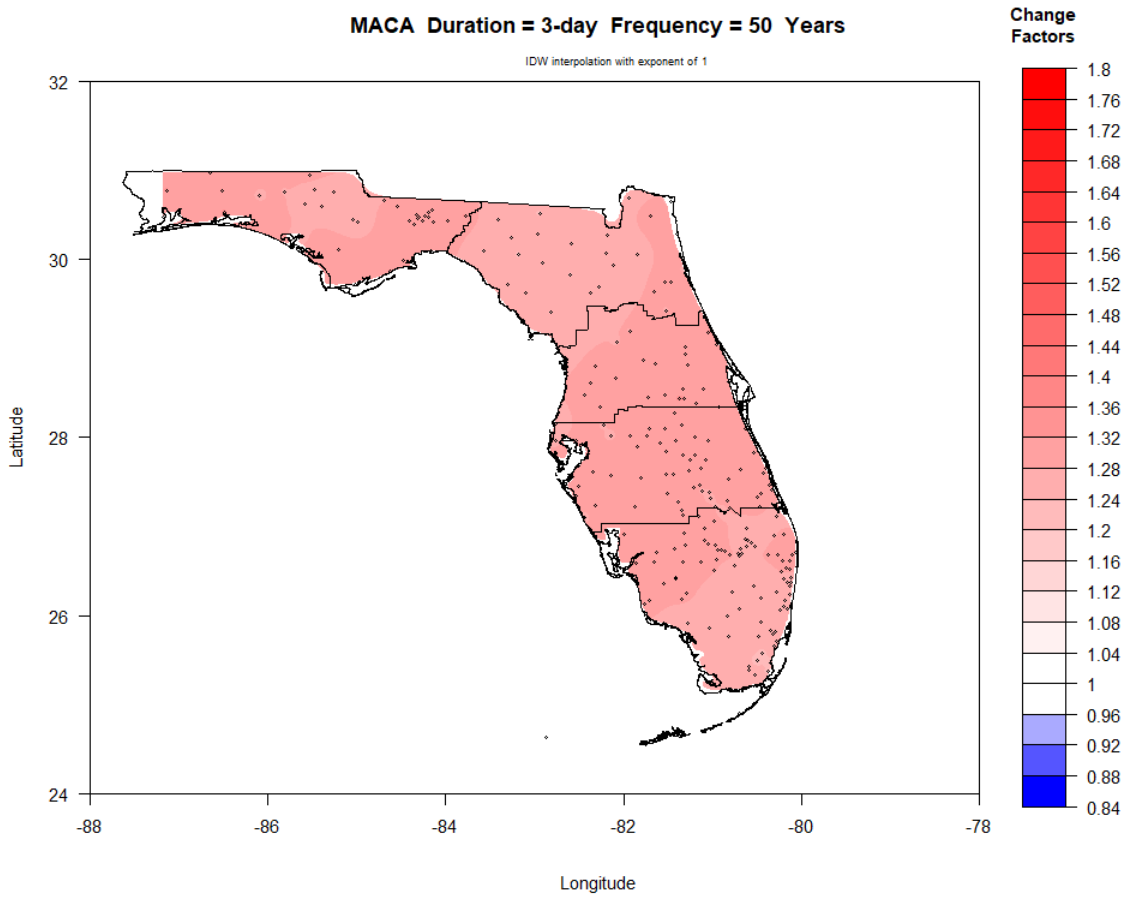

Figure III-58. Map of NEAR period (2030-2069) change factors across Florida for 3-day duration and 50-year return period.

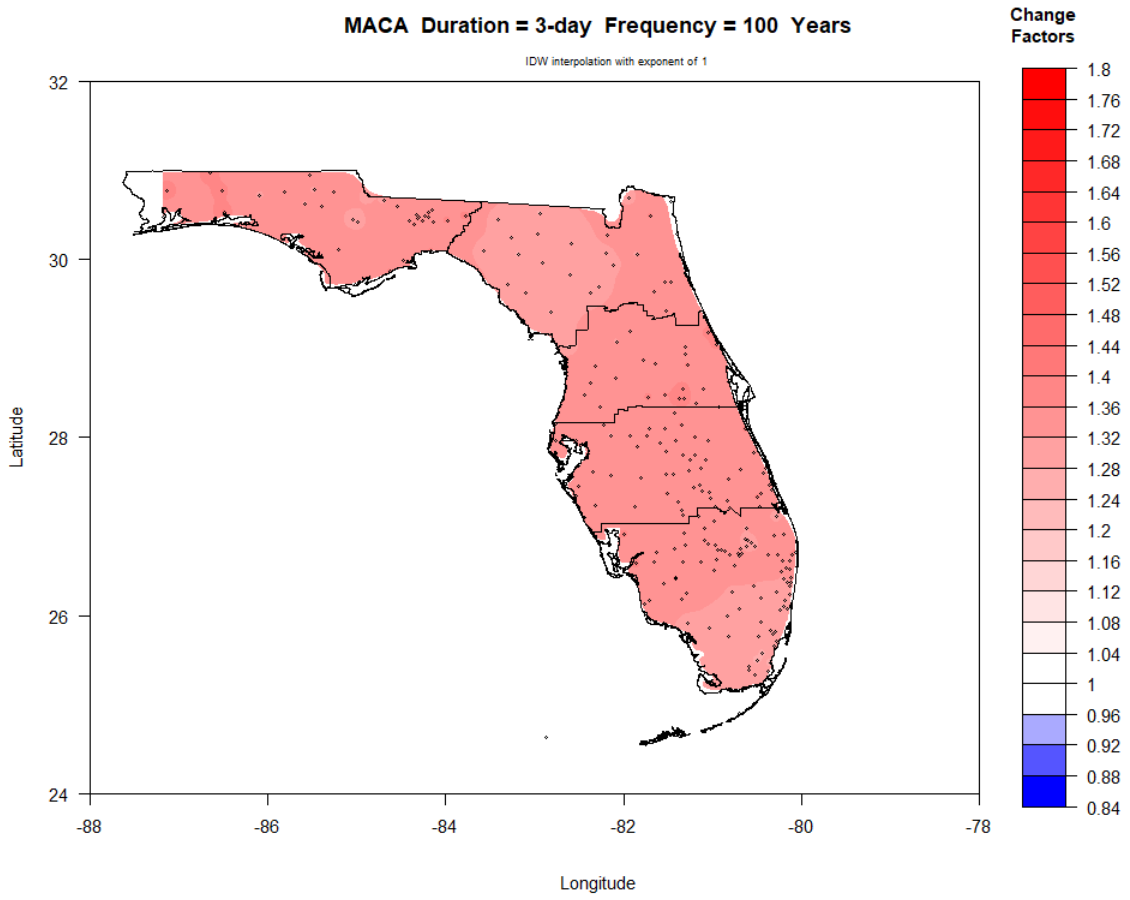

Figure III-59. Map of NEAR period (2030-2069) change factors across Florida for 3-day duration and 100-year return period.

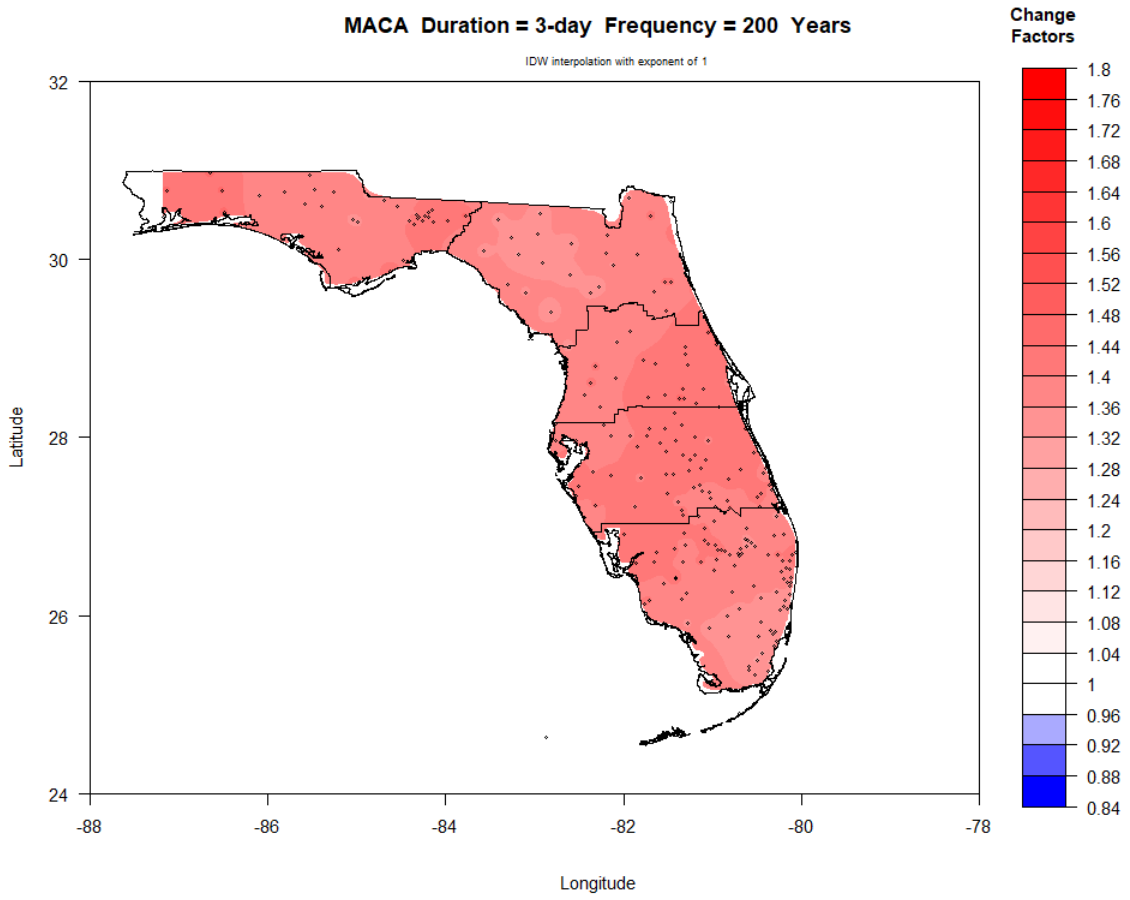

Figure III-60. Map of NEAR period (2030-2069) change factors across Florida for 3-day duration and 200-year return period.

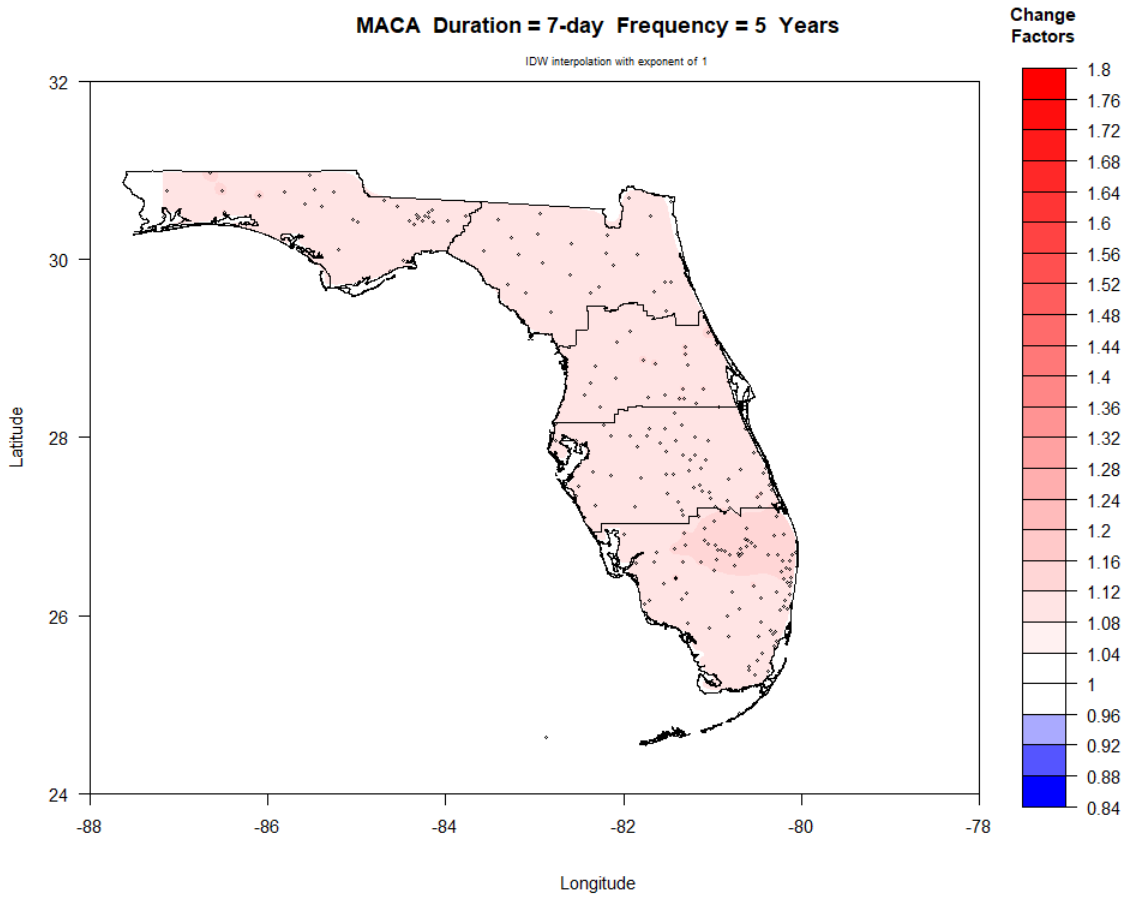

Figure III-61. Map of NEAR period (2030-2069) change factors across Florida for 7-day duration and 5-year return period.

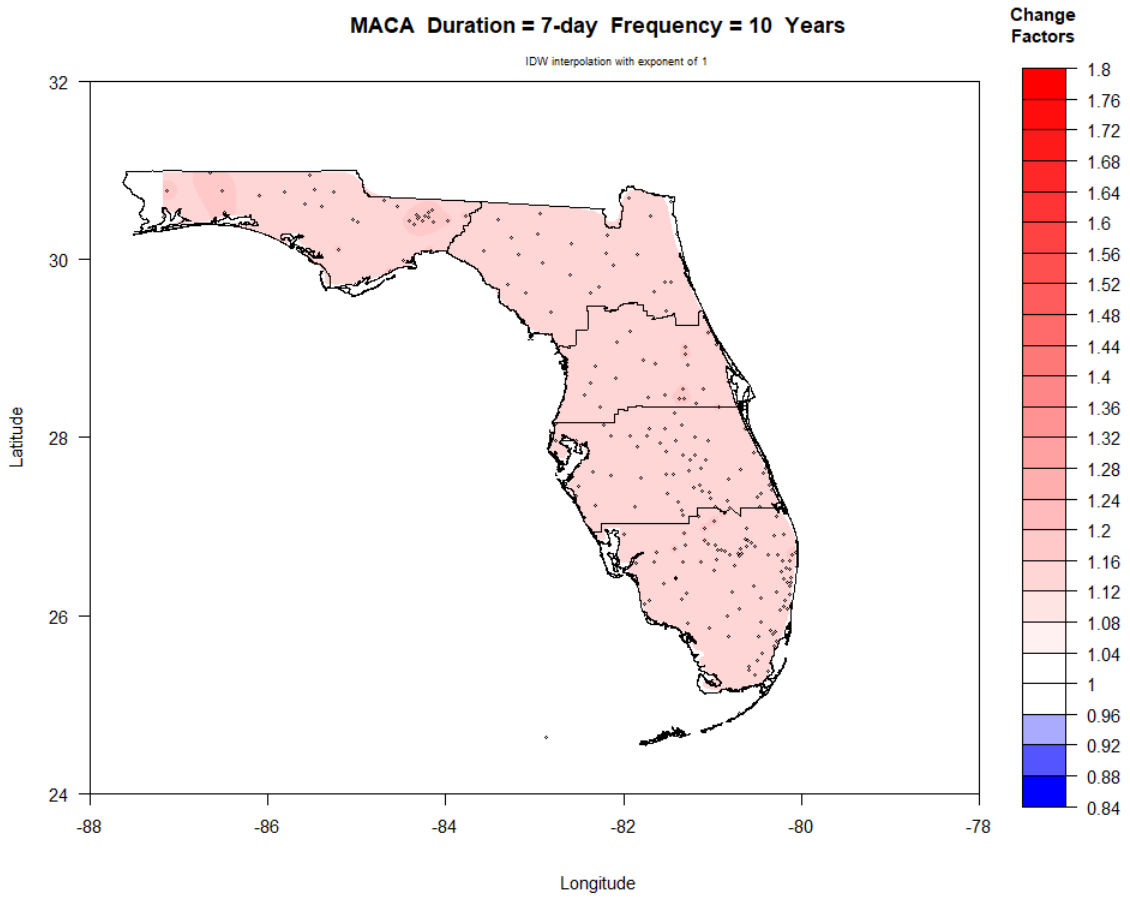

Figure III-62. Map of NEAR period (2030-2069) change factors across Florida for 7-day duration and 10-year return period.

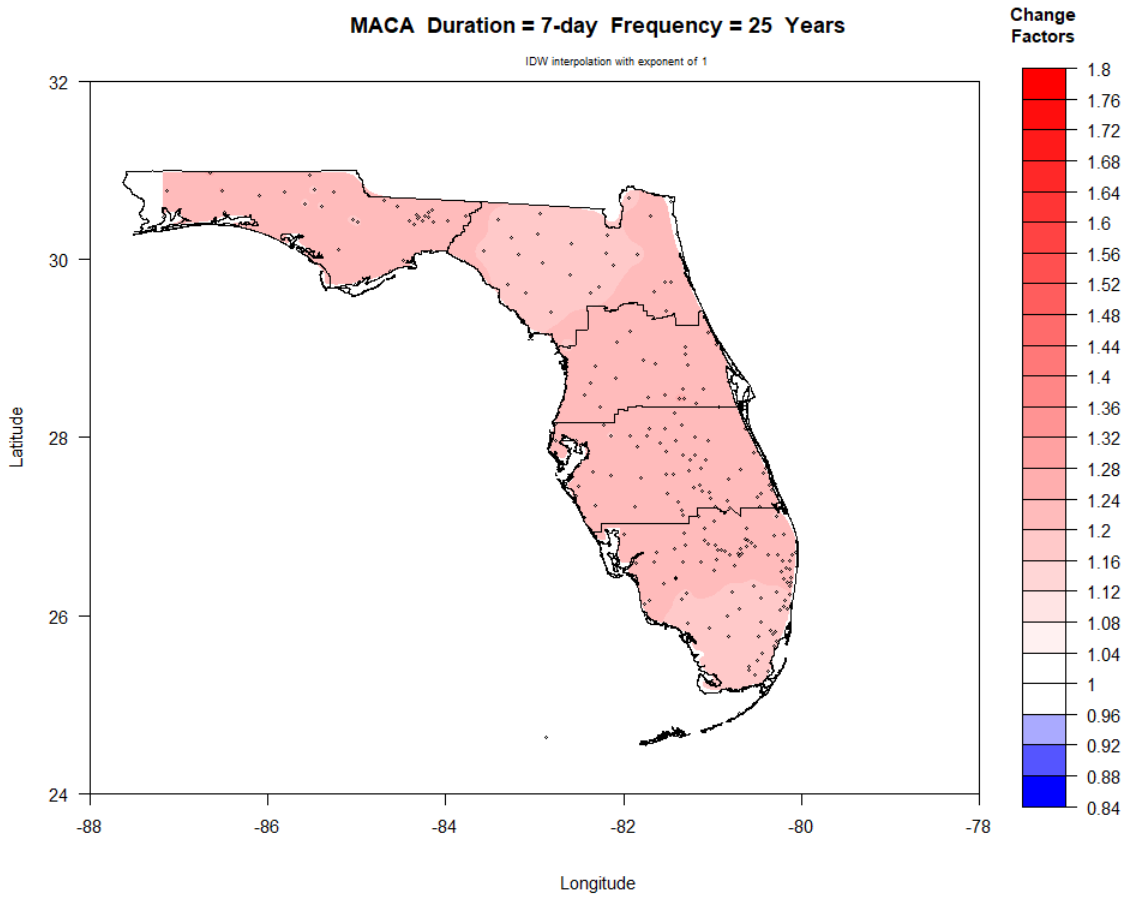

Figure III-63. Map of NEAR period (2030-2069) change factors across Florida for 7-day duration and 25-year return period.

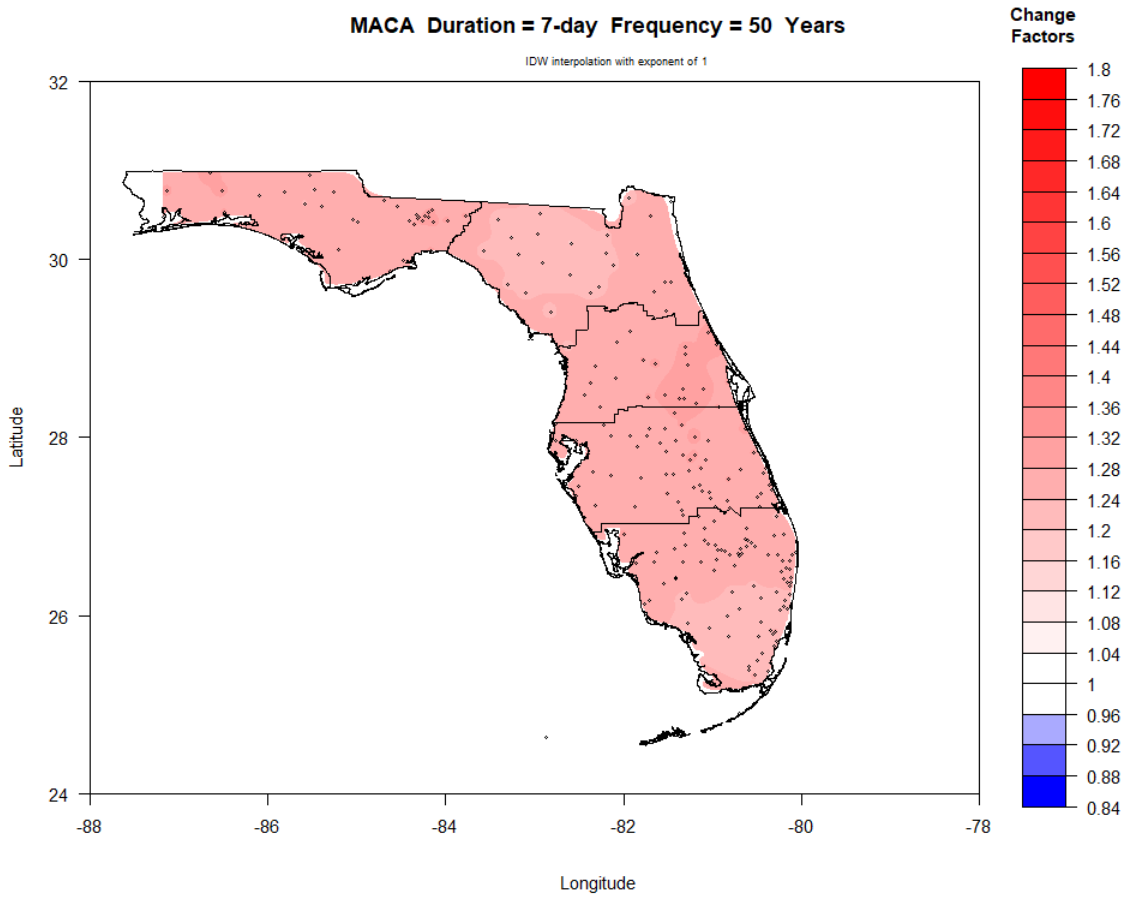

Figure III-64. Map of NEAR period (2030-2069) change factors across Florida for 7-day duration and 50-year return period.

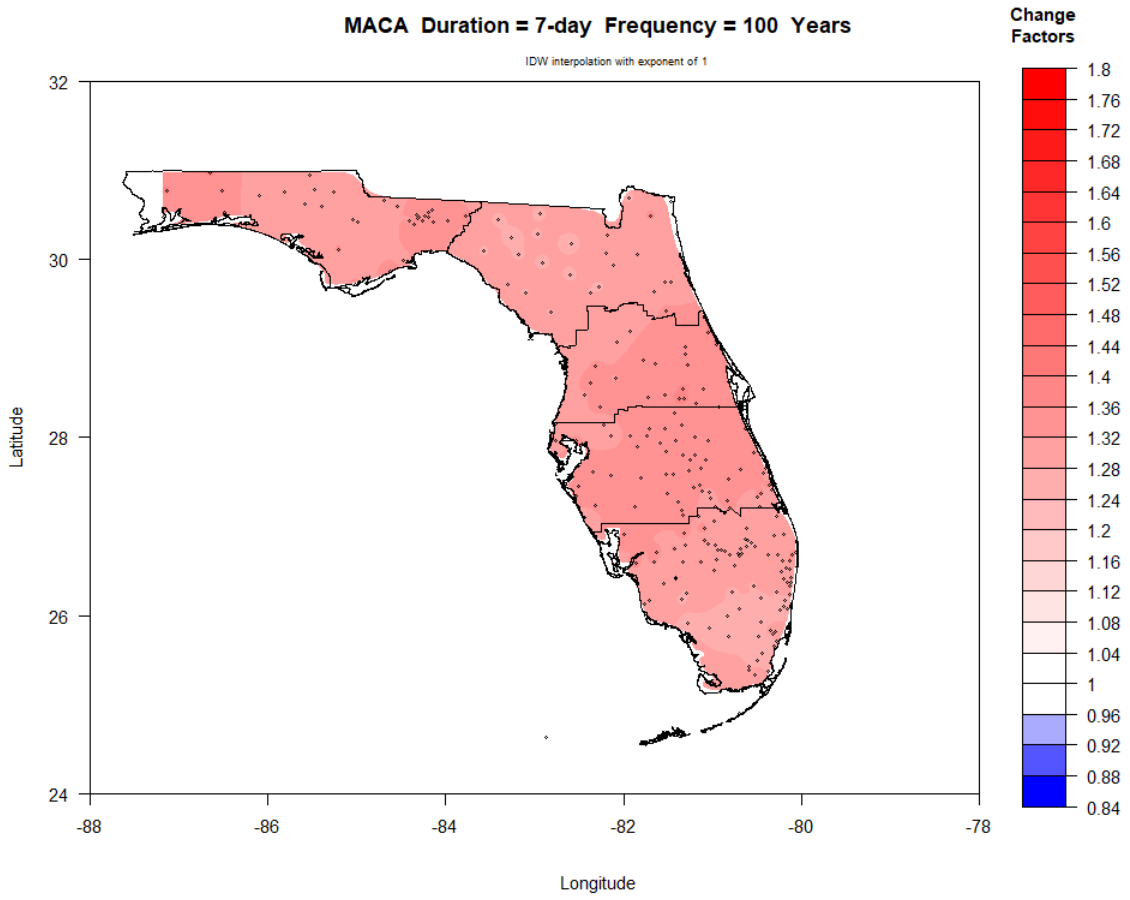

Figure III-65. Map of NEAR period (2030-2069) change factors across Florida for 7-day duration and 100-year return period.

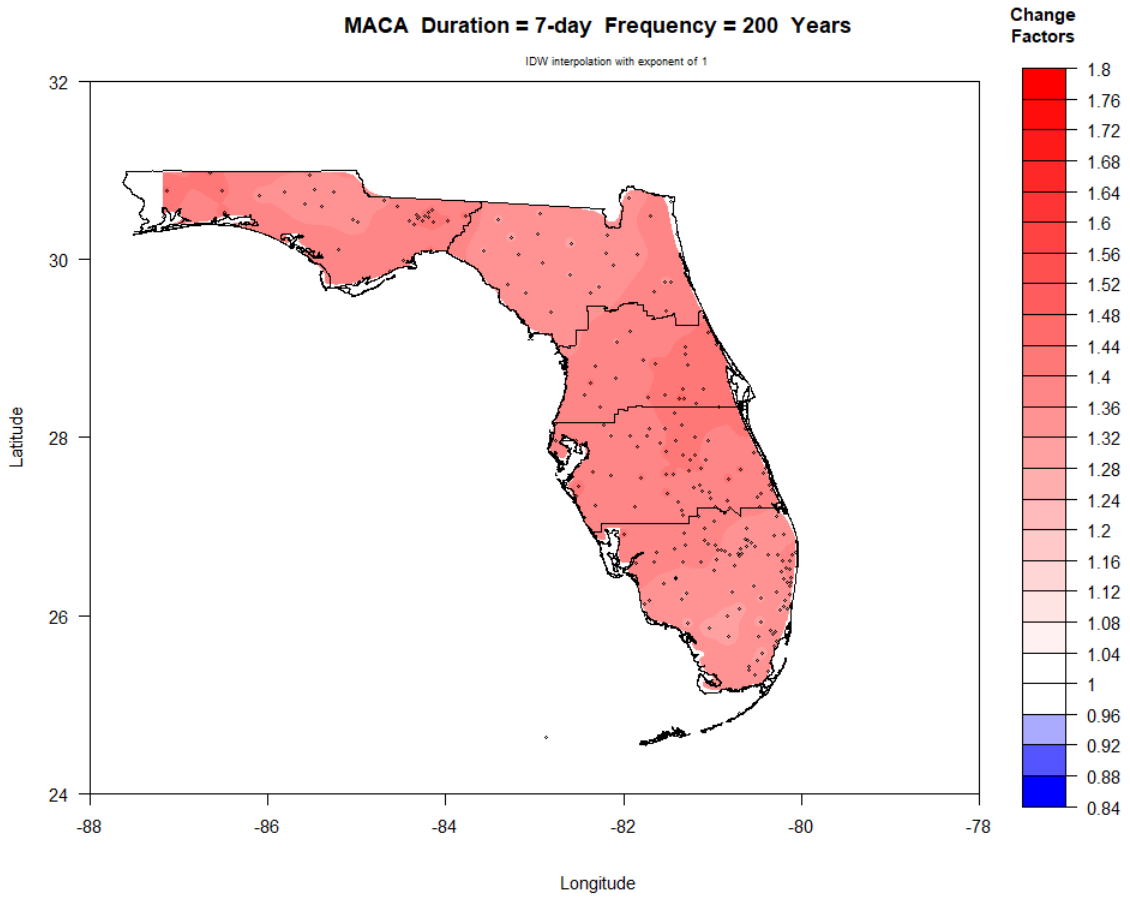

Figure III-66. Map of NEAR period (2030-2069) change factors across Florida for 7-day duration and 200-year return period.

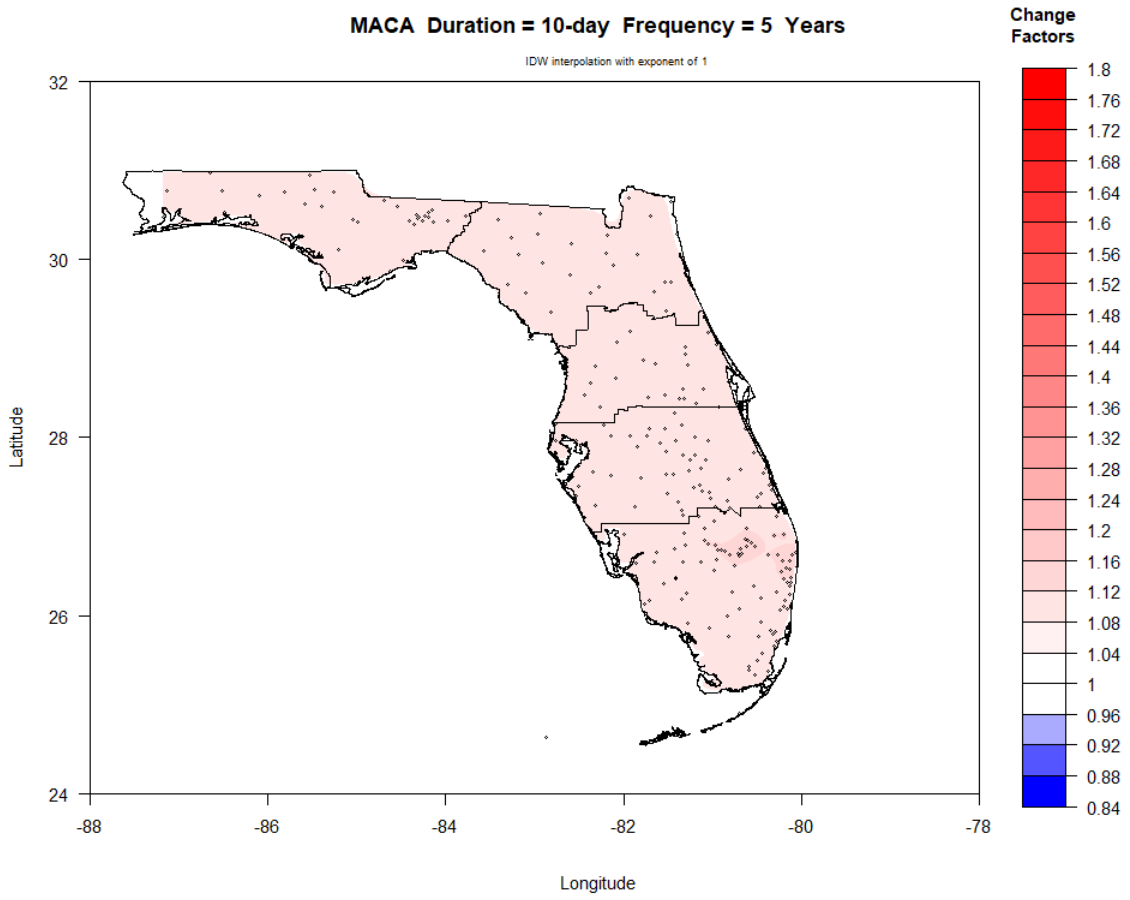

Figure III-67. Map of NEAR period (2030-2069) change factors across Florida for 10-day duration and 5-year return period.

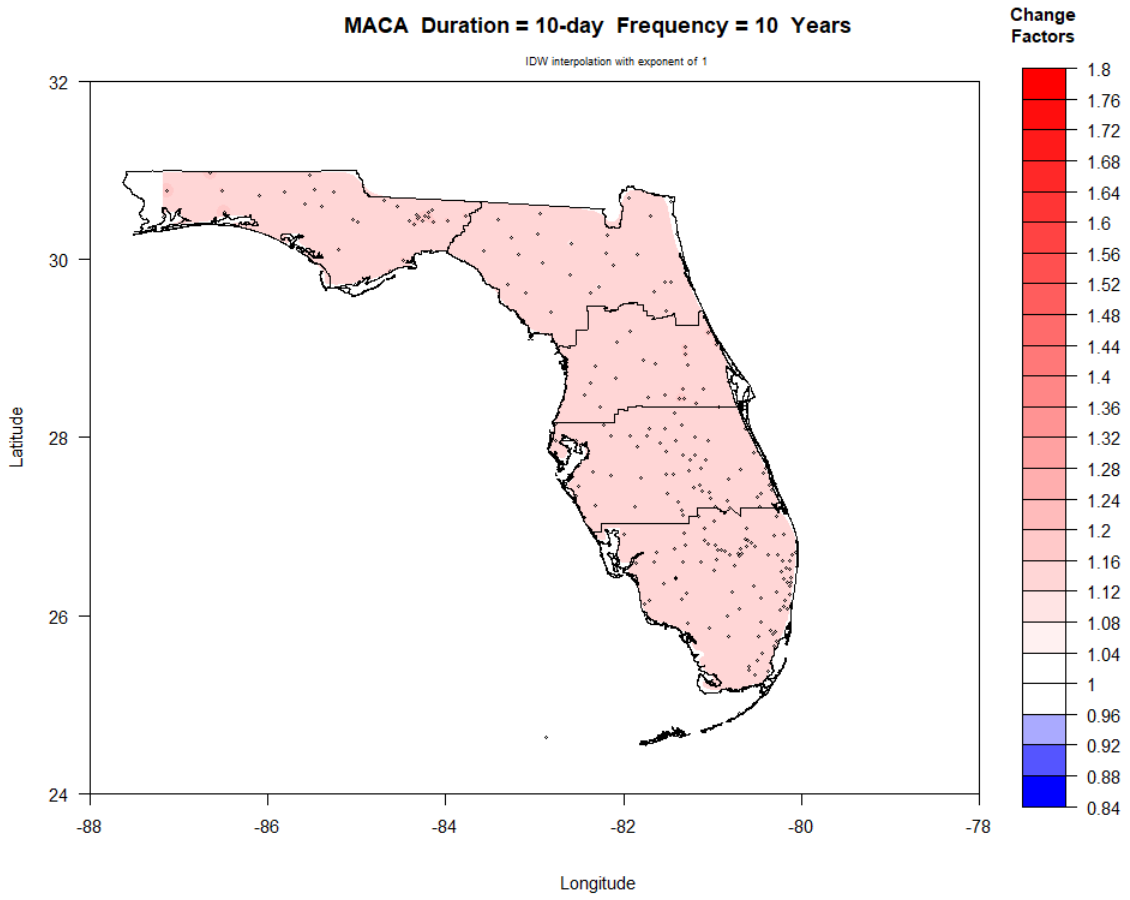

Figure III-68. Map of NEAR period (2030-2069) change factors across Florida for 10-day duration and 10-year return period.

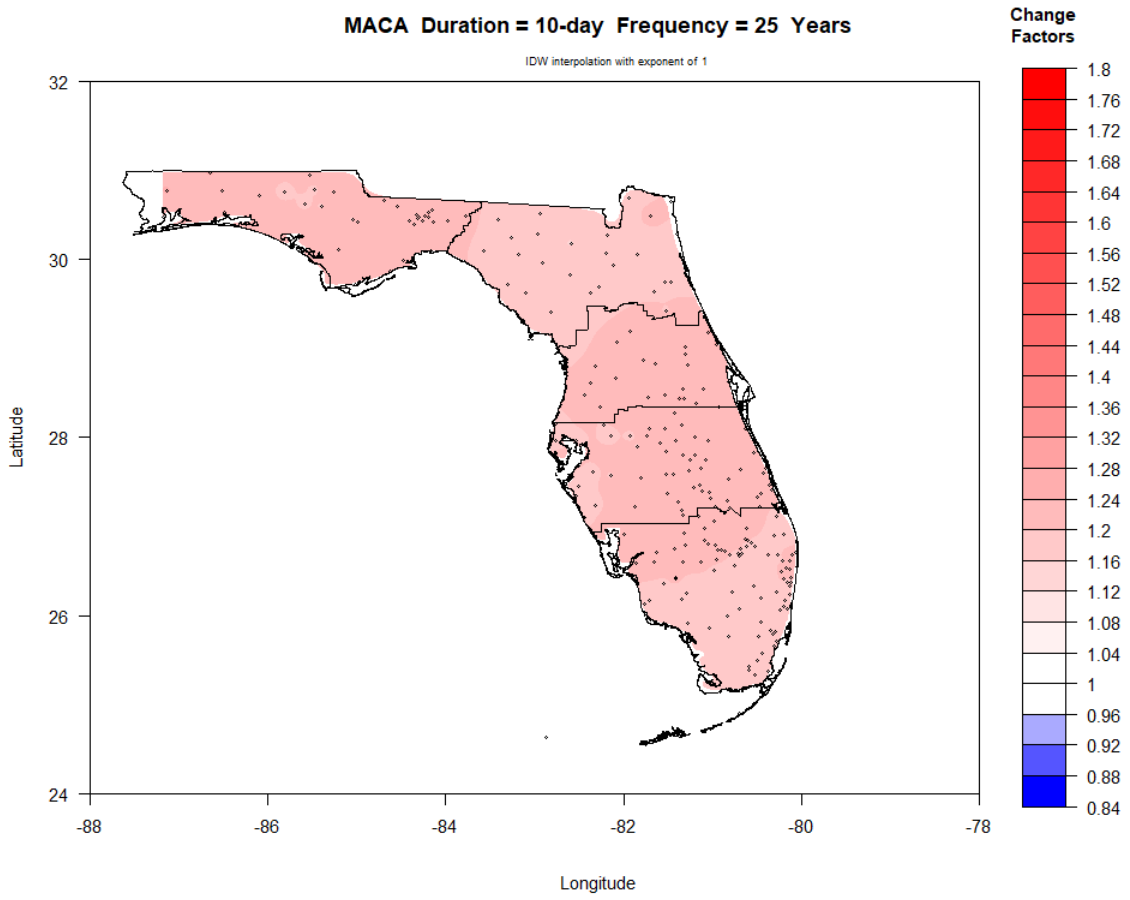

Figure III-69. Map of NEAR period (2030-2069) change factors across Florida for 10-day duration and 25-year return period.

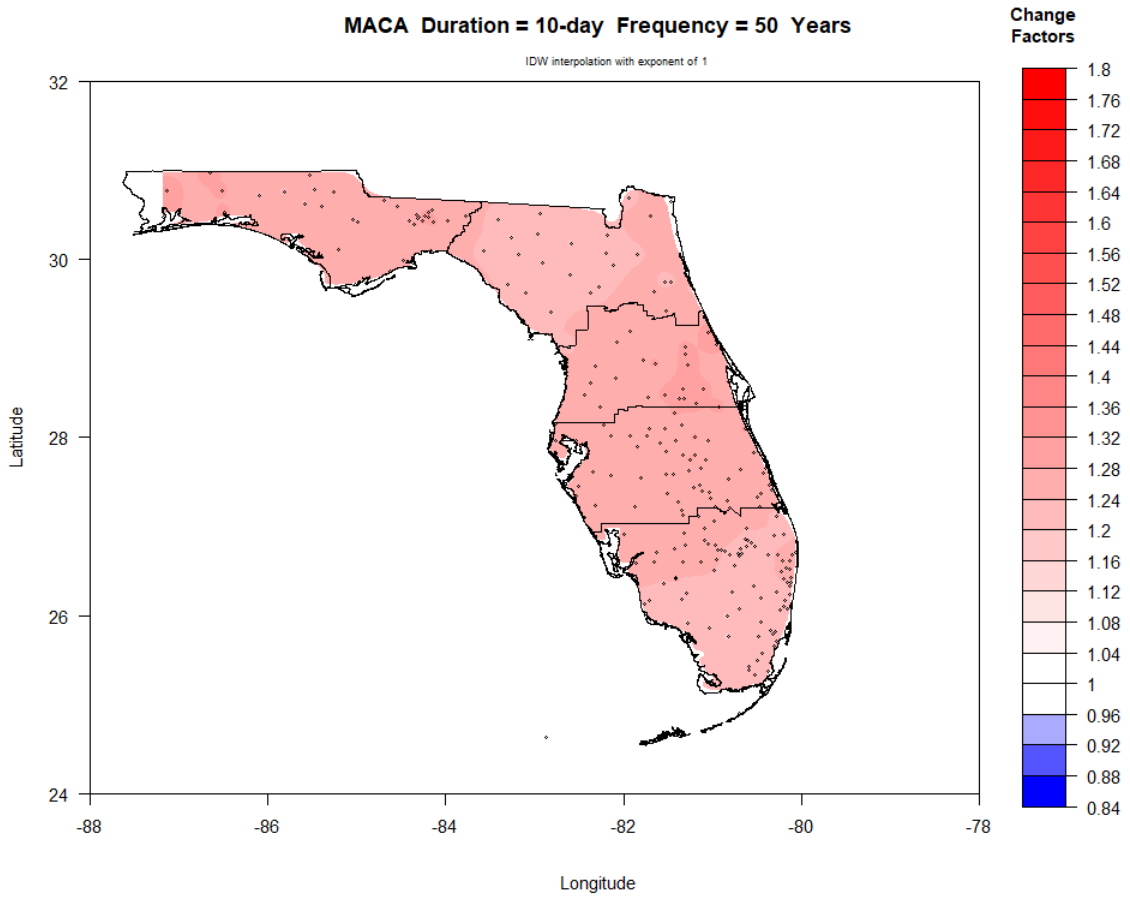

Figure III-70. Map of NEAR period (2030-2069) change factors across Florida for 10-day duration and 50-year return period.

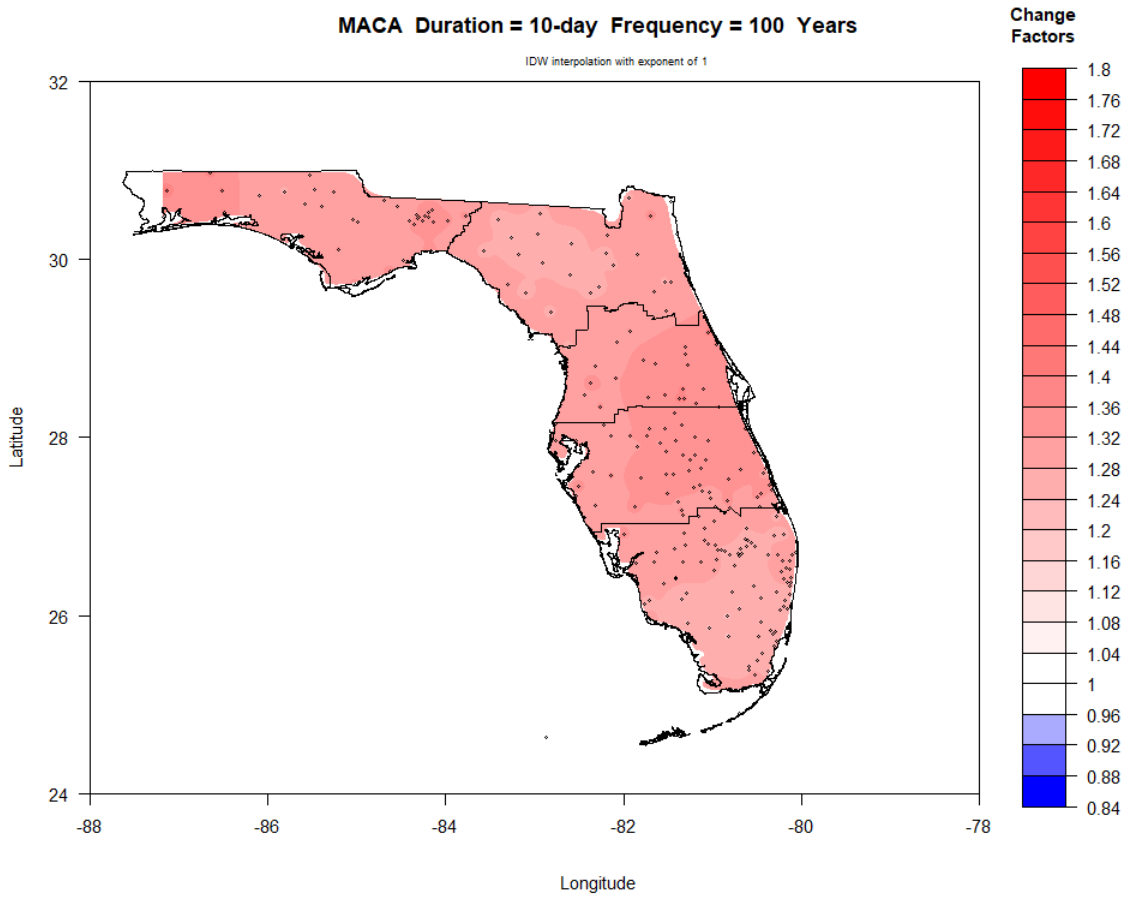

Figure III-71. Map of NEAR period (2030-2069) change factors across Florida for 10-day duration and 100-year return period.

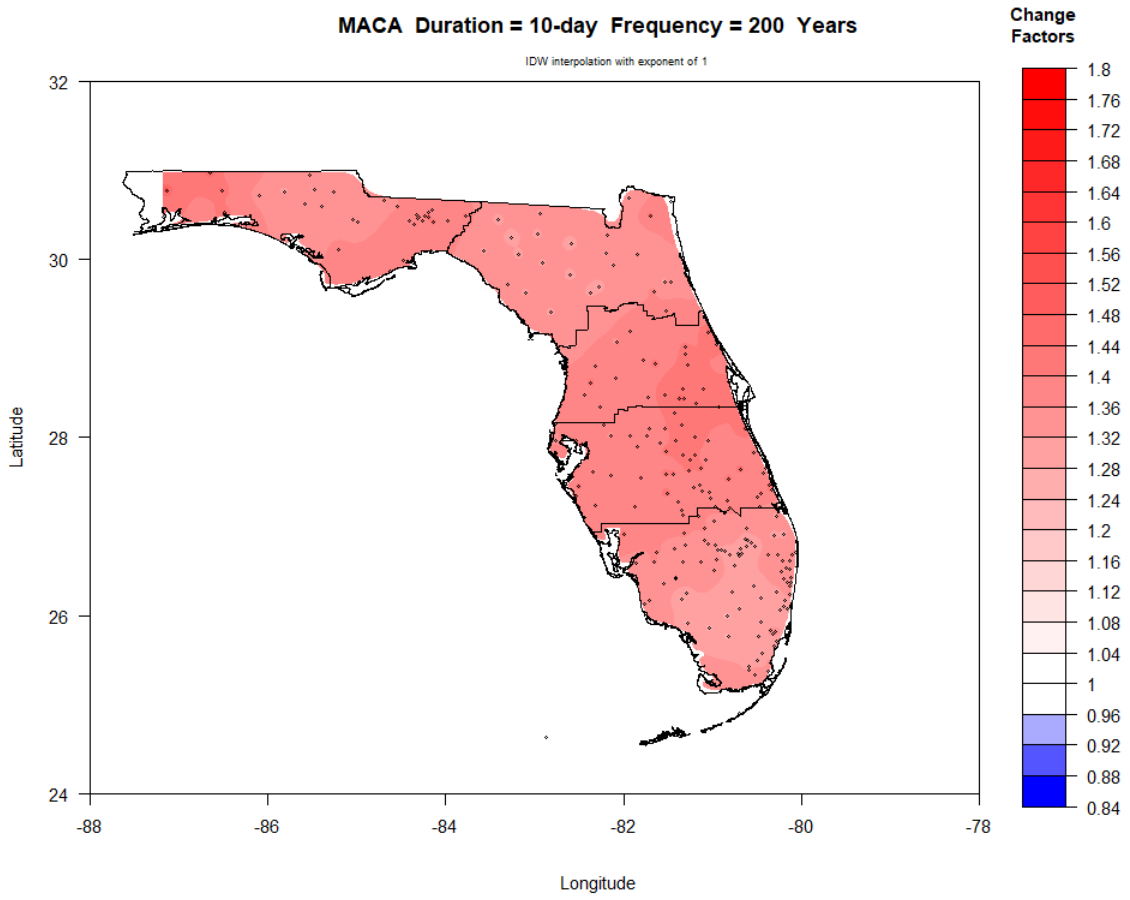

Figure III-72. Map of NEAR period (2030-2069) change factors across Florida for 10-day duration and 200-year return period.

APPENDIX IV. Change Factor Maps for FAR period (2060-2099)

Presented herein are maps of the change factors across Florida for the FAR period (2060-2099) generated using IDW interpolation with an exponent of 1. The maps were created for durations: 24-hr, 3-day, 7-day and 10-day, and return periods: 5-yr, 10-yr, 25-yr, 50-yr, 100-yr and 200-yr.

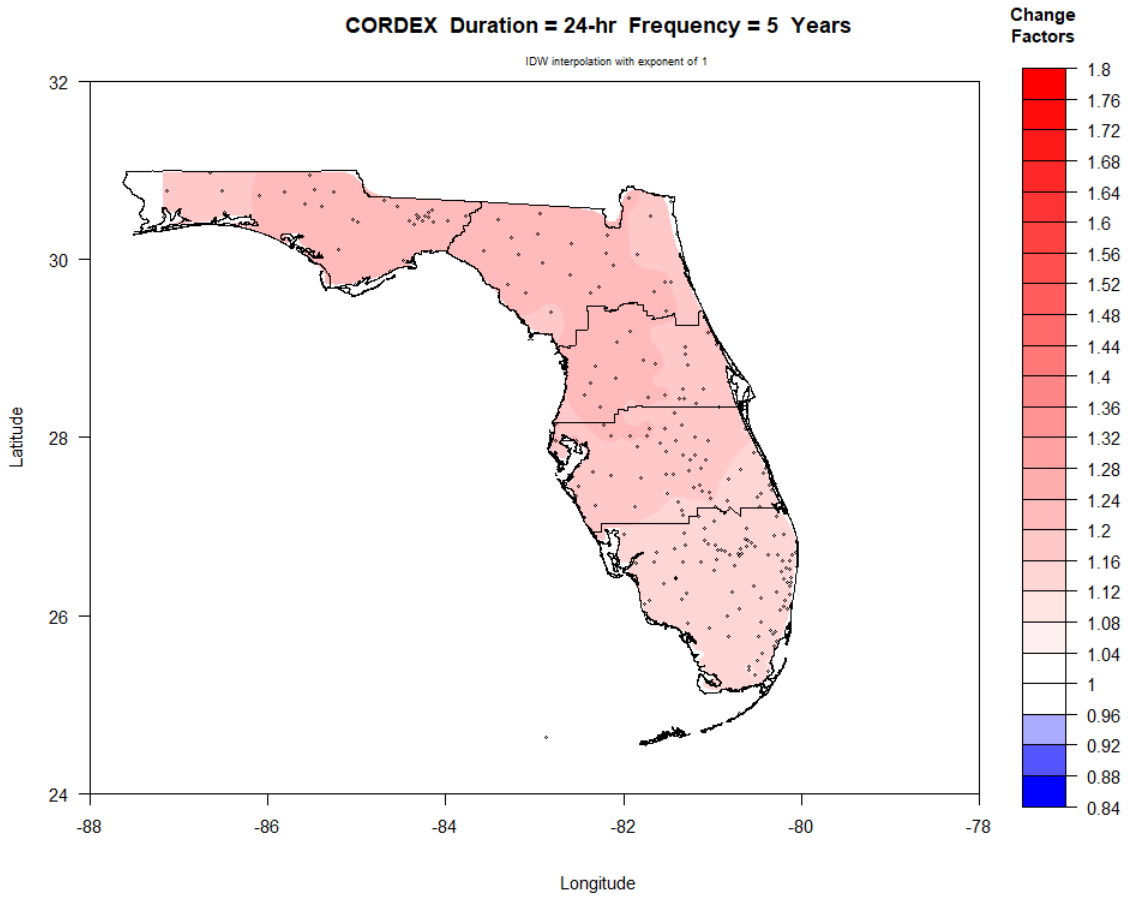

Figure IV-1. Map of FAR period (2060-2099) change factors across Florida for 24-hr duration and 5-year return period.

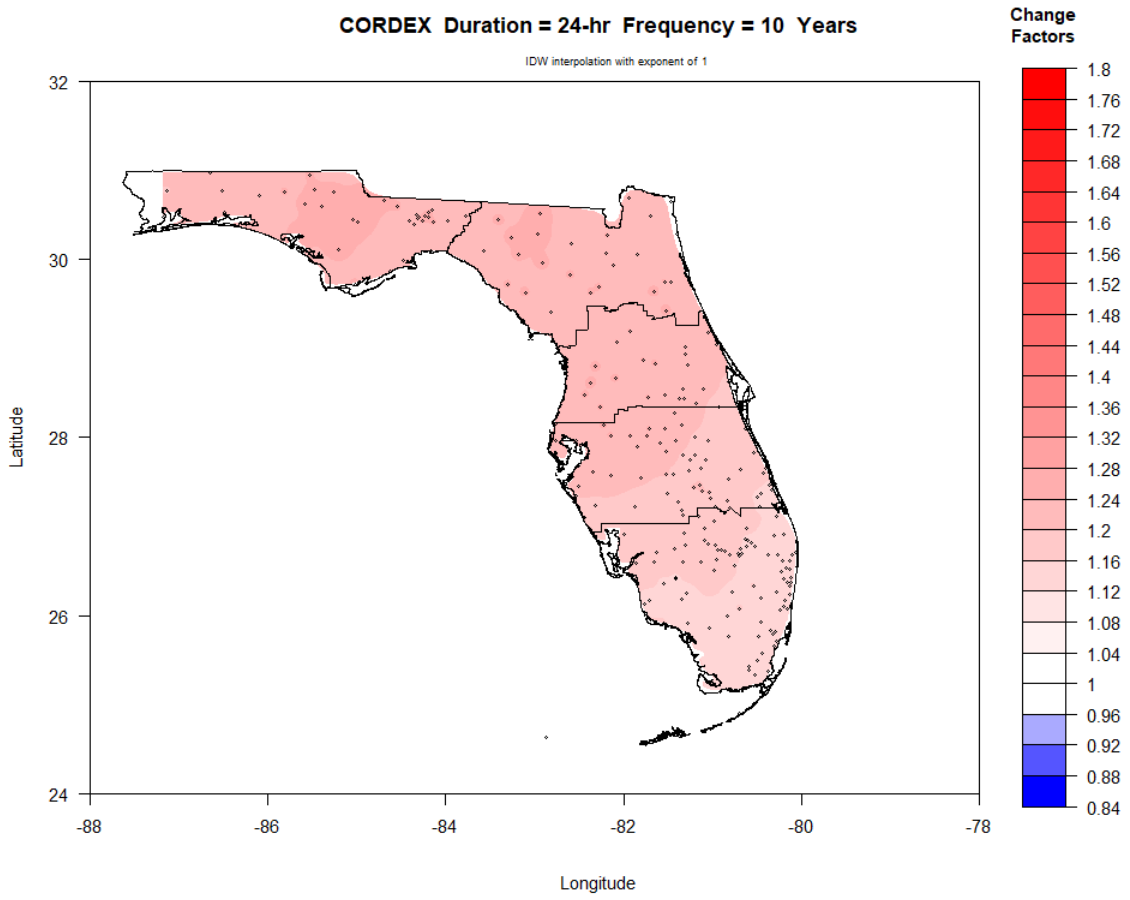

Figure IV-2. Map of FAR period (2060-2099) change factors across Florida for 24-hr duration and 10-year return period.

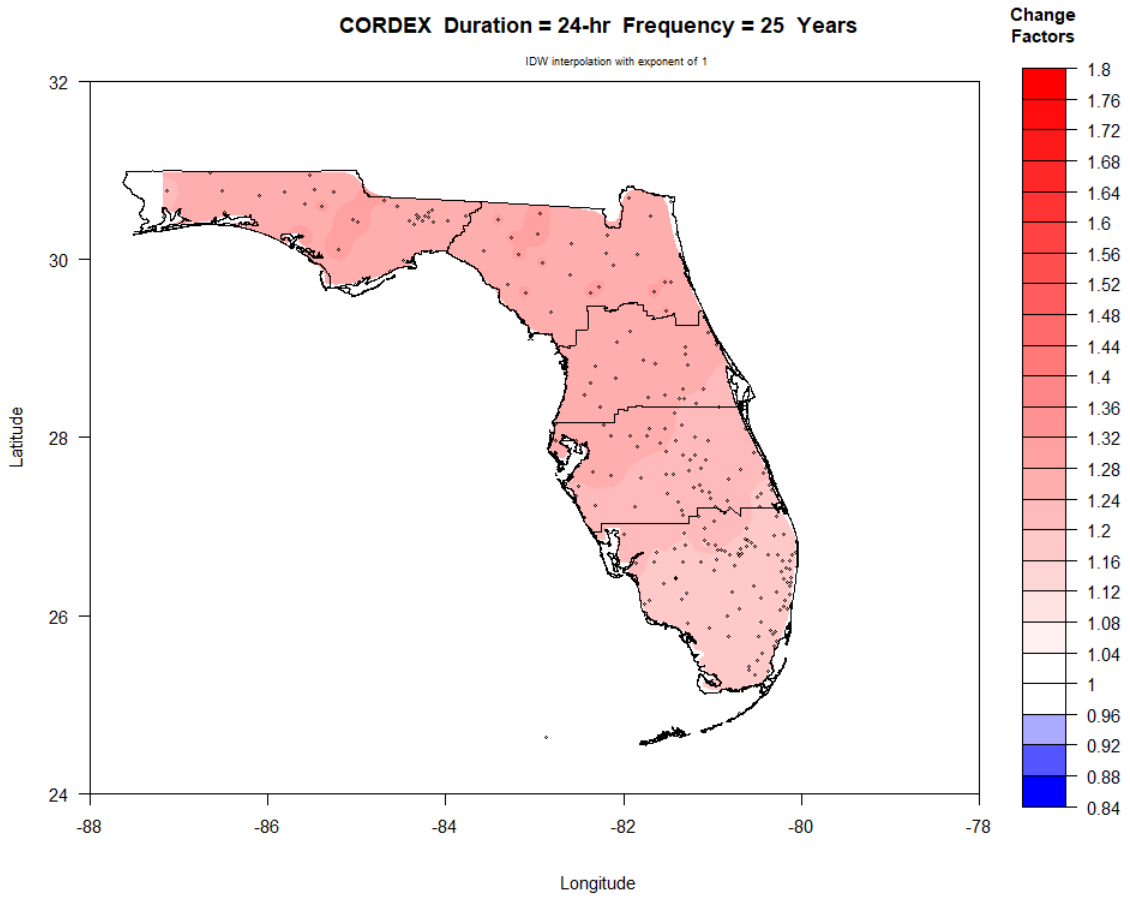

Figure IV-3. Map of FAR period (2060-2099) change factors across Florida for 24-hr duration and 25-year return period.

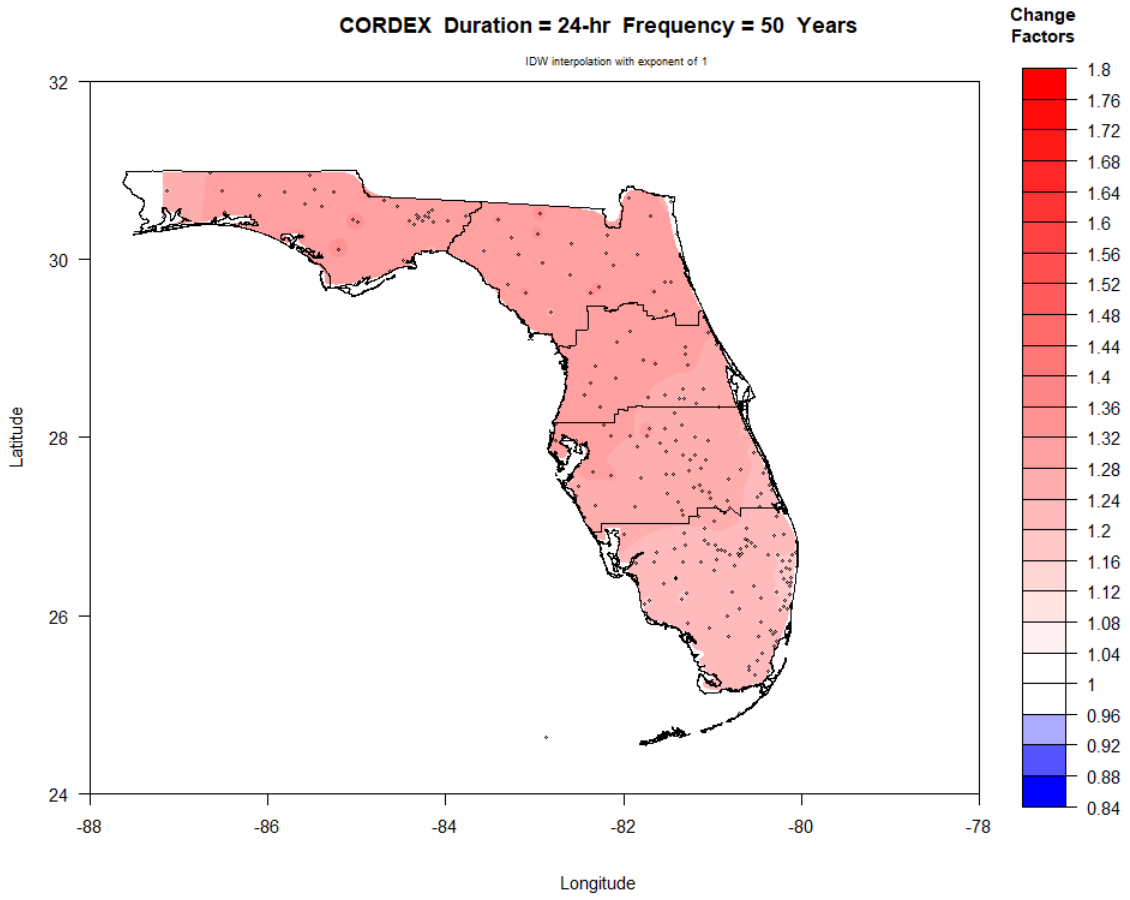

Figure IV-4. Map of FAR period (2060-2099) change factors across Florida for 24-hr duration and 50-year return period.

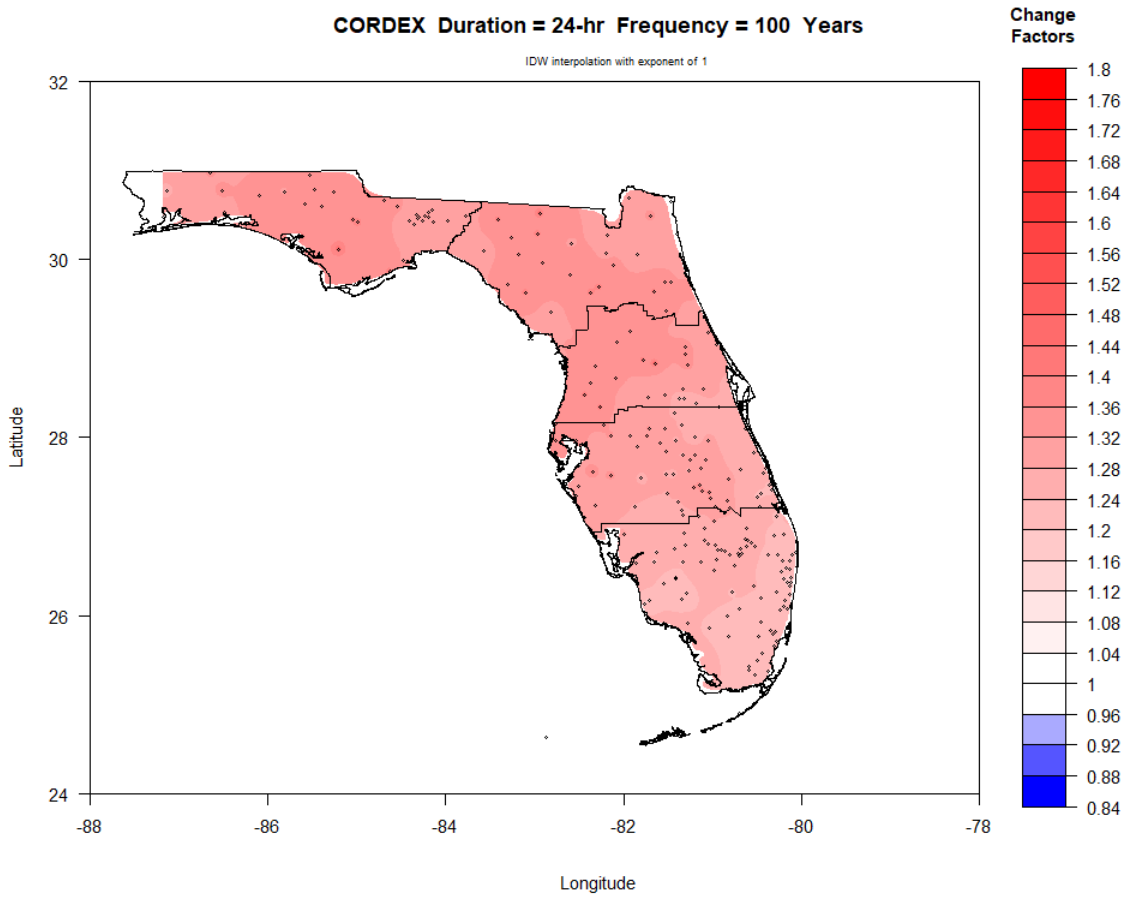

Figure IV-5. Map of FAR period (2060-2099) change factors across Florida for 24-hr duration and 100-year return period.

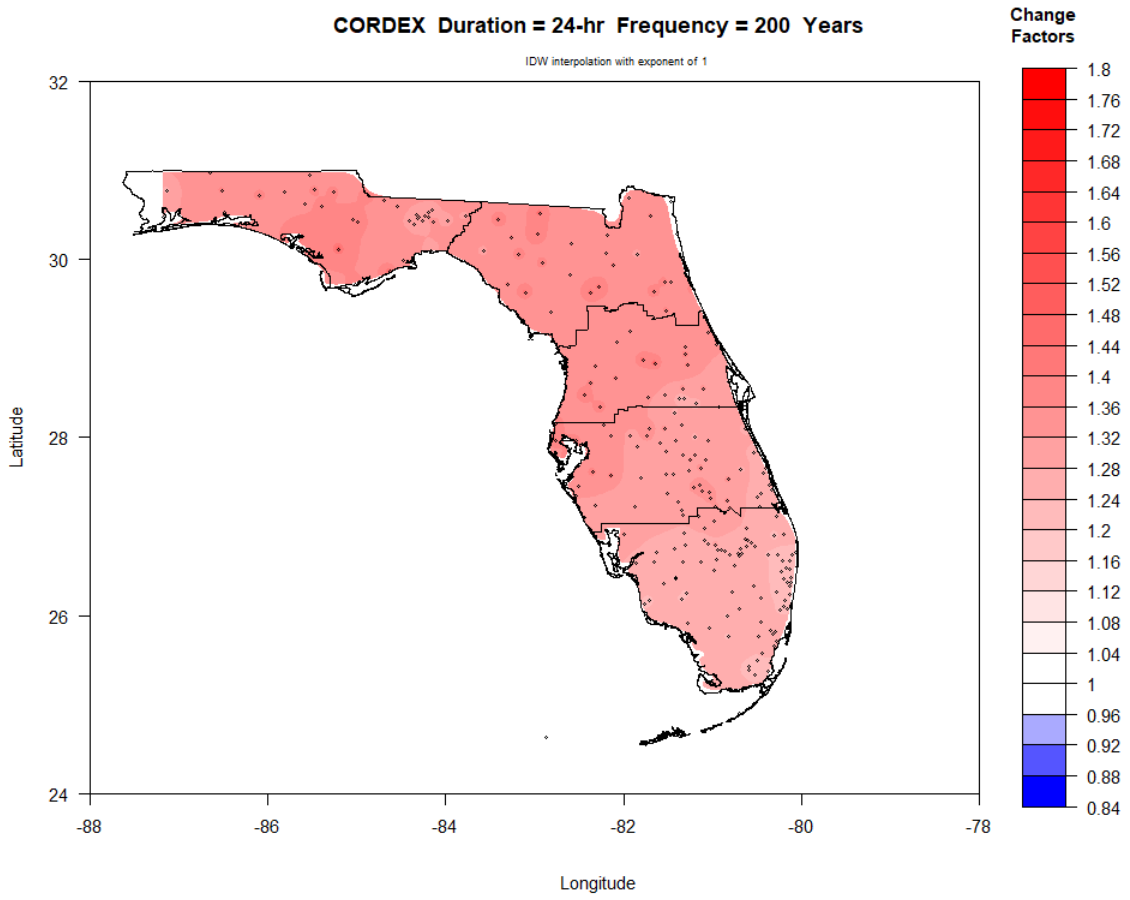

Figure IV-6. Map of FAR period (2060-2099) change factors across Florida for 24-hr duration and 200-year return period.

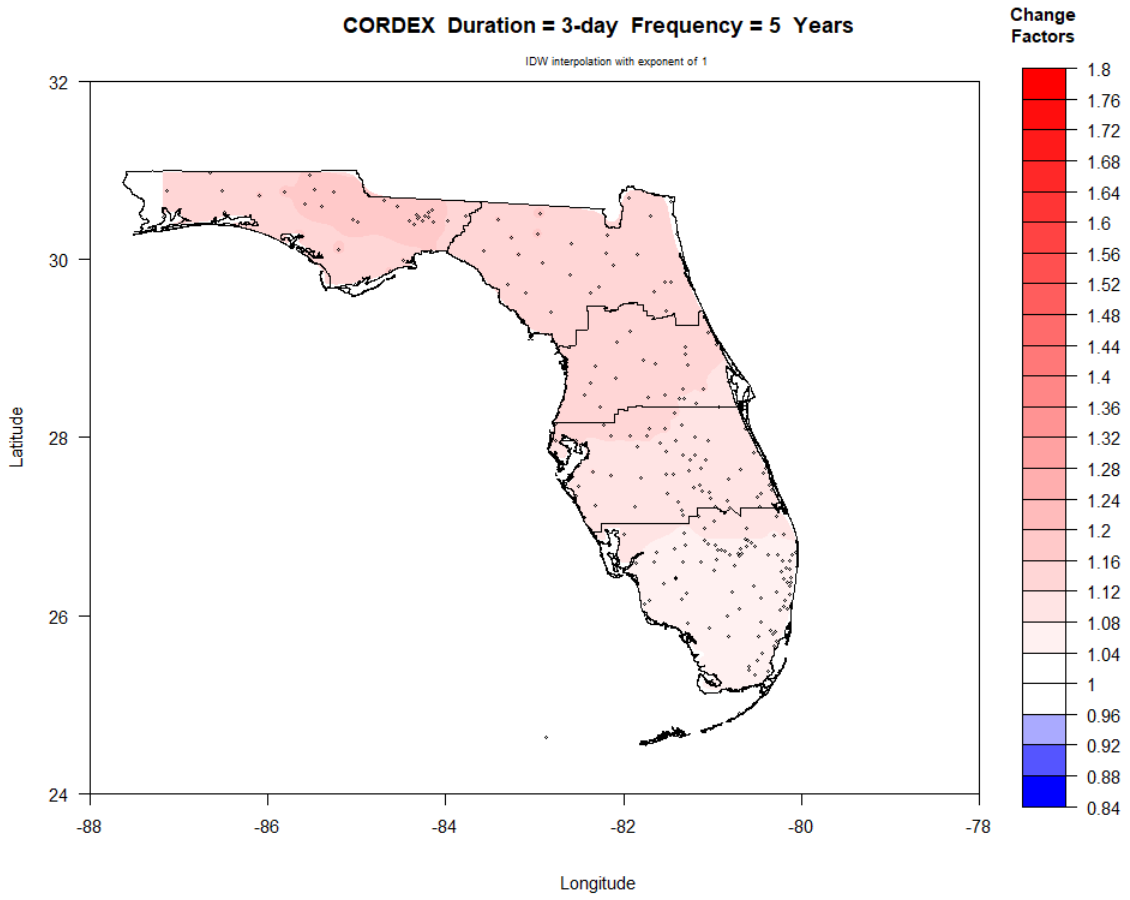

Figure IV-7. Map of FAR period (2060-2099) change factors across Florida for 3-day duration and 5-year return period.

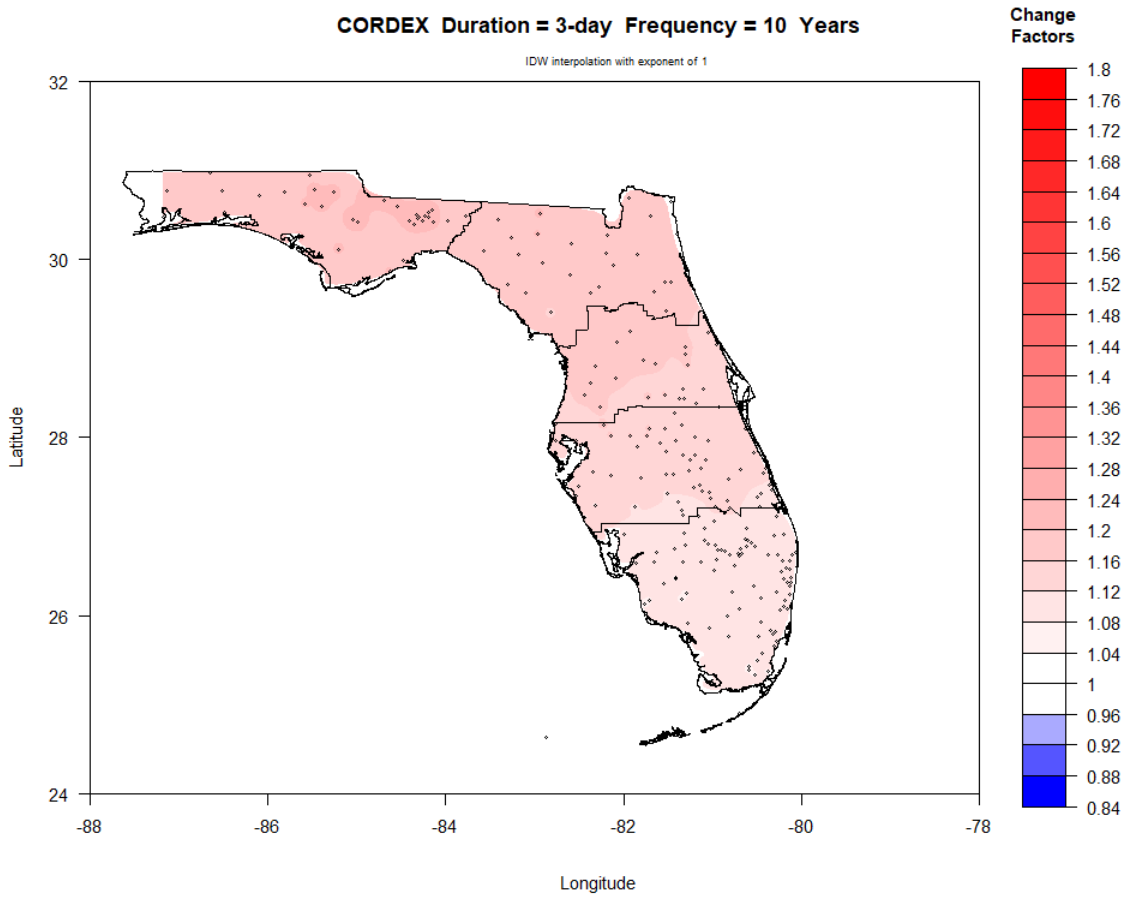

Figure IV-8. Map of FAR period (2060-2099) change factors across Florida for 3-day duration and 10-year return period.

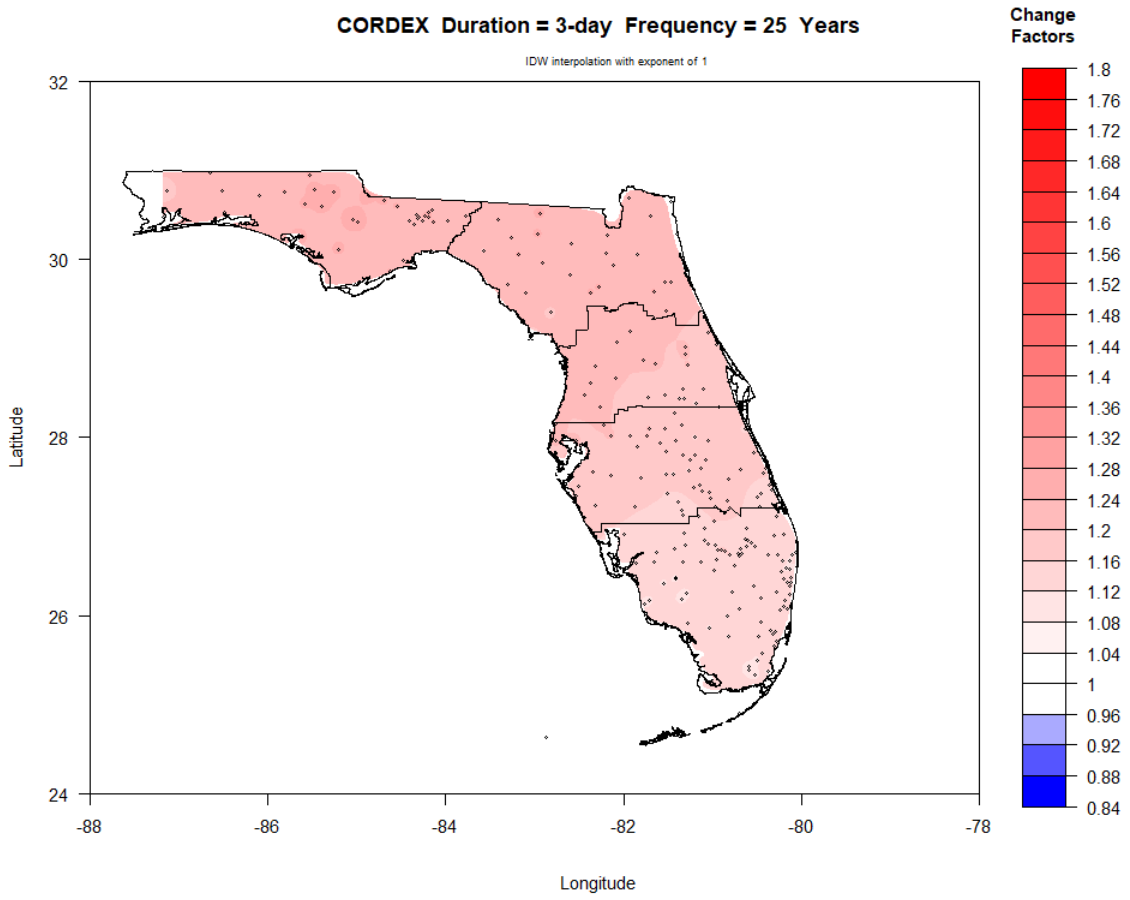

Figure IV-9. Map of FAR period (2060-2099) change factors across Florida for 3-day duration and 25-year return period.

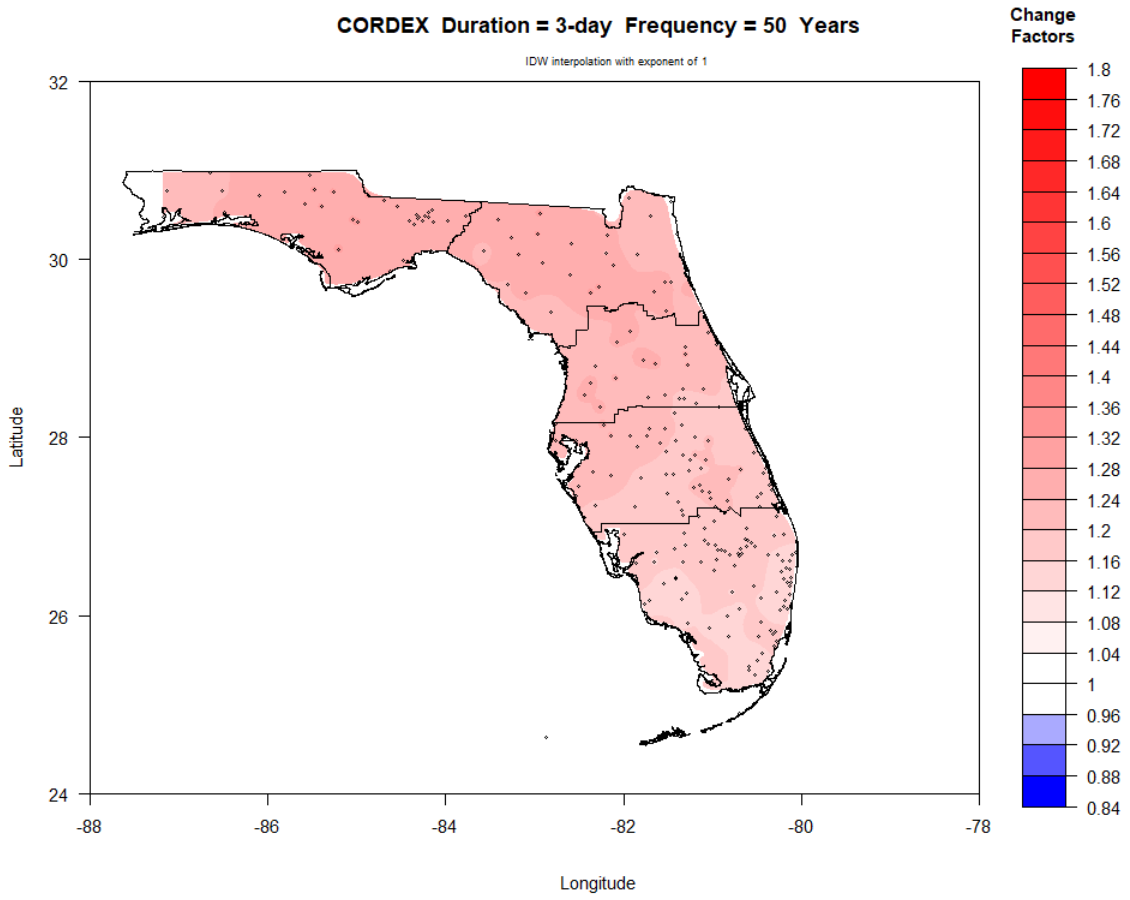

Figure IV-10. Map of FAR period (2060-2099) change factors across Florida for 3-day duration and 50-year return period.

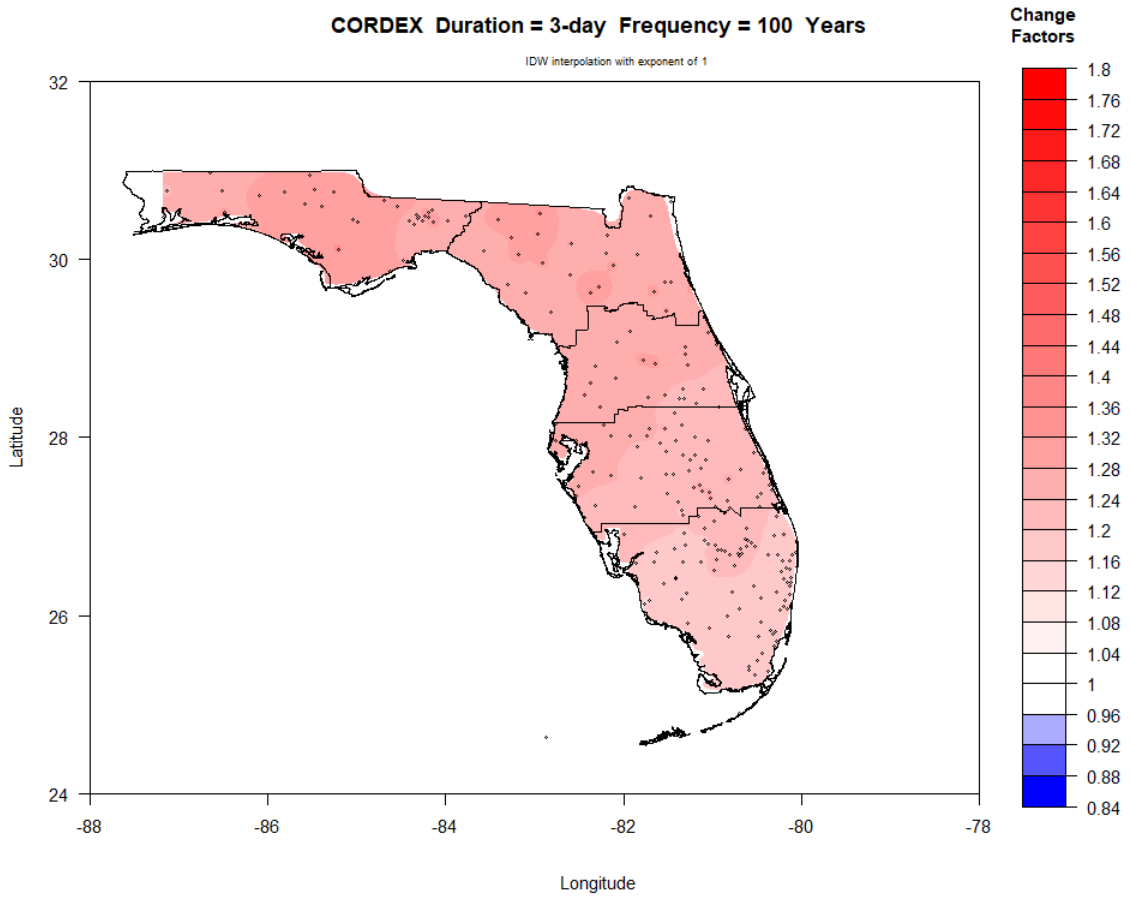

Figure IV-11. Map of FAR period (2060-2099) change factors across Florida for 3-day duration and 100-year return period.

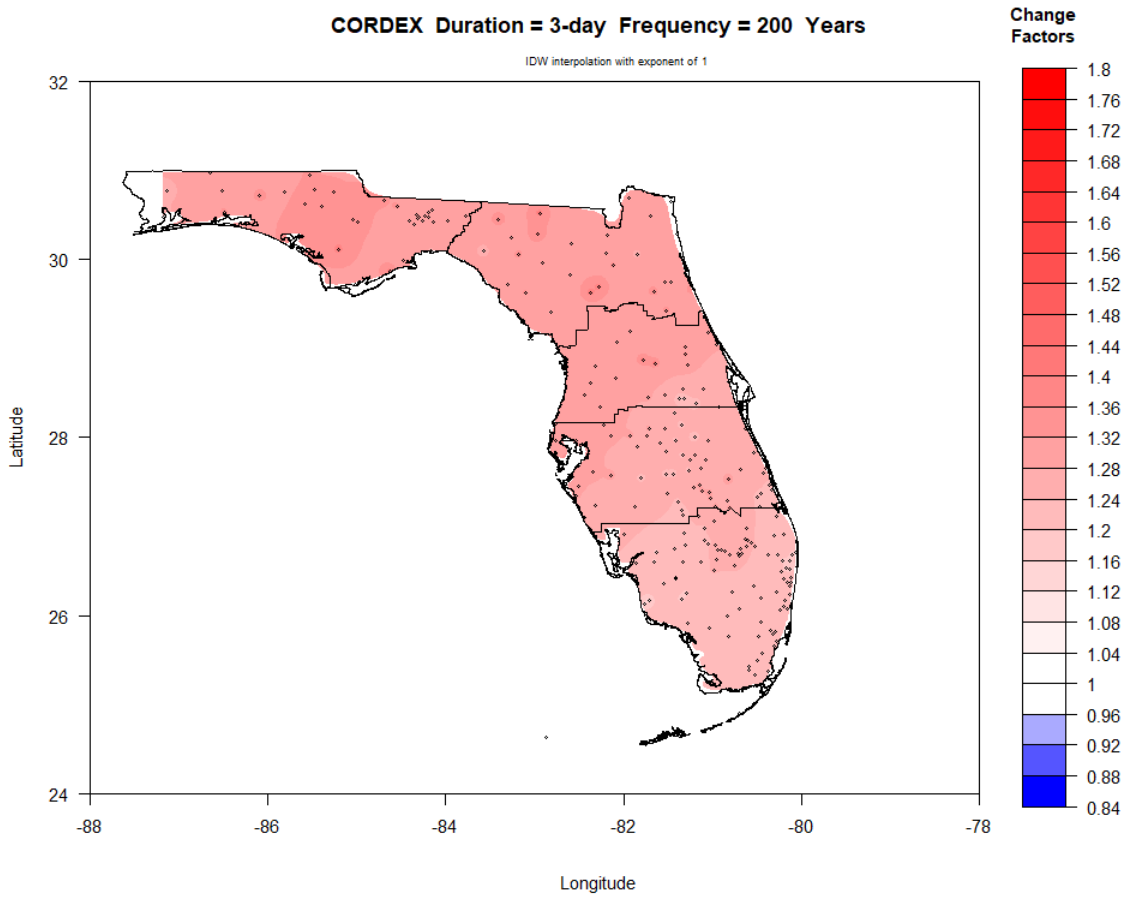

Figure IV-12. Map of FAR period (2060-2099) change factors across Florida for 3-day duration and 200-year return period.

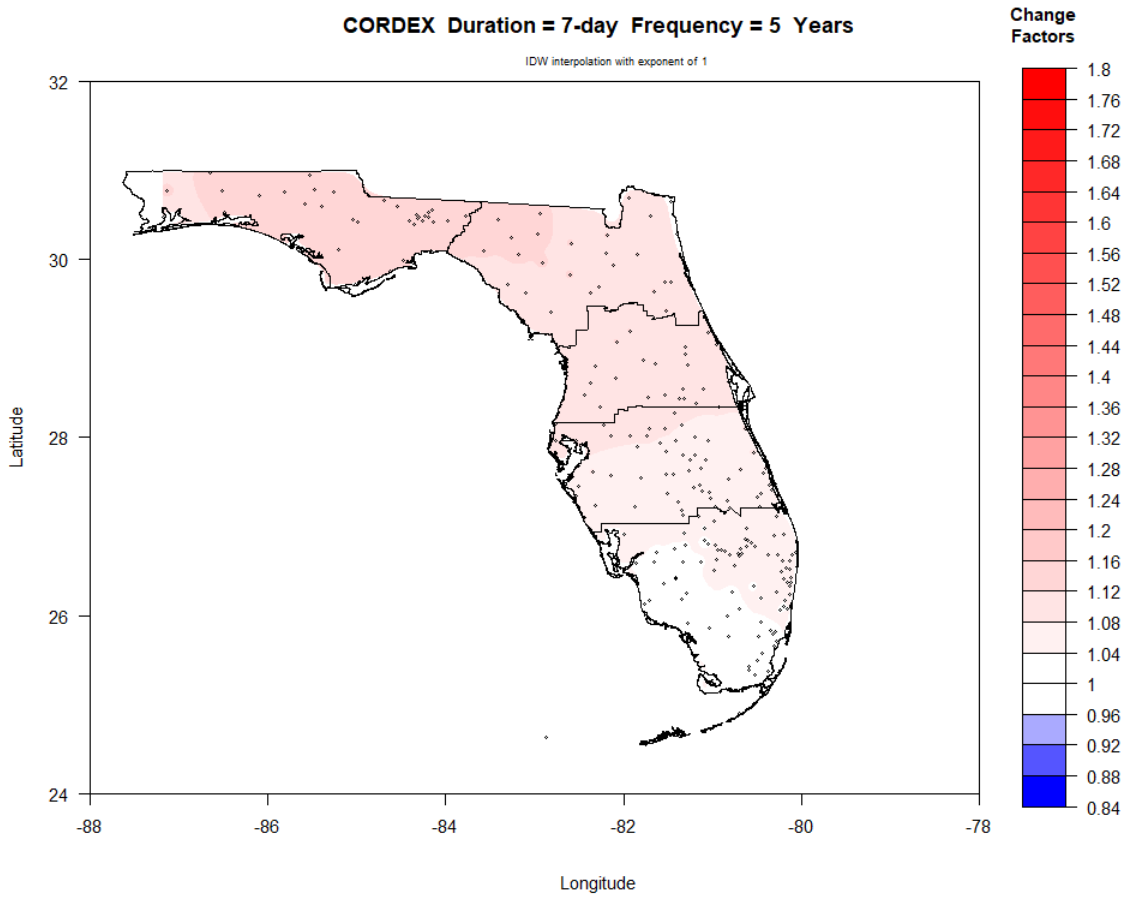

Figure IV-13. Map of FAR period (2060-2099) change factors across Florida for 7-day duration and 5-year return period.

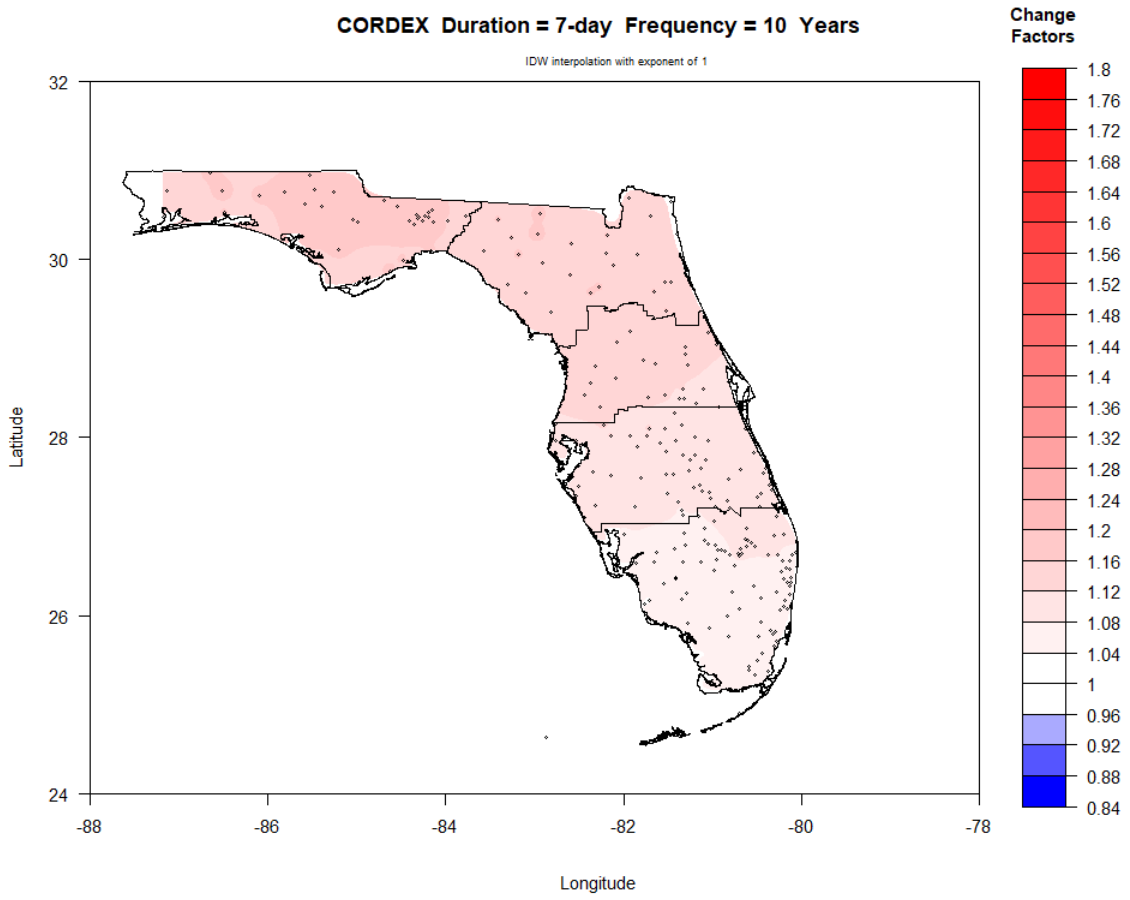

Figure IV-14. Map of FAR period (2060-2099) change factors across Florida for 7-day duration and 10-year return period.

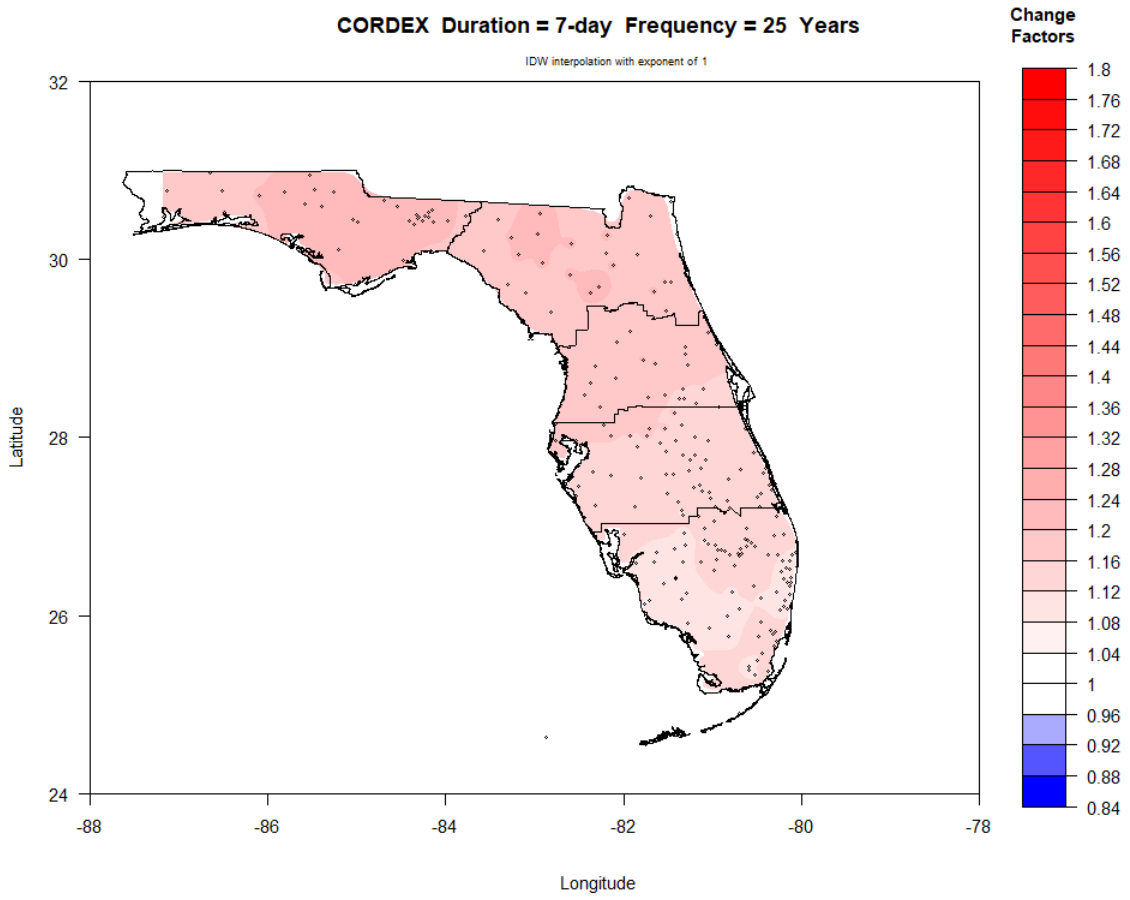

Figure IV-15. Map of FAR period (2060-2099) change factors across Florida for 7-day duration and 25-year return period.

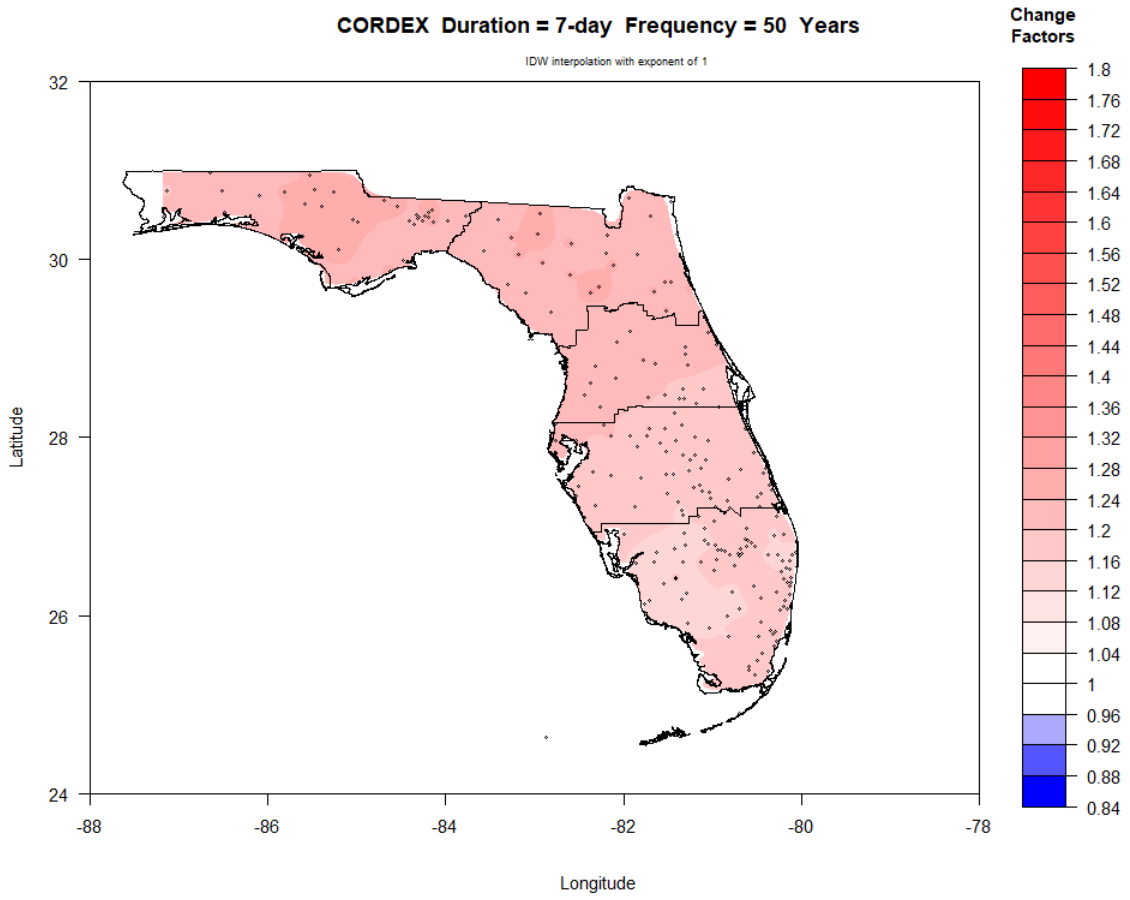

Figure IV-16. Map of FAR period (2060-2099) change factors across Florida for 7-day duration and 50-year return period.

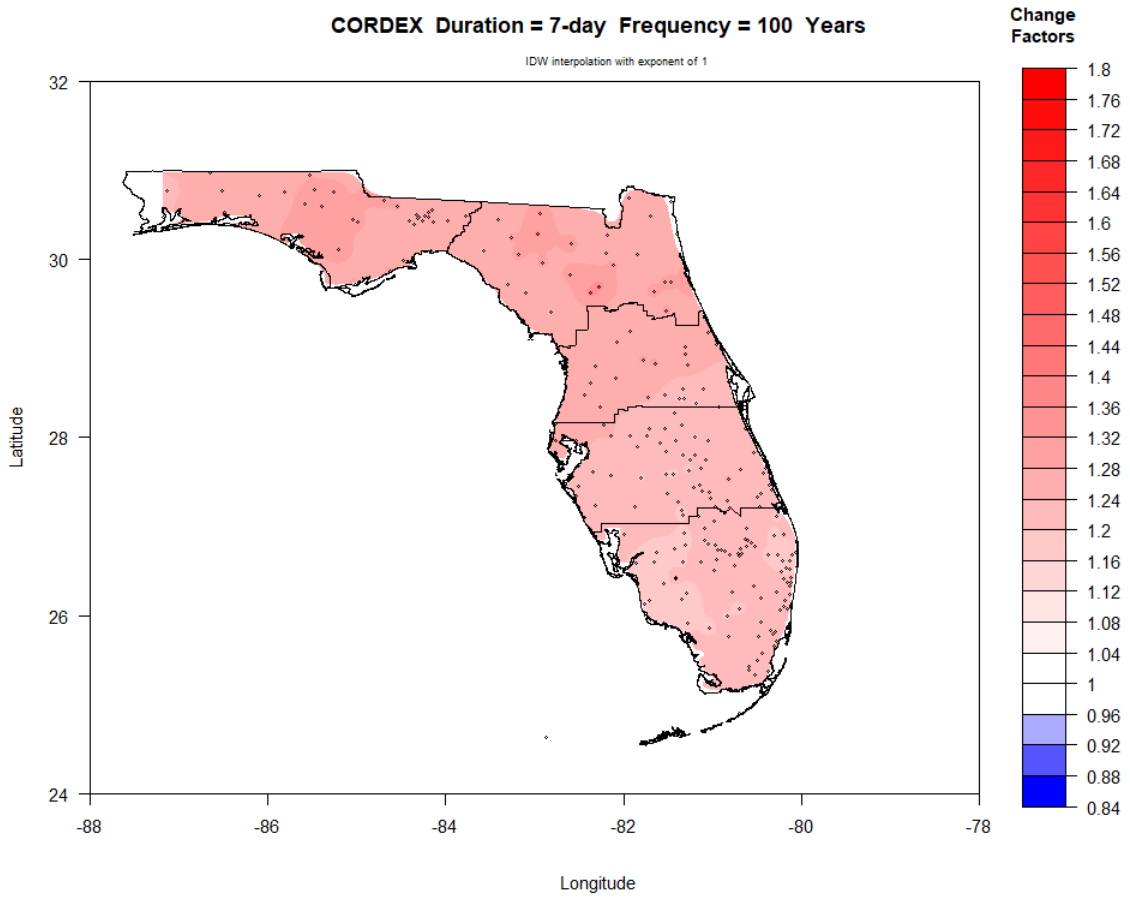

Figure IV-17. Map of FAR period (2060-2099) change factors across Florida for 7-day duration and 100-year return period.

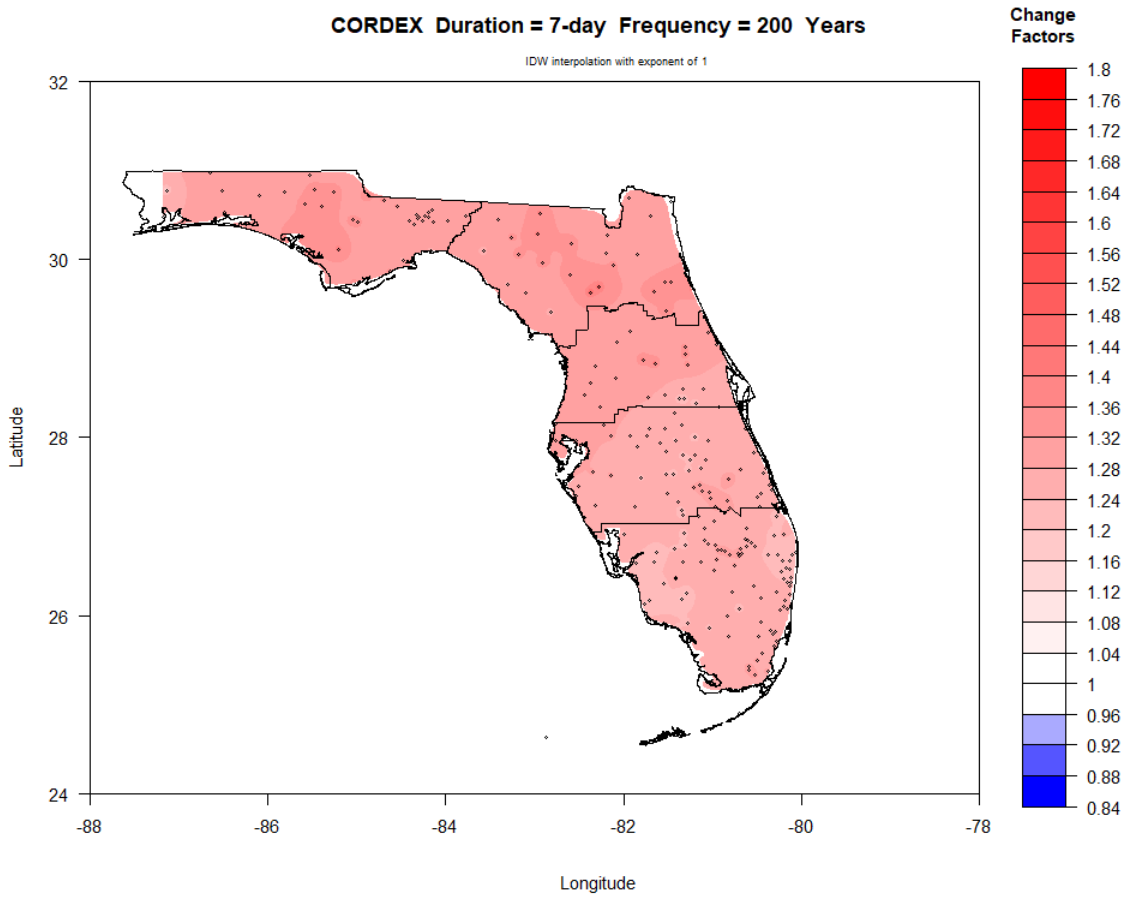

Figure IV-18. Map of FAR period (2060-2099) change factors across Florida for 7-day duration and 200-year return period.

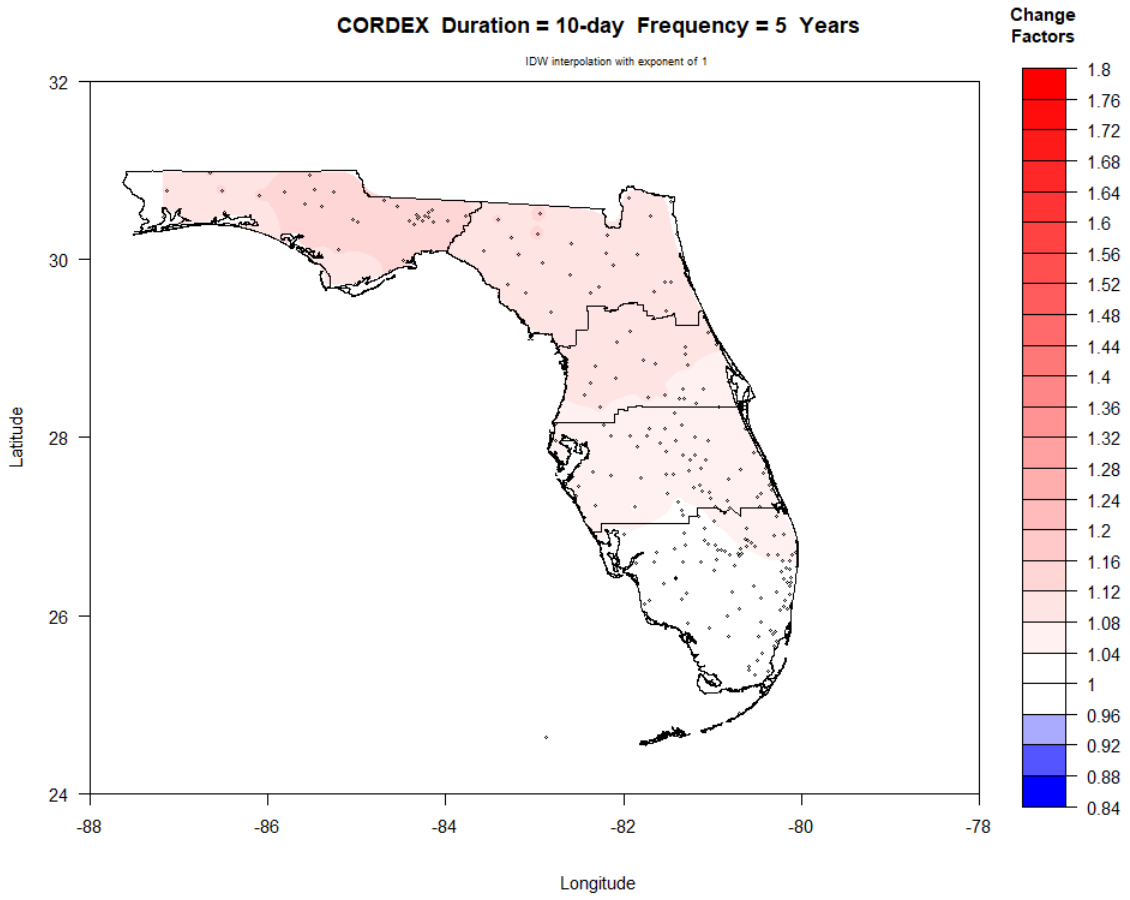

Figure IV-19. Map of FAR period (2060-2099) change factors across Florida for 10-day duration and 5-year return period.

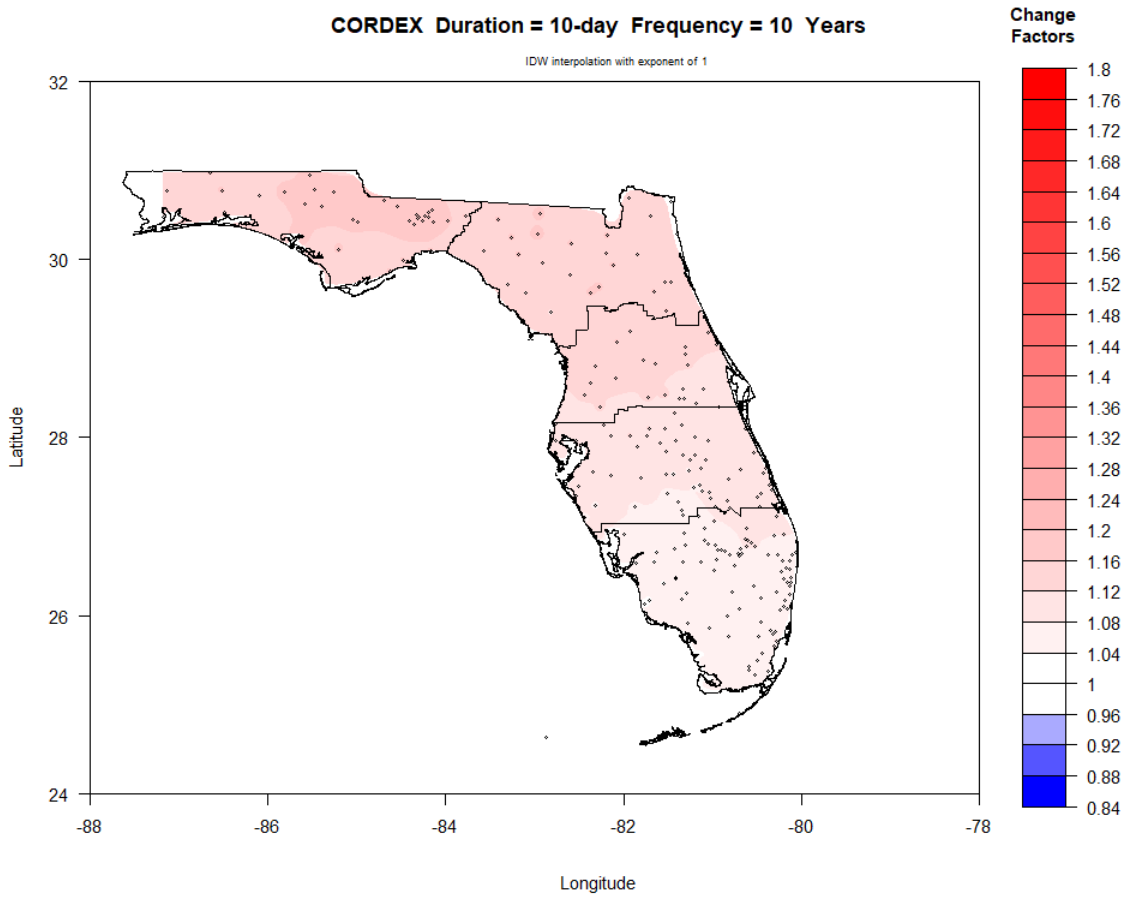

Figure IV-20. Map of FAR period (2060-2099) change factors across Florida for 10-day duration and 10-year return period.

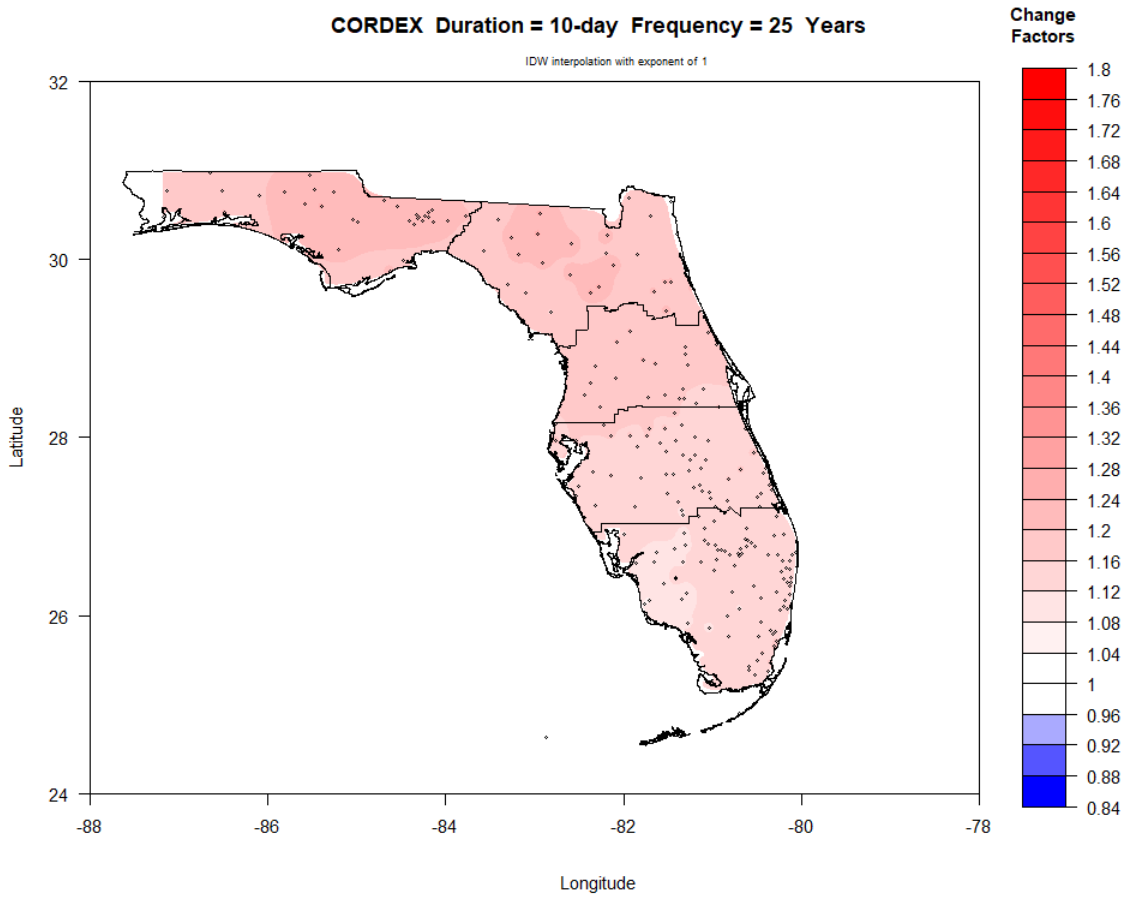

Figure IV-21. Map of FAR period (2060-2099) change factors across Florida for 10-day duration and 25-year return period.

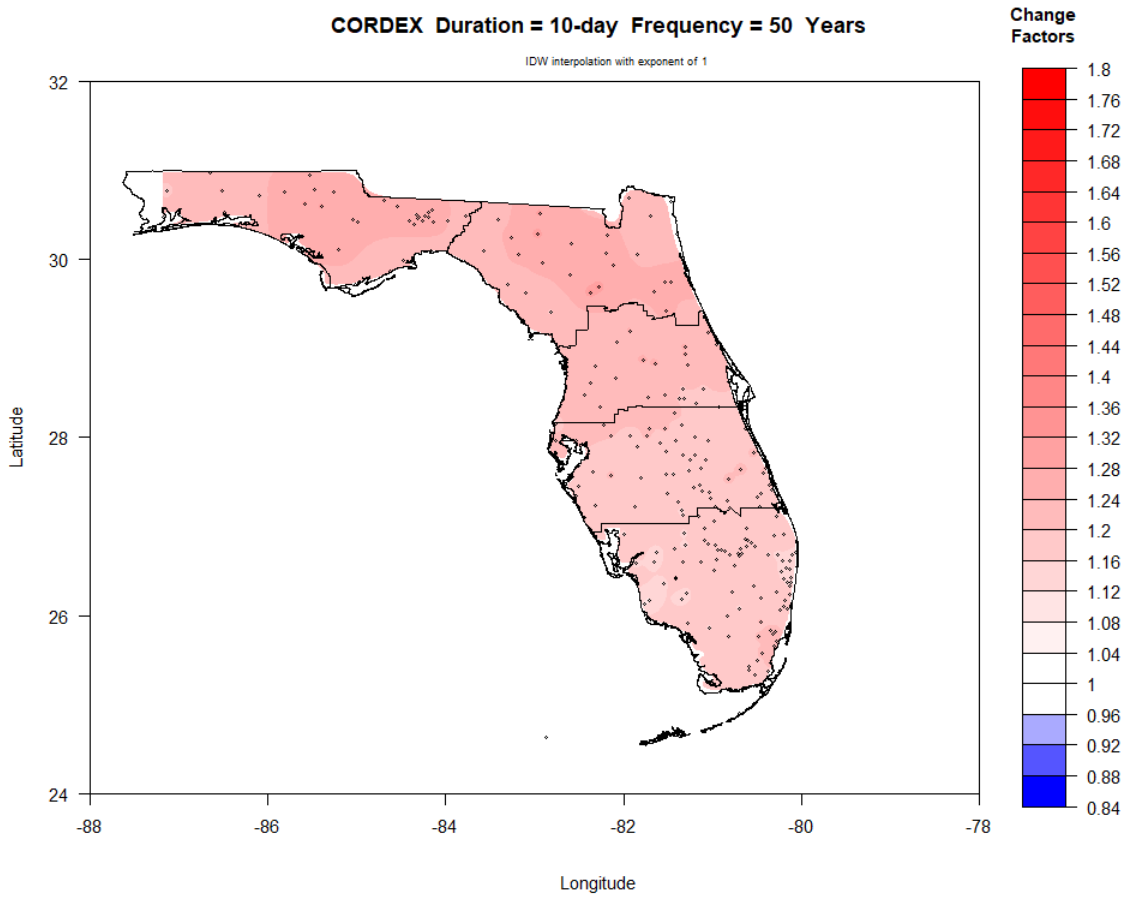

Figure IV-22. Map of FAR period (2060-2099) change factors across Florida for 10-day duration and 50-year return period.

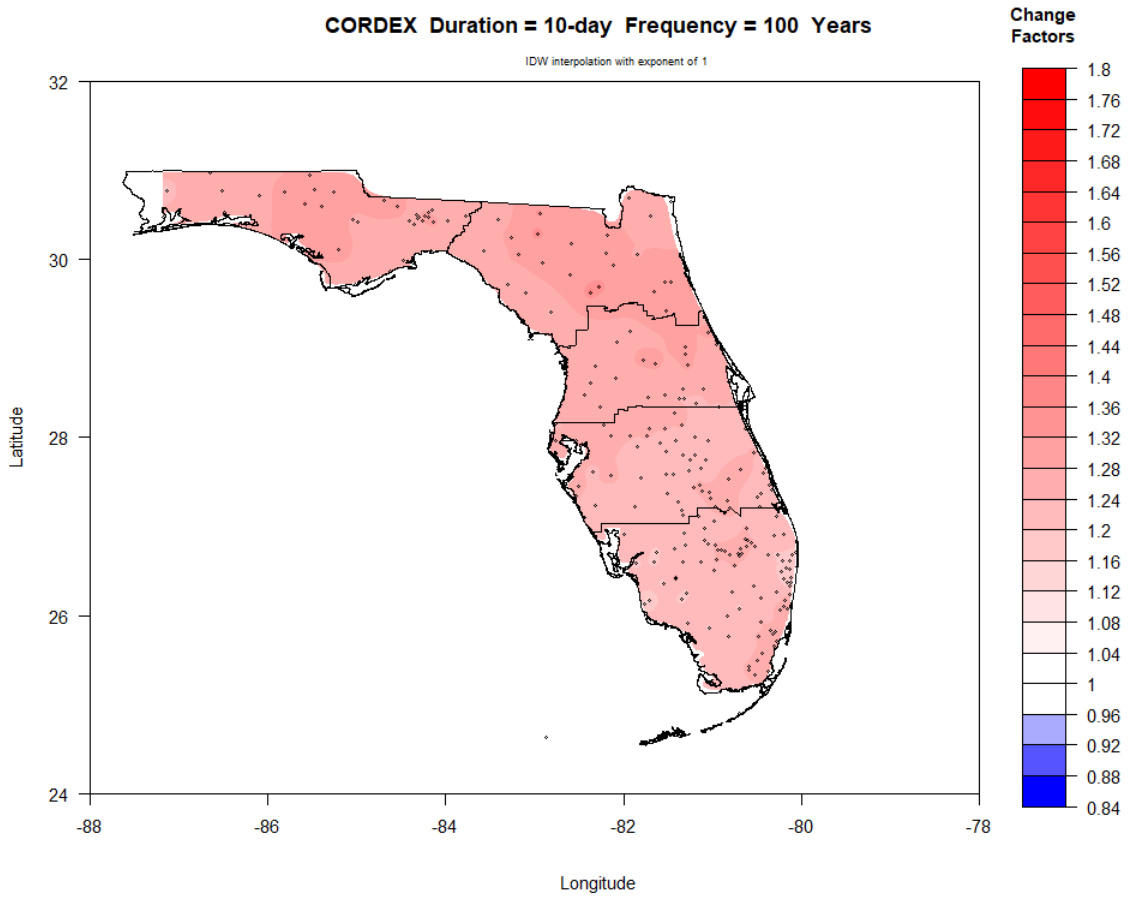

Figure IV-23. Map of FAR period (2060-2099) change factors across Florida for 10-day duration and 100-year return period.

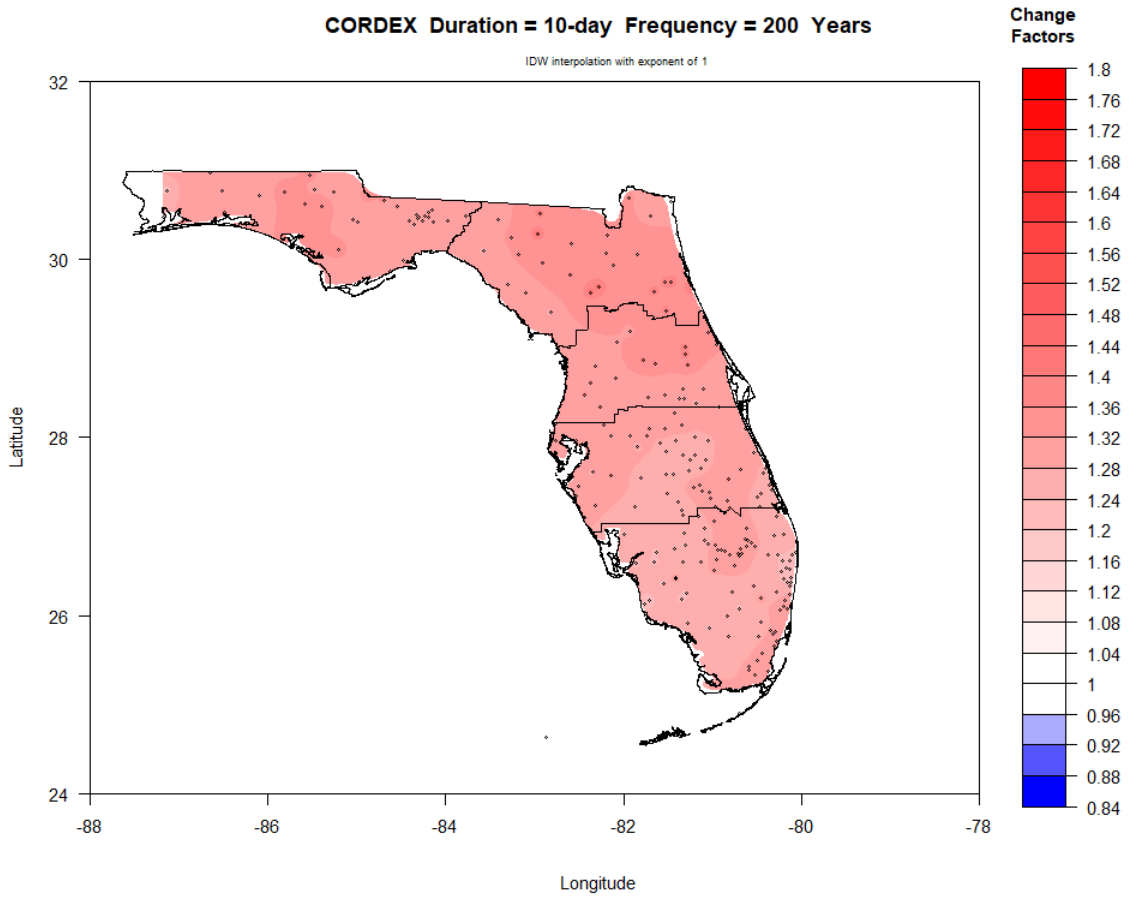

Figure IV-24. Map of FAR period (2060-2099) change factors across Florida for 10-day duration and 200-year return period.

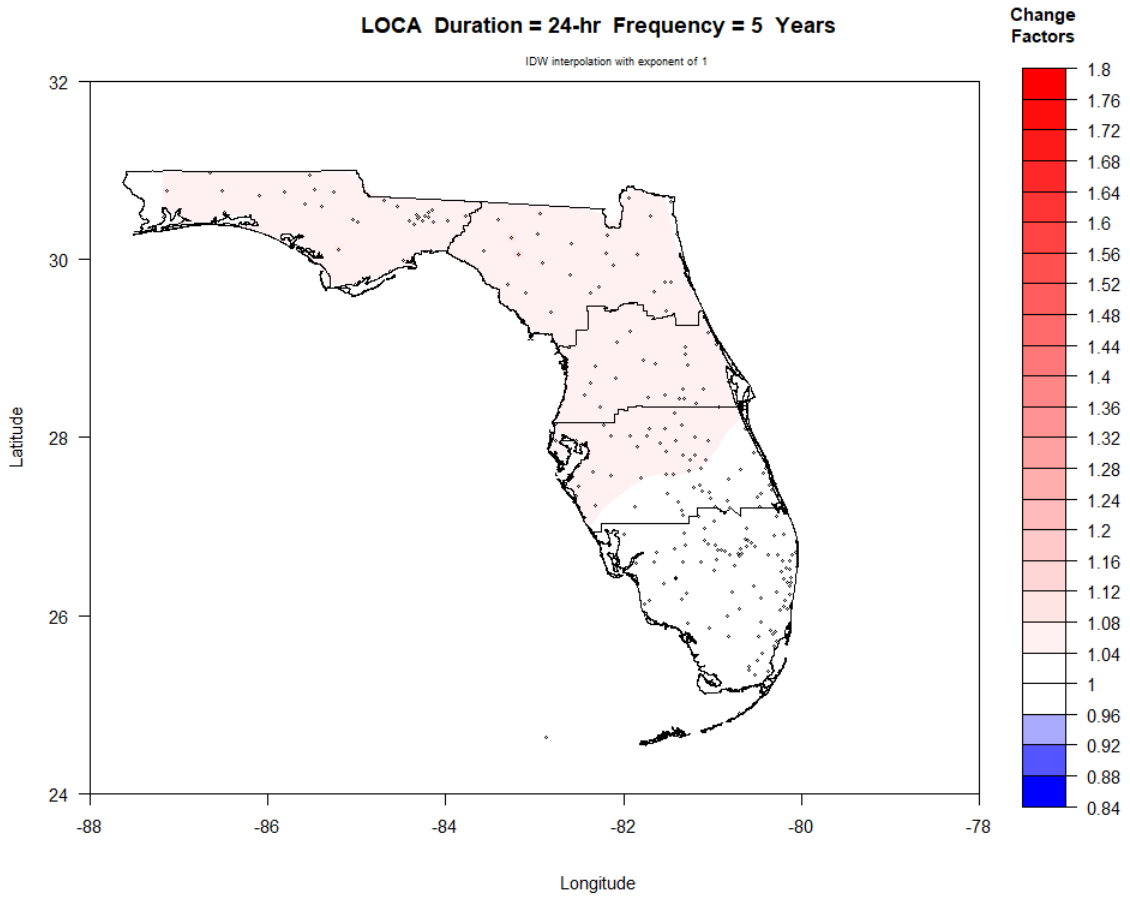

Figure IV-25. Map of FAR period (2060-2099) change factors across Florida for 24-hr duration and 5-year return period.

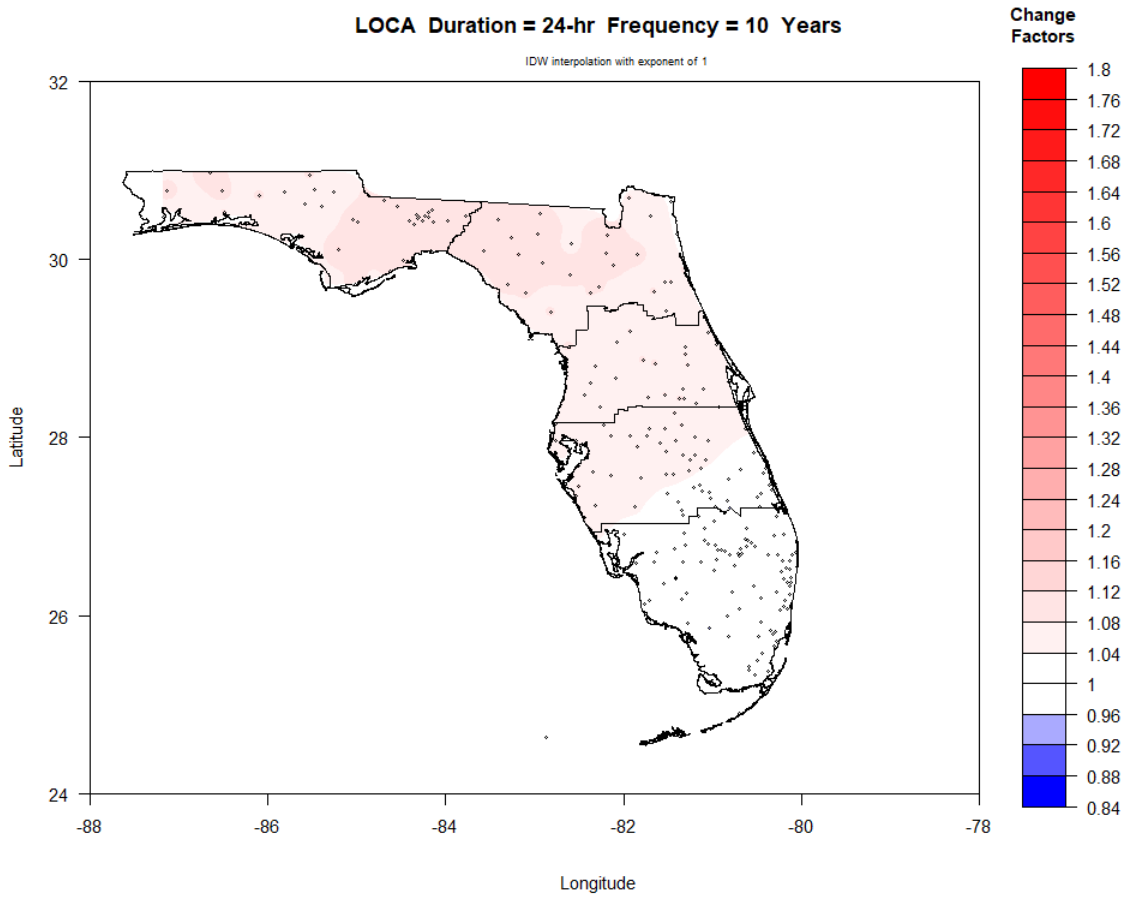

Figure IV-26. Map of FAR period (2060-2099) change factors across Florida for 24-hr duration and 10-year return period.

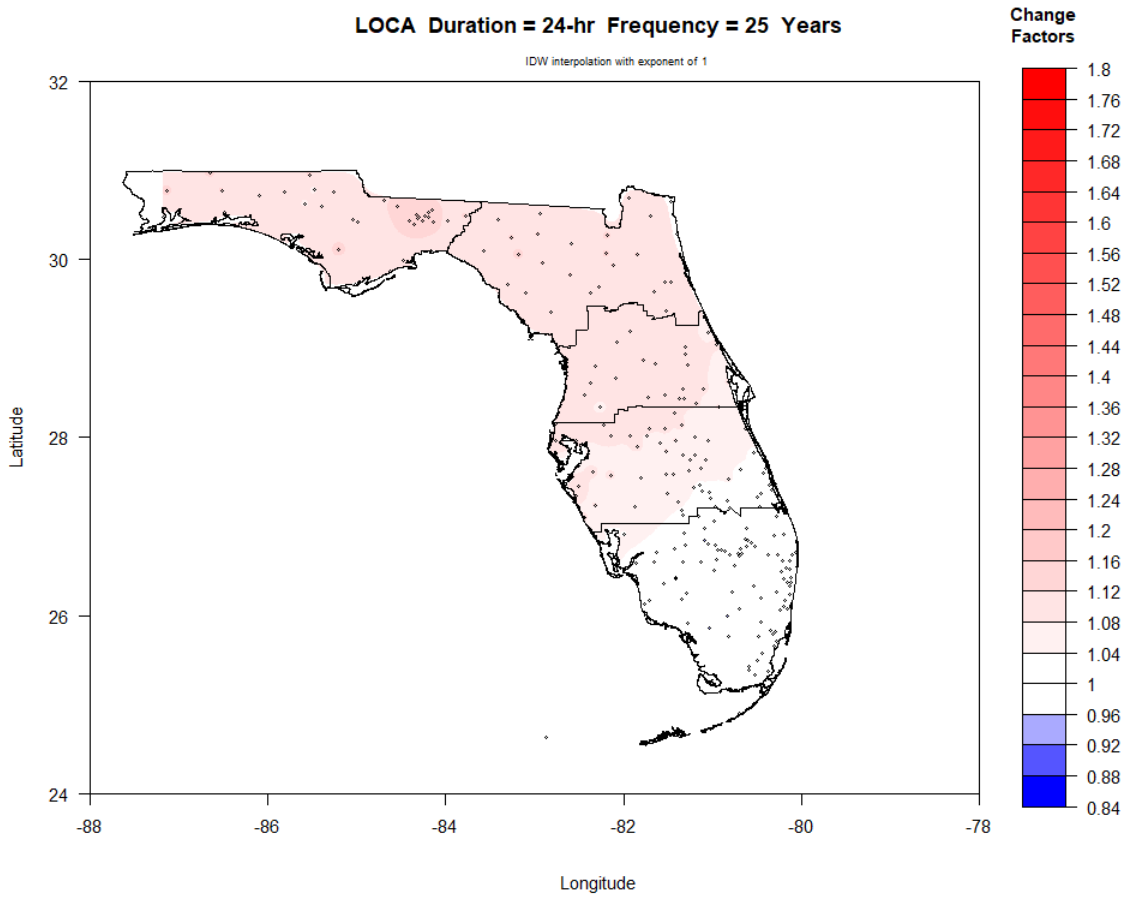

Figure IV-27. Map of FAR period (2060-2099) change factors across Florida for 24-hr duration and 25-year return period.

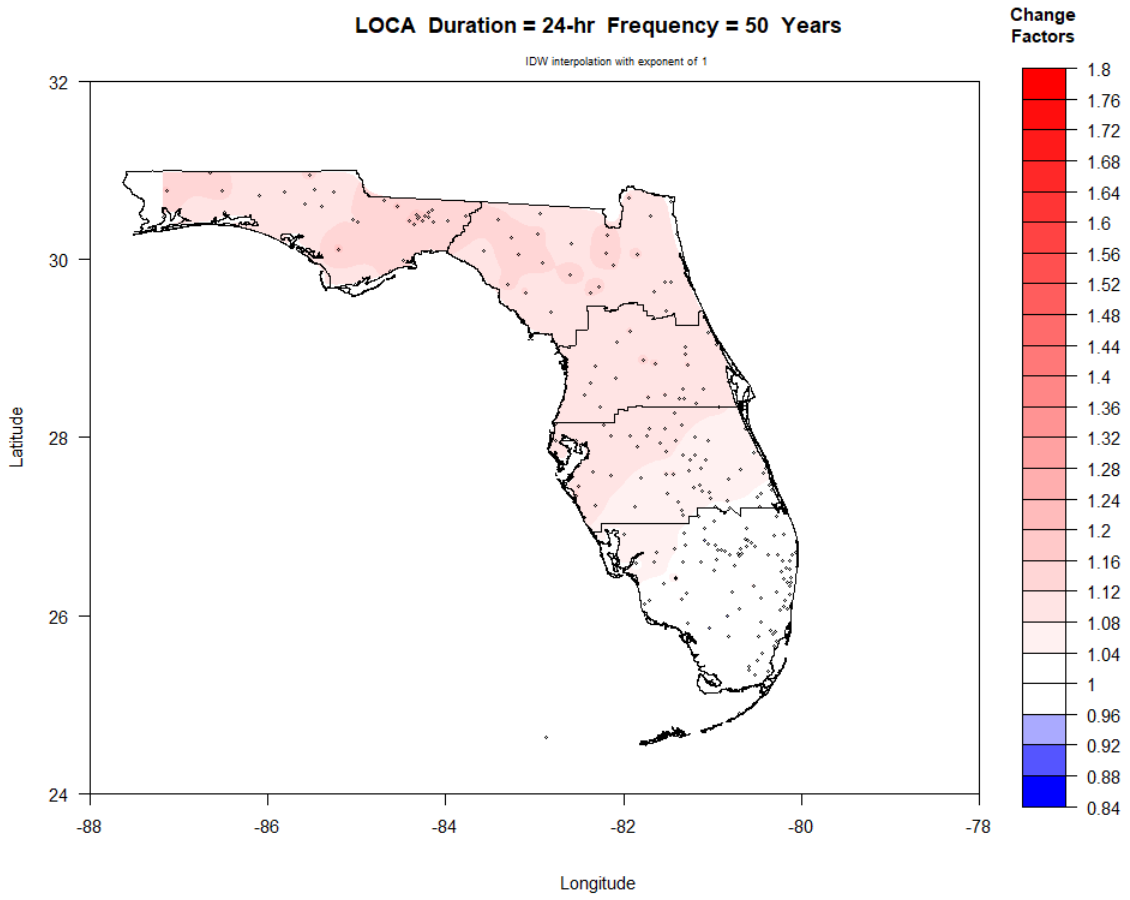

Figure IV-28. Map of FAR period (2060-2099) change factors across Florida for 24-hr duration and 50-year return period.

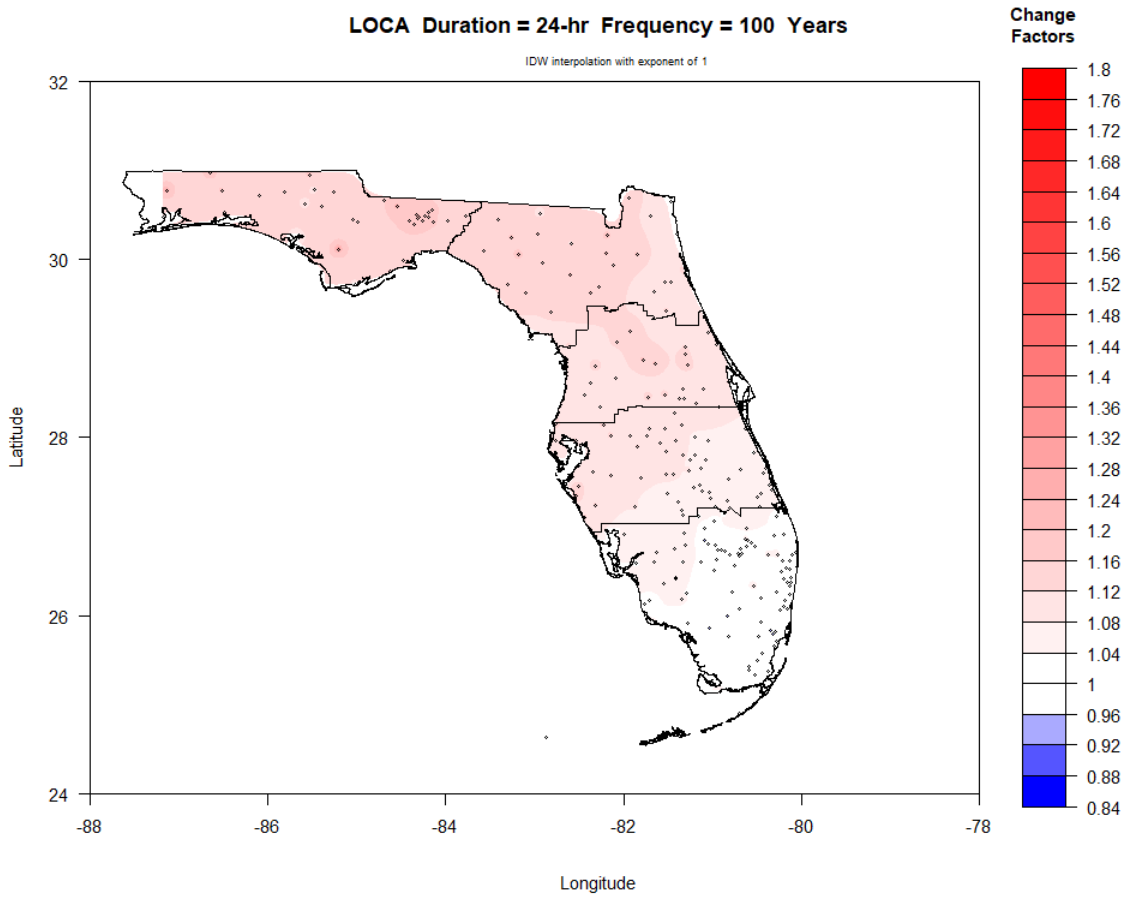

Figure IV-29. Map of FAR period (2060-2099) change factors across Florida for 24-hr duration and 100-year return period.

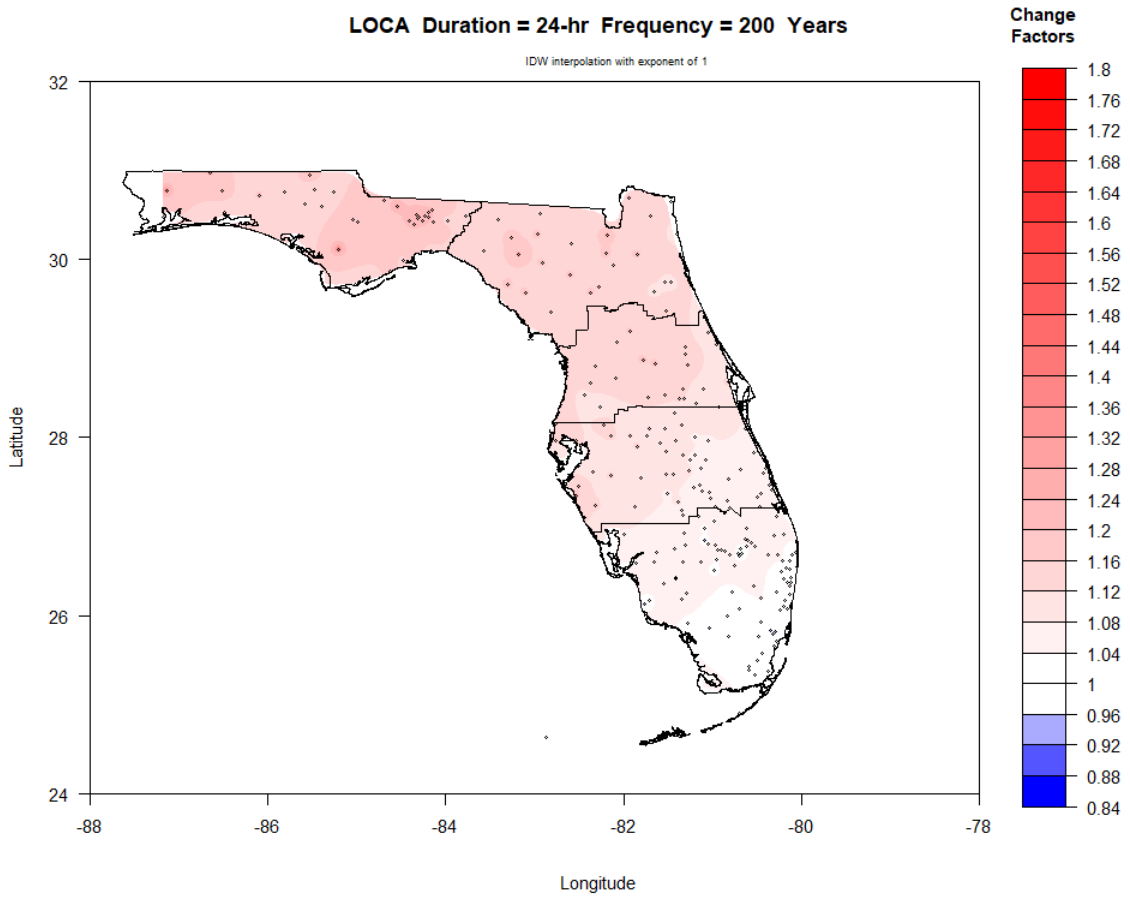

Figure IV-30. Map of FAR period (2060-2099) change factors across Florida for 24-hr duration and 200-year return period.

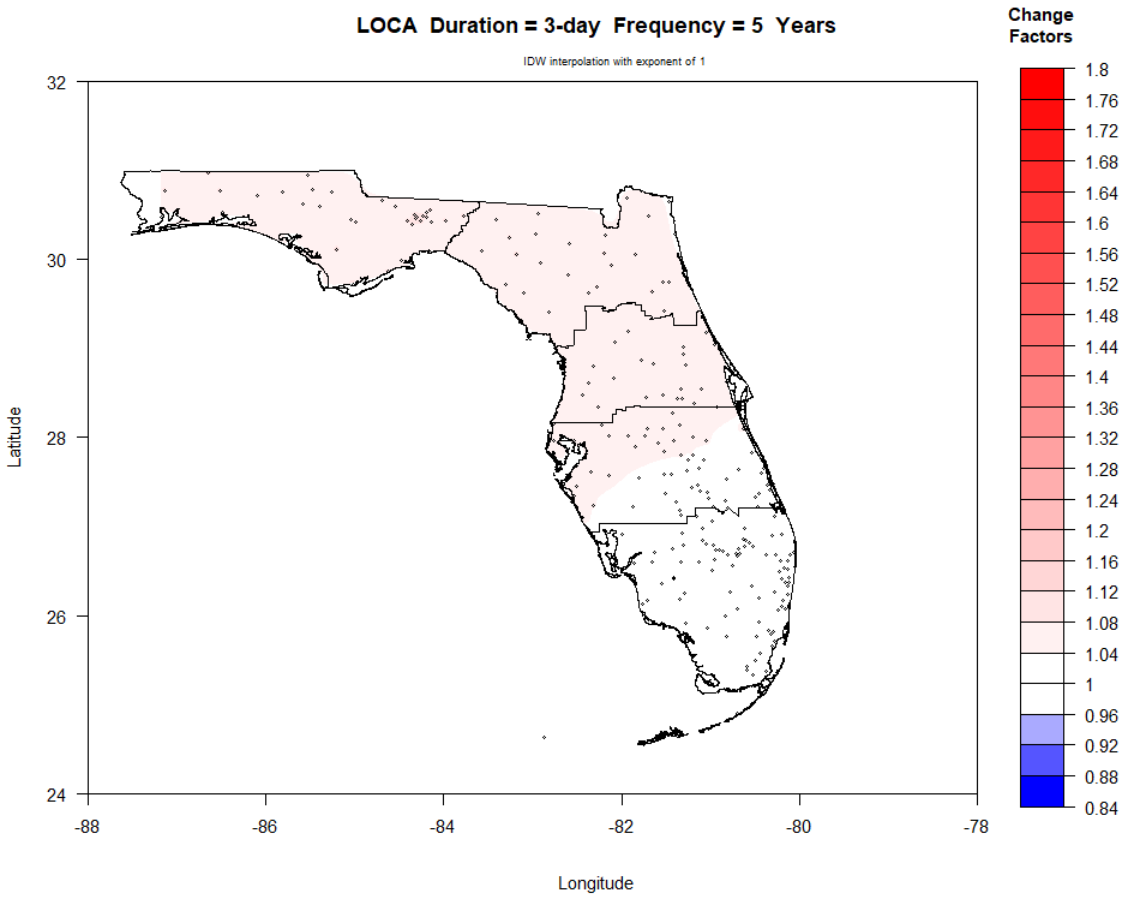

Figure IV-31. Map of FAR period (2060-2099) change factors across Florida for 3-day duration and 5-year return period.

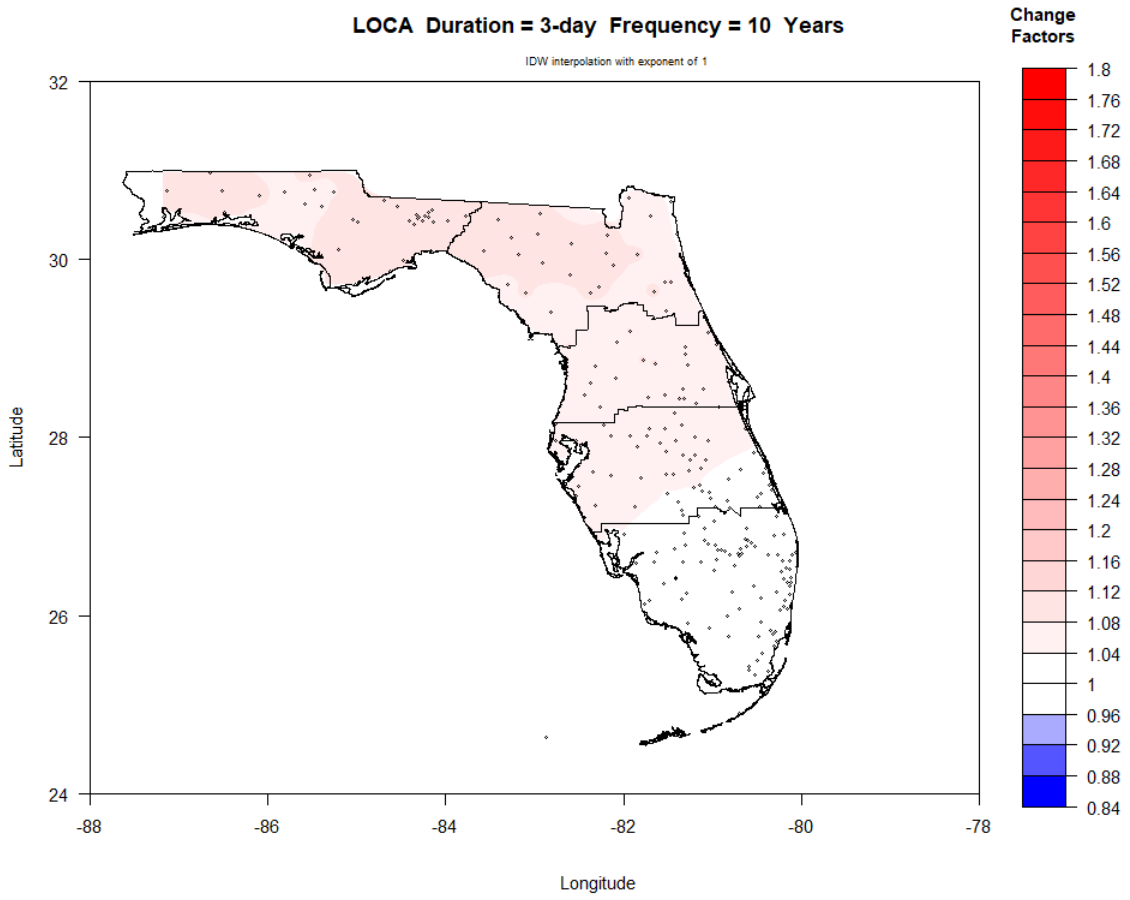

Figure IV-32. Map of FAR period (2060-2099) change factors across Florida for 3-day duration and 10-year return period.

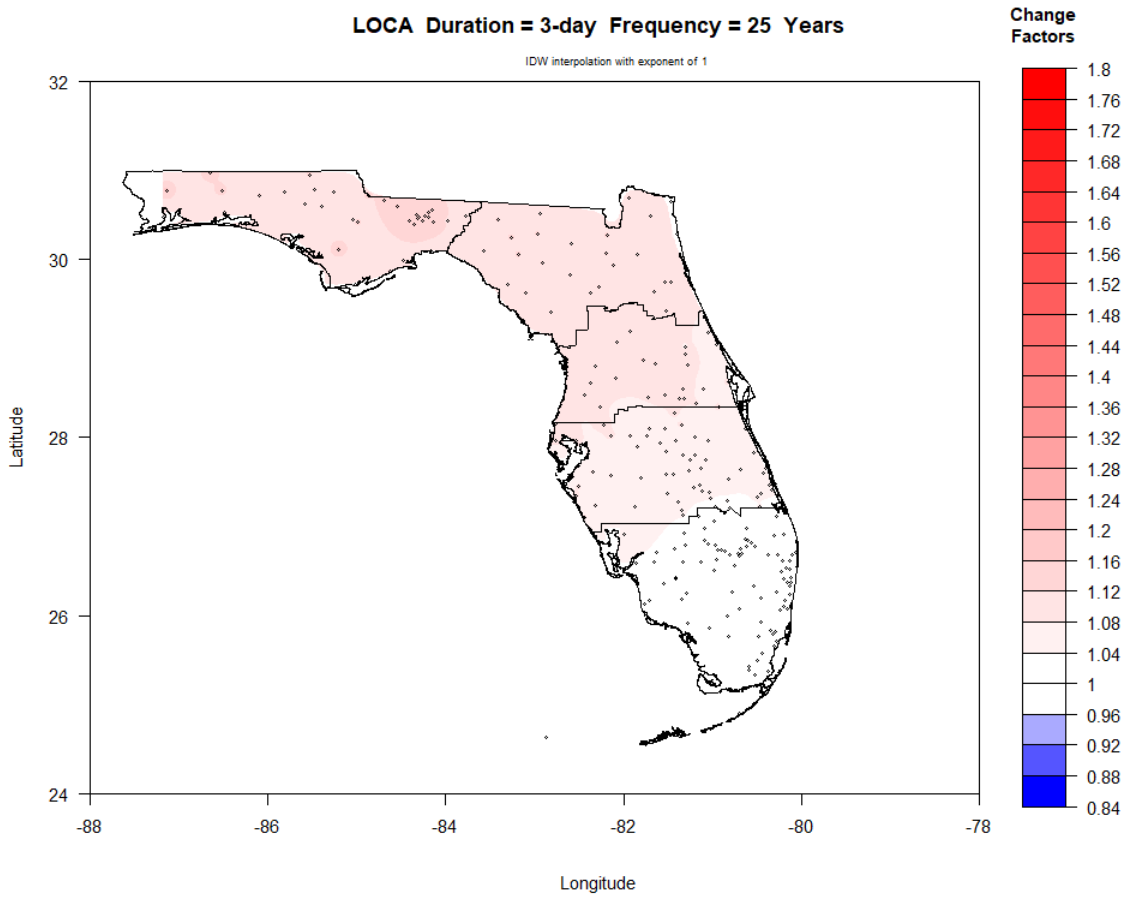

Figure IV-33. Map of FAR period (2060-2099) change factors across Florida for 3-day duration and 25-year return period.

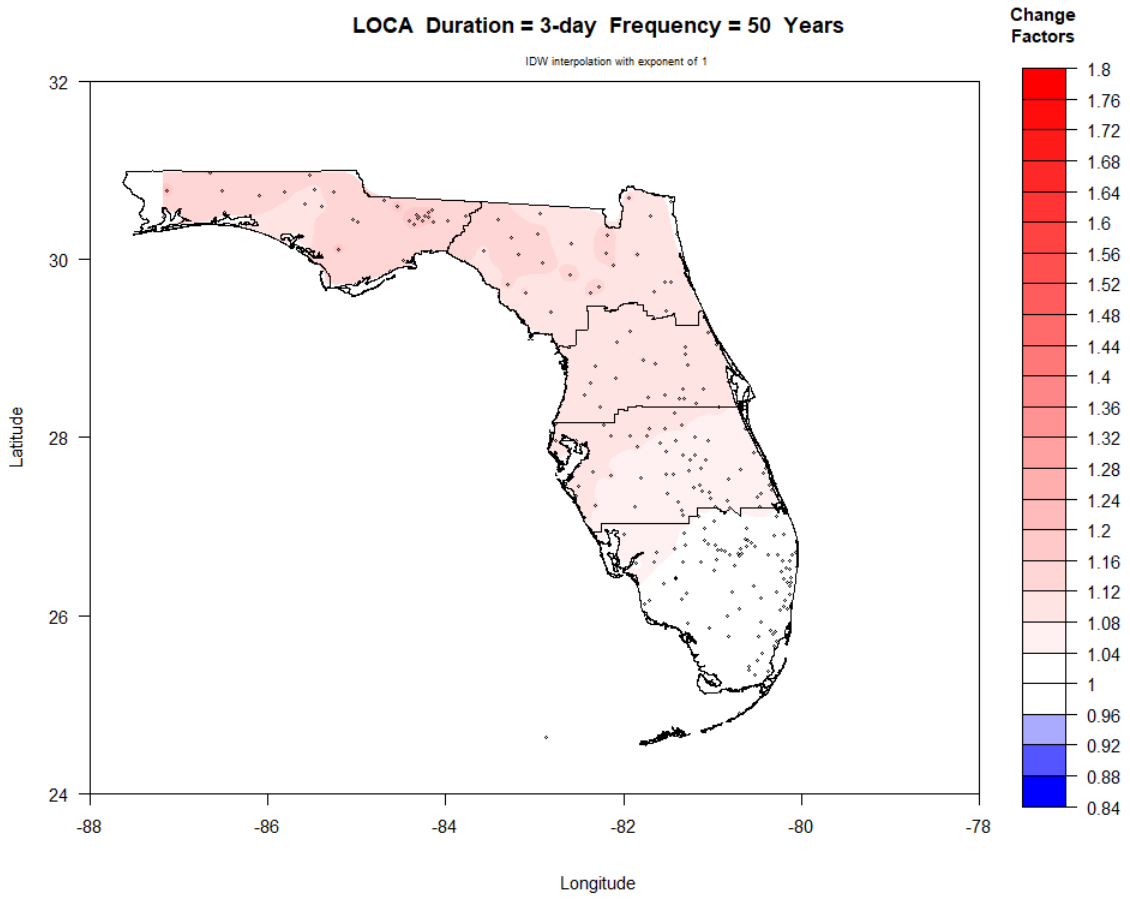

Figure IV-34. Map of FAR period (2060-2099) change factors across Florida for 3-day duration and 50-year return period.

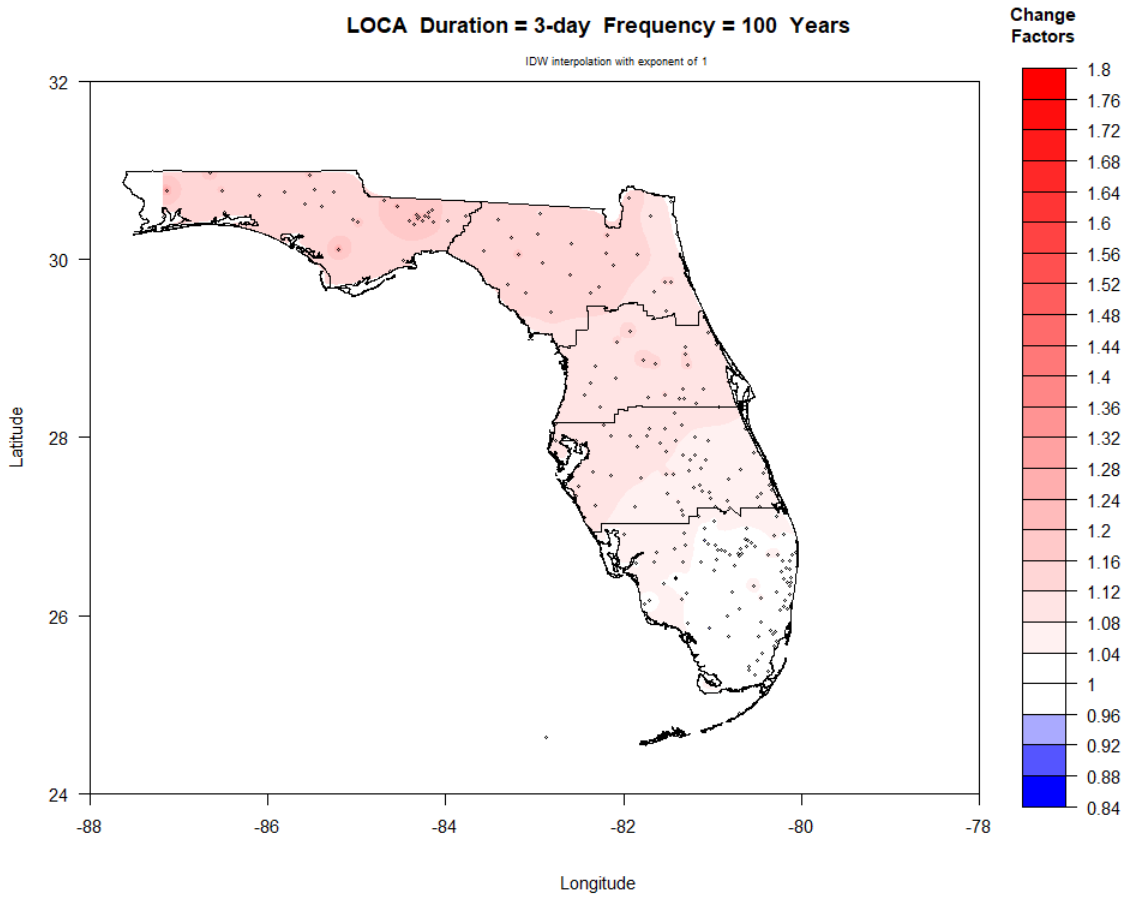

Figure IV-35. Map of FAR period (2060-2099) change factors across Florida for 3-day duration and 100-year return period.

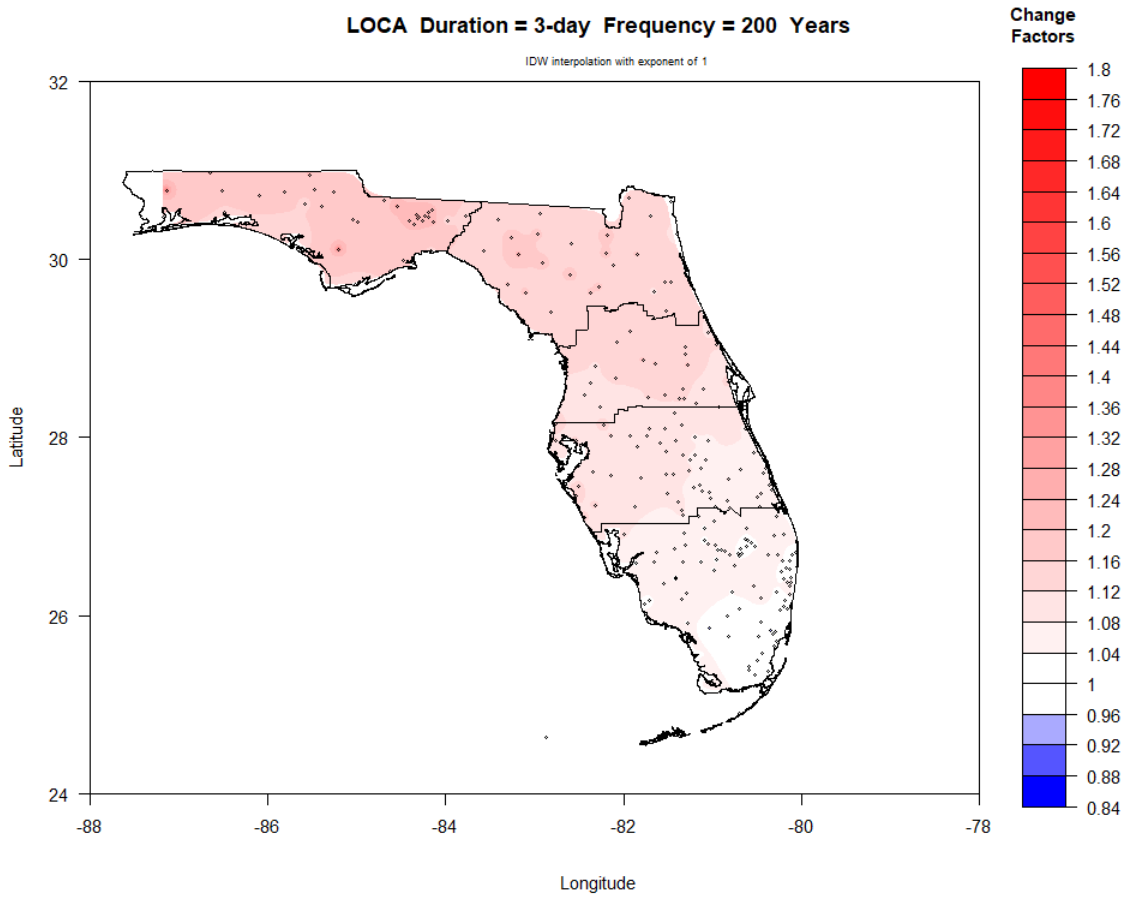

Figure IV-36. Map of FAR period (2060-2099) change factors across Florida for 3-day duration and 200-year return period.

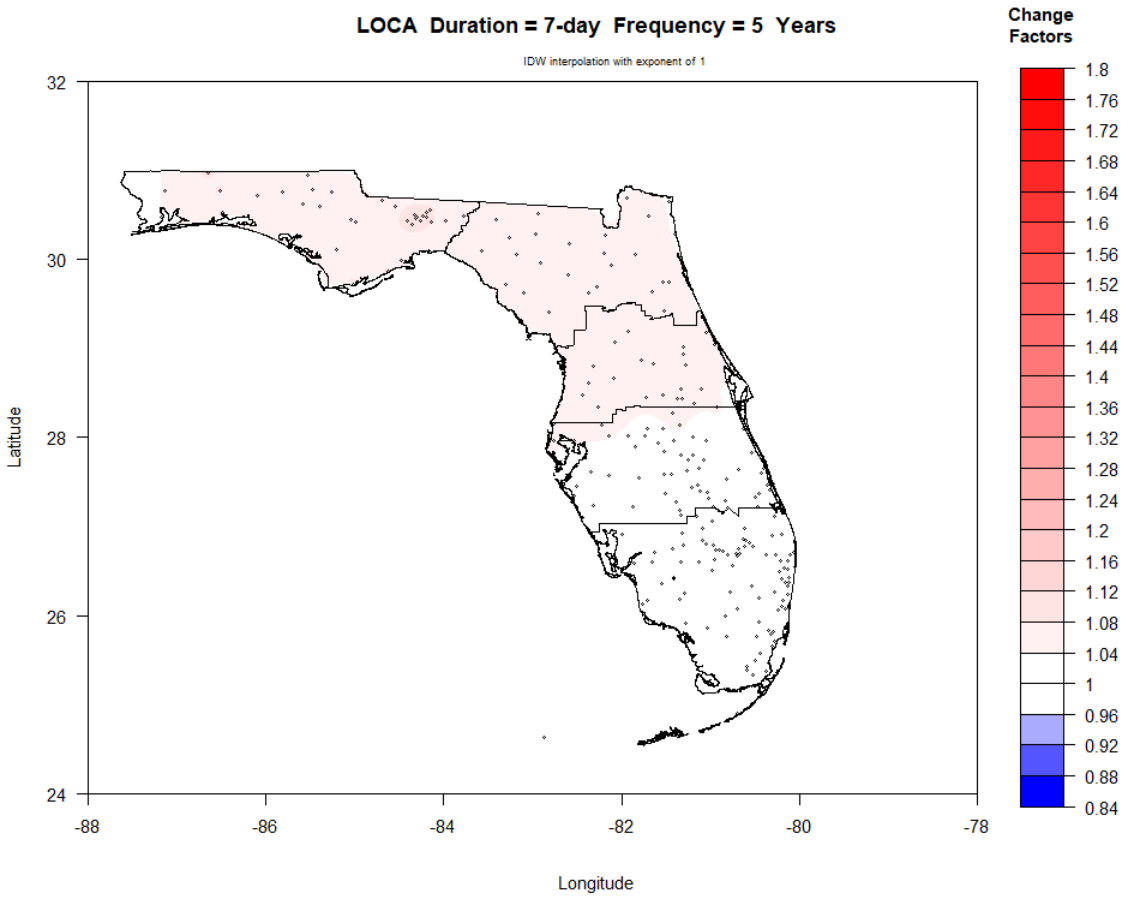

Figure IV-37. Map of FAR period (2060-2099) change factors across Florida for 7-day duration and 5-year return period.

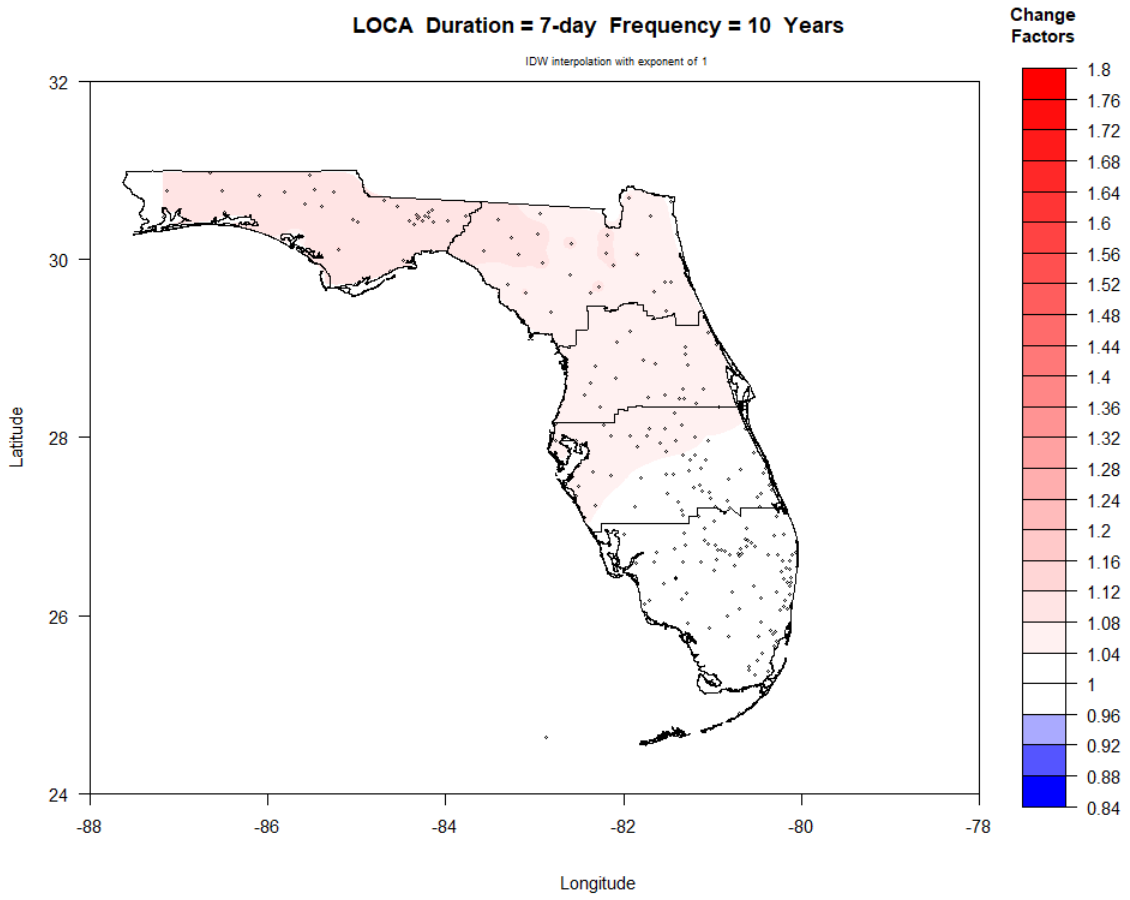

Figure IV-38. Map of FAR period (2060-2099) change factors across Florida for 7-day duration and 10-year return period.

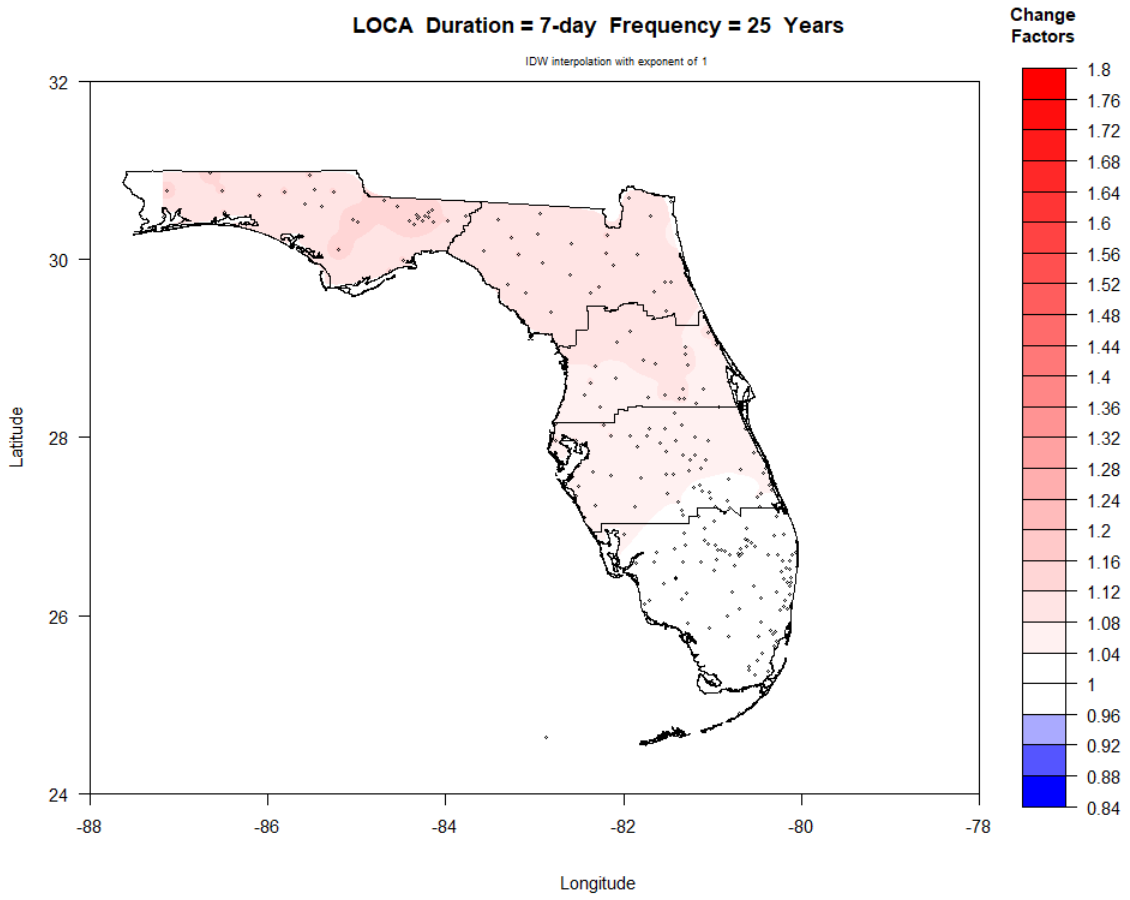

Figure IV-39. Map of FAR period (2060-2099) change factors across Florida for 7-day duration and 25-year return period.

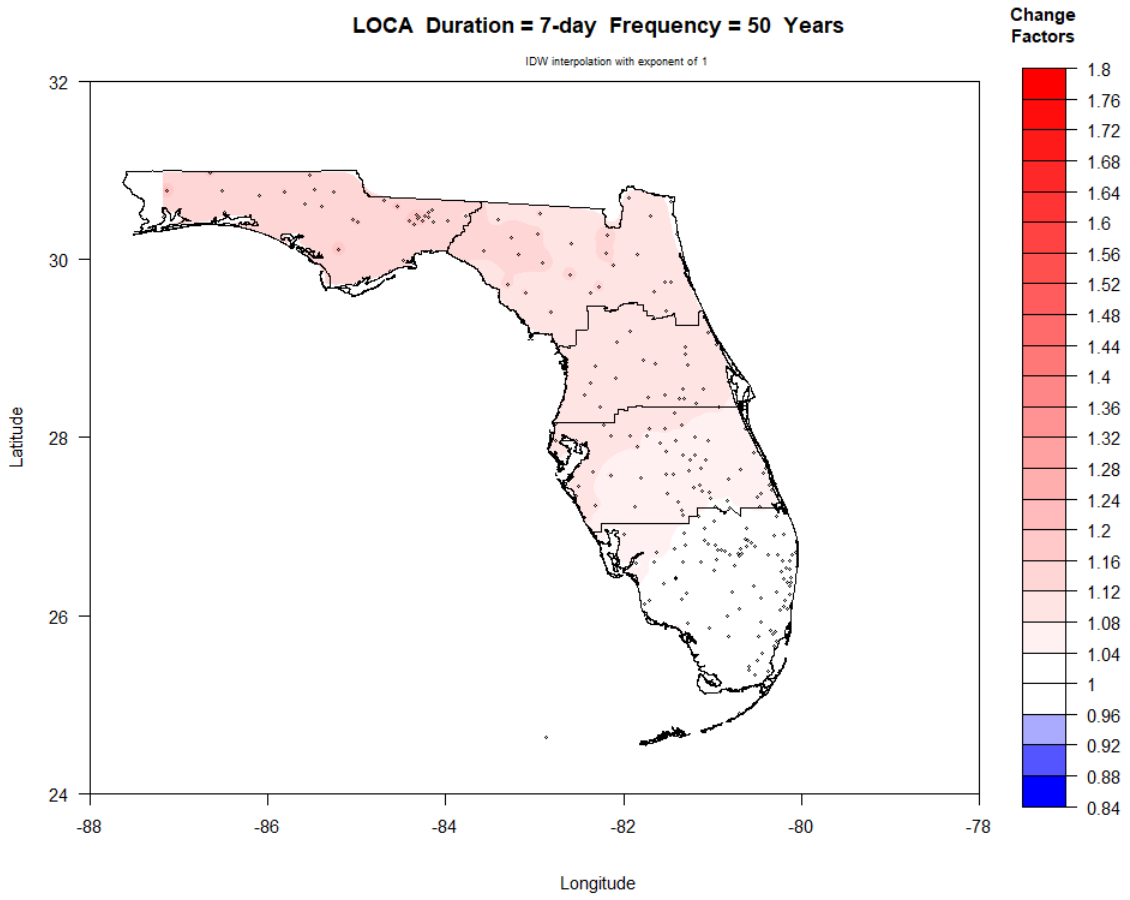

Figure IV-40. Map of FAR period (2060-2099) change factors across Florida for 7-day duration and 50-year return period.

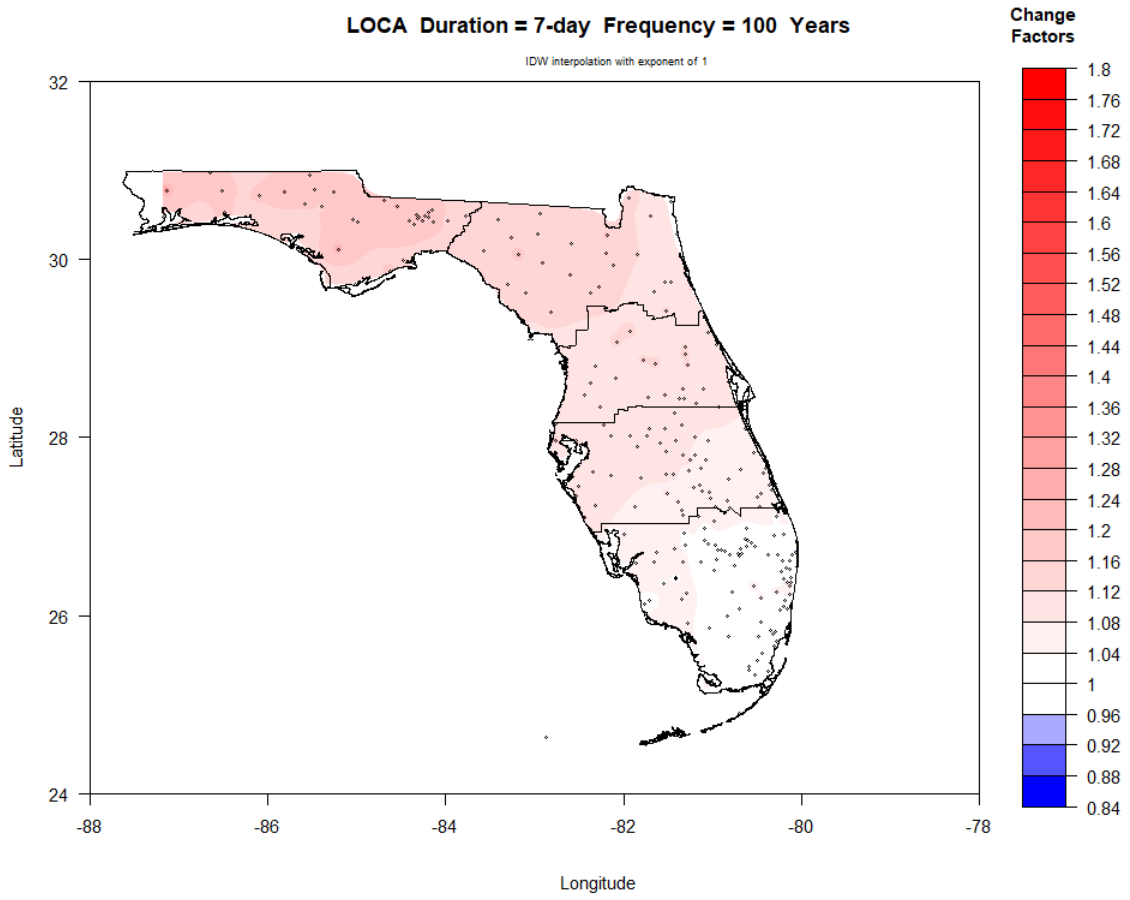

Figure IV-41. Map of FAR period (2060-2099) change factors across Florida for 7-day duration and 100-year return period.

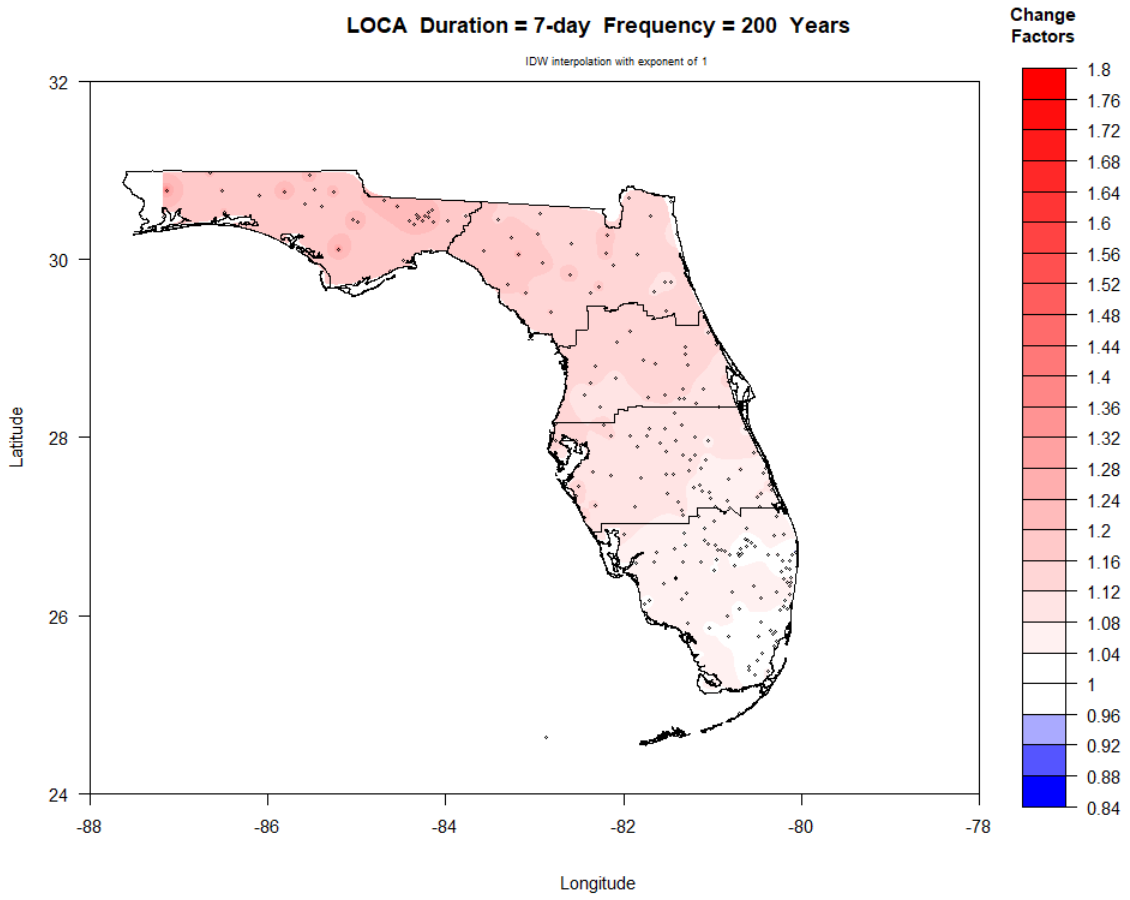

Figure IV-42. Map of FAR period (2060-2099) change factors across Florida for 7-day duration and 200-year return period.

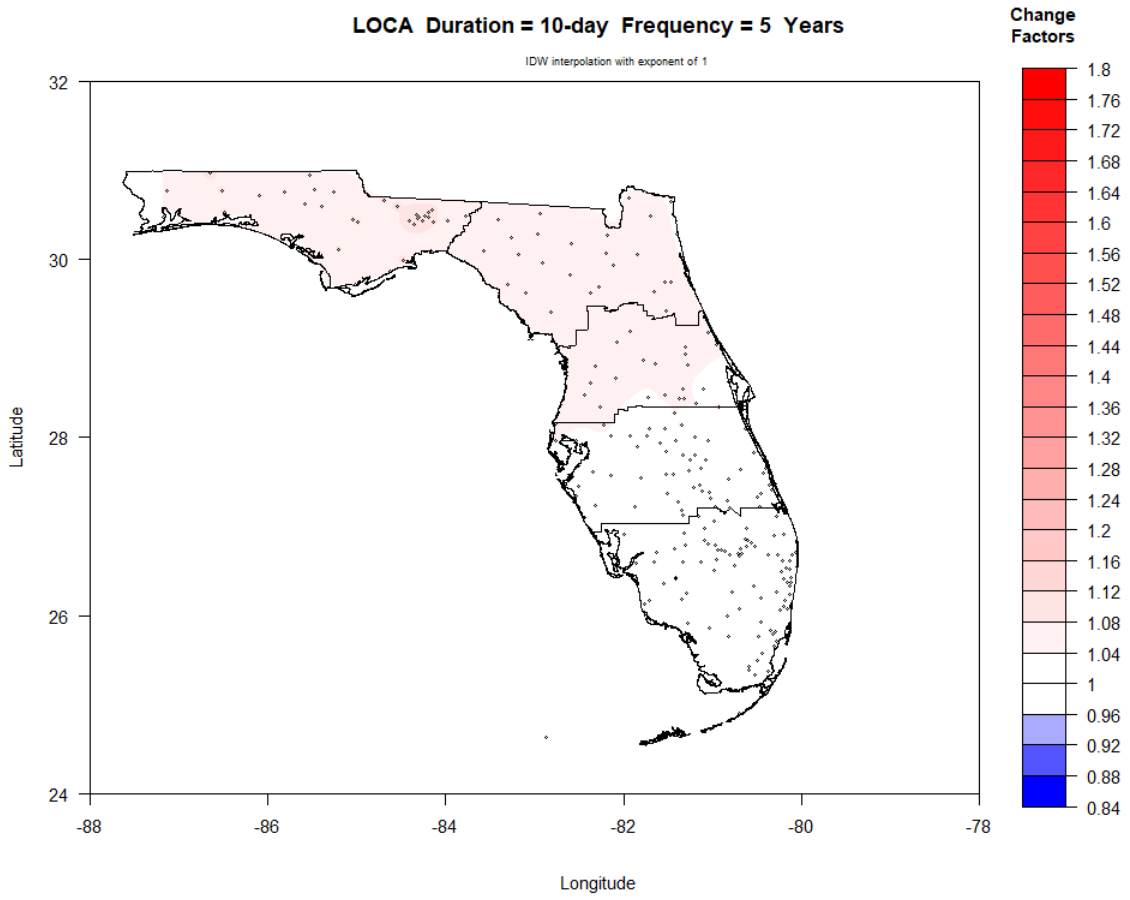

Figure IV-43. Map of FAR period (2060-2099) change factors across Florida for 10-day duration and 5-year return period.

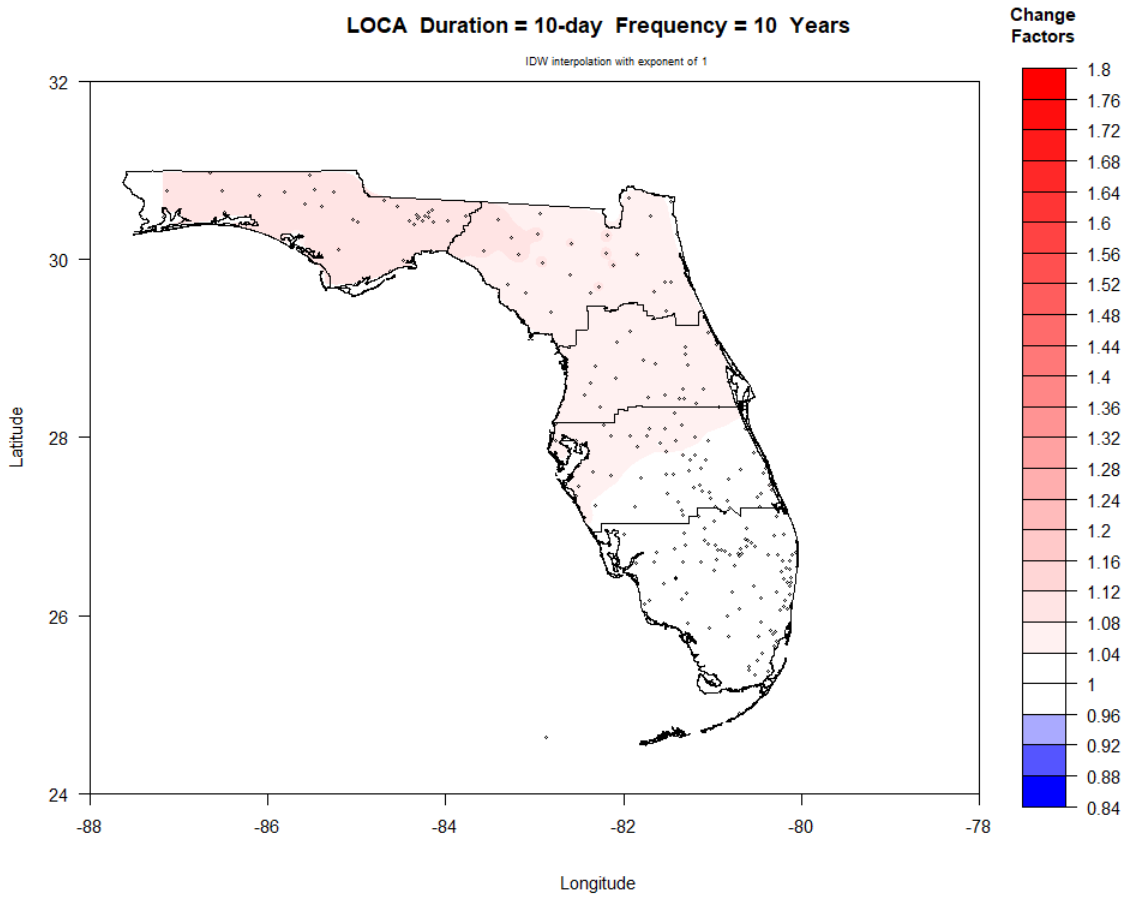

Figure IV-44. Map of FAR period (2060-2099) change factors across Florida for 10-day duration and 10-year return period.

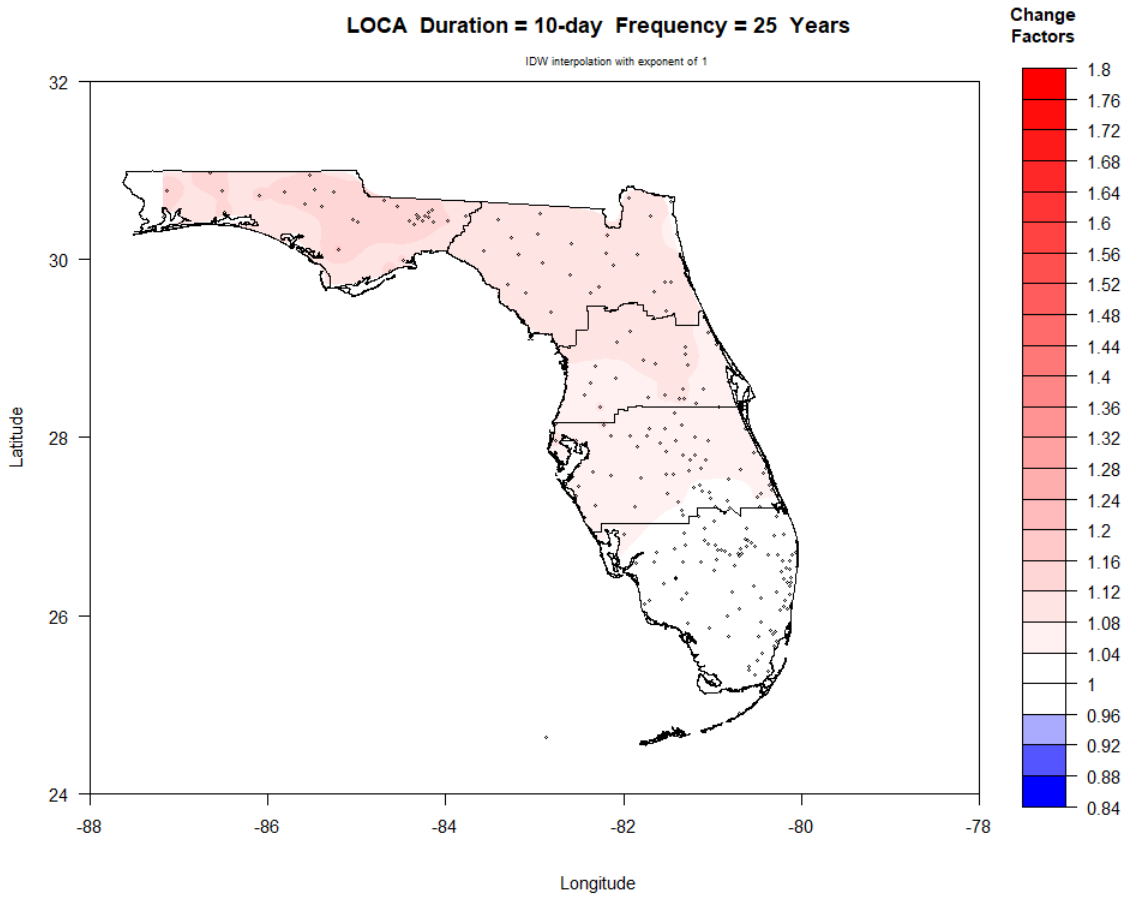

Figure IV-45. Map of FAR period (2060-2099) change factors across Florida for 10-day duration and 25-year return period.

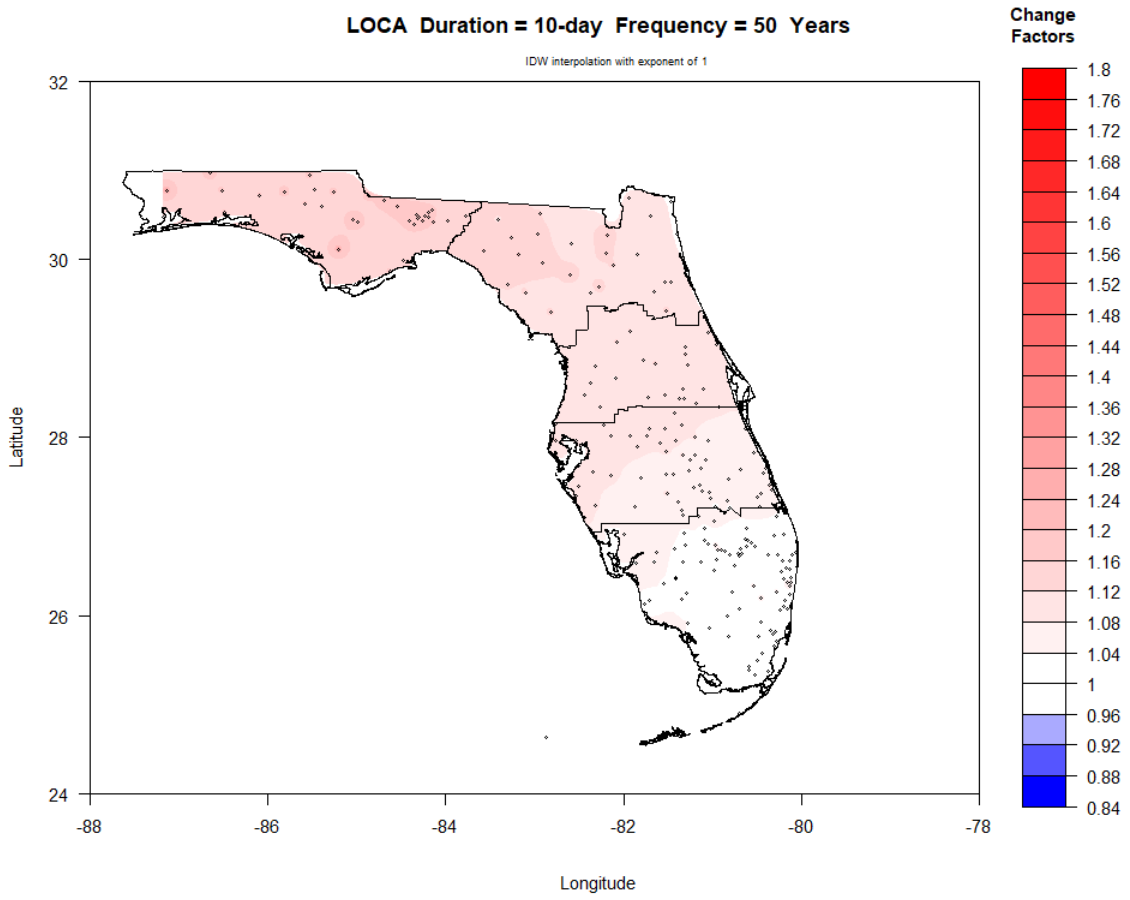

Figure IV-46. Map of FAR period (2060-2099) change factors across Florida for 10-day duration and 50-year return period.

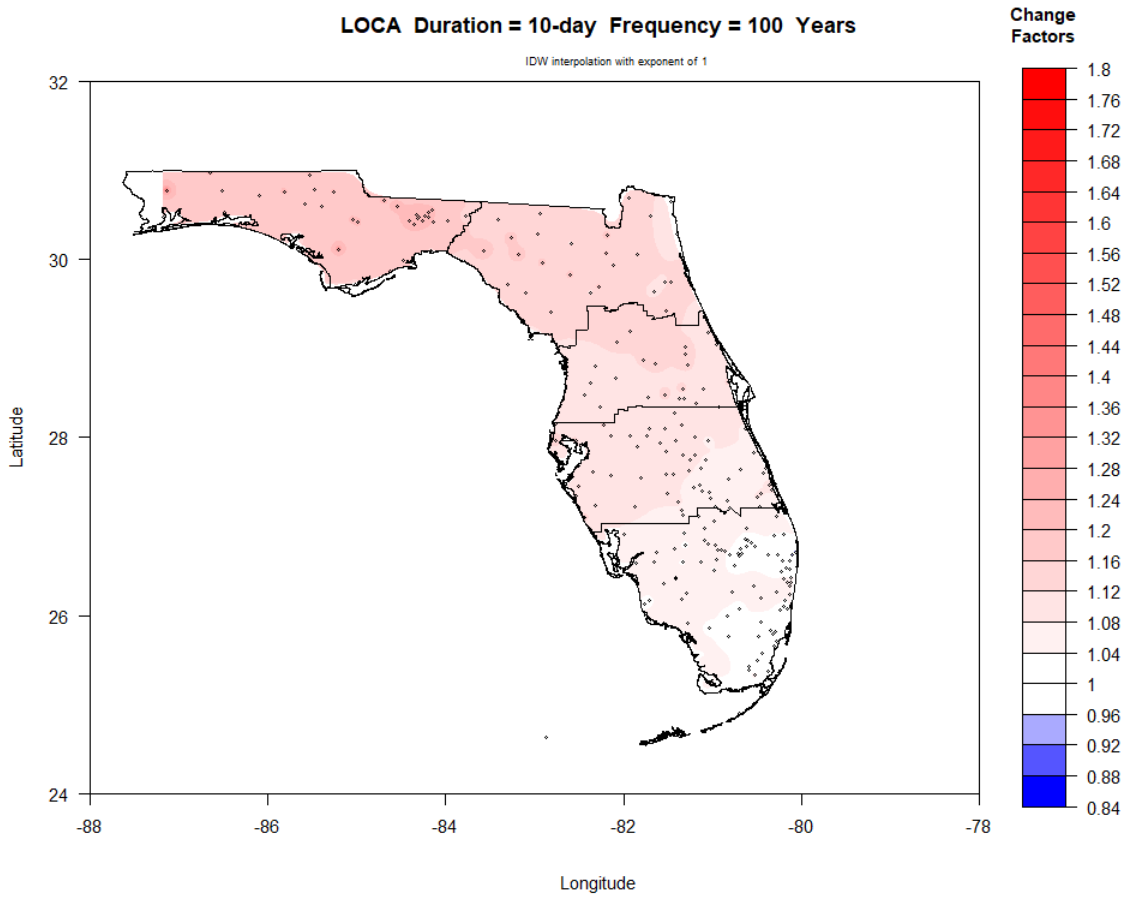

Figure IV-47. Map of FAR period (2060-2099) change factors across Florida for 10-day duration and 100-year return period.

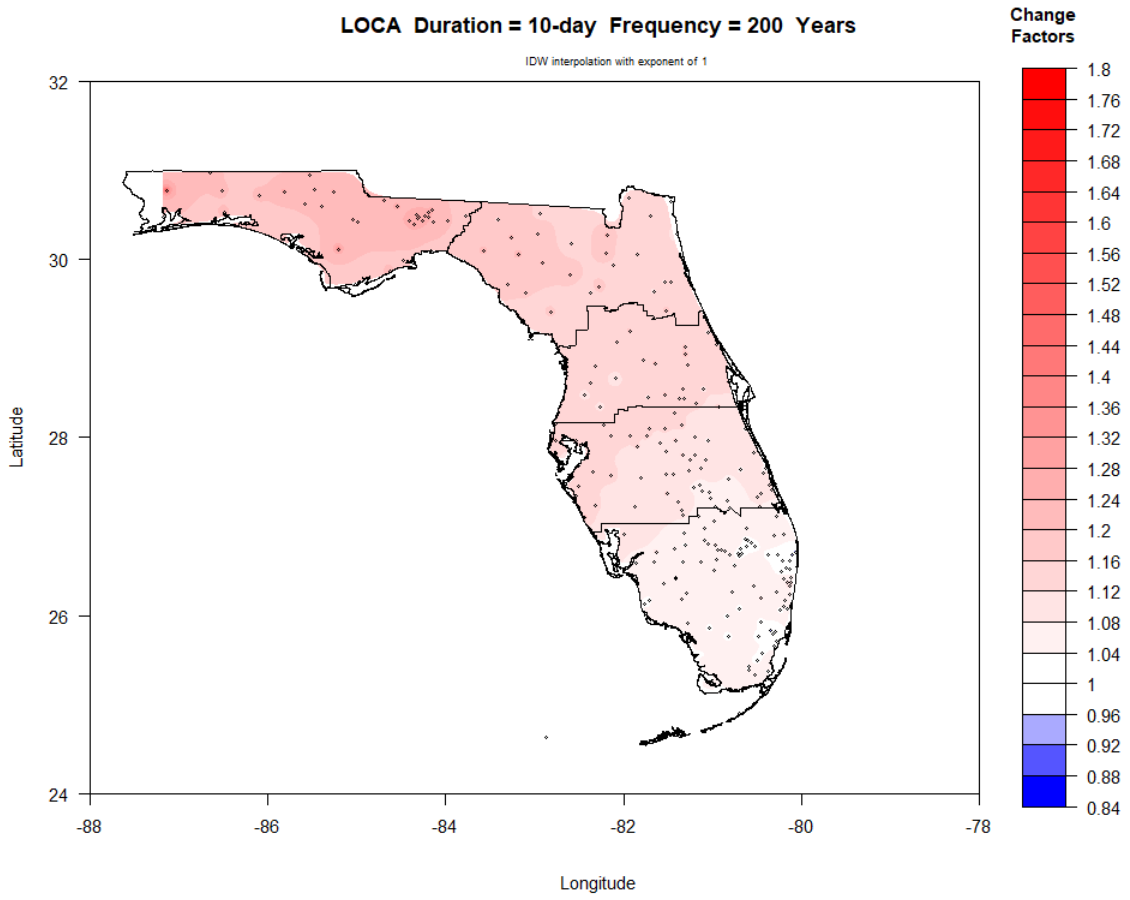

Figure IV-48. Map of FAR period (2060-2099) change factors across Florida for 10-day duration and 200-year return period.

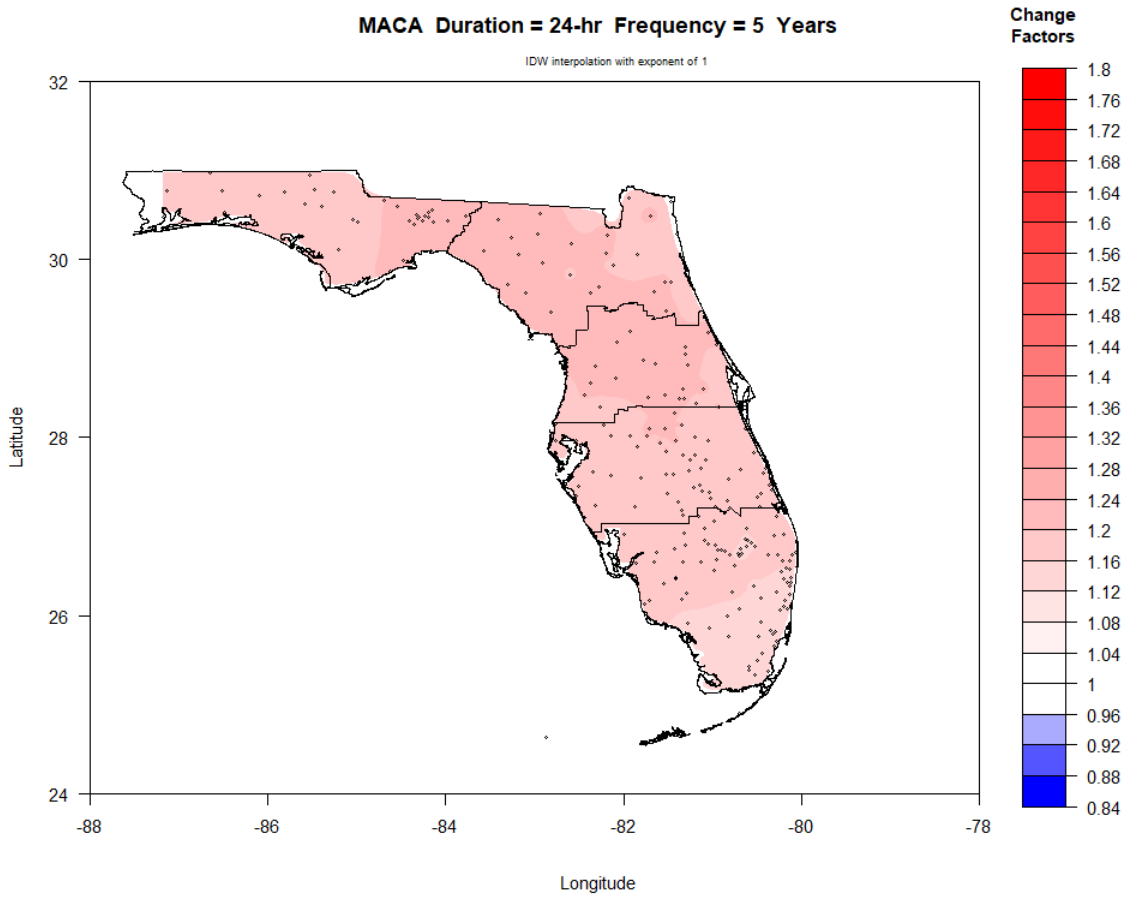

Figure IV-49. Map of FAR period (2060-2099) change factors across Florida for 24-hr duration and 5-year return period.

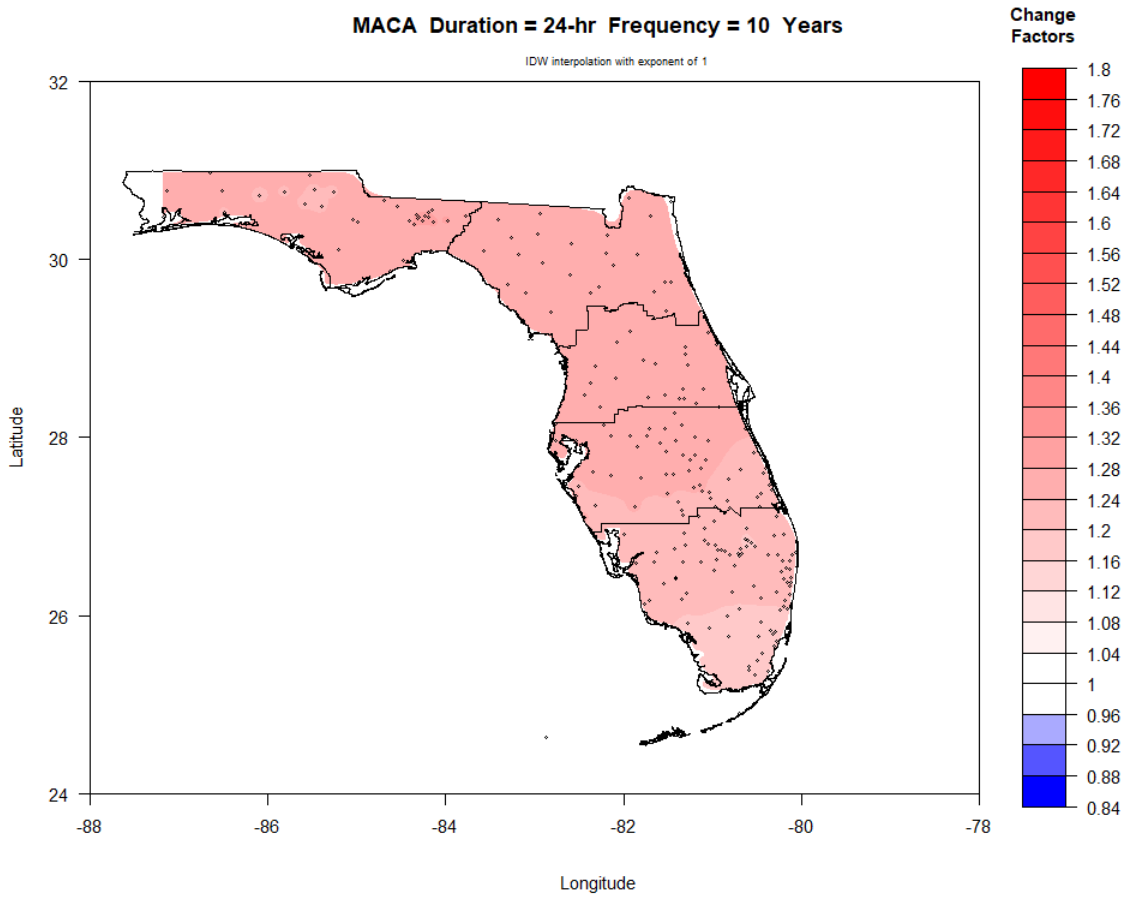

Figure IV-50. Map of FAR period (2060-2099) change factors across Florida for 24-hr duration and 10-year return period.

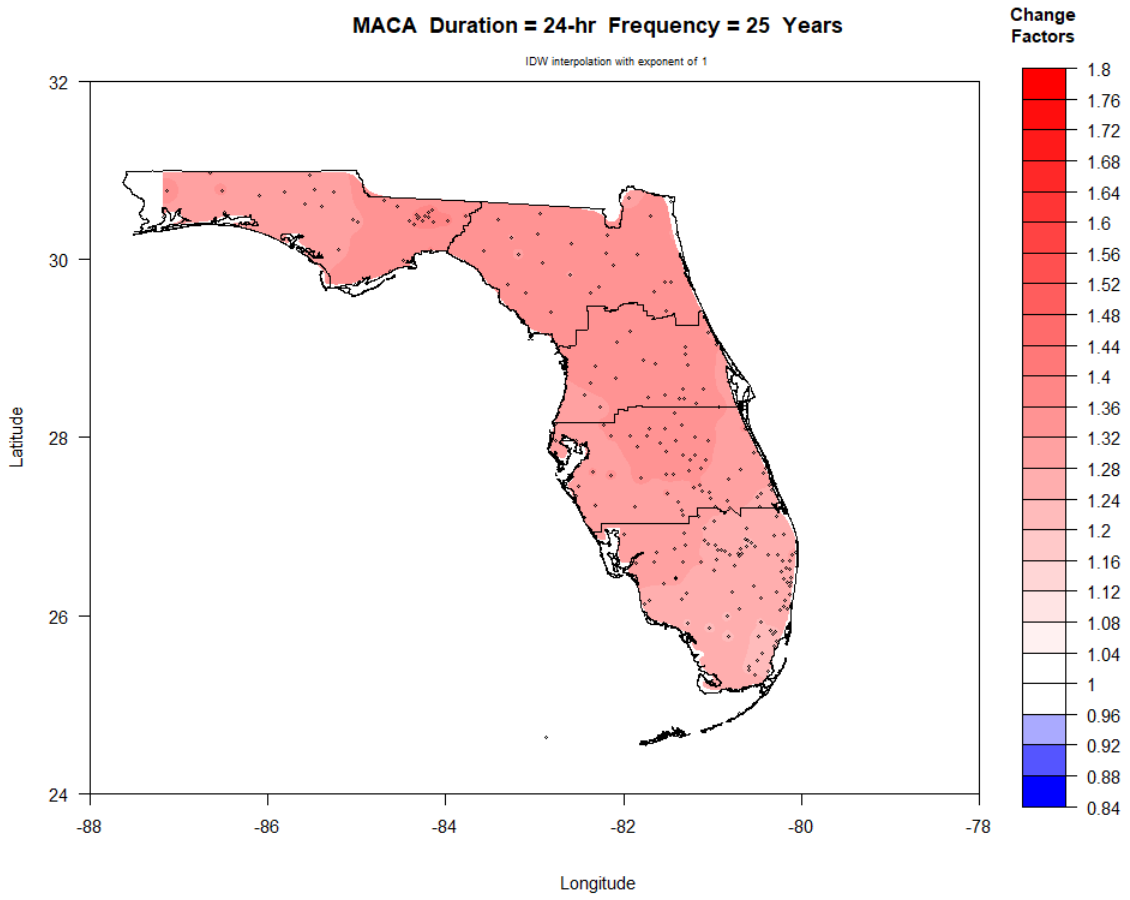

Figure IV-51. Map of FAR period (2060-2099) change factors across Florida for 24-hr duration and 25-year return period.

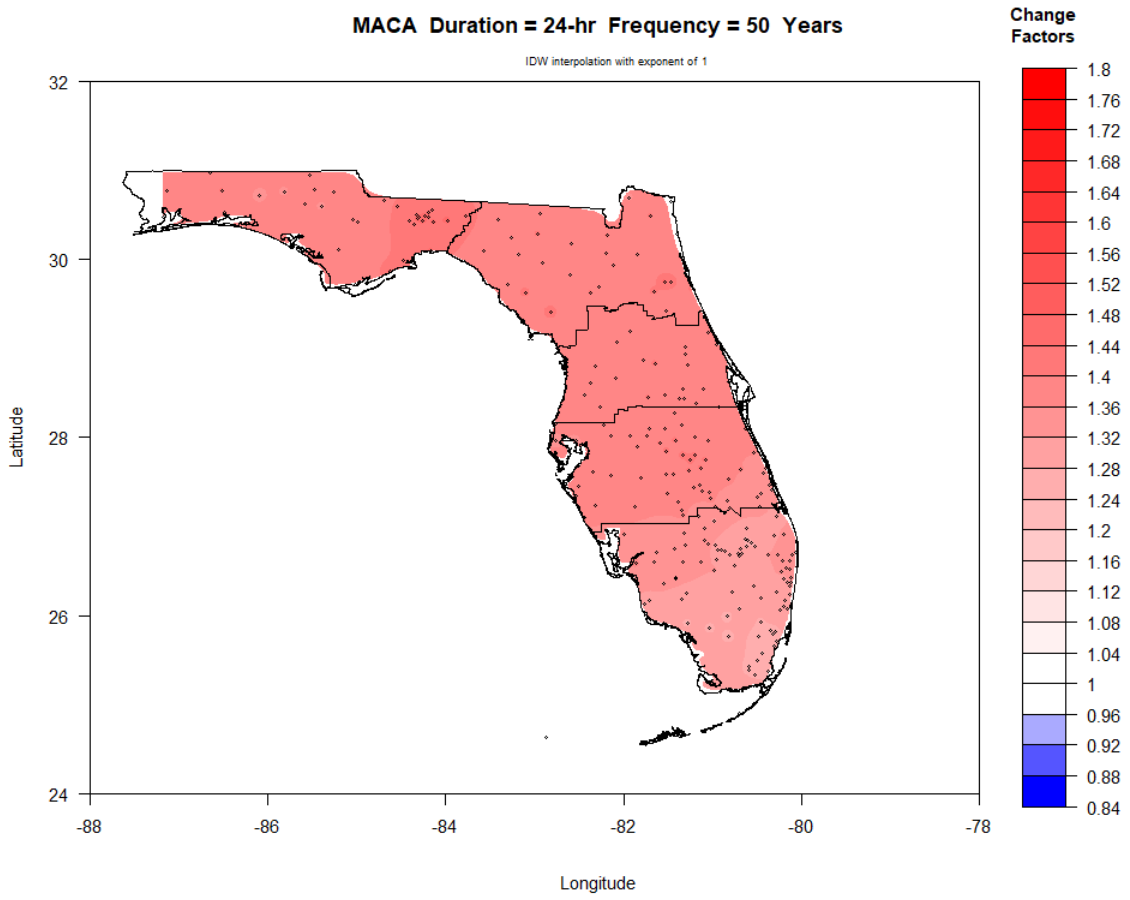

Figure IV-52. Map of FAR period (2060-2099) change factors across Florida for 24-hr duration and 50-year return period.

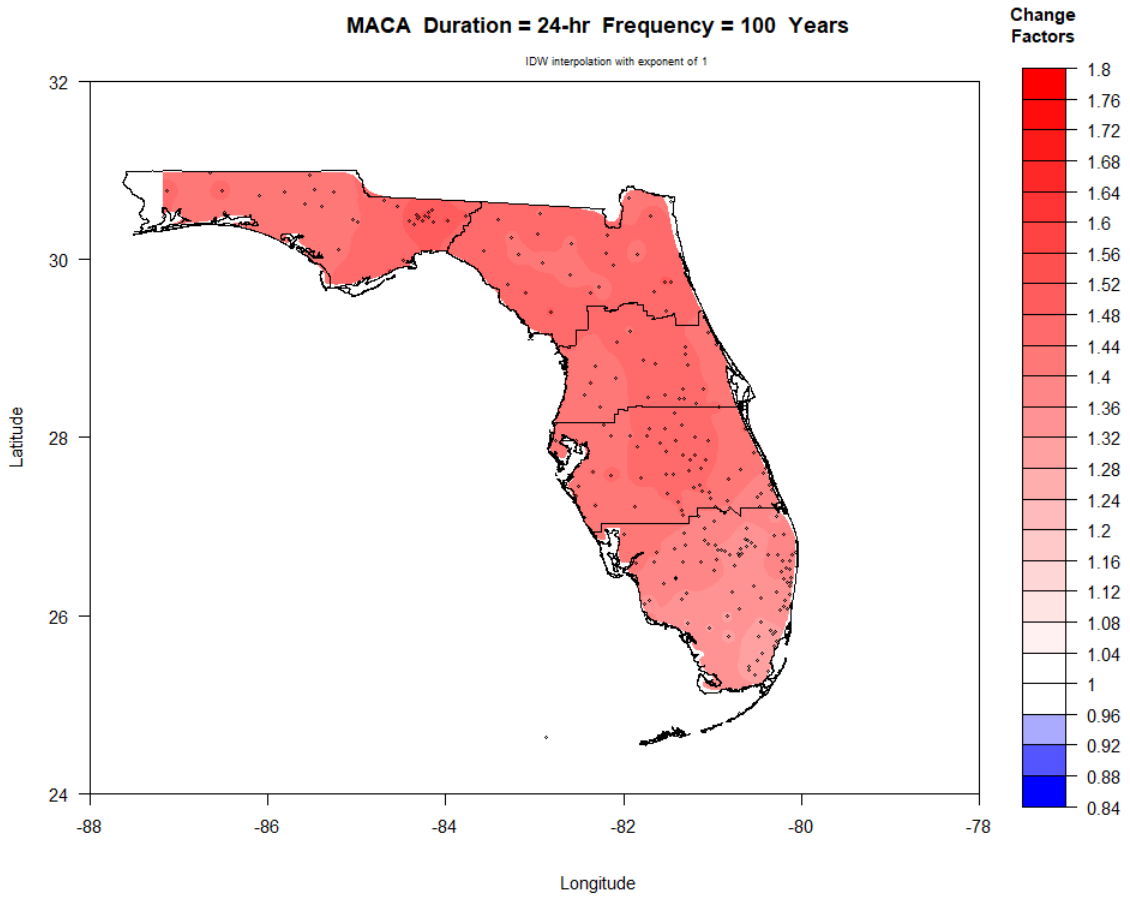

Figure IV-53. Map of FAR period (2060-2099) change factors across Florida for 24-hr duration and 100-year return period.

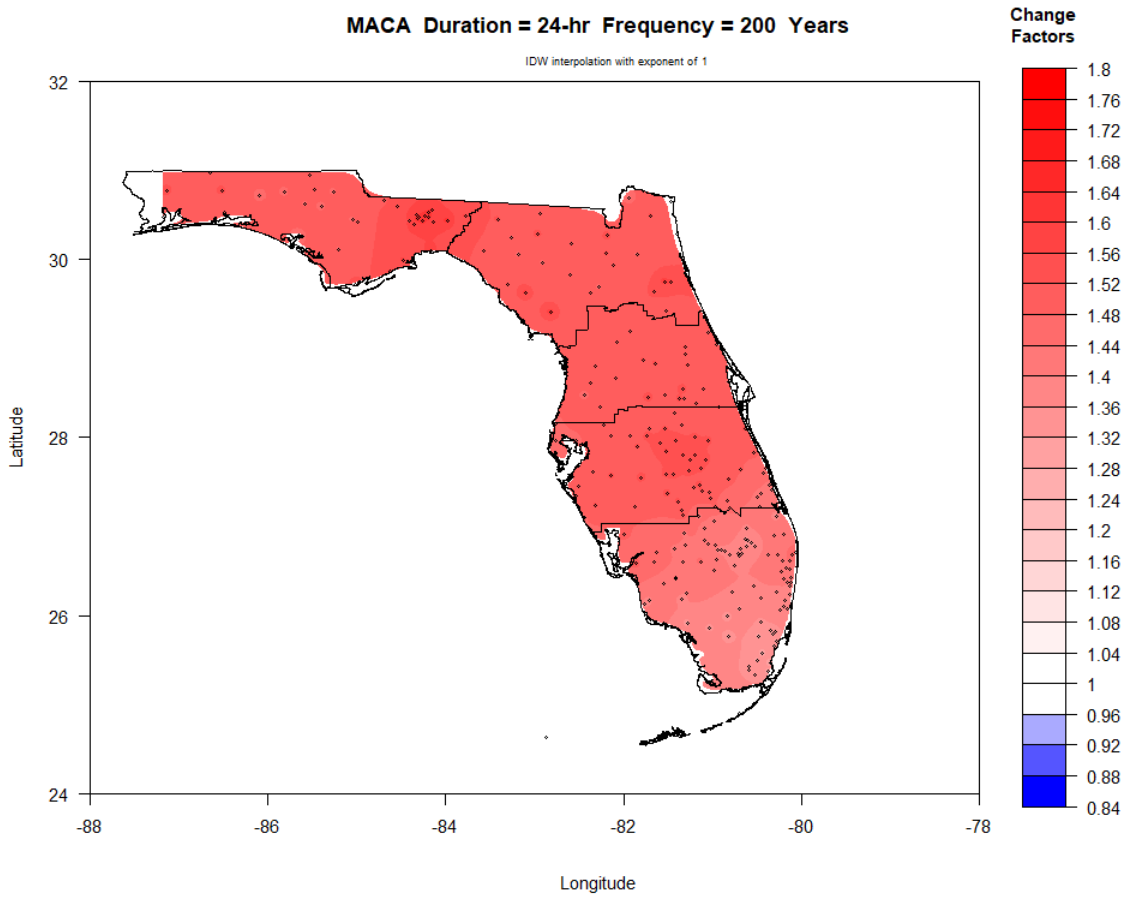

Figure IV-54. Map of FAR period (2060-2099) change factors across Florida for 24-hr duration and 200-year return period.

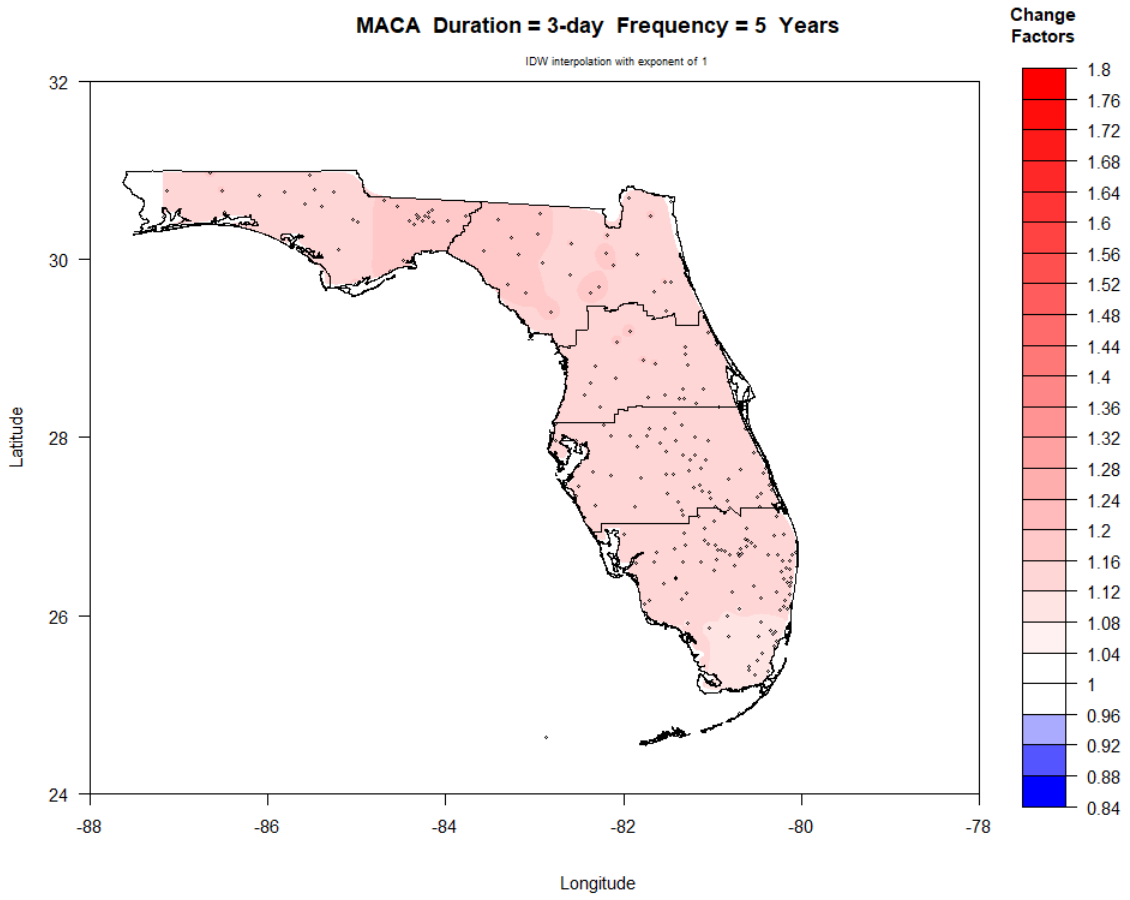

Figure IV-55. Map of FAR period (2060-2099) change factors across Florida for 3-day duration and 5-year return period.

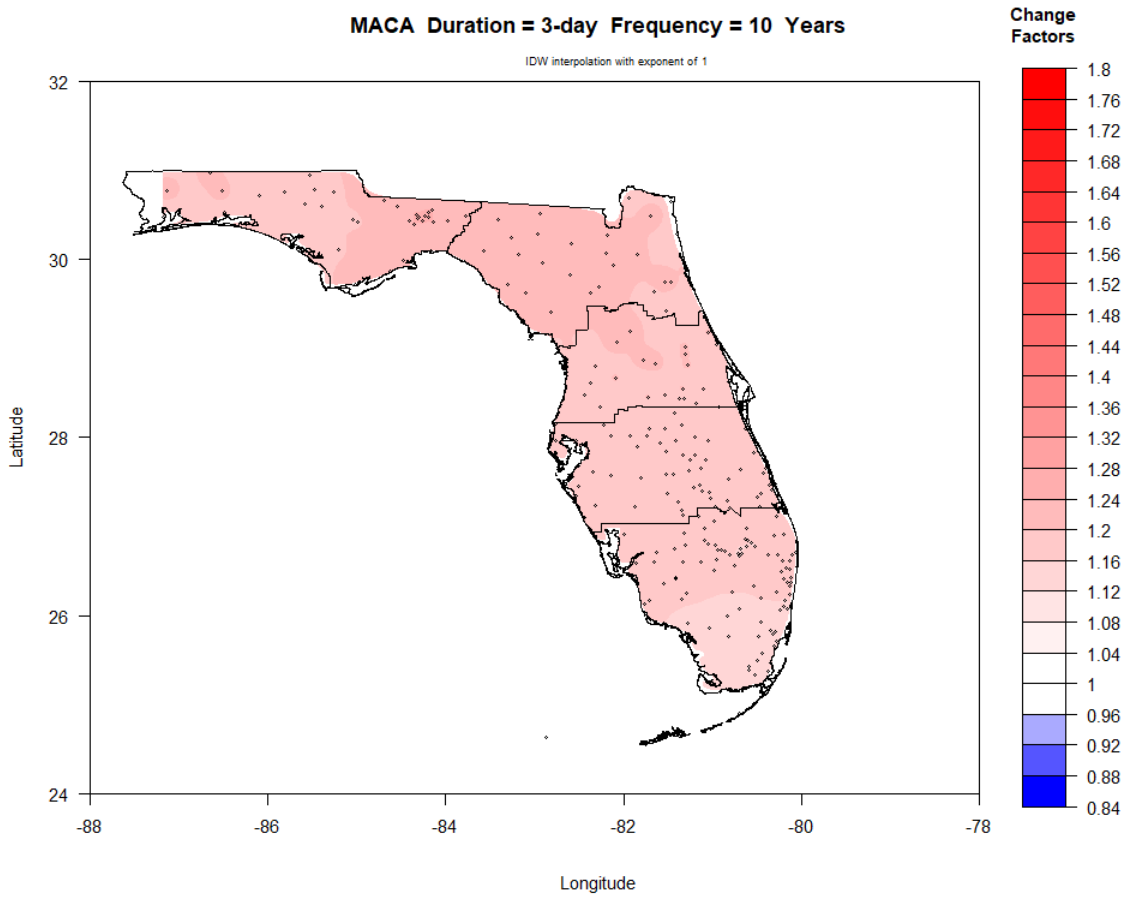

Figure IV-56. Map of FAR period (2060-2099) change factors across Florida for 3-day duration and 10-year return period.

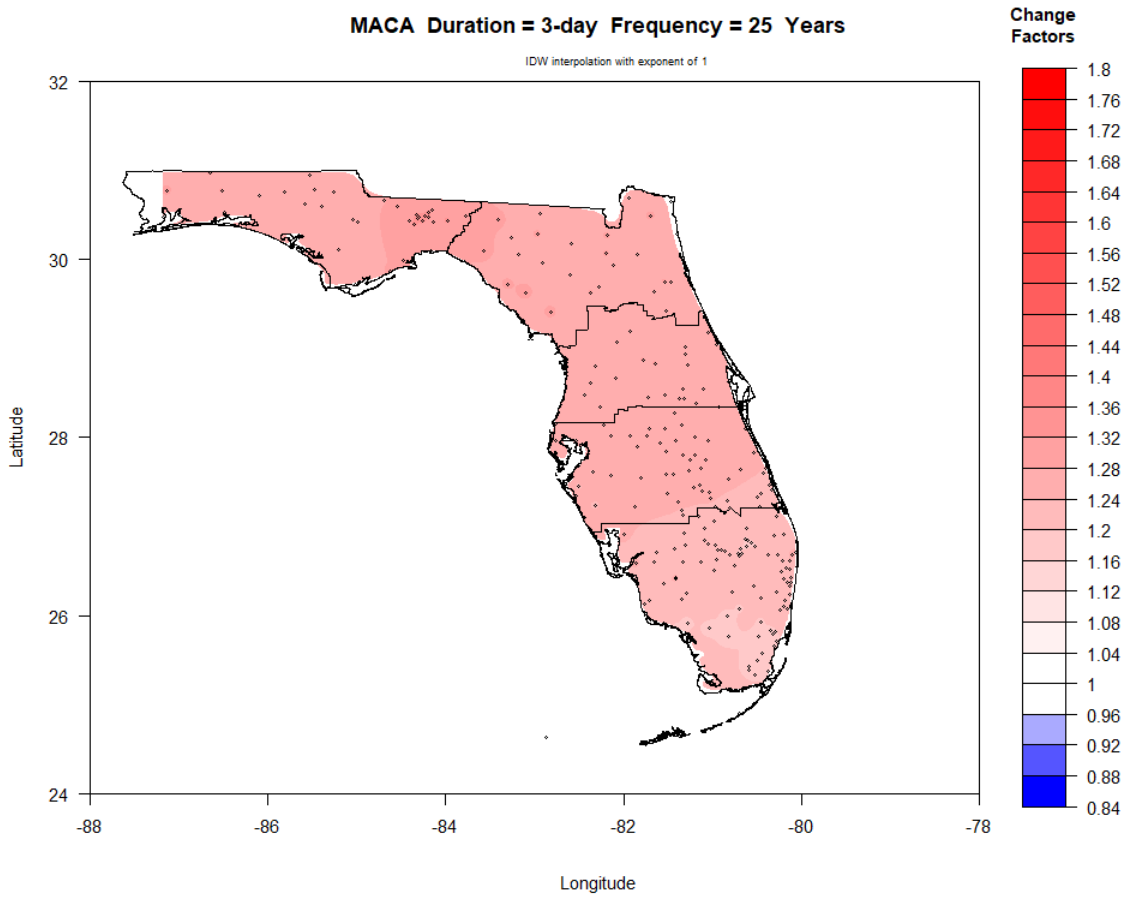

Figure IV-57. Map of FAR period (2060-2099) change factors across Florida for 3-day duration and 25-year return period.

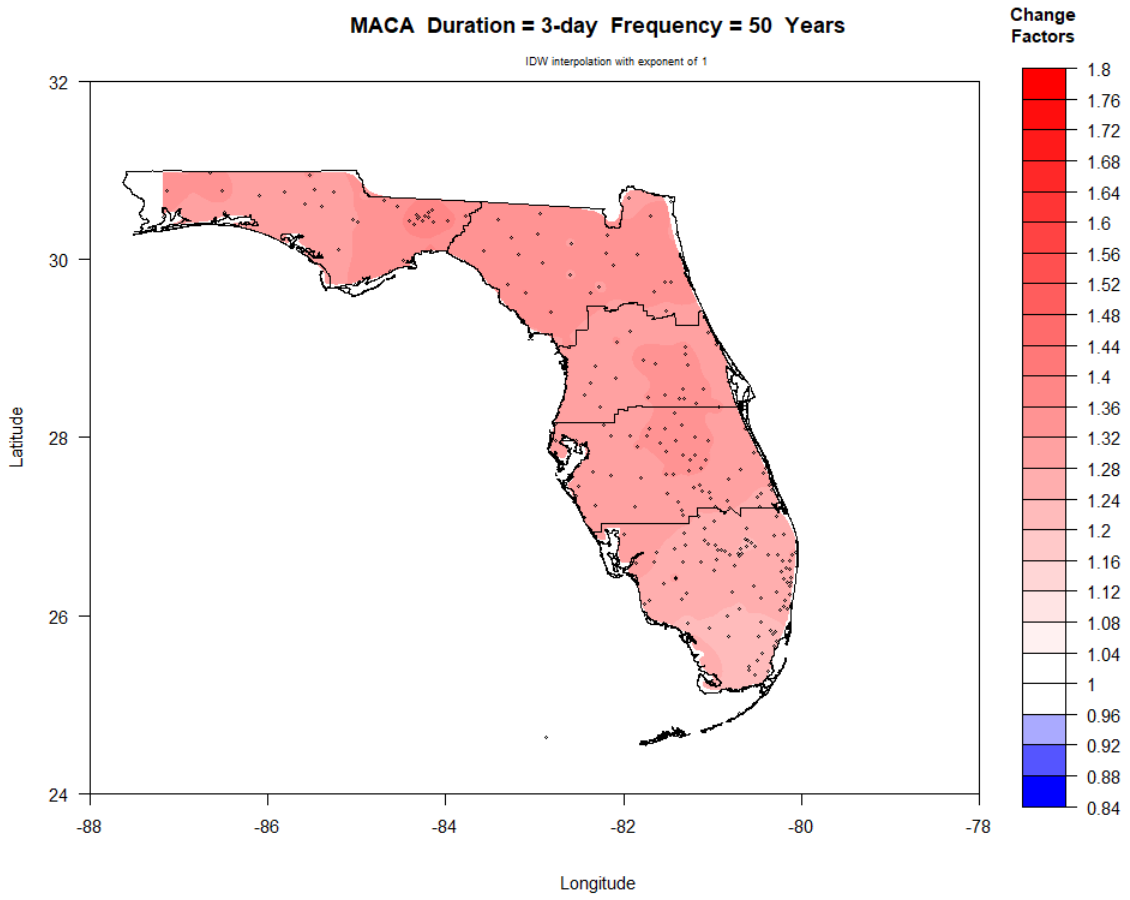

Figure IV-58. Map of FAR period (2060-2099) change factors across Florida for 3-day duration and 50-year return period.

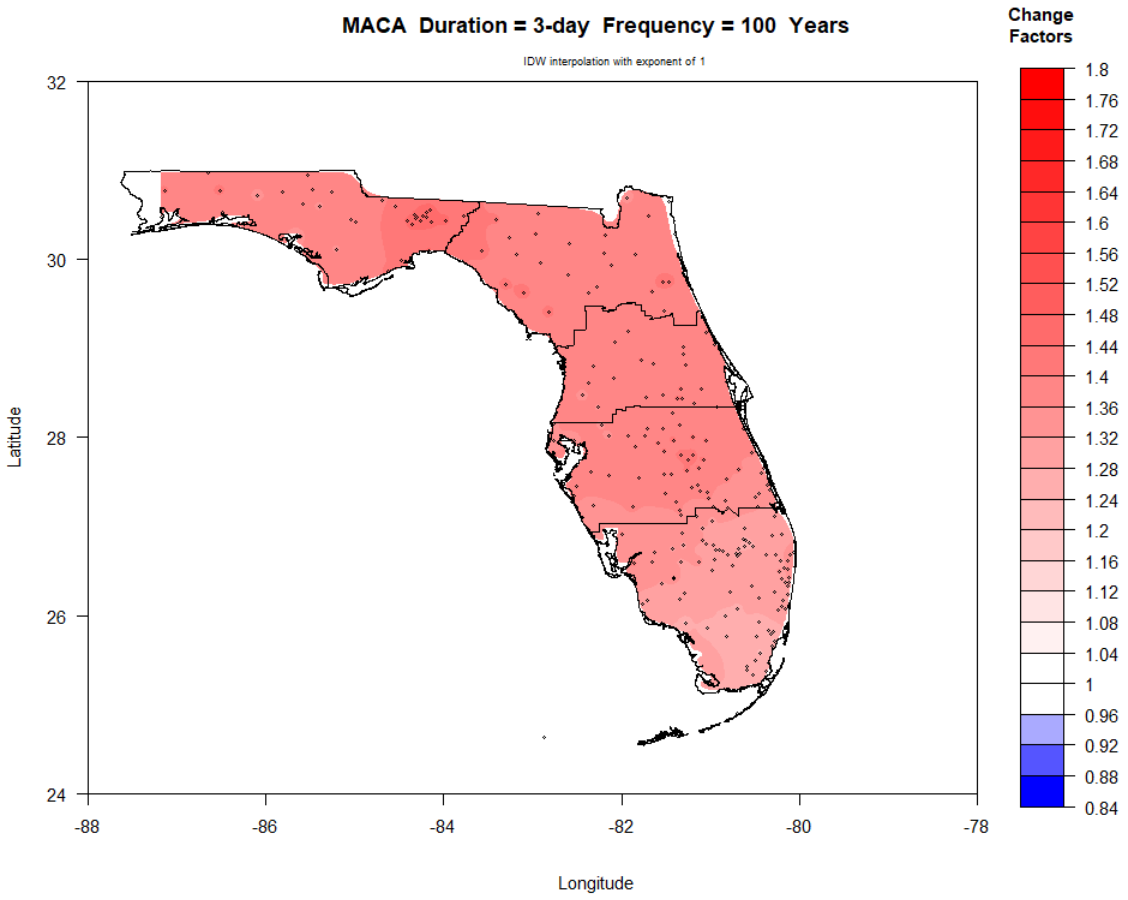

Figure IV-59. Map of FAR period (2060-2099) change factors across Florida for 3-day duration and 100-year return period.

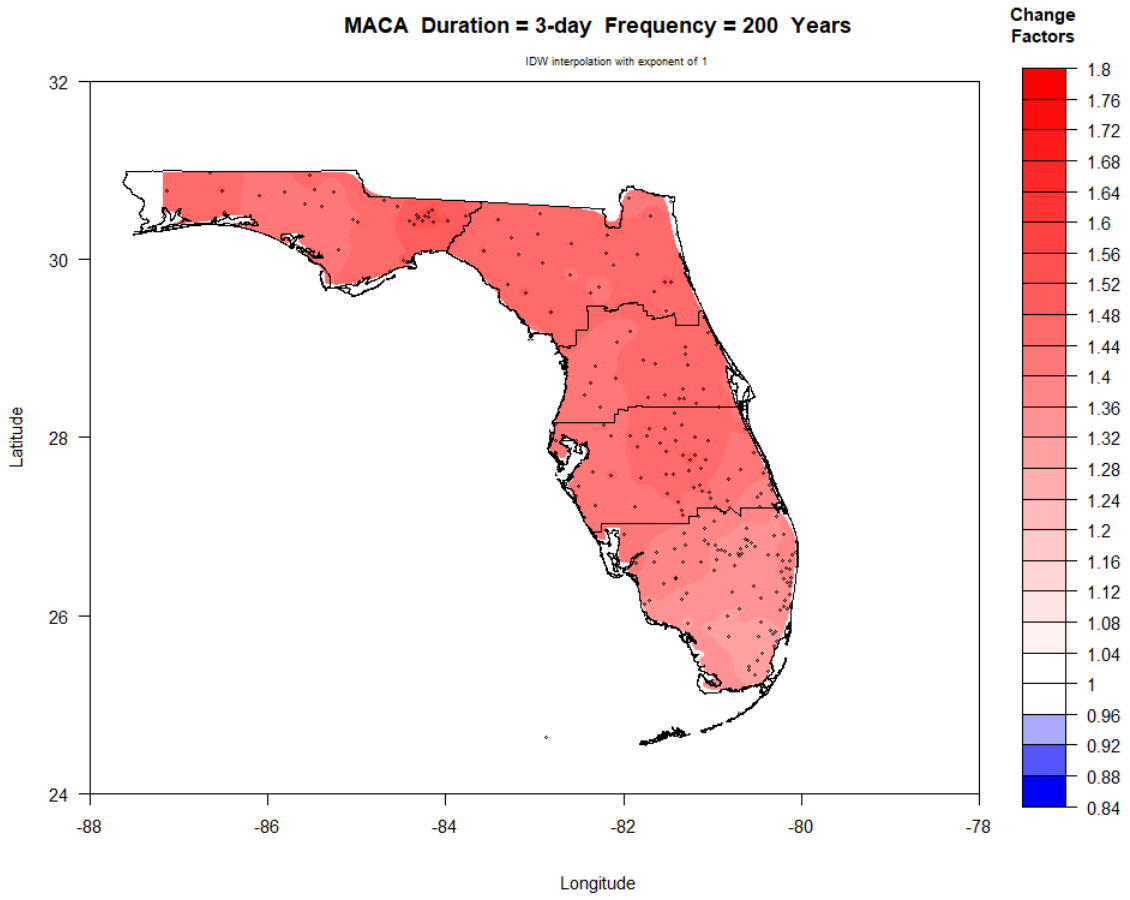

Figure IV-60. Map of FAR period (2060-2099) change factors across Florida for 3-day duration and 200-year return period.

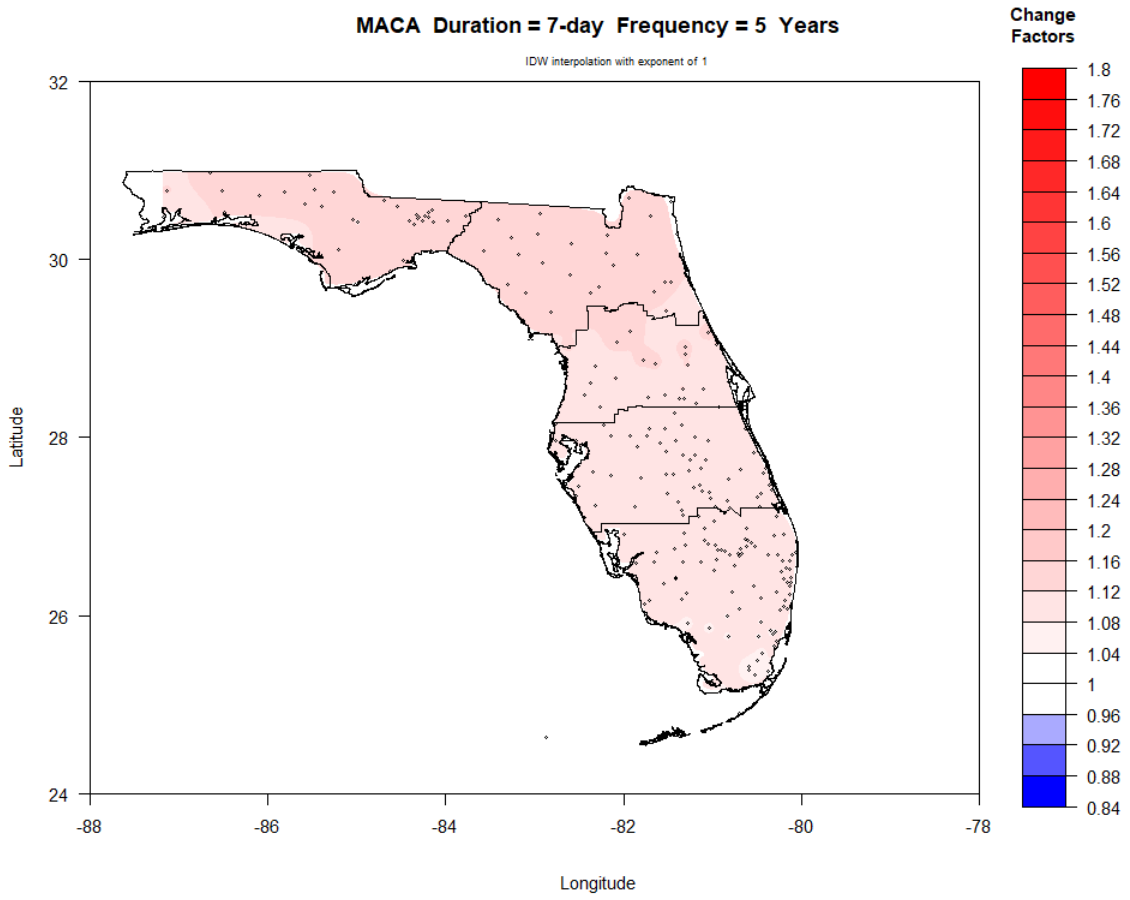

Figure IV-61. Map of FAR period (2060-2099) change factors across Florida for 7-day duration and 5-year return period.

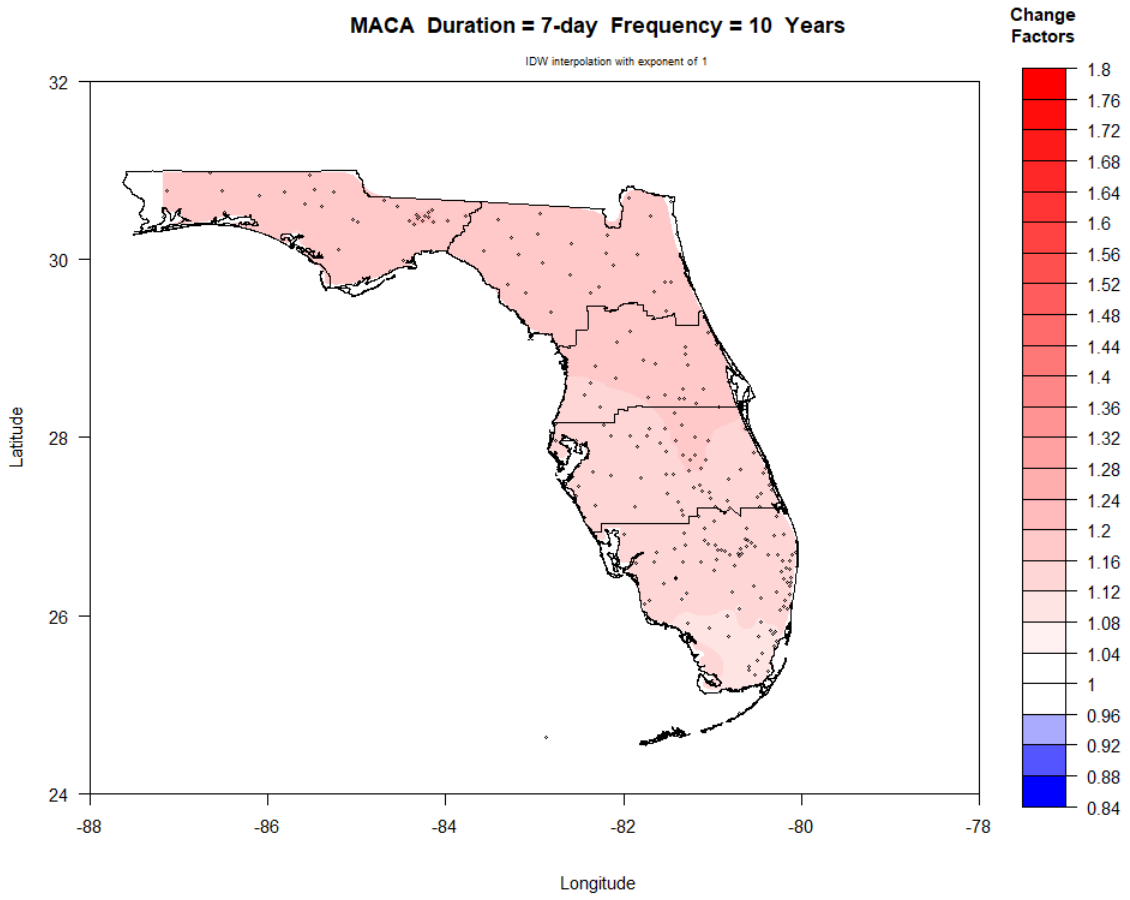

Figure IV-62. Map of FAR period (2060-2099) change factors across Florida for 7-day duration and 10-year return period.

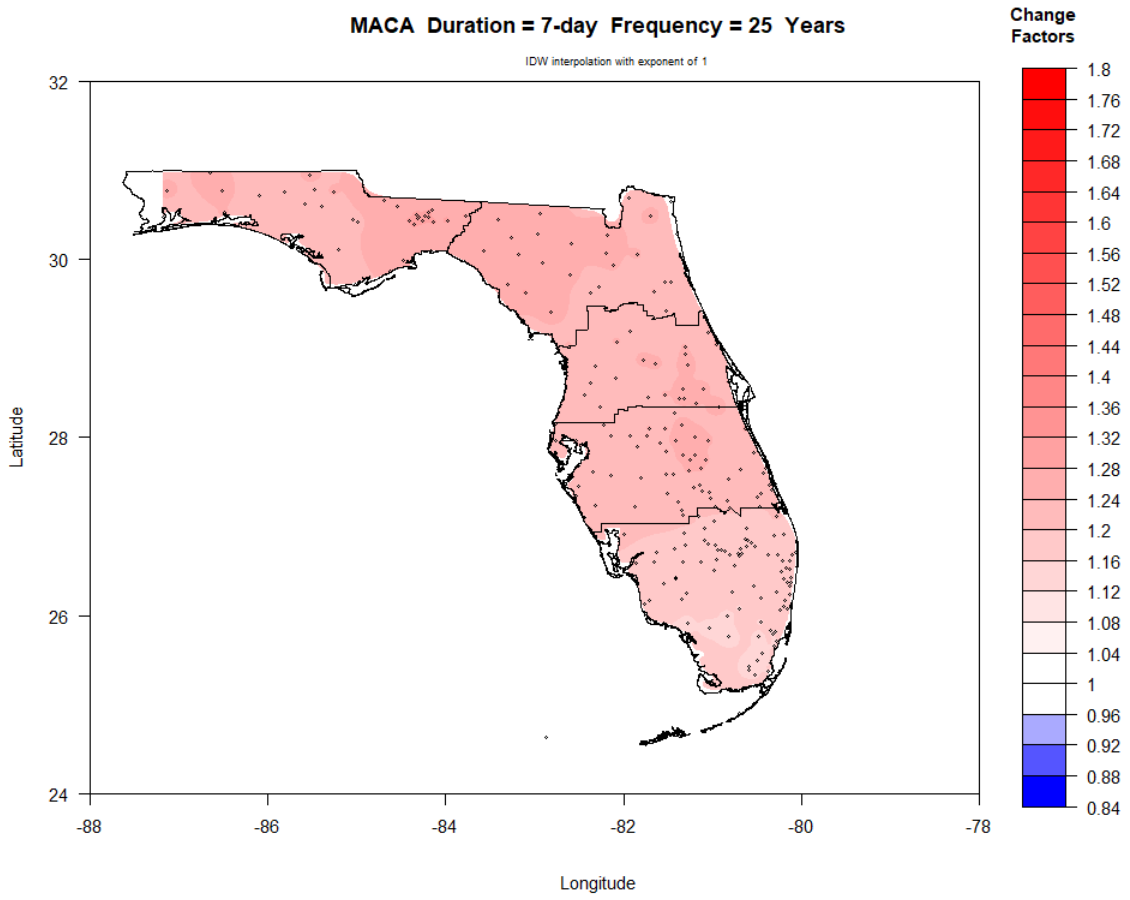

Figure IV-63. Map of FAR period (2060-2099) change factors across Florida for 7-day duration and 25-year return period.

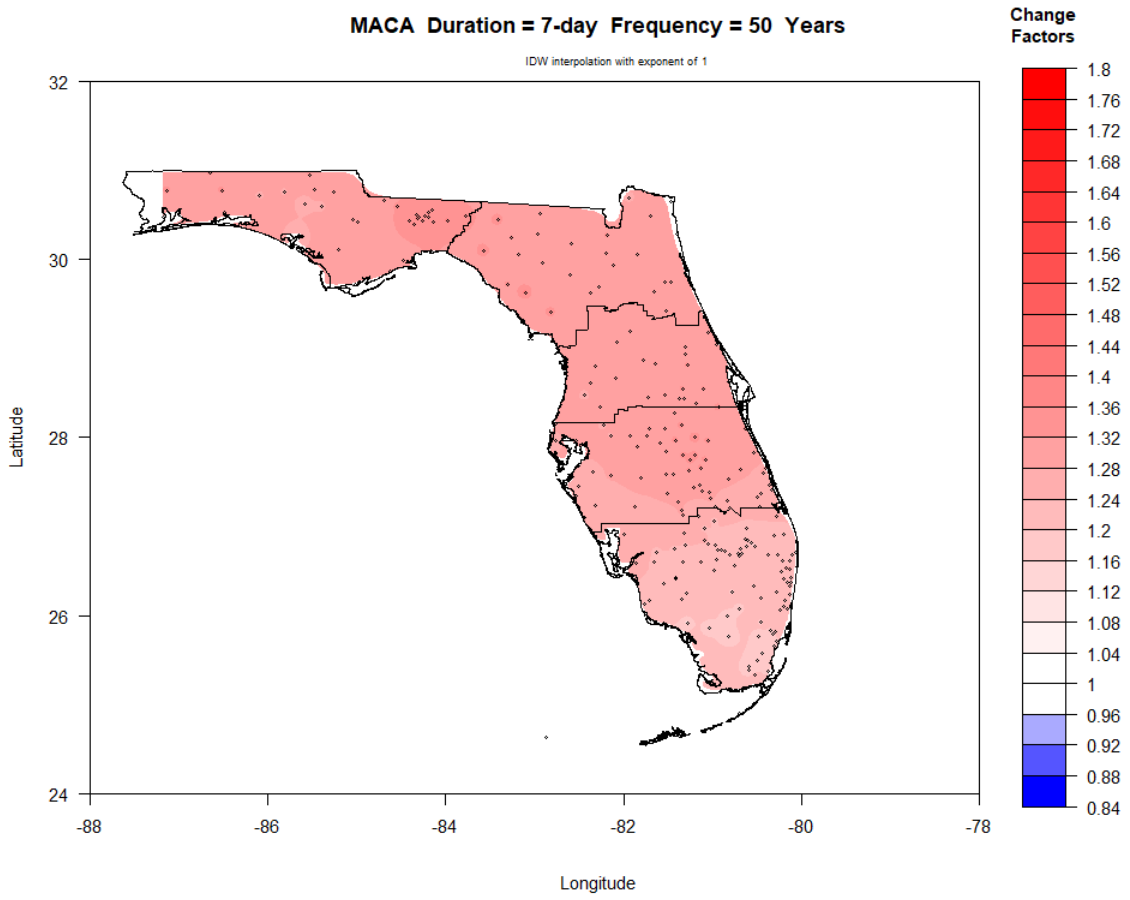

Figure IV-64. Map of FAR period (2060-2099) change factors across Florida for 7-day duration and 50-year return period.

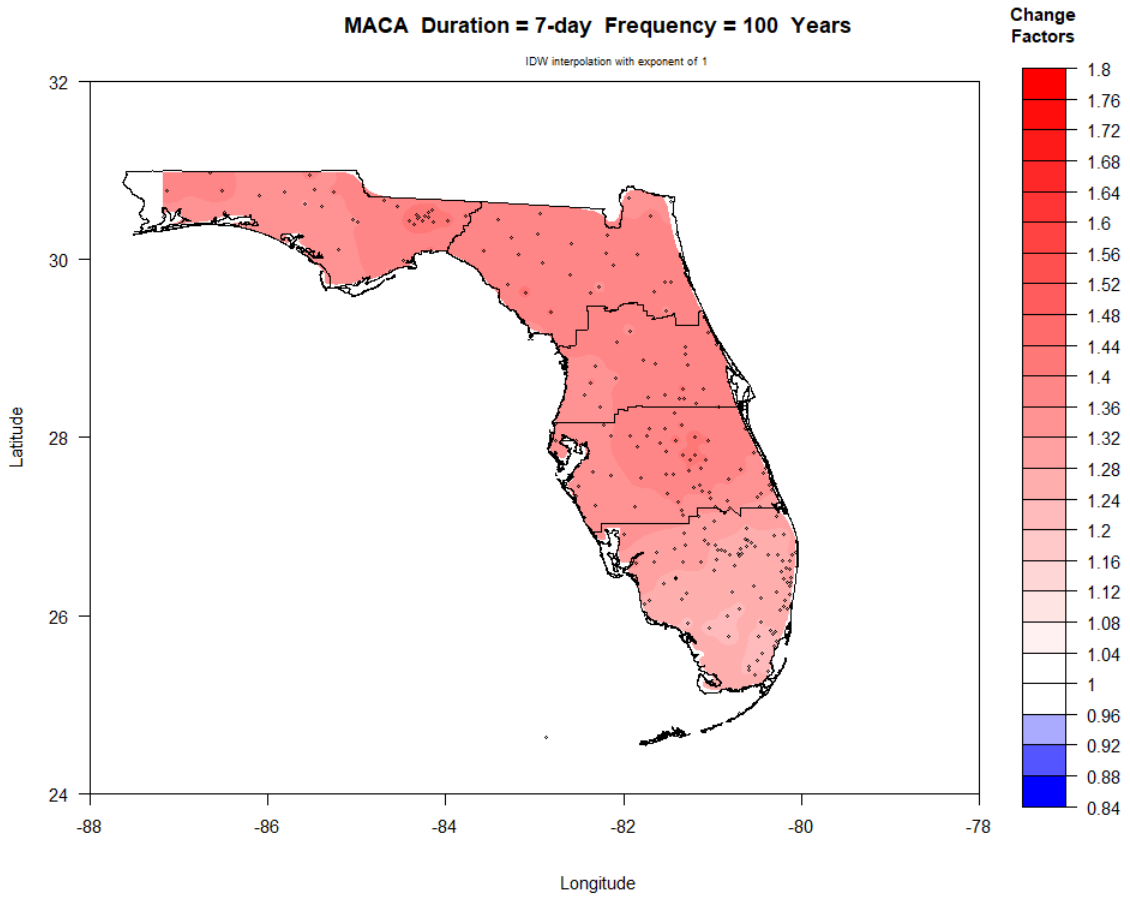

Figure IV-65. Map of FAR period (2060-2099) change factors across Florida for 7-day duration and 100-year return period.

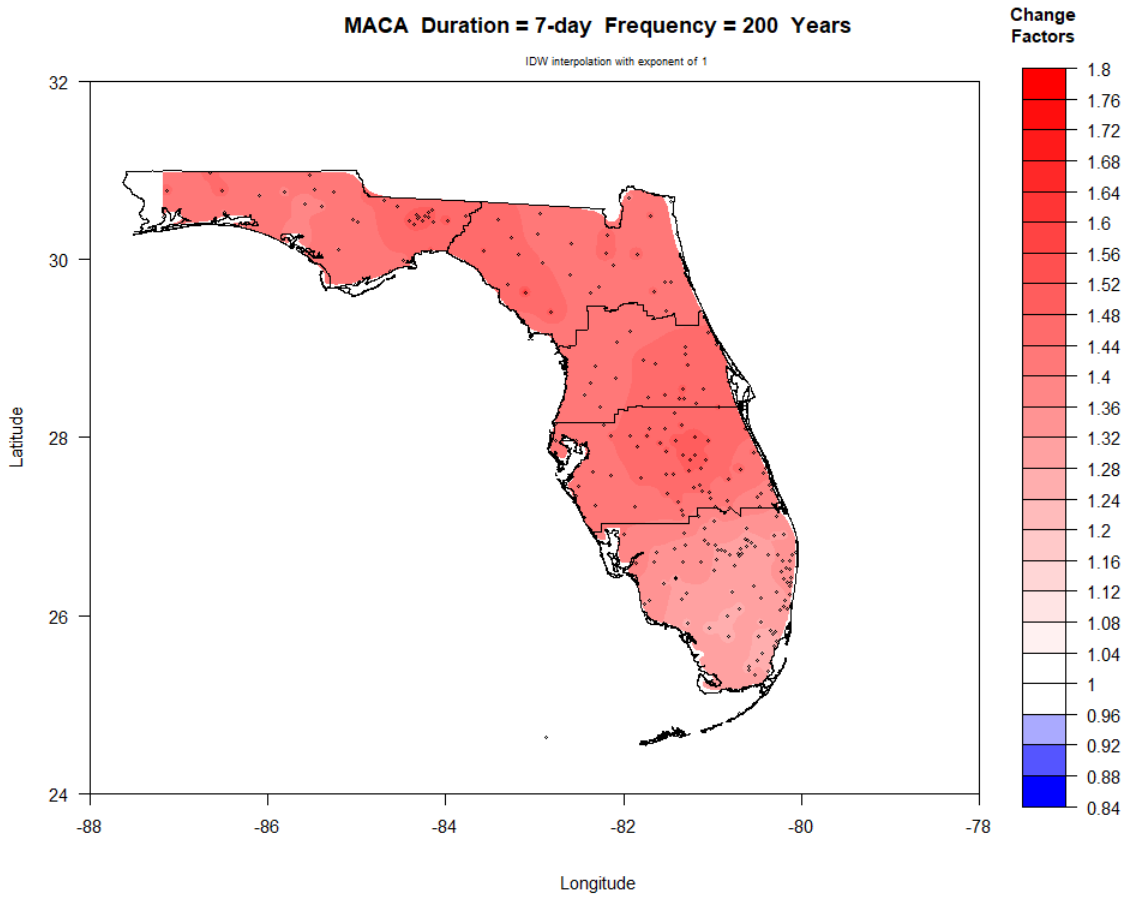

Figure IV-66. Map of FAR period (2060-2099) change factors across Florida for 7-day duration and 200-year return period.

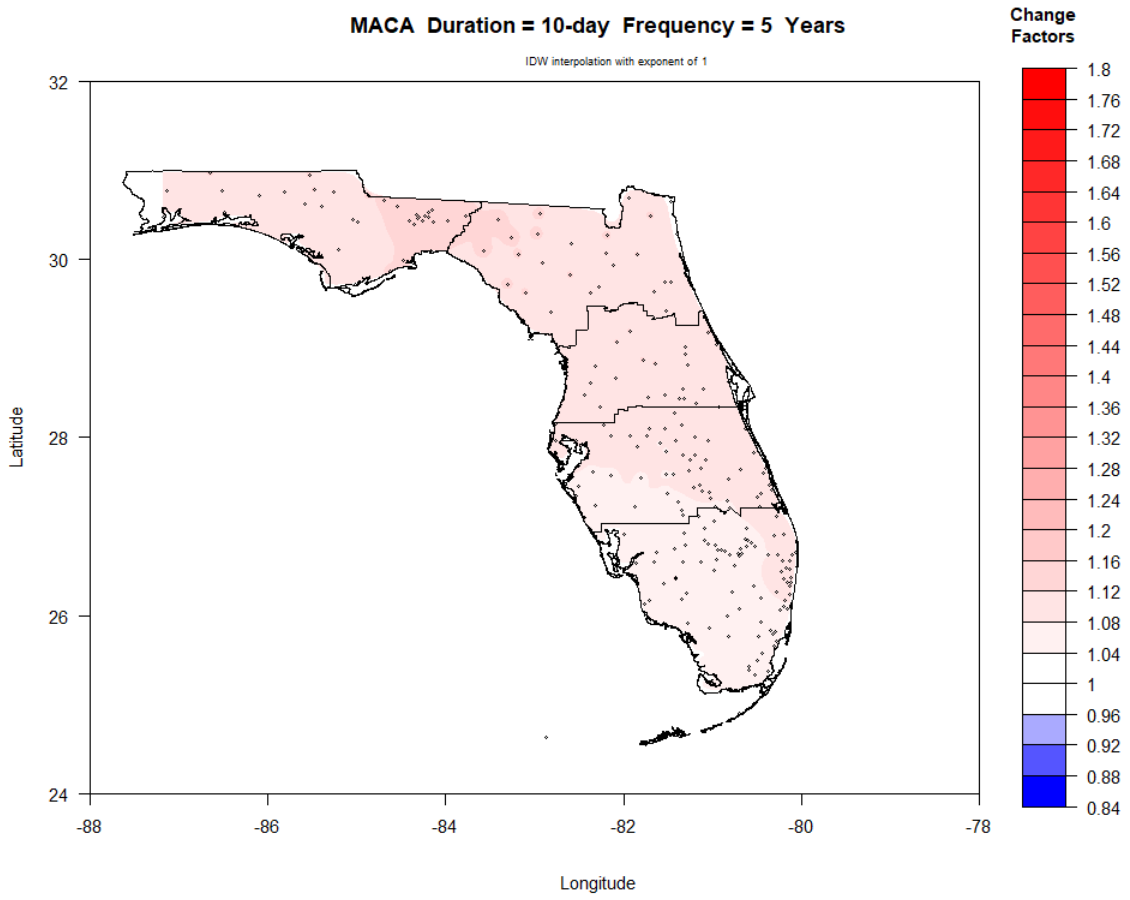

Figure IV-67. Map of FAR period (2060-2099) change factors across Florida for 10-day duration and 5-year return period.

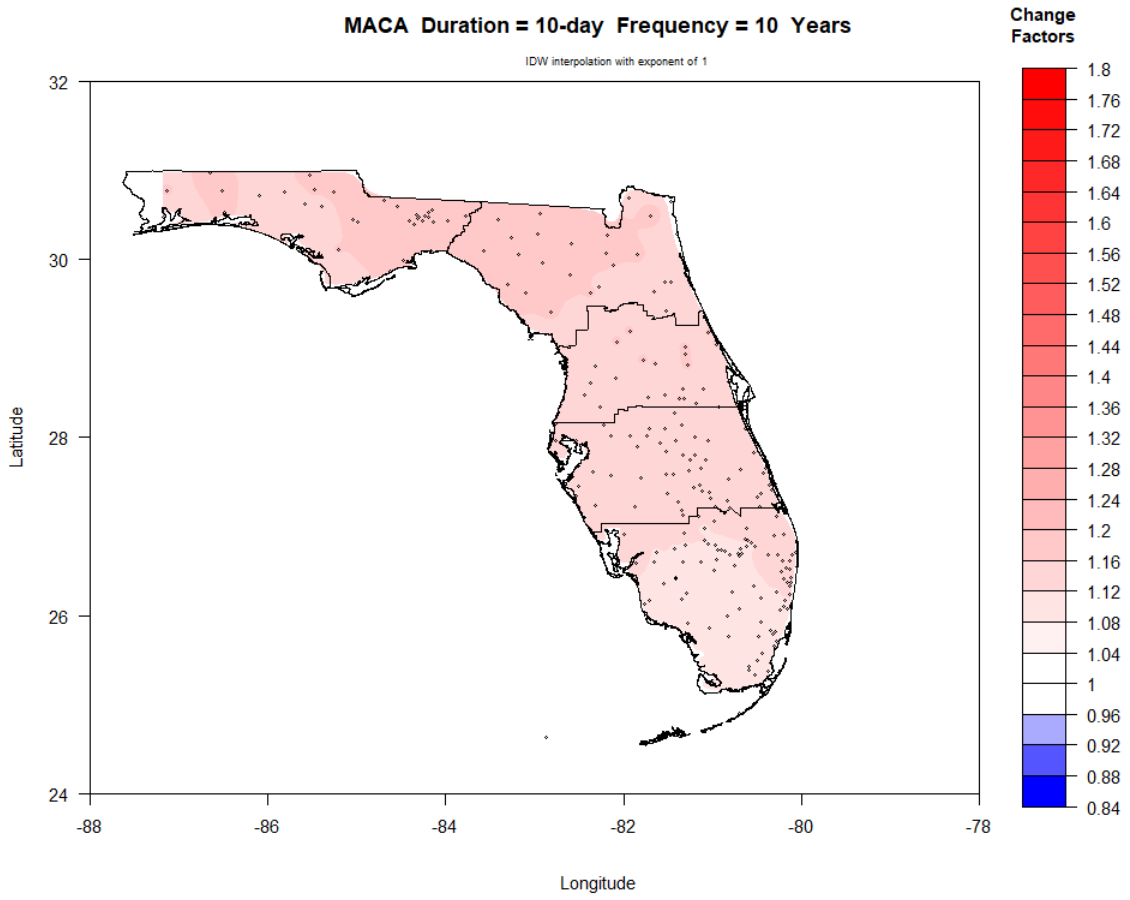

Figure IV-68. Map of FAR period (2060-2099) change factors across Florida for 10-day duration and 10-year return period.

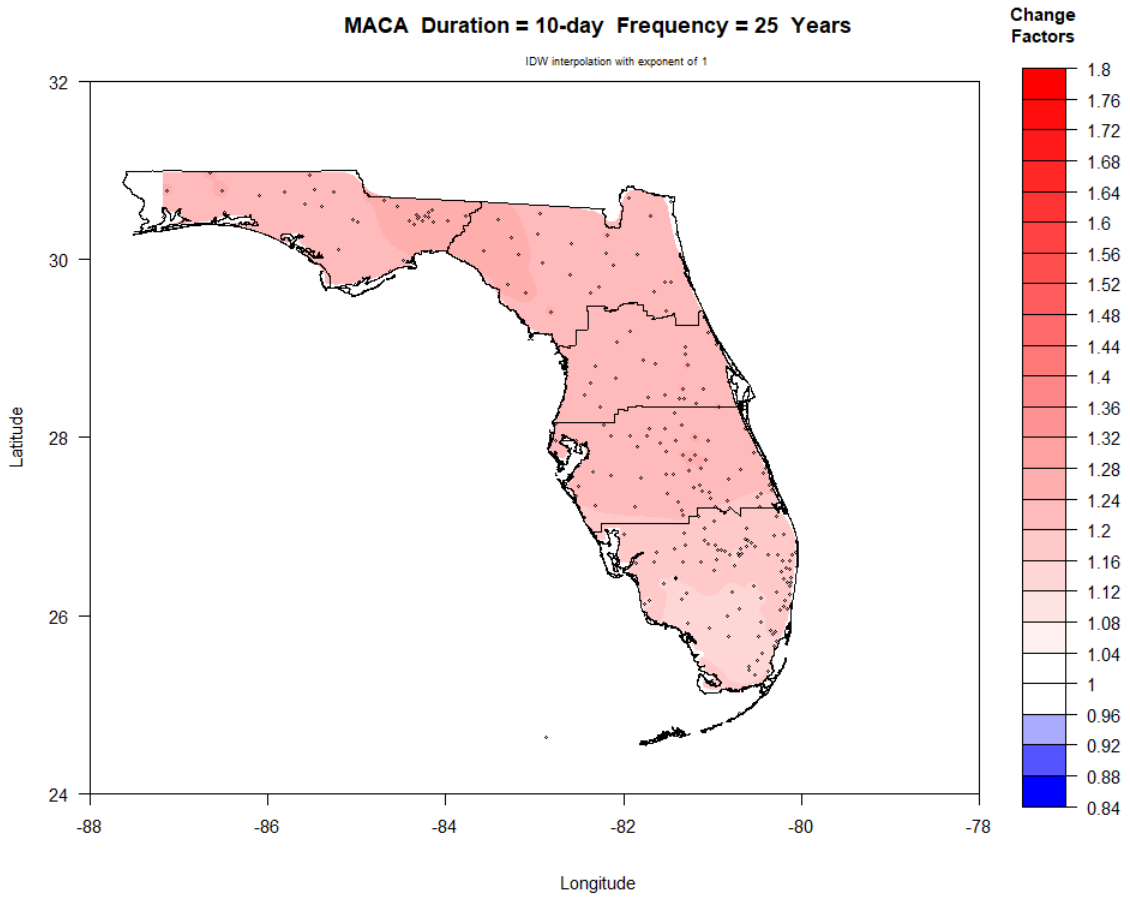

Figure IV-69. Map of FAR period (2060-2099) change factors across Florida for 10-day duration and 25-year return period.

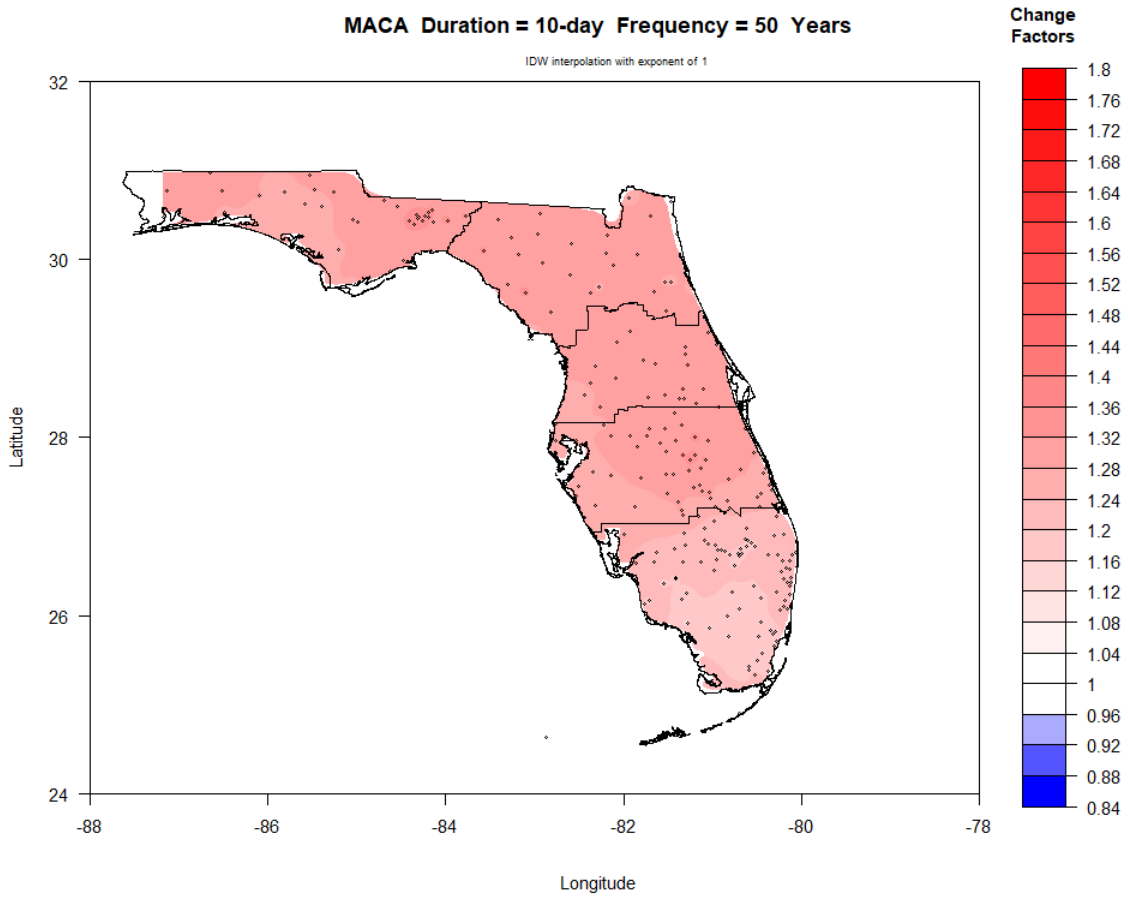

Figure IV-70. Map of FAR period (2060-2099) change factors across Florida for 10-day duration and 50-year return period.

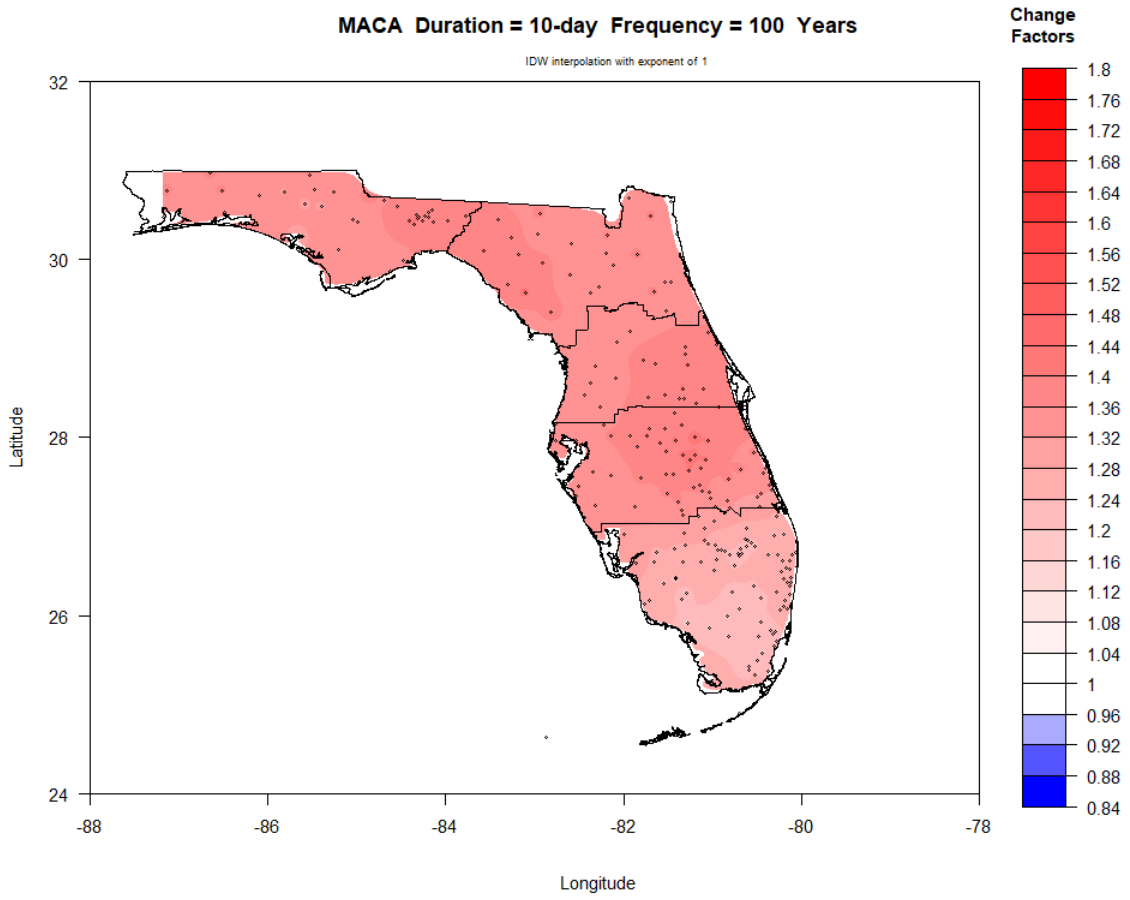

Figure IV-71. Map of FAR period (2060-2099) change factors across Florida for 10-day duration and 100-year return period.

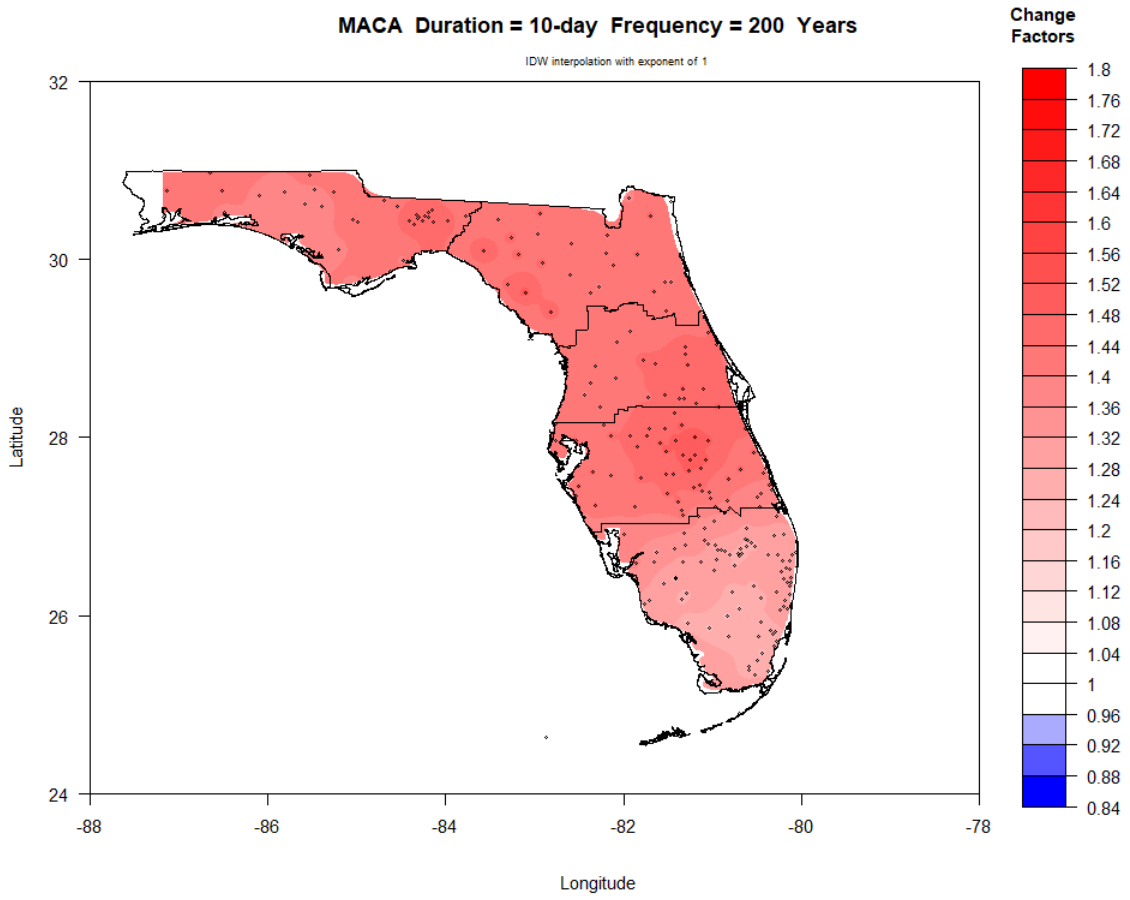

Figure IV-72. Map of FAR period (2060-2099) change factors across Florida for 10-day duration and 200-year return period.

APPENDIX V. Website

In response to the following task of the project scope, "FIU SLSC shall develop statewide, web-based user interface for making extreme rainfall projections available to communities across the state", web-access to the project results are provided using the Tableau software (https://public.tableau.com/). The public version of this software is a free platform to publicly share and explore data visualizations online.

For this project, the tables of Change Factors provided in Appendix I and II have been made available using the following Tableau Tool:
Updating the Statewide Extreme Rainfall Projections | Tableau Public

A snapshot of this interactive tool is shown below: